PETROLOGICAL AND ISOTOPIC EVIDENCE FOR DIAGENETIC EVOLUTION IN THE CHERRY VALLEY CARBONATES AND ADJACENT MUDROCKS OF THE MARCELLUS "SHALE" FROM WEST VIRGINIA, PENNSYLVANIA, AND NEW YORK

A Thesis
Presented to the Faculty of the Graduate School
of Cornell University
In Partial Fulfillment of the Requirements for the Degree of
Master of Science

by
Jonathan Casey Root

May 2018

ABSTRACT

The Cherry Valley carbonates are thin, laterally continuous limestones that separate the upper and lower organic-rich mudstones of the Marcellus "shale". Textural and compositional heterogeneity within these carbonates provide evidence of diagenetic evolution. The Cherry Valley carbonates contrast lithologically and petrophysically with bounding organic-rich mudstones, regionally the East Berne Member of the Oatka Creek Formation (overlying) and Bakoven Member of the Union Springs Formation (underlying), and comprise carbon isotope-depleted, methanogenic nodules and pelagic limestones. Petrologic evaluation of these units indicates the presence or absence of early nodule formation controlled the effect of burial, thermal, and exhumation diagenesis on these carbonates. The isotopic compositions of these nodular carbonates, which were deposited as fossiliferous mudstones, reflect an initial depletion of ^{13}C that was recrystallized by isotopically heavier carbon during burial diagenesis. In equivalent mudstones where nodules were not formed, isotopic compositions are comparable to that of unaltered dacryoconarid fossils which are the dominant source of calcite in these rocks.

Three depositional facies, which do not reflect subsequent alteration, are related to the Cherry Valley carbonates: (1) a basal calcareous mudstone facies that are rich in algal cysts; (2) an intermediate limestone rich in pelagic fossils that classically defines the Cherry Valley carbonates; (3) an upper-bounding calcareous mudstone facies.

Eight cores from West Virginia (3), Pennsylvania (2), and New York (3) are qualitatively and quantitatively described by petrologic methods, including thin section petrography and scanning electron microscopy, and geochemical analyses to integrate lithological, textural, and spatial relationships among the diagenetic framework of these rocks at a range of scales. Compositional analyses describe the distribution of mineral phases and textures, as determined by petrological observation, and include reflectance spectroscopy, X-ray diffraction, and energy dispersive X-ray spectroscopy. Stable carbon and oxygen isotope compositions of carbonate-derived CO_2 gas are measured using off-axis integrated cavity output laser spectroscopy.

The general diagenetic sequence for the Cherry Valley carbonates begins with (1) micritization of calcareous mudstones and bedded limestones; (2) methanogenetic formation of calcite or barite nodules; (3) prismatic calcite growth on fossils or allochemical grains (4) crystallization of organogenetic dolomite rhombohedra; (5) pore-filling cements that include sparry carbonates, barite, and pyrite; (6) catagenesis and mobilization of hydrocarbons via fractures and stylolites; (7) late stage calcite crystallization or dolomitization; (8) dedolomitization associated with exhumation.

BIOGRAPHICAL SKETCH

Casey Root is a native of Pennsylvania, splitting his childhood between the outskirts of Pittsburgh and the rural town of Lewisburg. He came to Cornell from Salt Lake City, Utah, after graduating from the University of Utah with a B.S. in Geological Sciences. While working at a core analysis lab as a sedimentary petrologist, Casey attended a guest lecture from his future advisor, Dr. Terry Jordan. This chance encounter ultimately led to their collaboration on this thesis. While at Cornell, Casey fully appreciated his time with his fellow graduate students and faculty while savoring the life of a local Ithacan. After finishing his degree, Casey and his wife, Erin, returned to their adopted home of Utah to begin his career with the U.S. Geological Survey.

For those that have tolerated me

ACKNOWLEDGMENTS

I have been the beneficiary of serendipity on more than one occasion, and my opportunity to come to Cornell University is no exception.

To my advisor, Dr. Terry Jordan, I am enormously thankful for the chance to study under her guidance and support. Since coming to Cornell, Terry has given me the opportunity to follow my nose with this research project while giving me the freedom to explore other interests such as my work with the U.S. Geological Survey. From the bottom of my heart, thank you for making this possible.

I'd like to thank my other committee member, Dr. John Thompson, for his guidance. John helped me through several roadblocks along the way and has been an invaluable source of support and knowledge.

Many thanks are due to others that have had a special influence on my academic life including Cornell professors Rick Allmendinger, Toby Ault, Bill White, and Rowena Lohman, all who made my teaching assistant duties a truly pleasurable experience. Thanks to my professors at the University of Utah, particularly to Dr. John Bowman for being a preeminent educator and teaching me what it means to be a good scientist. Thank you to my coworkers at TerraTek, including Dr. Patrick Gathogo and Doug Kolb, who taught and helped me so much, and special thanks to Kyle Tumpane and Ali Shearman for assisting in some analyses for this project.

Acknowledgment and thanks to Maura Weathers, Phil Carubia, Mick Thomas, and Don Werder for their training and patience on various lab equipment, as this work made use of the Cornell Center for Materials Research Shared Facilities which are supported through the NSF MRSEC program (DMR-1719875). Thanks to the AAPG Grants-in-Aid Foundation for their financial contribution through the Raymond C. Moore and Kenneth O. Stanley Memorial Grants. Thanks to: Brian Slater and Chuck Ver Straeten (New York State Museum); John Neubaum, Kristen Hand, and Stephen Shank (Pennsylvania Department of Conservation and Natural Resources); Phil Dinterman (West Virginia Geological and Economic Survey); Jaime Toro, Shikha Sharma, Tim Carr, and Greg Hammond (Department of Geology and Geography at West Virginia University); and Dustin Crandall (National Energy Technology Laboratory). Thanks to Chris Sherry and ASD Inc., a PANalytical company for lending a TerraSpec 4 and their continued guidance in the instrument's application, and to Ann Thompson for her expertise and advise in using the spectroscope. Thanks to Dick Lindemann of Skidmore College for his insights on Marcellus paleontology.

This experience would not have been nearly as much fun without the support of many friends. Thank you to my fellow graduate students – it was such an honor to get to know all of you and be a part of your life. Thank you to my predecessor, John Mason, whose big shoes inspired me to keep pushing this project. Special thanks to Chris Siron who showed me Ithaca's best watering holes and was always kind enough to run at my pace. Many thanks to Arna Pálsdóttir, Andres Aguirre, Kyle Murray, Paula Burgi, Laura Sinclair, Kevin Reath, Reed Huegerich, Paul Morgan, Katie Grant, and all of those that filled in to entertain my weekly pub trivia fix and lead Team 6th Place to legendary status. Thanks to those that participated in three amazing Friendsgiving celebrations. Thanks to D.K. Kim, Diego Quiros, Lauren McLeod, Irene del Real, and Jood Al Aswad, who all suffered sharing office space with me. Thanks to Jack Galian for his unwavering optimism.

I would like to offer special thanks to Dr. Frank Brown, Mike Getty, and Thom Horgos who, although no longer with us, continue to inspire me every day.

To my family, thank you for always being supportive. To my mom, for your dedication to your children that will never be wholly appreciated. To my big sister, for always going first and showing me the way. To my baby sister, for making me want to be better tomorrow than I am today. To my dad, for showing me it is okay to do things my way. To my grandparents, who each left on me their own indelible impression. To my brother-in-law, for reminding me never to blow it. To my in-laws, for their eagerness to help whenever possible.

To Erin, thank you for your relentless love and support in every walk of life.

TABLE OF CONTENTS

CHAPTER ONE : INTRODUCTION

This study aims to better constrain the post-depositional, or diagenetic, changes in the Cherry Valley Member carbonate and its equivalents of the Middle Devonian Marcellus subgroup in the Appalachian Basin of New York, Pennsylvania and West Virginia. A first objective is to determine the relationships between depositional conditions and burial diagenesis. Thereafter, the objective is to describe the successive diagenetic stages and their relationship to the broad scale burial and exhumation history of the basin. The development of diagenetic models is important to better understand how mudstones evolve and can be a tool for prediction of the properties of an unconventional hydrocarbon reservoir.

Though the Marcellus subgroup is one of the most studied units in the United States due to its economic potential, little work has been done to document the changes in lithology, composition, and texture from one portion of the basin to another as a function of diagenesis. The evolution of diagenesis has largely been studied within discrete zones of the basin, identifying compositional trends without specifying the diagenetic stage to which any mineral or chemical product corresponds. These carbonates provide a unique opportunity to examine diagenetic changes to a basin-wide, contemporaneous unit that was subjected after deposition to a range of burial regimes during the Late Paleozoic Alleghanian orogeny.

STUDY AREA

The study materials (Fig. 1.1) for this project consist of cored rock taken from eight wells in the states of West Virginia (3), Pennsylvania (2), and New York (3). These well locations were selected for their linear relationship that is parallel to the Appalachian orogenic axis. These well locations demonstrate similar trends in diagenetic evolution in the Cherry Valley carbonates of the Marcellus "shale" along strike of the basin. Well information for each core is included in Table 1.

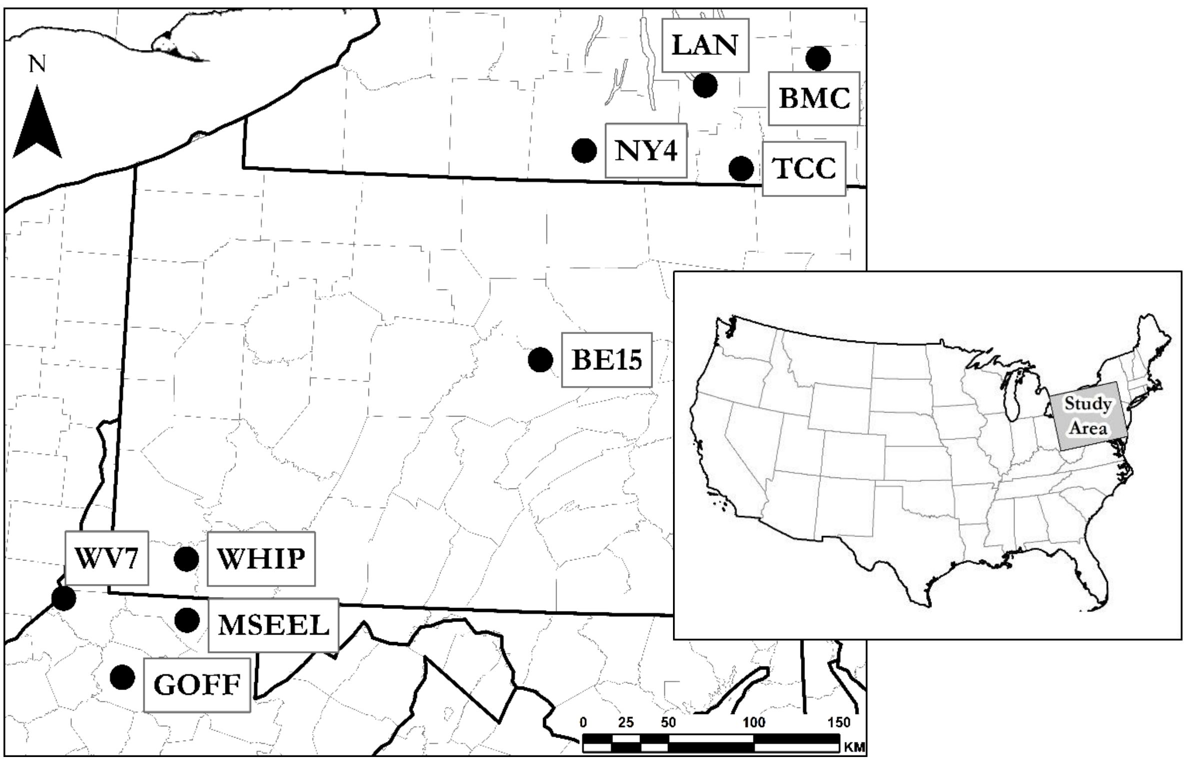

Figure 1.1: Study area map of the eastern United States. Black dots and well identification labels indicate the location of core material used in this study. See Table 1.1 for more information on each well.

Table 1.1: Well information for studied Marcellus core material. See corresponding study area map (Fig. 1.1) for well locations.

Well Name	ID	County	State	API	Latitude	Longitude
Nathan Goff #55	GOFF	Harrison	WV	4703305106	39.281369 N	80.392692 W
MIP 3H / MSEEL	MSEEL	Monongalia	WV	4706101707	39.601749 N	79.976171 W
EGSP WV-7	WV7	Wetzel	WV	4710300645	39.678200 N	80.823700 W
St. Whipkey #1	WHIP	Greene	PA	3705924715	39.923565 N	80.003158 W
Bald Eagle 2015	BE15	Centre	PA	CEN027-0384	41.053550 N	77.619509 W
Strong #1	TCC	Tioga	NY	31107264660000	42.085672 N	76.239269 W
EGSP NY-4 / Valley Vista View 1	NY4	Steuben	NY	31101152680000	42.163710 N	77.353910 W
Cargill Core Test	LAN	Tompkins	NY	31109131730000	42.523030 N	76.504860 W
Beaver Meadow 1	BMC	Chenango	NY	31017230060000	42.672370 N	75.699630 W

GEOLOGICAL BACKGROUND

Geological History

The Appalachian Basin functioned as a foreland basin during deposition of the Marcellus “shale” in response to the Alleghanian orogen (Fig. 1.2). As early diagenesis advanced, the position of the proximal basin margin and adjacent thrust belt became progressively closer to the strata through time. The Appalachian Basin is a thick and elongate stack of sedimentary rocks (Sak et al., 2012). The basin subsided on continental crust and between the orogenic highlands and the adjacent craton during the Paleozoic.

Biostratigraphy and radiometric dating demonstrate changes in tectonic activity during the Paleozoic. Direct analyses of depositional timing include U-Pb zircon ages of volcanic ashes (Tucker et al., 1998). These radiometric dates, in conjunction with conodont biostratigraphy, have enabled studies to constrain precise time periods (± 1.0-2.0 m.y.) within the Devonian during deposition of the Marcellus sediments.

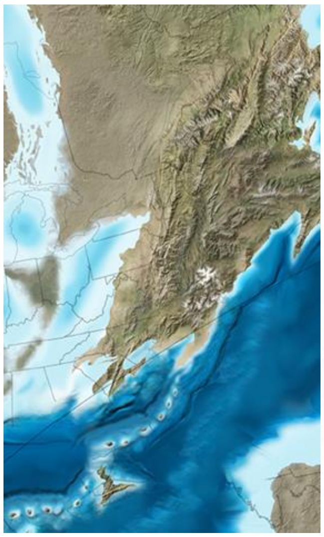

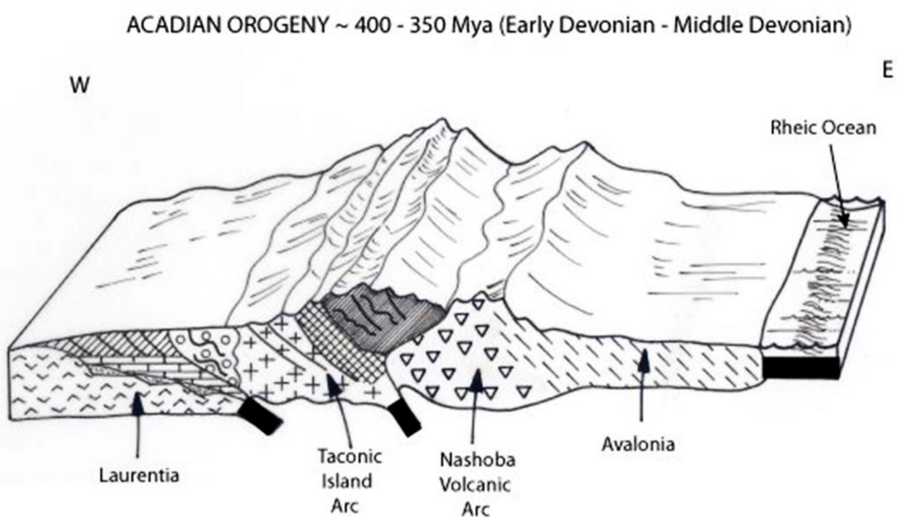

Figure 1.2: Paleogeographic map of the Appalachian orogen during the Middle Devonian (left, Blakey, 2016, ©2013 Colorado Plateau Geosystems Inc, licensed to Teresa E. Jordan) with corresponding tectonic-scale cross-sections that depict the general orogenic processes involved with Appalachian Basin formation (right, Coleman, 2005).

Chronostratigraphic data show the rate of burial beneath Pennsylvanian-age strata were approximately 100 m/m.y. in West Virginia (Reed et al., 2005). The maximum depth of burial of the Devonian strata is variable along strike of the basin axis, and quite uncertain. Estimates from various studies range to 3-4 km in western New York (Heitzler and Harrison, 1998), 3.4 km in central and northeastern Pennsylvania (Roden and Miller, 1989) 3-4 km in the Catskill region of New York and 2-3 km for western New York (Miller and Duddy, 1989), 3.1 km in Maryland, West Virginia, and Virginia (Roden, 1991) and greater than 4.5 km in central Pennsylvania (Lash and Engelder, 2005).

Exhumation is tracked using thermochronological studies, including apatite fission-track ages on detrital grains from various portions of the Appalachian Basin. These illuminate the timing of unroofing after the Alleghanian Orogeny (Blackmer et al., 1994; Roden and Miller, 1989; Roden, 1991; Roden-Tice et al., 2000). Early exhumation rates were approximately 10 m/m.y. from the late Permian until the early Cretaceous, and thereafter accelerated to 30-50 m/m.y. through the late Cretaceous. Since then, exhumation slowed to approximately 20-25 m/m.y. and has remained constant through present day (Reed et al., 2005). The cessation of Alleghanian loading was followed by rifting in the North Atlantic during the late Triassic or early Jurassic (Pitman and Talwani, 1972) which may have influenced the exhumation rates (Reed et al., 2015).

Stratigraphic Overview

Deposition in the Appalachian Basin took place throughout the Paleozoic in shallow subtropical seas as the North American craton was then located south of the equator. Global sea level shows a gradual rise through the Cambrian, reaching a maximum in the Ordovician, withdrawing through the Silurian, and into its minimums during the Devonian (Haq and Schutter, 2008). Widespread and persistent deposition of siliciclastics in the foredeep are characteristic of the Middle Devonian, including the Marcellus "shale", and throughout Lower Mississippian strata (Harper and Patchen, 1996). Foredeep deposits account for more than 10 km of present-day deposition in thickest portions of the basin (Fig. 1.3). As relative sea level regressed, turbidite-slope to delta-front deposits sediments were deposited. Other foreland basin components, including the forebulge and back-bulge basins, are still intact in the distal portions of the foreland basin. Lower to Middle Devonian strata mark the forebulge position via the distribution of unconformities and shallow marine or reef carbonates that formed during retrograde migration of this elongate, orogen-parallel area of positive relief (Lash and Engelder, 2000; Ver Straeten and Brett, 2000). In contrast with foredeep deposits, the forebulge and backbulge zones are vertically minor, on the order of 20-50 m in positive relief (Ver Straeten and Brett, 2000).

As subsidence ceased during the Lower Permian, erosion removed much of those youngest strata from the Appalachian Basin (Ryder et al., 2012), particularly in the northern portions of the basin where Pennsylvanian and Permian units are largely absent. Despite this, basin strata presently extend to nearly 10 km depth despite having over 250 million years of subaerial exposure.

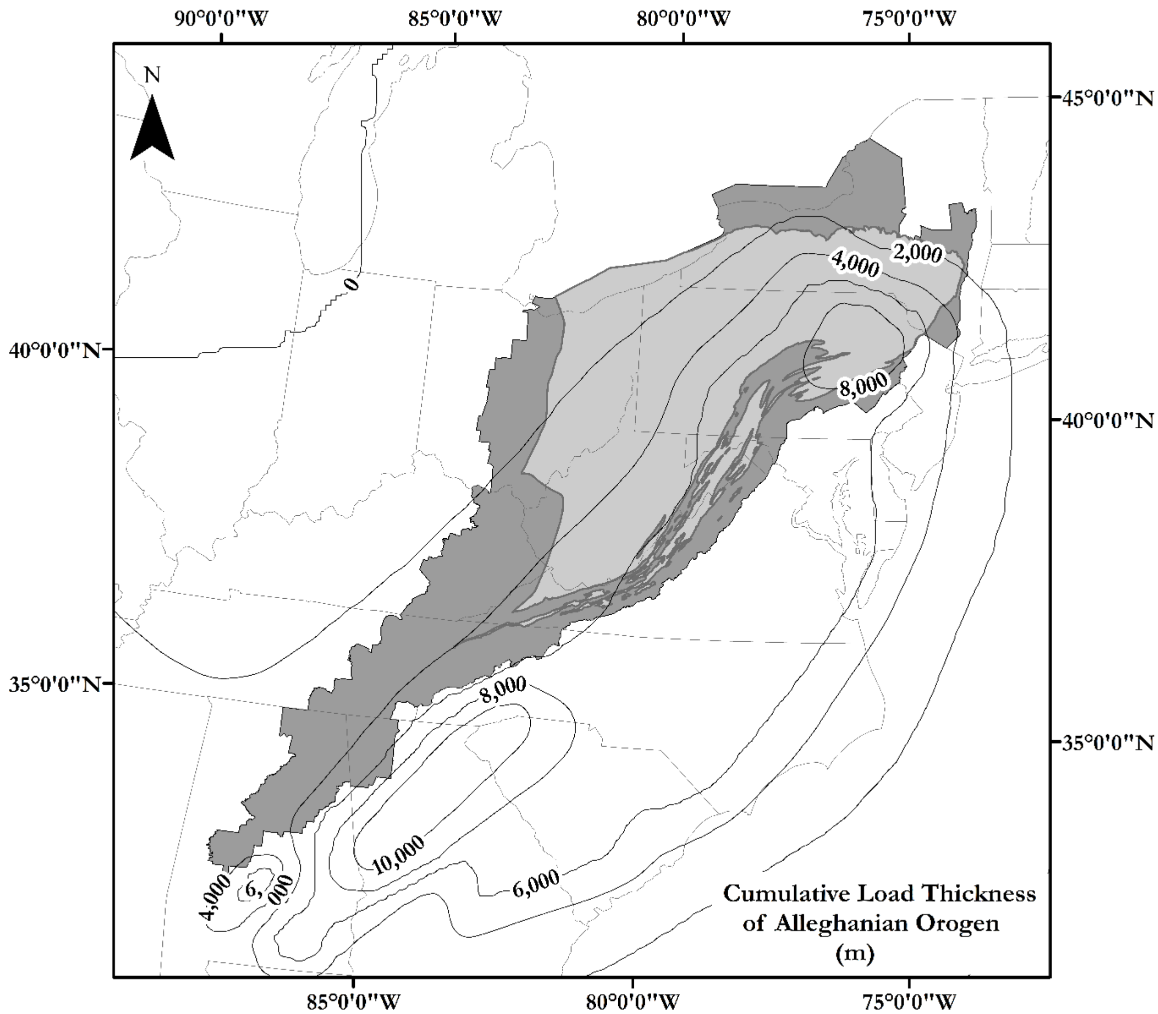

Figure 1.3: Isopach map of the cumulative load thickness of Alleghanian crustal loading. Dark grey marks the extent of Appalachian Basin deposits; light grey marks the extent of Marcellus deposition. See Table 1.1 for more information on each well.

Middle Devonian strata, namely the Eifelian to Givetian-aged Hamilton Group deposits, of the Appalachian Basin accumulated in the elongate foreland basin and are typically considered part of the Catskill delta succession. Using New York-based stratigraphic nomenclature, the Hamilton Group includes the Marcellus subgroup which comprises the Union Springs and Oatka Creek Formations. Regionally, the Hamilton Group is underlain by the Onondaga Formation (lower Eifelian) and overlain by the Tully Limestone (upper Givetian). Though stratigraphic nomenclature differs by state (Fig. 1.4), the Marcellus subgroup/Formation comprises upper (Oatka Creek Formation/Shale) and lower mudstone units (Union Springs Formation/Shale) that are generally separated by the Cherry Valley carbonates (Fig. 1.5). In New York, the base of the Oatka Creek Formation is defined by the Hurley Member, if present, or more commonly the base of the Cherry Valley Member. Across the basin, the Cherry Valley carbonates are thinner than 4.0 meters (Fig. 1.6) and are characterized by dacryoconarid- and goniatite-rich wacke/packstones with nodular, interbedded, organic-rich mudstones. In eastern areas, where deposition was more proximal to the Catskill delta, the Cherry Valley carbonates may include considerable siliciclastic components and, locally, is a grain-supported sandstone. As the organic-rich mudstones of the Marcellus "shale" are economically important, well log data of the Cherry Valley carbonates is readily available and is easily discerned from the mudstones as a low-gamma zone (Fig. 1.7).

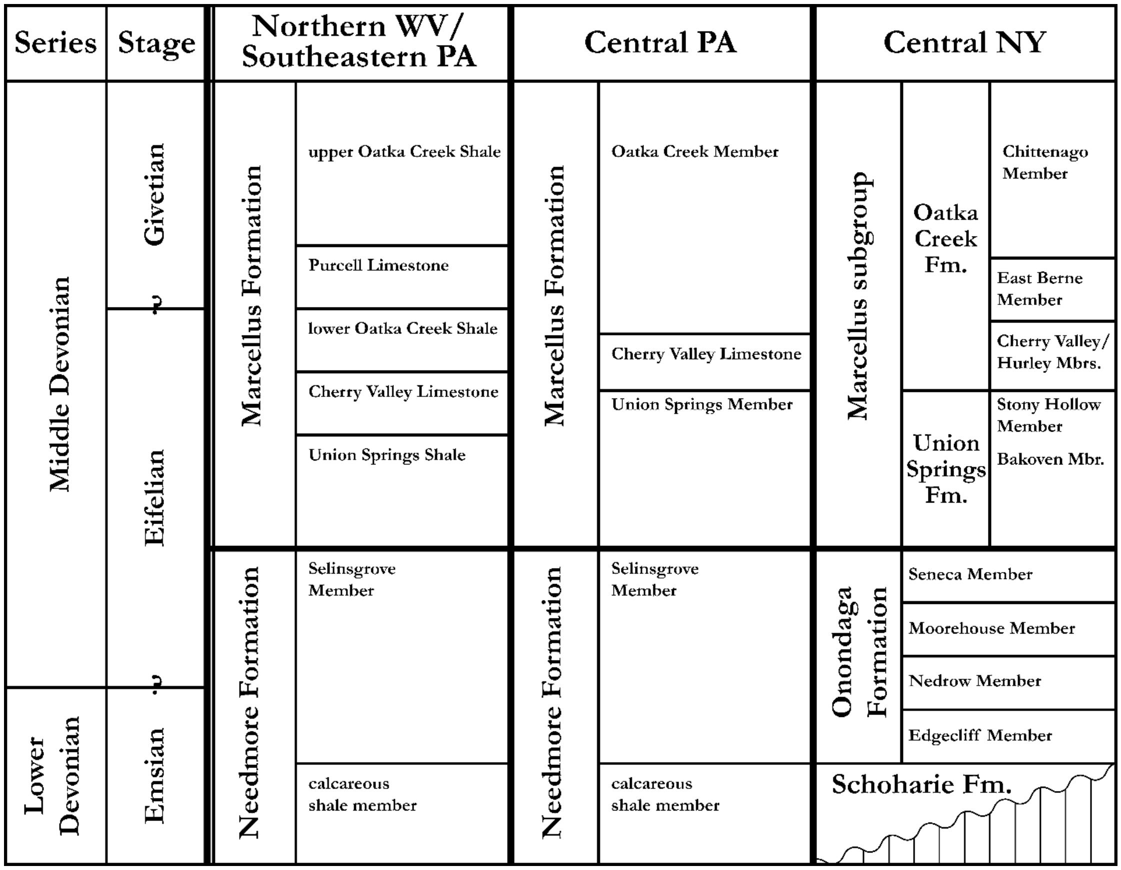

Figure 1.4: Stratigraphic synthesis of Lower Devonian (Emsian) to Middle Devonian (Eifelian to Givetian) siliciclastic and carbonate units in the Appalachian Basin. The location-specific summaries are organized parallel to the axis of the basin, from northern West Virginia/southeastern Pennsylvania (modified from Chen, 2016) to central Pennsylvania (modified from Lash and Engelder, 2011) to central New York (modified from Ver Straeten, 2011). The studied core material is representative of these stratigraphic units in these three areas.

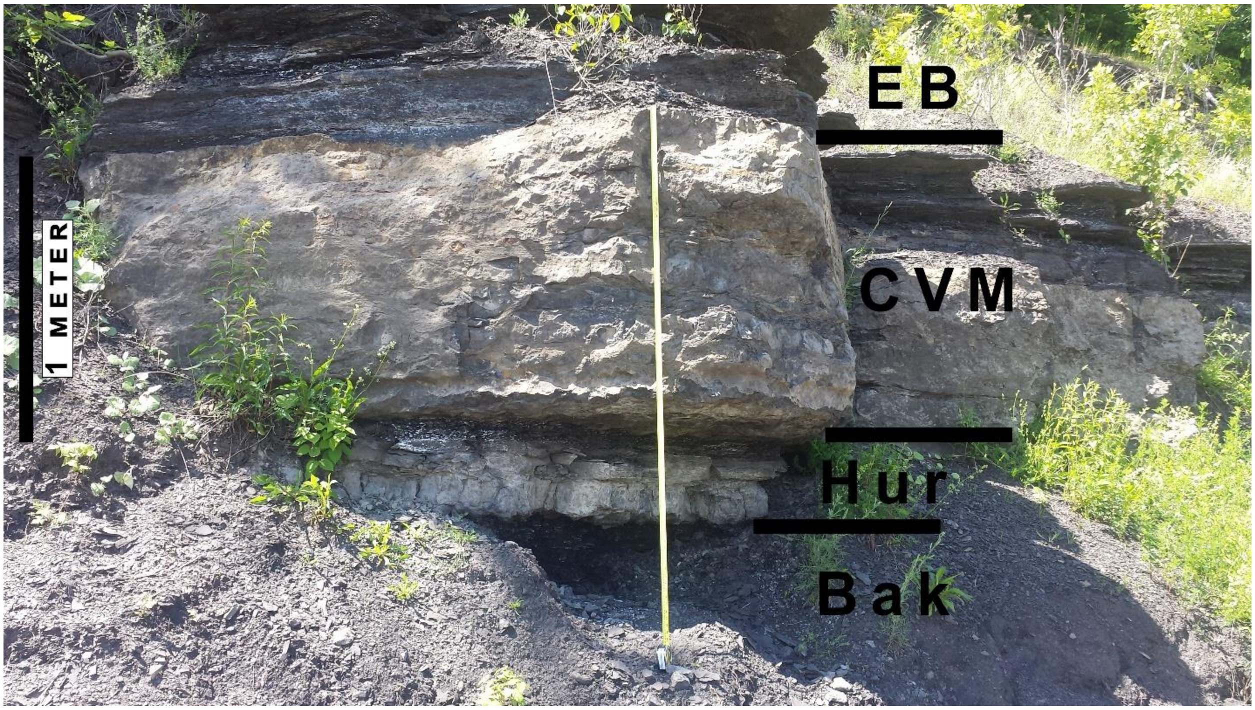

Figure 1.5: Photograph of the Cherry Valley Member outcrop at Chestnut Street, Cherry Valley, New York, showing the representative sequence from the Union Springs Formation (Bakoven Member) into the Oatka Creek Formation (Hurley Member and overlying named members). EB = East Berne Member; CVM = Cherry Valley Member; Hur = Hurley Member; Bak = Bakoven Member.

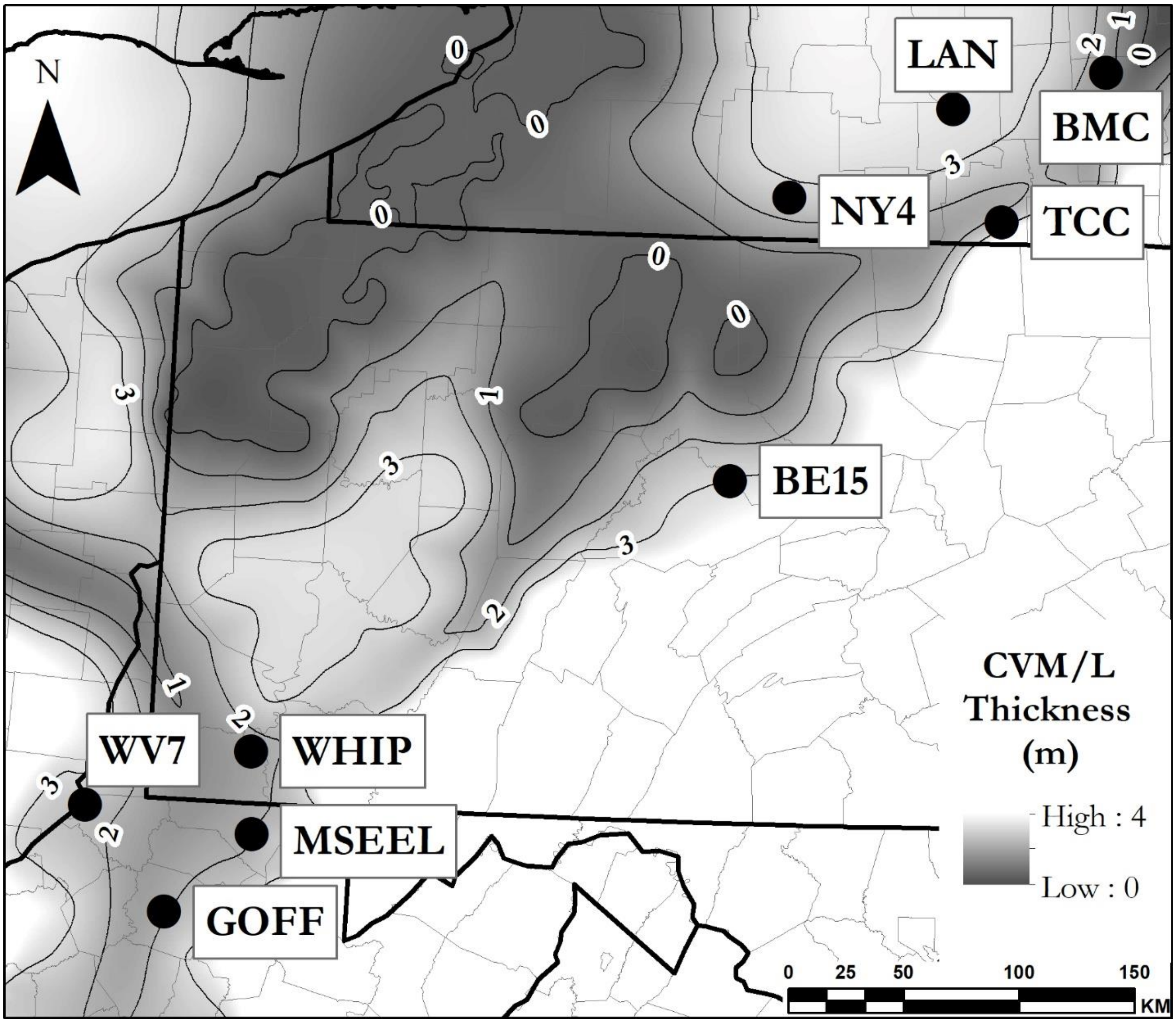

Figure 1.6: Generalized and interpolated isochore map of the Cherry Valley carbonates based on previous studies and well log data (Lash and Engelder, 2011).

.

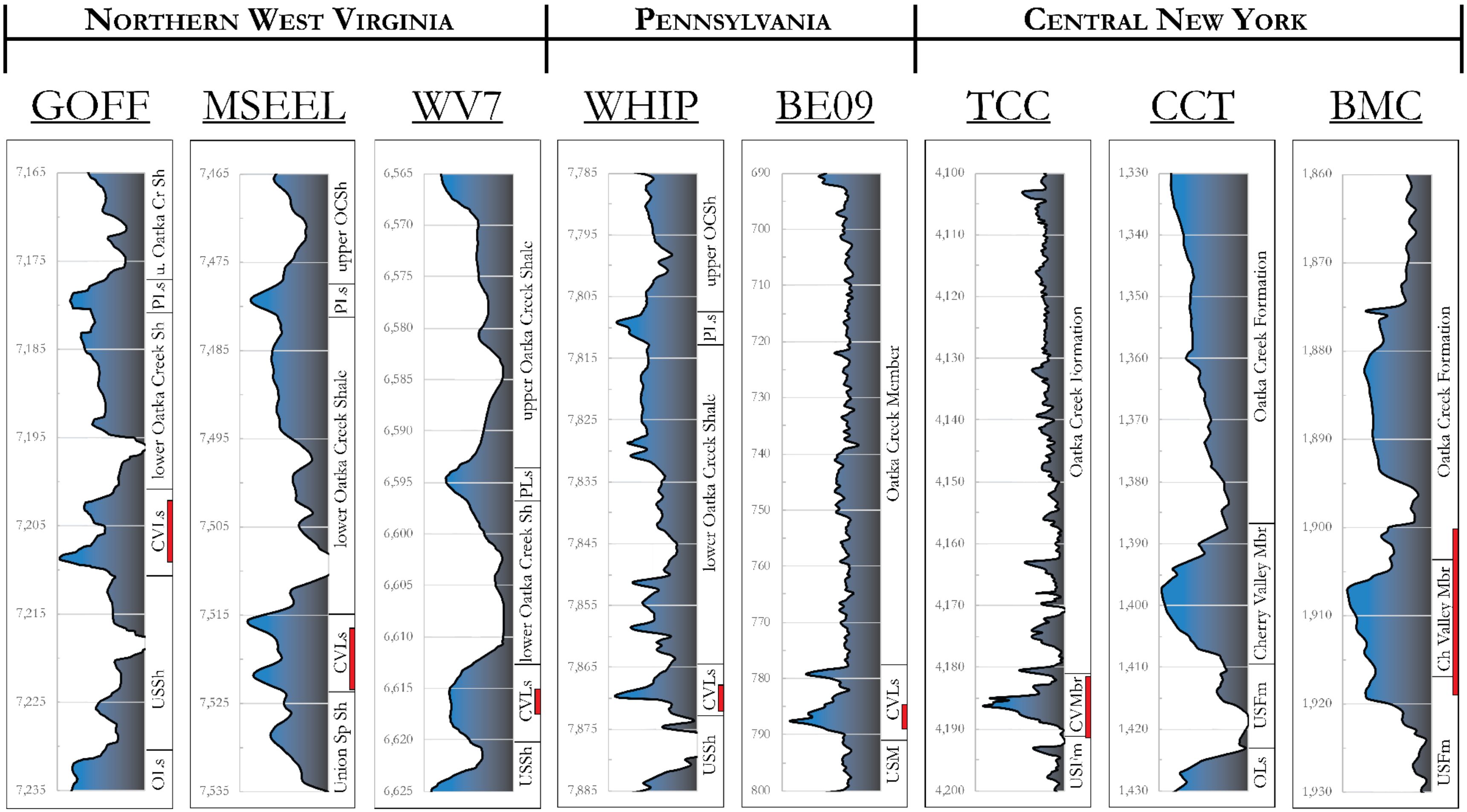

Figure 1.7: Gamma logs from select cores used in this study, exaggerated to highlight the low gamma response in the thin carbonates of the Marcellus subgroup. Stratigraphy reflects the naming conventions from each respective state. Note: no wireline measurements were taken for BE15, though logs do exist for a sister well that was drilled approximately one mile away in 2009 (BE09). Red bars adjacent to stratigraphic names denotes sampled interval in available cores (BE09 is inferred from core comparisons with BE15). CVL is Cherry Valley Limestone; USSh is Union Springs shale; OLs is Onondaga Limestone; Pls is Purcell Limestone, and OCSh is Oatka Creek shale.

Thermal and Geochemical Summary

Various studies and models have been developed to discern the burial and thermal conditions of Devonian strata in the Appalachian Basin (Beaumont et al., 1987; Heizler and Harrison, 1998; Miller and Duddy, 1989; Roden and Miller, 1989; Roden, 1991; Quinlan and Beaumont, 1984). Maximum burial of Paleozoic strata of the Appalachian Basin occurred between 300-250 Ma, or concurrent with Alleghanian tectonism (Heizler and Harrison, 1998; Reed et al., 2005). The thermal maximum (275-300 °C) of crystalline basement was reached at approximately 300 Ma, near the beginning of the Permian, as terranes obducted within the Appalachian and Ouachita orogens, which thickened the crust (Beaumont et al., 1987; Heizler and Harrison, 1998). This period was followed by unroofing and consequent cooling during the Mesozoic. Estimates for thermal conditions within the Marcellus "shale" vary. Lower Devonian to Upper Pennsylvanian strata in northeast Pennsylvania and southeastern New York cooled from greater than 110 °C during the early post-Alleghanian period (Roden and Miller, 1989). In western New York, Upper Devonian rocks cooled from lower temperatures (80-110 °C) (Miller and Duddy, 1989). Reed et al. (2005) finds a range of of 132-171 °C in Pennsylvanian strata in West Virginia, and the Marcellus is approximately 460 m below. Assuming the same geothermal gradient (30 °C/km), the paleomaximum temperature in the Marcellus ranges between 146-185 °C.

Exposure to these burial temperatures thermally matured the organic material within the black shales of the Marcellus, resulting in liquid- and gas-prone source rocks across the basin. Geochemical indicators of thermal maturity, including as conodont alteration index (CAI) and vitrinite reflectance (R_o)(Repetski et al., 2008), in addition to apatite-fission track analyses (Miller and Duddy, 1989; Roden and Miller, 1989; Roden-Tice et al., 2000) illuminate the thermal history of Devonian rocks in the Appalachian Basin. Interpolated models of CAI and R_o (Fig. 1.8) from published data of selected Marcellus production wells suggest the studied cores represented a range of thermal environments (CAI: 2.0 - 4.0; R_o: 1.0 - 2.0). Though the accuracy of these thermal proxies is limited, they are an industry standard that can provide generalized spatial regimes of burial conditions.

Organic matter of the Marcellus subgroup was deposited in anoxic, possibly euxinic, conditions that were intermittently interrupted by episodes of dysoxia during deposition in the Acadian foreland basin (Lash and Blood, 2014). Though many studies have been conducted to define a precise understanding of how organic material matured, they universally result in a regional pattern in which thermal maturity increases with decreasing distance the Appalachian front. Natural gas in central to northeastern Pennsylvania is typically postmature (dry gas) and may decrease to early-mature (late wet gas) along the northwest flank of the Appalachian Basin (Laughrey and Baldassare, 1998; Milliken et al., 2013). Basin-wide fracturing may have occurred as a consequence of abnormal fluid pressures generated during thermal maturation of kerogen to hydrocarbons, causing natural hydraulic joints when maximum burial was reached

(Engelder et al., 2009; Lash and Engelder, 2009). These joints sets, commonly referred to as the J1 (north-northeast striking) and J2 (northwest striking) joints, are one hypothesis as to why the Devonian shales of the Appalachian Basin are such an economic boon, as these fractures heavily increase transmission and connectivity to natural gas production wells.

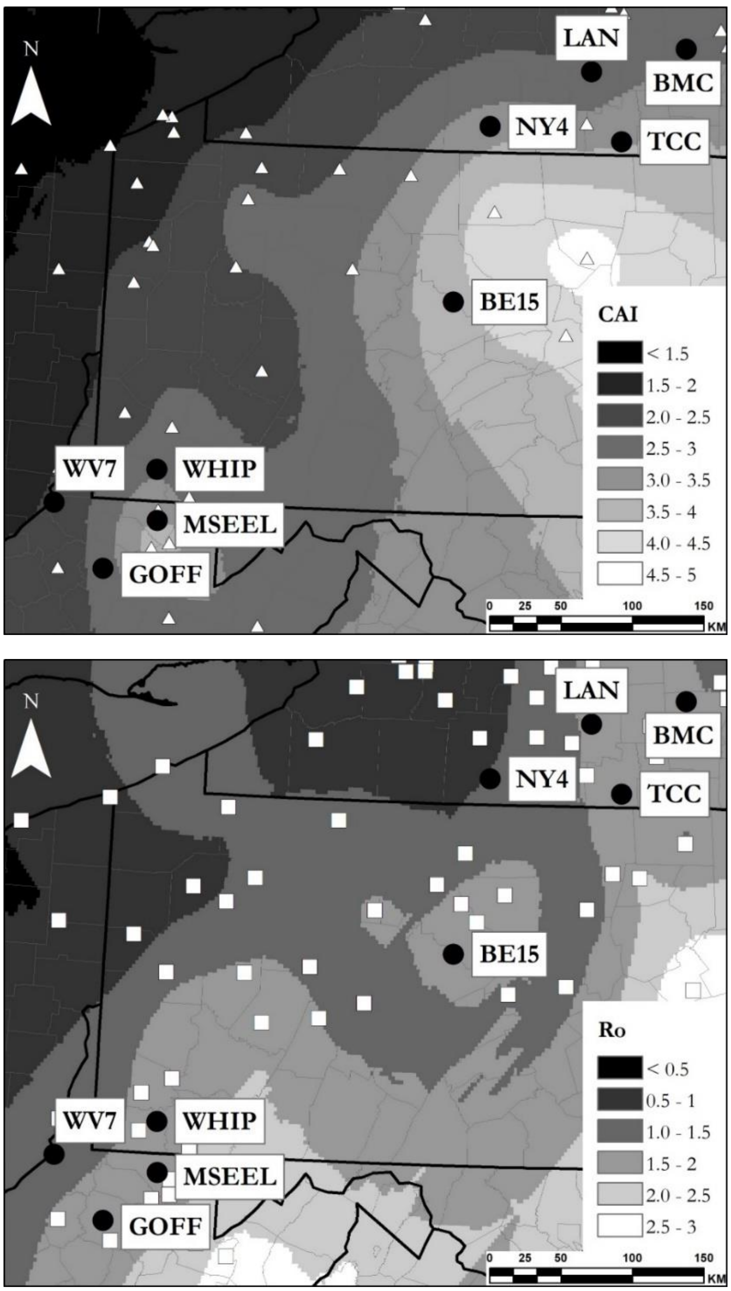

Figure 1.8: Maps of thermal maturity of the Marcellus organic-rich mudstones, including conodont alteration index (CAI - top) and vitrinite reflectance (R_o - bottom), from public data of selected Marcellus production wells. Each prediction map used ordinary kriging with a spherical model on ArcGIS 10.4. The CAI is an estimation of maximum temperature that was reached based on the approximate color of the apatite in conodonts (CAI of 0-1 is less than 80°C; 1-2 = 60-140°C; 2-3 = 110-200°C; 3-4 = 190-300°C; 4-5 = greater than 300°C), and the interpolation was performed using 80 wells (white triangles) from Repetski et al. (2008). R_o is a normalized measure of incident light that is reflected off the surface of particles of vitrinite, and 135 wells (white squares) were used for this interpolation (from Repetski et al. 2008).

PURPOSE

The evolution of diagenesis has largely been studied within discrete zones of the basin (Lash and Blood, 2014; Laughrey and Baldassare, 1998; Milliken et al., 2013; Pommer, 2013; Wang et al., 2015). These studies have developed spatial relationships between Devonian shales and the Appalachian orogenic axis. Milliken et al. (2013) and Laughrey and Baldassare (1998), for instance, find the degree of organic maturity increases as distance from the Appalachian orogenic axis decreases. Lash and Blood (2014) determined the diagenetic history of the Marcellus subgroup includes several horizons of authigenic calcium carbonate concretions and distinct barium enrichment that reflect the effects of non-steady-state microbial diagenesis within a methane-rich environment. Wang (2014) produced a thesis on the origin of the Cherry Valley Limestone in central Pennsylvania and identified the primary facies observed as well as addressing some of the depositional conditions that resulted in the formation of authigenic nodules.

However, key questions about the controls on diagenesis would be better addressed by examining depositionally similar rocks across a spatial gradient of burial conditions. This strategy is applied to the Cherry Valley carbonates, which share depositional characteristics across a majority of the basin, yet after deposition they were exposed to a variety of burial conditions. This unit therefore provides a unique opportunity to observe how varying pressure, temperature, and fluid interactions at interfaces between strata with distinct lithologic and petrophysical properties have controlled diagenesis of interbedded organic-rich, clay-rich or calcareous mudstones and limestones. Better understanding of the diagenetic outcomes, such as cement precipitation and dissolution, within mixed carbonate systems may provide insight into the evolution of the Appalachian Basin rocks. This study will show how varying post-depositional conditions alter the principal compositional and textural features in interbedded carbonates and organic-rich mudstones.

CHAPTER TWO : METHODS

Analyses ranging from visual petrographic analysis to chemical and isotopic analyses were performed for 87 samples acquired for eight cores from West Virginia, Pennsylvania, and New York, representing the East Berne and Cherry Valley Members of the Oatka Creek Formation and the Bakoven Member of the Union Springs Formation (or equivalents). The Strong #1 well (TCC – Tioga County, NY) acted as the pilot well in this study and was continuously sampled throughout the Cherry Valley Member as well as the immediately adjacent mudstones above and below. Sample selections for all other cores were chosen based on core description and composition (short-wave infrared spectroscopy or existing datasets). Oil and gas well logs and data, made available through the state-run databases (New York State ESOGIS, Pennsylvania EDWIN, West Virginia PIPELINE), were used to find appropriate core that included the Cherry Valley Member. Cores were selected based on location, availability, and condition, as many wells did not core the Cherry Valley Member interval or had been sampled out during previous studies.

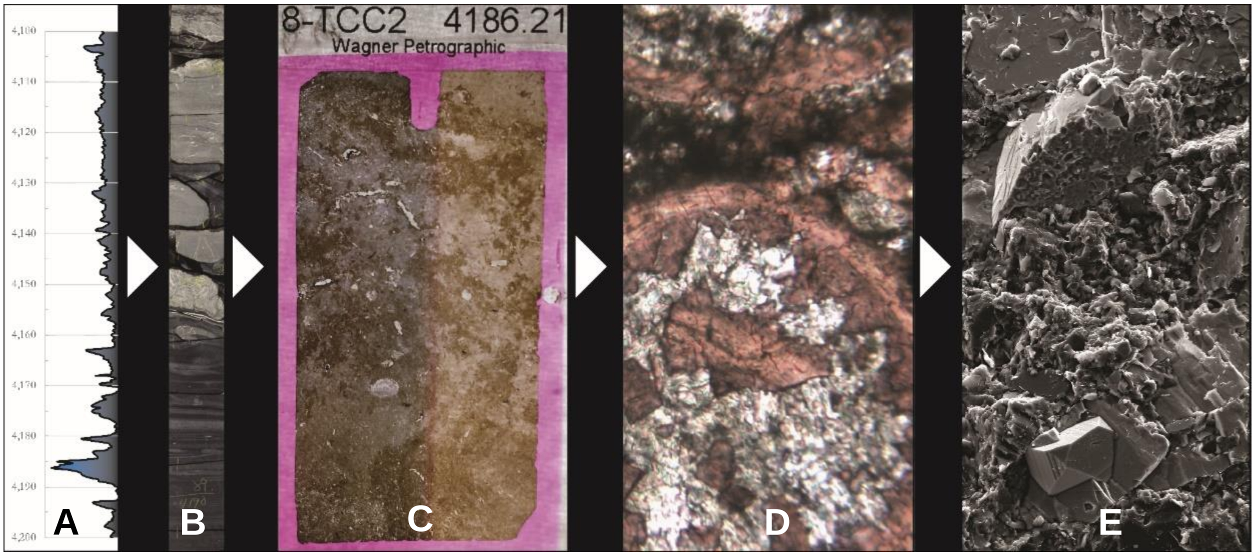

Figure 2.1: Outline of the scaled workflow (from left to right), starting with (A) confirming the presence of the Cherry Valley Member in borehole logs (kilometer- to meter-scale), (B) visual inspection and description of core material (meter-scale), (C) sample selection and preparation for analysis (centimeter-scale), (D) thin-section petrography (millimeter-scale), and (E) electron microscopy (micron-scale). Each component reinforces the next and ensures reliable upscaling of petrologic details.

REFLECTANCE SPECTROSCOPY

Shortwave near-infrared reflectance spectroscopy (SWIR) is used on core to detect compositional changes among horizons and to narrow sample selection. The instrument measures the optical energy that is reflected by, absorbed into, or transmitted through a sample. Optical energy refers to a wavelength range that is greater than the visible wavelengths, and is often called electromagnetic radiation or optical radiation (ASD Inc., a PANalytical Company, 2015). This spectrum is generally characteristic of a singular mineral. In carbonates, the reflectance spectrum varies based on the cation present, hence the mineralogy of the carbonate can be identified based on the spectrum (Fig. 2.2).

A TerraSpec 4 Standard-Res Mineral Analyzer was used on each of the eight cores. The spectroscope analyzes at the visible near-infrared and shortwave infrared wavelength range between 350 and 2500 nm at a resolution of 3-10 nm and a scanning time of 100 milliseconds.

To collect a spectrum, core is first cleaned and dried to remove drilling mud or other material that may interfere with the analysis. Analyses are spaced approximately 3-4 cm apart (Fig. 2.3), with closer spacing within the Cherry Valley Member and wider in mudstones. A handheld contact probe fitted with a halogen bulb is white-balanced and then held against the surface of the core to collect for approximately 10 seconds before moving down the core to the next location. White balancing must be redone every 10 minutes to ensure consistent results. Mineralogy is matched to spectra using the Spectral Geologist (TSG®) Pro mineral analysis software to determine an on-the-spot, preliminary mineralogy and assist picking suitable horizons to sample for thin section preparation, X-ray diffraction, and scanning electron microscopy. A known error occurred throughout testing where siderite was identified as a dominant mineral by the software. This error is likely the result of poor quality spectra of carbonate minerals in rocks with low reflectance such as mudstones (Halley, 2016). Subsequent petrographic observation confirmed the error by a visual absence of siderite.

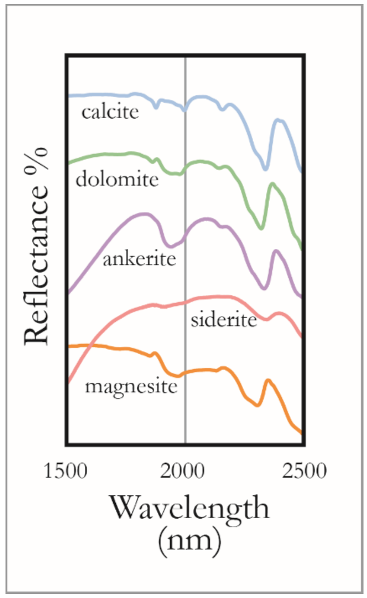

Figure 2.2: Stacked plot of characteristic spectra of carbonate minerals from The Spectral Geologist® Reference Library on a scale of relative percent reflectance. Reflectance values are relative to the individual minerals and represent a qualitative (i.e., pattern matching) identification of mineral phases.

Figure 2.3: The TerraSpec 4 Standard-Res Mineral Analyzer measures direct transmittance as a percent, representing the ratio of the incident light beam that is transmitted by the sample. The spectroscope (top left) is placed on the surface of core material to collect data for approximately ten seconds. The short collection time allows for a closely spaced interval of sampling, for which each is marked by the red and blue stickers.

THIN SECTION PREPARATION AND PETROGRAPHY

Core material was cut for thin sections and prepared by Wagner Petrographic in Lindon, Utah. Billets were mounted to standard glass slides and ground to a thickness of 30 microns. Thin sections are treated with a dual carbonate stain, including Alizarin Red and potassium ferricyanide, to highlight calcite (pink), ferroan calcite (purple), and ferroan dolomite or ankerite (blue). The prepared thin sections are observed under plane-polarized, cross-polarized, and reflected UV light at various magnifications on a Leitz Laborlux 12-POL petrographic microscope fitted with a Leica DFC 400 camera. All thin sections and photomicrographs are oriented normal to bedding.

Lithologic naming is based upon the composition, texture, fossils, organic content, and detrital content of a sample as observed in thin section. Limestone is classified are based on the Dunham (1962) naming classification (Fig. 2.4). Mudstone is classified utilizes the Folk (1974) organization (Fig. 2.5) based on mineralogy, and may be modified by the matrix composition or other rock properties including fossil or visible organic content. For the rocks in this study, the matrix may be argillaceous (clay mineral-rich), calcareous, dolomitic, or a combination of these. Carbonate mudstone is used here as a term based on the Dunham (1962) scheme and implies that the calcite mud (i.e., micrite) is depositional in origin. It is distinguished from the term calcareous mudstone, based on the Folk (1974) classification, which is inclusive of diagenetic calcite, i.e., a calcite cement within an originally clay-rich, or argillaceous, mudstone.

Other distinctions in rock name include compositional ("baritic", "organic", "pyritic", "sideritic") or textural ("microsparitic", "felted", "silty", "fossiliferous") variations.

Carbonate textures are described using terminology from Folk (1965) to relate diagenetic processes such as recrystallization, neomorphism, and replacement (Fig. 2.6). Further textural descriptions of crystalline fabrics are used to describe carbonate cement morphology (Fig. 2.7) or diagenetic textures (Figs. 2.8 and 2.9).

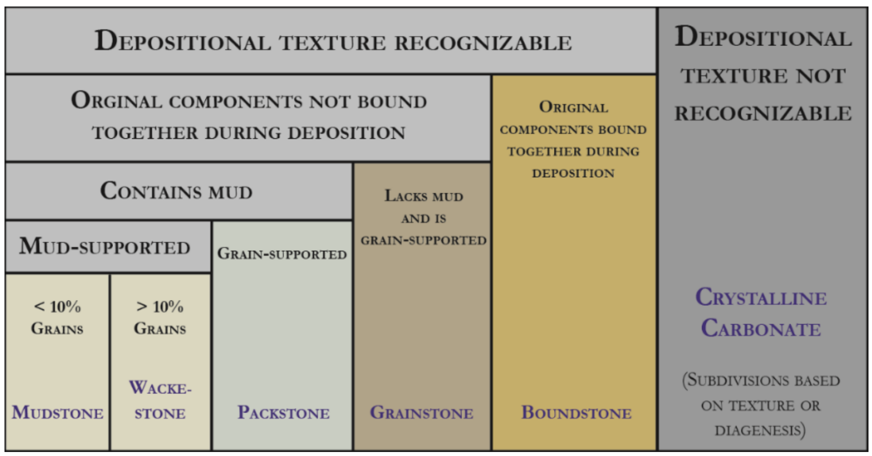

Figure 2.4: The Dunham classification of carbonate rocks (1962) is based on depositional textures with an emphasis on whether the particle structure supported by matrix (micrite mud) or grains (i.e., fossil). Highly altered rocks that have resulted in the destruction of depositional fabrics and textures are considered crystalline carbonates, although relic fossils and framework grains may still be apparent. Dunham's definition of a mudstone has been refined with the mudstone naming classification represented in Figure 2.5.

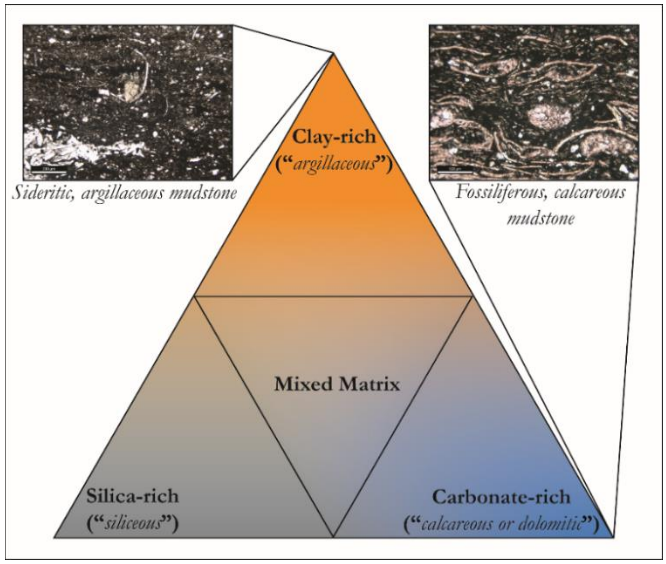

Figure 2.5: Mudstone classification scheme is based on the Folk (1974) definition of a mudrock as a fine-grained rock that is predominantly composed of mud-sized particles, whose composition is either clay or carbonate. Additionally, these rocks are matrix supported, where the matrix is defined as the material composed of crystals or crystallites that are less than 4 microns in diameter, and include diagenetic mineralization or cementation. Compositional end-members within mudstones include clay-rich ("argillaceous"), carbonate-rich ("calcareous or dolomitic"), and silica-rich ("siliceous").

<table>
<tr><th>PROCESS</th><th>EXAMPLE</th><th colspan="4">FOLK TERMINOLOGY</th></tr>
<tr><td>One mineral replaces another of different compositions</td><td>Calcite → dolomite, ankerite, pyrite, etc</td><td colspan="4">REPLACEMENT</td></tr>
<tr><td>Mineral is replaced by its polymorph</td><td>Aragonite feature → calcite mosaic</td><td rowspan="3">Psuedoreplacement</td><td rowspan="2">Recrystal-lization</td><td>Inversion</td><td rowspan="3">NEOMORPHISM</td></tr>
<tr><td>Deformed mineral changes to a mosaic of undeformed crystals</td><td>Strained calcite → unstrained calcite</td><td>Strain Recrystal-lization</td></tr>
<tr><td>Undeformed mineral changes its form, grain size or orientation</td><td>Calcite mud or fiber → calcite mosaic</td><td colspan="2">Recrystallization (and degrading recrystallization)</td></tr>
<tr><td>Mineral dissolves leaving a cavity; cavity is filled later</td><td>Allochem → cavity → calcite cement</td><td colspan="4">Solution-cavity Fill</td></tr>
</table>

Figure 2.6: Terminology of carbonate diagenetic processes and mineral alteration, modified from Folk (1965). Within this study, the terms *recrystallization* and *neomorphism* are synonymous and imply textural change, whereas *replacement* implies that a new mineral replaced the original. Additional modifiers to these terms, such as "aggrading neomorphism", or an increase in grain size, may be applied to further describe textural alteration.

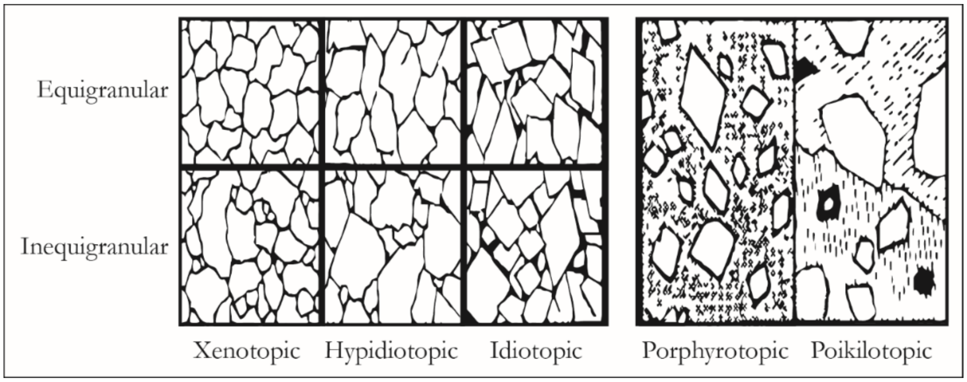

Figure 2.7: From Flügel (2004), end-member crystallization fabrics of carbonates are used to describe the relative size distribution of grains within a rock as well as crystal shape. Additionally, porphyrotopic and poikilotopic fabrics are inherently inequigranular, with a contrast of sizes between grain and matrix. Porphyrotopic fabrics include a fine-grained matrix, such as micrite, that supports other carbonate grains, fossils, or detritus. In contrast, a rock with a poikilotopic fabric recrystallizes the fine-grained matrix to form larger carbonate crystals that enclose smaller components.

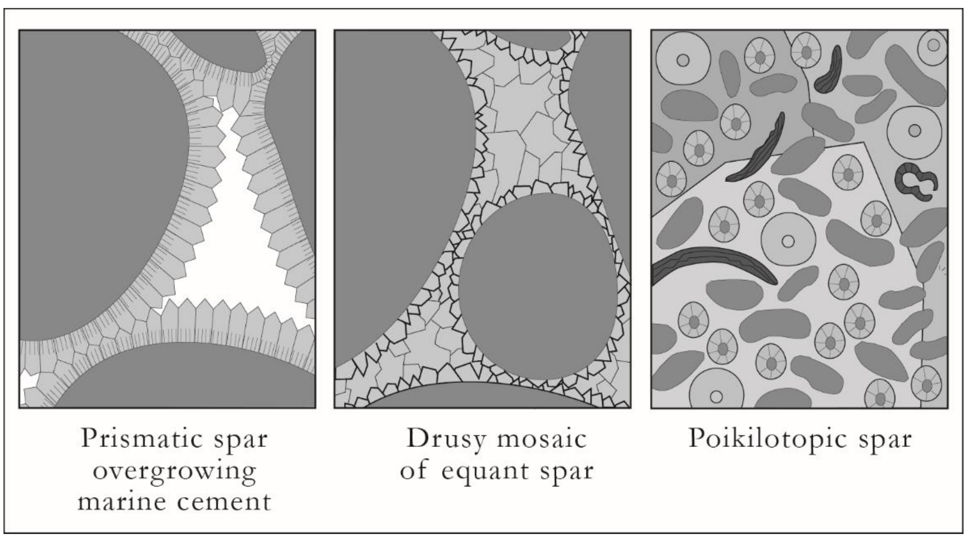

Figure 2.8: Cement textures from Scholle and Ulmer-Scholle (2006) are morphologies present in the burial-stage cements within the Cherry Valley Member carbonates. All three may also result from eogenetic diagenesis. Generally, these diagenetic growths occur in order, with prismatic spar overgrowing marine cement (see Fig. 2.9 for different types) crystallizing first during eogenesis. Drusy mosaic of equant spar subsequently occludes interparticle space or fills empty fossils. Poikilotopic spar is typically associated with deep-burial telogenesis.

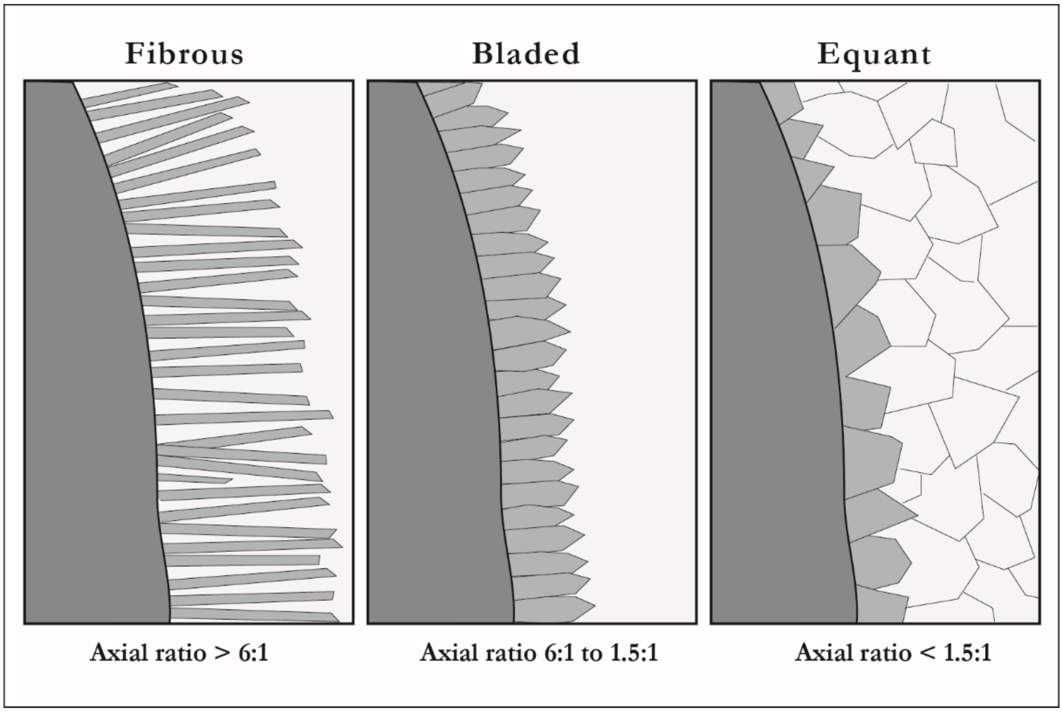

Figure 2.9: From Scholle and Ulmer-Scholle (2006) and Folk (1965), the terminology for carbonate crystal shapes based on the relative length-to-width ratios.

Detailed petrologic observations are intended to describe the relationship between texture and composition as they relate to diagenesis (Appendix I). In thin section, dominant matrix composition is distinguished from accessory minerals. Thin section analysis also is key to establishing the order of growth, dissolution, and replacement of multiple mineral species. Distribution of minerals, which is primarily supported by petrographic observation and aided by compositional analyses, is qualitatively described by determining whether a mineral is depositional or diagenetic. Textural description includes the presence of fractures, detritus, alignment of depositional components such as mica flakes or fossils, and diagenetic mineralization. Images and descriptions are representative of the dominant features of the rock.

In general, the Cherry Valley carbonates lack clay minerals, hence the clay mineral geochemistry is treated by a generalized method. Descriptions of mudstones directly above (East Berne Member of the Oatka Creek Formation) and below (Bakoven Member of the Union Springs Formation) rely on visual petrography. Minor authigenic clays, including kaolinite and chlorite, may be noted in the detailed petrologic descriptions.

X-RAY DIFFRACTION

Leftover core and thin section billets are crushed and disaggregated to a grain size of approximately 4 microns. A Bruker D8 Advance ECO powder diffractor analyzes the sample, mounted on a glass holder, from 18-45° two-theta (2θ) using Cu K-α radiation at 40kV and 25mA with a 0.2 second step time (1,389 total steps and 306.2 seconds total scan time). JADE software identifies mineralogy based on whole pattern fitting. This analysis yields data for the mineral phases that are present in the selected sample, though it does not quantify the proportions of minerals. The Cherry Valley carbonates are dominantly composed of calcite with minor amounts of other carbonates (Fig. 2.10). The spectrum produced by JADE has been transformed using color to indicate peak height so that they may be applied to a vertical scale (Fig. 2.11) Separate samples containing clay-sized particles are not prepared due to the typically negligible amount of clay minerals present in the carbonates-of-interest.

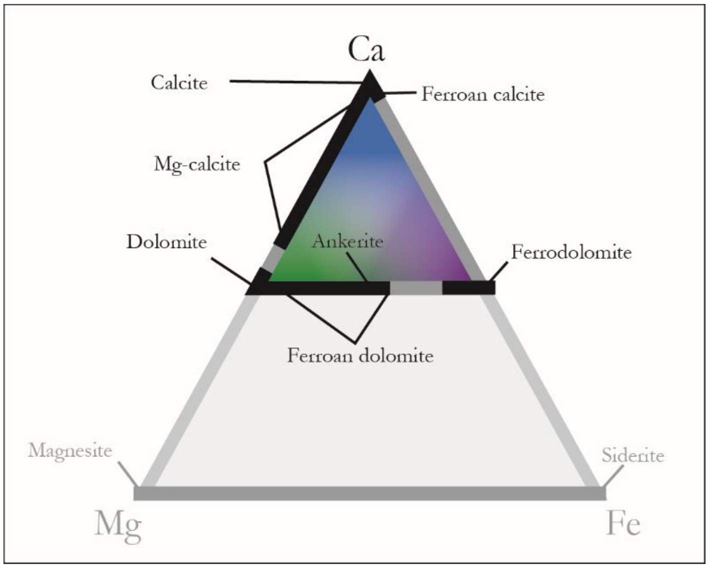

Figure 2.10: Modified from Scholle and Ulmer-Scholle (2006), a ternary plot of carbonate minerals that outline the colloquial terms including “ferroan calcite” or “ferroan dolomite”. Carbonate minerals within the Cherry Valley Member are largely restricted to the upper portion of the plot.

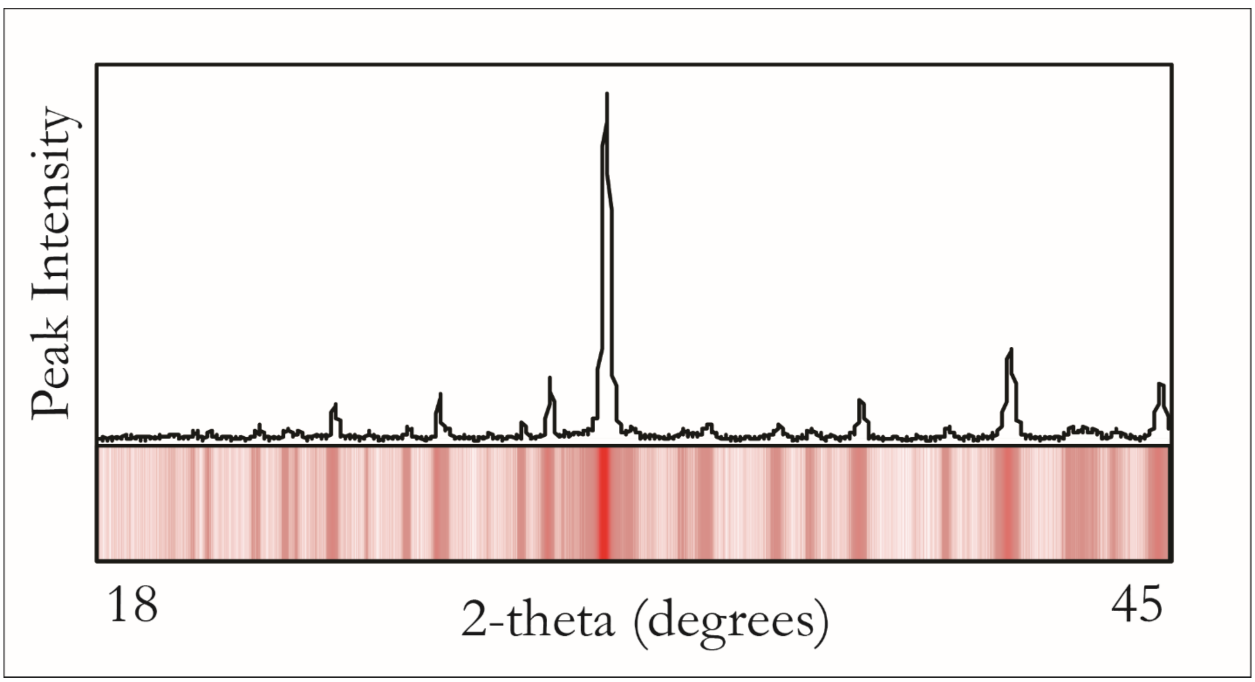

Figure 2.11: X-ray diffraction spectrum of a dolomite in the Strong #1 well. Spectra are converted to one dimensional graphs for log view (see Results). Red portions of these one-dimensional graphs represent peaks with increasing intensity.

SCANNING ELECTRON MICROSCOPY

The leftover thin section billet is broken with a hydraulic splitter across bedding to expose a fresh surface for electron microscopy that can be directly related to petrographic descriptions. The sample, matching the length of its corresponding thin section, is mounted on a standard aluminum SEM pin stub and sputter-coated with a conductive metal such as iridium, platinum/palladium alloy, or palladium/gold alloy. The samples are then imaged in a field emission scanning electron microscope, including a LEO 1550 FE-SEM or FEI Quanta 650 FEG, equipped with an energy dispersive X-ray spectrometer. Samples are viewed primarily with a secondary electron detector, with lesser use of a backscatter electron detector, to describe microtextural and compositional elements.

SEM imaging is used to describe depositional fabric or the arrangement of diagenetic minerals. Microtextural, compositional, distribution and degradation of organic material, and the paragenetic relationships between diagenetic minerals are assessed under SEM observation. Semi-quantitative composition data, as determined by energy dispersive X-ray spectroscopy, complements the morphological data.

STABLE ISOTOPE GEOCHEMISTRY

Stable isotope geochemistry analyses were collected by Dr. Greg Dipple at the University of British Columbia using laser spectroscopy to measure the $^{13}C/^{12}C$ and $^{18}O/^{16}O$ composition of carbonate minerals (Barker et al., 2011). Approximately 20 mg of pure carbonate was required for each analysis. This material was extracted from thin-section billets (Fig. 2.19) with a diamond-tipped drill bit (approximately 3 mm). Due to the disparity in size between drill bit and rock components (micron-scale), heterogeneity in isotopic composition is expected. The carbonate minerals are reacted with phosphoric acid to release CO_2 gas. The isotope compositions of this gas are measured using off-axis integrated cavity output laser spectroscopy. Carbon isotopes are reported in permil relative to VPDB and oxygen isotopes to VSMOW. The oxygen isotopes have been converted to VPDB for the entirety of this thesis.

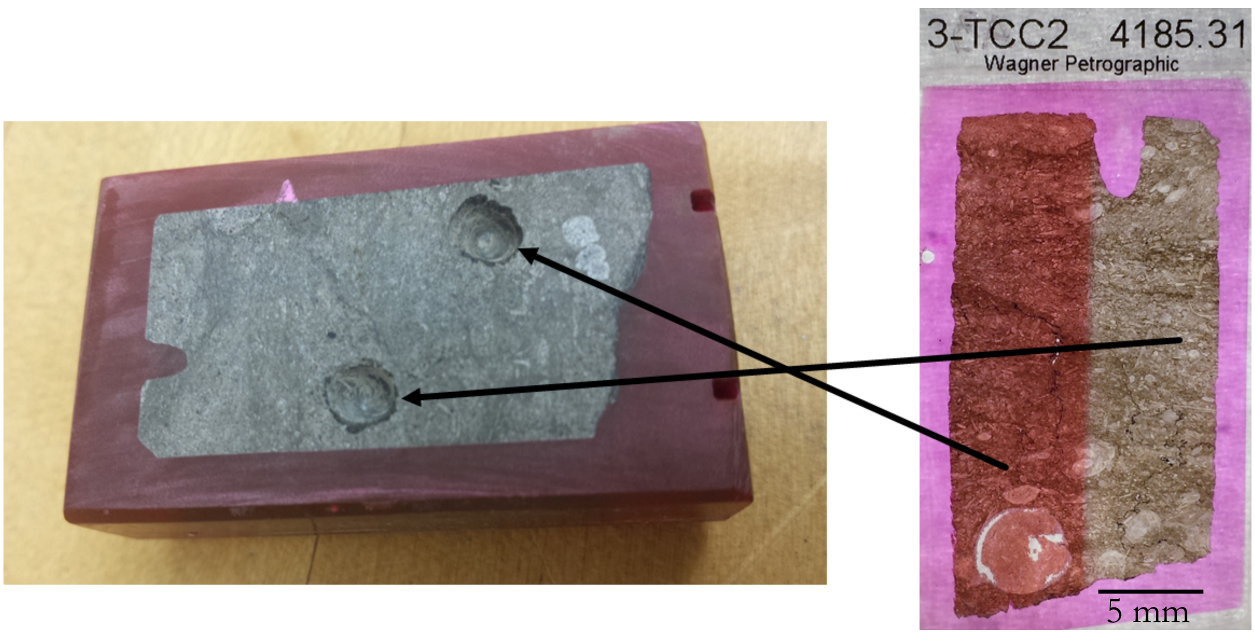

Figure 2.12: Material for isotope analysis was taken from thin-section billets or remaining core material that could be directly correlated back to thin sections.

DEVELOPMENT OF A PARAGENETIC SEQUENCE

Textural and compositional heterogeneity provide important evidence to diagenetic environments and alteration. Discrete steps of mineralization or recrystallization, or a rock's *paragenetic sequence*, may be determined by documenting the relationships among various mineral phases or crystalline textures. Accurate reconstruction of the paragenetic sequence is dependent upon determining the order of diagenetic stages. The use of transmitted light petrography in conjunction with scanning electron microscopy permit observation of rock properties at different scales. Transmitted light petrography illuminates crystalline fabrics and morphology as well as composition. Scanning electron microscopy offers qualitative evidence of timing with regard to recrystallization or replacement. Essentially, these tools are used to reveal microscopic cross-cutting relationships.

The timing of each step in a paragenetic sequence is a well-studied area of carbonate petrology. Scholle and Ulmer-Scholle (2003) and Flügel (2010) were the primary sources of information on diagenesis for this study. Crystalline textures in marine carbonates are associated with various diagenetic environments, including early or syngenetic diagenesis, eogenesis, mesogenesis, and telogenesis. In these rocks, recrystallization is treated as a constant and ongoing process. Previous studies that constrain the timing of basin-wide features, namely the burial history (Reed et al., 2005) or development of jointing (Lash and Engelder, 2009), provide temporal support for the paragenetic sequence.

SYNTHESIS OF THE PARAGENETIC SEQUENCE WITH ISOTOPIC DATA

Isotopic compositions in limestones are used to learn about processes involved with the crystallization of carbonate mineral phases. Stable isotopes provide evidence of conditions (e.g., temperature) or processes which operate at a scale that may be larger than the scale available for visual observation. Nodule formation is one example where isotopes can be paramount in upscaling microscopic observations, as these nodules often produce ambiguous textures (Bojanowski et al., 2014; Irwin et al., 1977). Isotopes provide evidence of depositional or paleoenvironmental conditions (Frappier et al., 2015), as well as about diagenetic alteration (Choquette and James, 1987; Flügel, 2010), although diagenetic isotopic signature often masks the paleoenvironmental signals.

This study used bulk analysis of carbonate minerals, and a certain degree of heterogeneity is expected. Differences in the compositions of "sister" samples are attributed to this compositional heterogeneity, or sampling bias, rather than an erroneous analysis (Brodie et al., 2018). The disparity between these measurements can be attributed to multiple carbonate minerals from different times of crystallization, and phases of minerals with trace amounts are likely lost due to recrystallization or replacement. In support of a paragenetic sequence, isotopic data does not directly distinguish diagenetic processes and must be integrated with petrologic analysis to precisely define paragenesis.

CHAPTER THREE : RESULTS

PETROGRAPHIC AND MINERALOGICAL RESULTS

Detailed petrographic analysis was performed on 87 core samples acquired from eight cores from West Virginia (GOFF, MSEEL, WV7), Pennsylvania (WHIP, BE15), and New York (TCC, NY4, BMC). A majority of these samples are altered limestones within the Cherry Valley Member of the Oatka Creek Formation within the Marcellus subgroup. Descriptions of select mudstones from immediately above and below the Cherry Valley carbonates are included.

The following sections include a summary of the petrographical descriptions of primarily the Cherry Valley carbonates within each of the sampled cores in West Virginia, Pennsylvania, and New York. Table 1 includes the well identification, stratigraphic position, sample identification, and sample depth of all samples. Detailed petrologic descriptions of all 87 samples, including thin section petrography and SEM analysis, may be found for each respective sample in Appendix I. A summary of lithologies, or rock names, from all 87 samples is shown in Figure 3.1. Compositional logs, as well as sample locations, are available for each core in Figure 3.2.

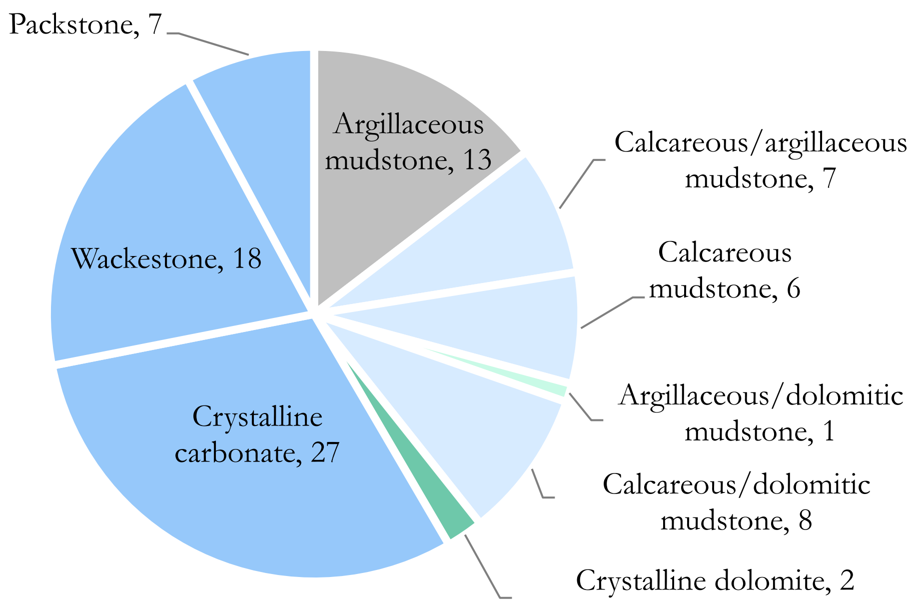

Figure 3.1: Distribution of lithologies from all sampled cores as base categories (i.e., without individual modifiers). Colors associated with lithologies are: Dark Blue – Dunham limestones; Light Blue – Folk mudstones (calcareous); Gray – Folk mudstones (argillaceous); Dark Green – Crystalline dolomite; Light Green – Folk mudstones (dolomitic).

Table 3.1: Lithologies of sampled core material. See Appendix I for details. Dark Blue – Dunham limestones; Light Blue – Folk mudstones (calcareous); Gray – Folk mudstones (argillaceous); Dark Green – Crystalline dolomite; Light Green – Folk mudstones (dolomitic).

Well	Stratigraphy		Sample ID	TS Depth (ft)	Lithology
West Virginia					
GOFF	Marcellus Formation	Cherry Valley Limestone	**GOFF-10/11**	7,204.75	Microsparitic crystalline carbonate
			GOFF-17	7,205.25	Microsparitic crystalline carbonate
			GOFF-19/20	7,205.42	Microsparitic crystalline carbonate
			GOFF-26/27	7,205.96	Microsparitic crystalline carbonate
			GOFF-31/32	7,206.25	Microsparitic crystalline carbonate
			GOFF-35/36	7,206.50	Microsparitic crystalline carbonate
			GOFF-39/40	7,206.92	Microsparitic crystalline carbonate
West Virginia					
MSEEL	Marcellus Fm.	Cherry Valley Ls.	**MSEEL-15**	7,518.17	Microsparitic crystalline carbonate
			MSEEL-58/59	7,524.08	Microsparitic crystalline carbonate
West Virginia					
WV7	Marcellus Formation	Cherry Valley Limestone	**WV7-1**	6,615.17	Microsparitic packstone
			WV7-3	6,615.33	Microsparitic packstone
			WV7-6	6,615.67	Microsparitic wackestone
			WV7-8	6,615.83	Microsparitic wackestone
			WV7-12	6,616.08	Microsparitic crystalline carbonate

Table 3.1 (cont): Lithologies of sampled core material. See Appendix I for details.

Well	Stratigraphy		Sample ID	TS Depth (ft)	Lithology
Pennsylvania					
WHIP	Marcellus Formation	Cherry Valley Limestone	**WHIP-36**	7,868.58	Microsparitic crystalline carbonate
			WHIP-3	7,869.83	Organic, pyritic, argillaceous mudstone
			WHIP-9	7,870.50	Microsparitic crystalline carbonate
			WHIP-12	7,870.75	Microsparitic crystalline carbonate
			WHIP-17	7,871.25	Fossiliferous, organic, argillaceous mudstone
			WHIP-23	7,872.25	Fossiliferous, calcareous/argillaceous mudstone
			WHIP-28	7,872.67	Fossiliferous, calcareous mudstone

Pennsylvania					
BE15	Marcellus Formation	OC Mbr.	**BE15-10**	335.00	Argillaceous mudstone
		Cherry ValleyLimestone	**BE15-16**	335.50	Fossiliferous, calcareous/dolomitic mudstone
			BE15-23	336.25	Calcareous/dolomitic mudstone
			BE15-33	337.25	Microsparitic crystalline carbonate
			BE15-38	337.70	Silty, calcareous/dolomitic mudstone
			BE15-42	338.00	Calcareous/dolomitic mudstone
			BE15-45	338.25	Calcareous/dolomitic mudstone
			BE15-49	338.60	Fossiliferous, calcareous/dolomitic mudstone
		Union Springs	**BE15-52**	338.95	Calcareous/dolomitic mudstone
			BE15-54	339.13	Nodular, argillaceous/dolomitic mudstone

Table 3.1 (cont): Lithologies of sampled core material. See Appendix I for details.

Well	Stratigraphy			Sample ID	TS Depth (ft)	Lithology
New York						
TCC	Oatka Creek Formation	E. Berne Member		**1-TCC2**	4,183.46	Fossiliferous, calcareous/argillaceous mudstone
				2-TCC2	4,183.79	Fossiliferous, calcareous mudstone
		Cherry Valley Member		**2-TCC1**	4,185.00	Packstone
				3-TCC2	4,185.31	Packstone
				4-TCC2	4,185.44	Fossiliferous, calcareous/argillaceous mudstone
				5-TCC2	4,185.58	Wackestone
				6-TCC2	4,185.83	Crystalline carbonate
				7-TCC2	4,186.08	Baritic crystalline carbonate
				8-TCC2	4,186.21	Crystalline dolomite
				9-TCC2	4,186.42	Crystalline dolomite
				10-TCC2	4,186.71	Dolomitic crystalline carbonate
				11-TCC2	4,186.96	Fossiliferous, dolomitic, calcareous/argillaceous mudstone
				12-TCC2	4,187.08	Fossiliferous, dolomitic, calcareous/argillaceous mudstone
				3-TCC1	4,187.25	Fossiliferous, baritic, calcareous mudstone
				13-TCC2	4,187.33	Baritic wackestone
				14-TCC2	4,187.50	Baritic wackestone
				15-TCC2	4,187.71	Felted, baritic, calcareous/dolomitic mudstone
				16-TCC2	4,187.83	Organic, pyritic, argillaceous mudstone
				17-TCC2	4,188.00	Felted, microsparitic crystalline carbonate
				4-TCC1	4,188.25	Felted, baritic, microsparitic crystalline carbonate
				5-TCC1	4,188.50	Organic, pyritic, argillaceous mudstone
				18-TCC2	4,188.50	Microsparitic crystalline carbonate

Table 3.1 (cont): Lithologies of sampled core material. See Appendix I for details.

Well	Stratigraphy		Sample ID	TS Depth (ft)	Lithology
New York					
TCC	Oatka Creek Fm.	Ch. Valley Member	**19-TCC2**	4,188.75	Microsparitic crystalline carbonate
			6-TCC1	4,189.00	Felted, microsparitic crystalline carbonate
	Union Springs Formation	Bakoven Member	**20-TCC2**	4,189.21	Argillaceous mudstone
					Microsparitic crystalline carbonate
			21-TCC2	4,189.42	Argillaceous mudstone
			7-TCC1	4189.67	Fossiliferous, organic, pyritic, argillaceous mudstone
			22-TCC2	4189.88	Argillaceous mudstone
			8-TCC1	4190.33	Argillaceous mudstone
			9-TCC1	4190.58	Pyritic, argillaceous mudstone
			23-TCC2	4191.17	Fossiliferous, argillaceous mudstone

New York					
NY4	Oatka Creek Formation	Cherry Valley Member	**NY4-20**	3,844.45	Microsparitic wackestone
			NY4-22	3,844.70	Felted, microsparitic crystalline carbonate
			NY4-24	3,844.95	Felted, microsparitic crystalline carbonate
			NY4-29	3,845.50	Microsparitic wackestone
			NY4-35	3,846.36	Microsparitic wackestone
			NY4-39	3,846.78	Microsparitic wackestone
			NY4-43	3,847.33	Microsparitic wackestone
			NY4-47	3,847.92	Microsparitic wackestone
			NY4-50	3,848.25	Microsparitic packstone
					Fossiliferous, calcareous mudstone
			NY4-52	3,848.58	Microsparitic wackestone

Table 3.1 (cont): Lithologies of sampled core material. See Appendix I for details.

Well	Stratigraphy		Sample ID	TS Depth (ft)	Lithology
New York					
BMC	Oatka Creek Formation	E. Berne Member	**BMC-NYSM-2**	1,900.00	Organic, argillaceous mudstone
			BMC-NYSM-3	1,901.00	Fossiliferous, calcareous mudstone
		Cherry Valley Member	**BMC-13**	1,902.58	Microsparitic wackestone
			BMC-NYSM-4	1,903.00	Silty wackestone
			BMC-21	1,903.50	Microsparitic packstone
			BMC-26	1,904.25	Microsparitic wackestone
			BMC-30	1,904.75	Microsparitic packstone
			BMC-35	1,905.33	Microsparitic wackestone
			BMC-40	1,905.83	Microsparitic wackestone
			BMC-43	1,906.17	Microsparitic wackestone
			BMC-NYSM-5	1,906.50	Microsparitic crystalline carbonate
			BMC-48	1,906.75	Microsparitic crystalline carbonate
	Union Springs	Bakoven Member	**BMC-NYSM-6**	1,909.00	Silty, fossiliferous, calcareous mudstone
			BMC-NYSM-7	1,915.00	Argillaceous/calcareous mudstone
			BMC-NYSM-8	1,917.00	Argillaceous/calcareous mudstone

WEST VIRGINIA

Nathan Goff #55 (GOFF)

The Cherry Valley carbonates in the GOFF core is composed of crystalline carbonates, with SWIR and XRD finding calcite to be the dominant mineral at the sampled intervals (Fig. 3.2). Aspectral SWIR results in the overlying and underlying mudstones mark the extents of the Cherry Valley carbonates.

Crystalline carbonates

Seven samples between the depths of 7,204.75 and 7,206.92 feet in the GOFF core are characterized as crystalline carbonates with a microsparitic texture (Fig 3.3). The matrices of these crystalline carbonates are predominantly composed of calcite (Fig 3.3A/C) based on petrography and compositional analyses. A nonlaminated texture is generally observed in all samples as diagenesis has largely rendered depositional fabrics unrecognizable. The matrices, which are composed of diagenetic calcite, are recrystallized or neomorphosed to xenotopic, inequigranular microspar.

The diagenetic mineral assemblage includes recrystallized calcite with lesser amounts of ferroan calcite, barite (Fig 3.3C), and dolomite. These latter three minerals occur as minor cements that crystallized within cysts that are walled by organic material. Subvertical fractures are common and filled with calcite that is of the same phase as the matrix. Irregular, anastomosing, organic-filled stylolites propagate parallel to bedding in all samples and are generally associated with agglomerated baroque dolomite (Fig 3.3B). Pyrite is typically associated with organic material which is mostly observed as highly degraded, fine, amorphous kerogen that is disseminated throughout the matrix.

All samples contain a significant number of fossils, though identification and quantity estimates are made difficult by diagenesis. Collapsed, organic-walled cysts (Fig 3.3A/C) are likely algal and are the best-preserved fossils. Other nondescript fossil fragments are apparent and not identifiable (Fig 3.3D).

Figure 3.2 (facing page): Compositional results for the GOFF core. The central sector is dominated by calcite, corresponding to the Cherry Valley carbonates (between blue lines), whereas the top and bottom intervals are clay-rich mudstones. Note the position in feet of the top and bottom of the core interval studied. The red bars at far left represent a sampled interval. Columns of data include: left column are core photographs; second column from left are raw SWIR data; second column from right is SWIR-based automated mineralogy; right column shows mineralogy based on XRD.

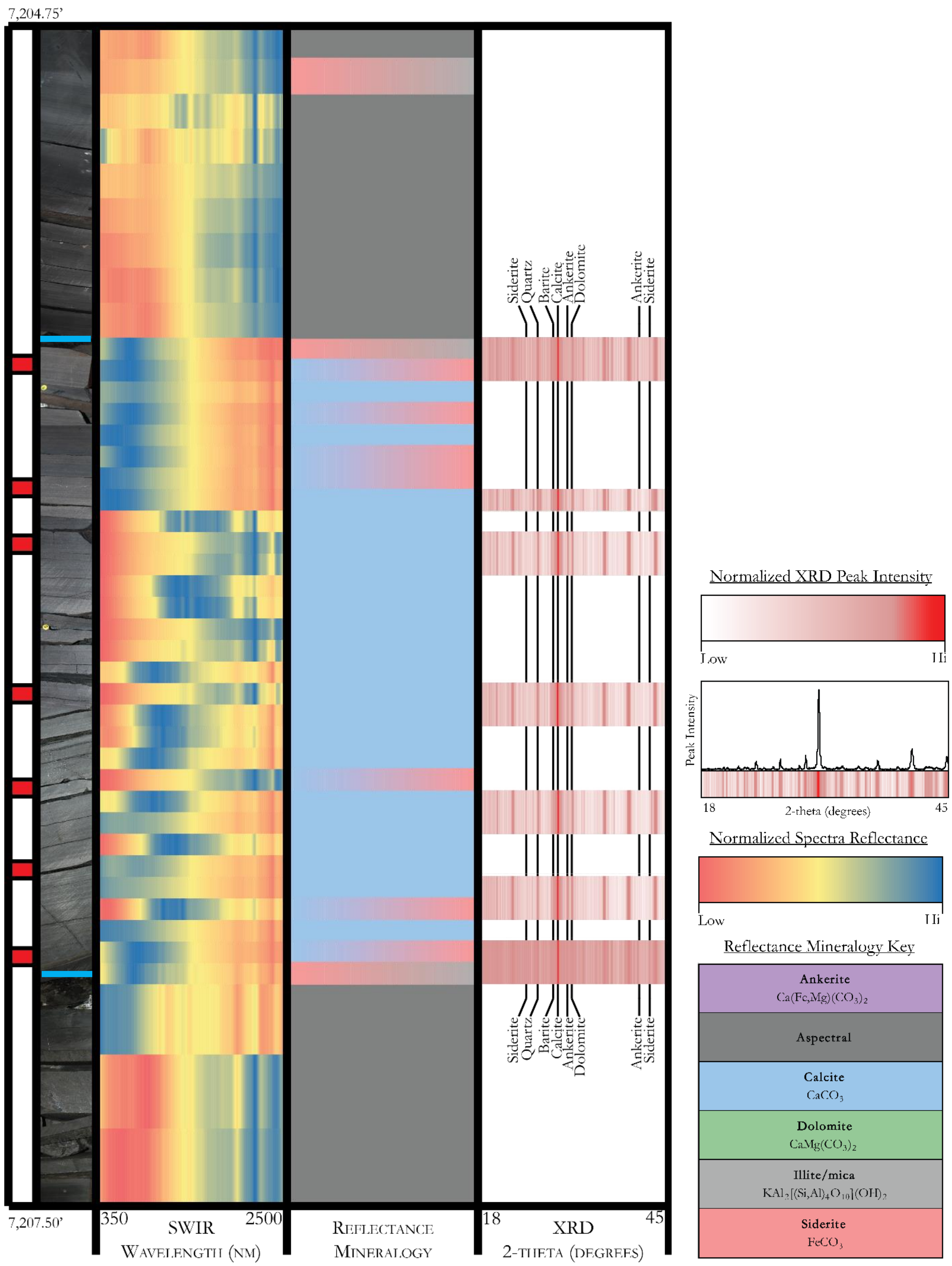
7,204.75'
7,207.50'
350
2500
SWIR
Wavelength (nm)
Reflectance
Mineralogy
18
45
XRD
2-theta (degrees)
Siderite
Quartz
Barite
Calcite
Ankerite
Dolomite
Ankerite
Siderite
Normalized XRD Peak Intensity
Low
Hi
Peak Intensity
18
2-theta (degrees)
45
Normalized Spectra Reflectance
Low
Hi
Reflectance Mineralogy Key
Ankerite
Ca(Fe,Mg)(CO3)2
Aspectral
Calcite
CaCO3
Dolomite
CaMg(CO3)2
Illite/mica
KAl2[(Si,Al)4O10](OH)2
Siderite
FeCO3

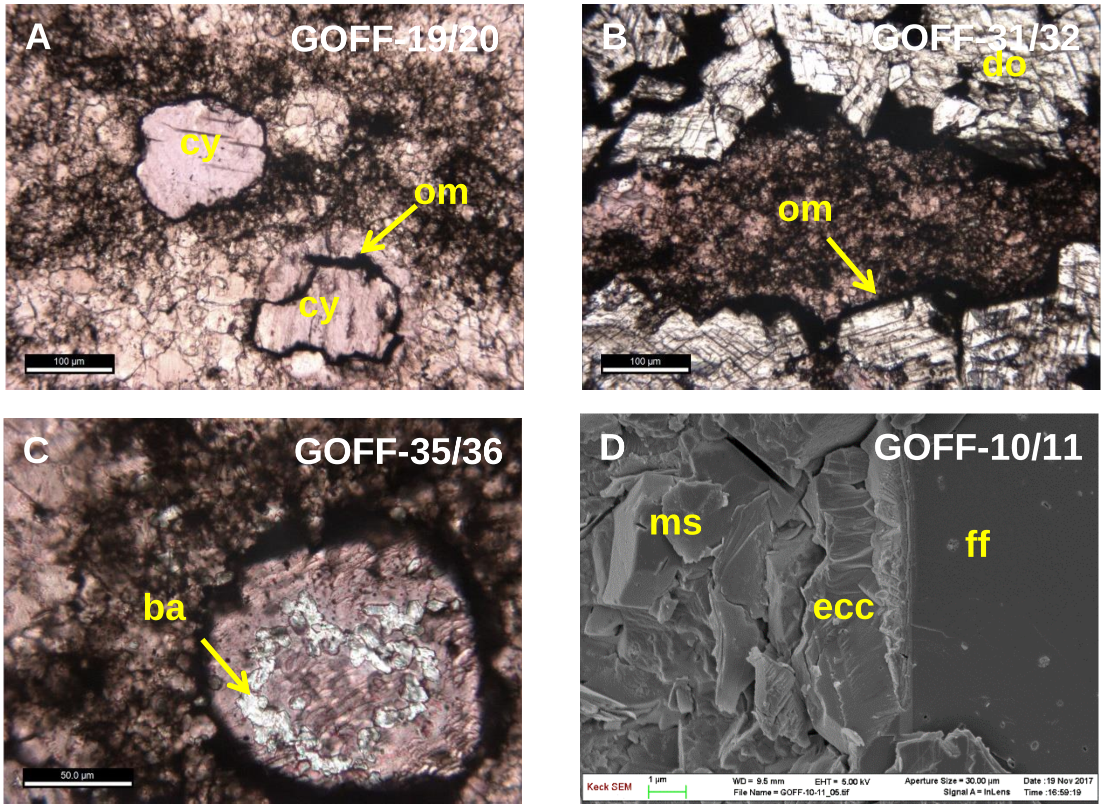

Figure 3.3: GOFF core petrologic images. **A**–GOFF-19/20 (7,205.42 ft) collapsed cysts (cy) with an organic wall (om) in a microsparitic crystalline carbonate (Plane-polarized light. Scale bar = 100 µm); **B**–GOFF-31/32 (7,206.25 ft) dolomite (do) may be associated with organic material (om) and stylolites (Plane-polarized light. Scale bar = 100 µm); **C**–GOFF-35/36 (7,206.50 ft) a collapsed, organic-walled cyst is filled with a slight ferroan calcite and barite (ba) (Plane-polarized light. Scale bar = 50 µm); **D**–GOFF-10/11 (7,204.75 ft) equant calcite (ecc) is crystallized on the surface of a fossil fragment (ff). ms = microspar (Secondary electron detector. Scale bar = 1 µm).

MIP 3H (MSEEL)

Two limestone sections delineate the extent of the Cherry Valley carbonates in the MSEEL core, with SWIR and XRD finding calcite to be the dominant mineral, and interbedded mudstones between the crystalline carbonates were not sampled (Fig. 3.4). Minor dolomite was detected in the lower limestone bed which contains comparatively higher amounts of fossils than the upper interval.

Crystalline carbonates

Two samples taken at 7,518.17 and 7,524.08 feet in the MSEEL core are characterized as crystalline carbonates with a microsparitic texture (Fig. 3.5). The matrices of these crystalline carbonates are predominantly composed of diagenetic calcite based on petrography and compositional analyses. A nonlaminated texture is generally observed in both samples as diagenesis has largely rendered depositional fabrics unrecognizable (Fig. 3.5A/C). At 7,518.17 feet, indistinct bedforms and laminae are weakly evident at low magnifications, though these textures are lost are higher magnifications. A depositionally chaotic texture is visible at 7,524.08 feet as demonstrated by irregular fossil orientations (Fig. 3.5B). These textures are largely overprinted by diagenesis at higher magnification as the matrices are recrystallized or neomorphosed to xenotopic to hypidiotopic, inequigranular microspar.

Calcite is the predominant mineral in these two samples (Fig. 3.5). Minor ferroan calcite is generally associated with fossils or crystallized within fossils cysts that are walled by organic material. Irregular, anastomosing, organic-filled stylolites propagate normal to bedding in both samples and are generally associated with agglomerated dolomite rhombohedra. Pyrite is typically associated with organic material which is mostly observed as highly degraded, fine, amorphous kerogen that is disseminated throughout the matrix.

Fossil content varies from one depth to the next. Nondescript fossil fragments and collapsed, organic-walled cysts (Fig. 3.5A) are the only identifiable fossil present at 7,518.17 feet. A more diverse assemblage at 7,524.08 feet includes dacryoconarids (Fig. 3.5B), gastropods, crinoids, ostracods, and trilobites, as well as organic-walled cysts. Fossils are highly recrystallized and commonly feature circumgranular, bladed or equant calcite growth (Fig. 3.5C). Ferroan calcite is commonly associated with more robust fossils such as crinoid or trilobite fragments.

Figure 3.4 (following facing pages): Compositional results for the MSEEL core. The Cherry Valley carbonates (between the blue lines) are represented by an upper and lower calcite-rich zone with a clay-rich mudstone in between. Clay-rich mudstones are above and below the sampled interval. Note the position in feet of the top and bottom of the core interval studied. The red bars at far left represent a sampled interval. Columns of data include: left column are core photographs; second column from left are raw SWIR data; second column from right is SWIR-based automated mineralogy; right column shows mineralogy based on XRD.

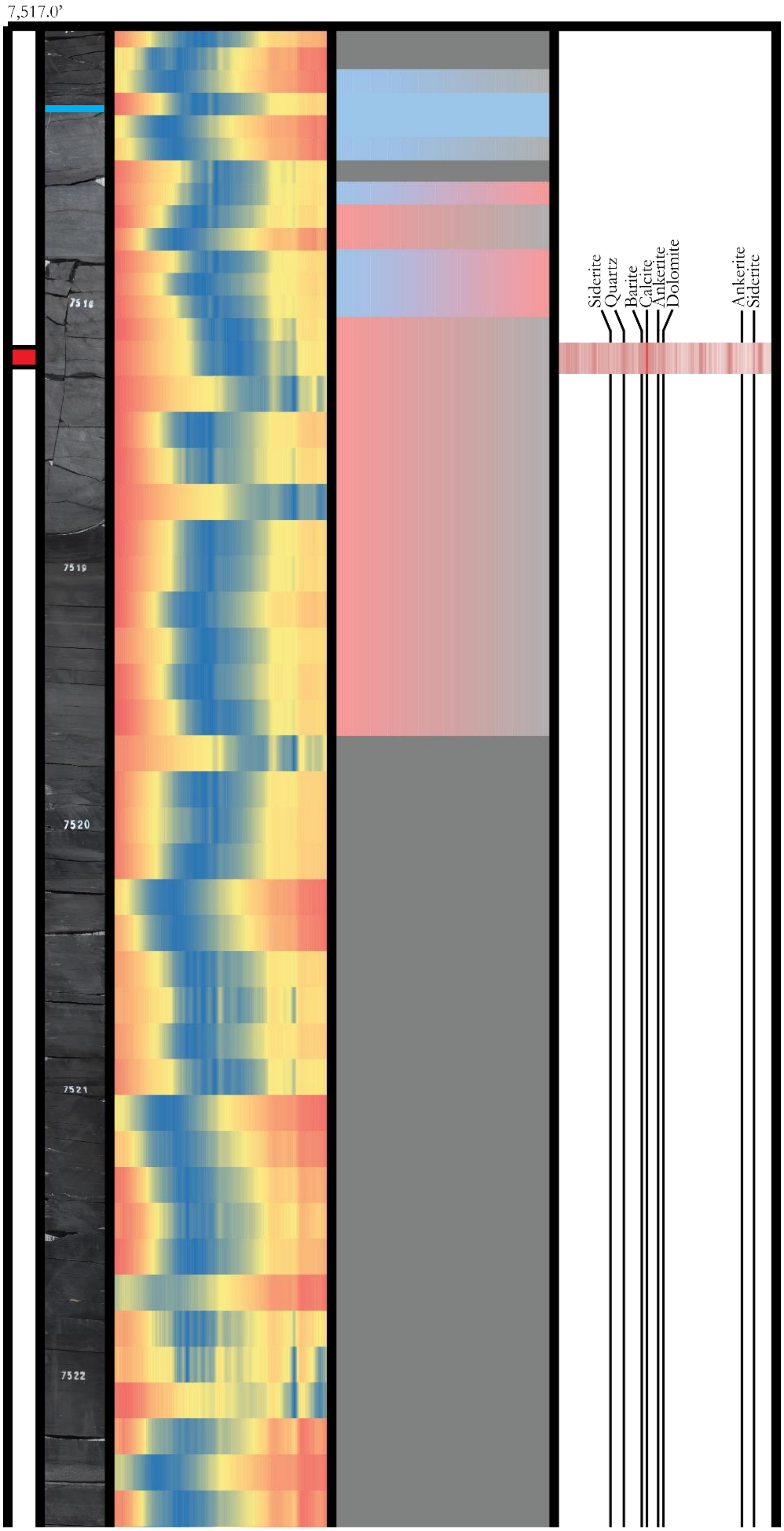
7,517.0'
7518
7519
7520
7521
7522
Siderite
Quartz
Barite
Calcite
Ankerite
Dolomite
Ankerite
Siderite

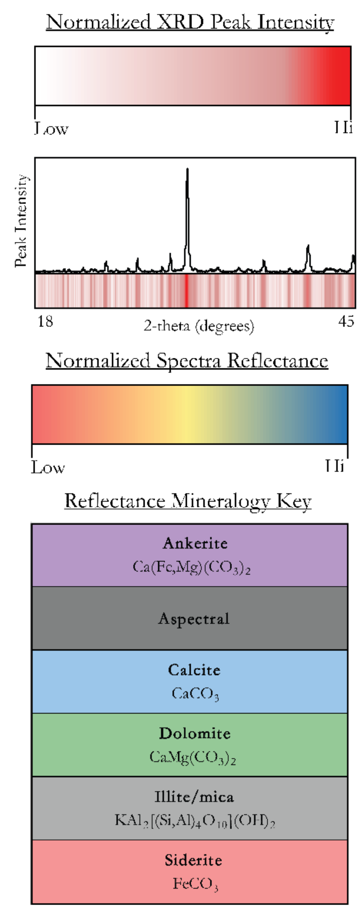
Normalized XRD Peak Intensity
Low
Hi
Peak Intensity
18
2-theta (degrees)
45
Normalized Spectra Reflectance
Low
Hi
Reflectance Mineralogy Key
Ankerite
Ca(Fe,Mg)(CO3)2
Aspectral
Calcite
CaCO3
Dolomite
CaMg(CO3)2
Illite/mica
KAl2[(Si,Al)4O10](OH)2
Siderite
FeCO3

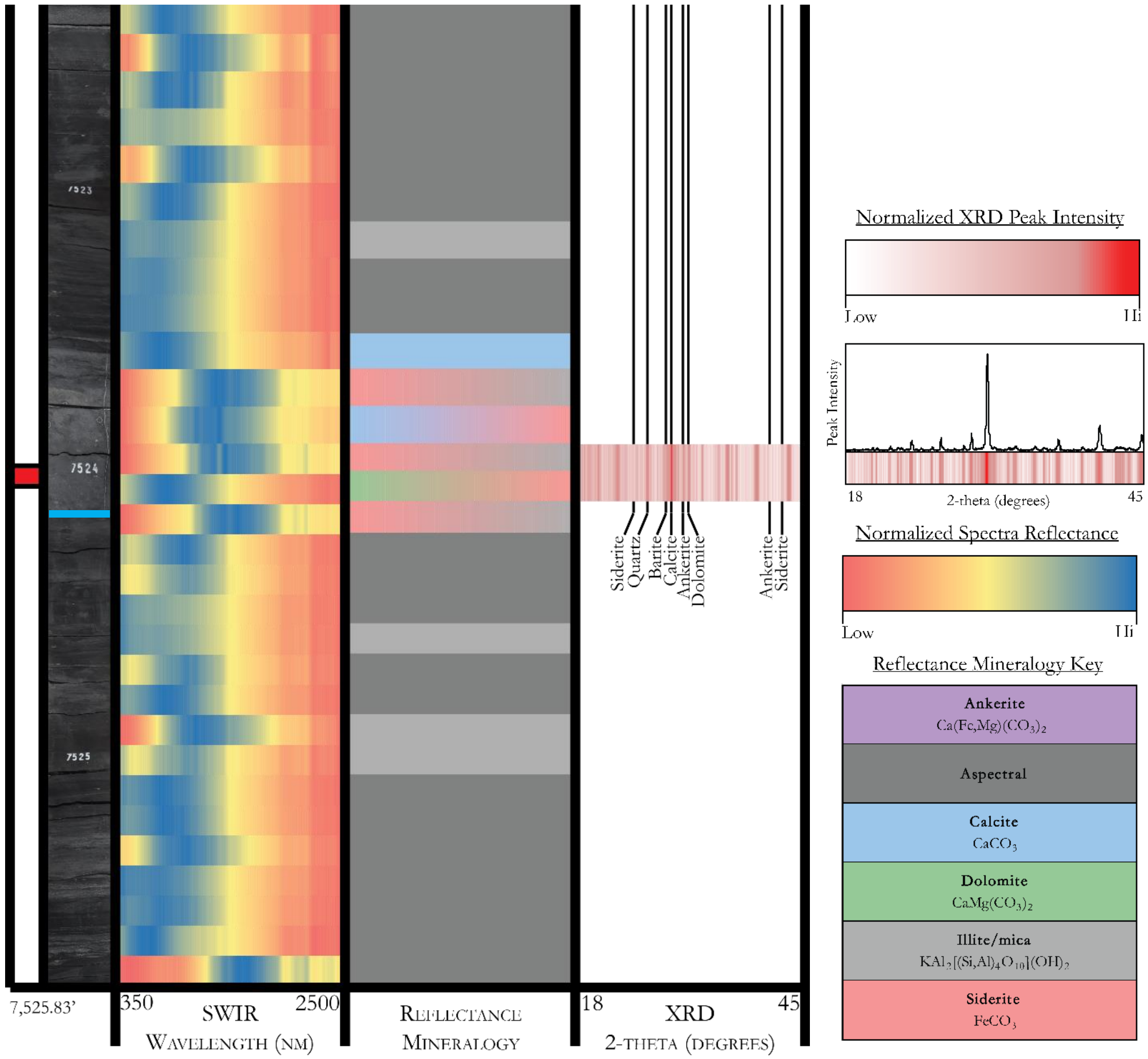
7523
7524
7525
7,525.83'
350
SWIR
2500
Wavelength (nm)
Reflectance
Mineralogy
18
XRD
45
2-theta (degrees)
Siderite
Quartz
Barite
Calcite
Ankerite
Dolomite
Ankerite
Siderite
Normalized XRD Peak Intensity
Low
Hi
Peak Intensity
18
2-theta (degrees)
45
Normalized Spectra Reflectance
Low
Hi
Reflectance Mineralogy Key
Ankerite
Ca(Fe,Mg)(CO3)2
Aspectral
Calcite
CaCO3
Dolomite
CaMg(CO3)2
Illite/mica
KAl2[(Si,Al)4O10](OH)2
Siderite
FeCO3

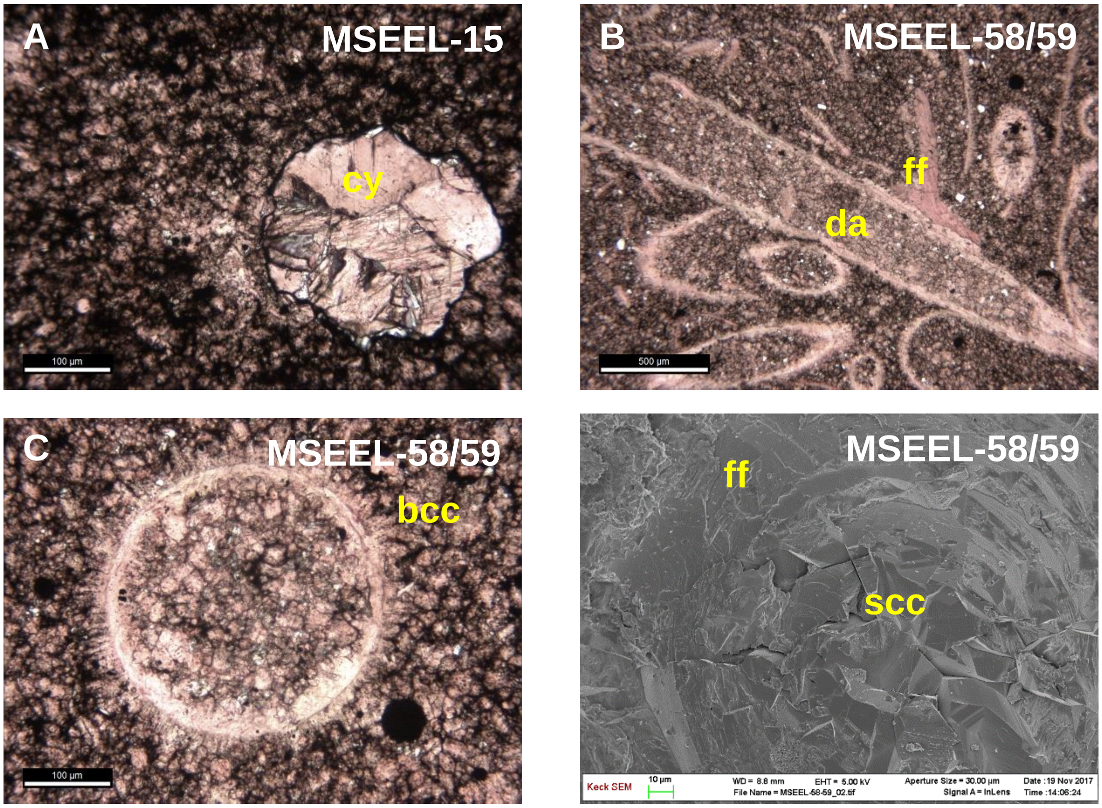

Figure 3.5: MSEEL core petrologic images: **A**–MSEEL-15 (7,818.17 ft) collapsed, organic-walled cyst (cy) in a microsparitic crystalline carbonate (Plane-polarized light. Scale bar = 100 µm); **B**–MSEEL-58/59 (7,824.08 ft) recrystallized dacryoconarids (da) and fossil fragments (Plane-polarized light. Scale bar = 500 µm); **C**–MSEEL-58/59 (7,824.08 ft) a fossil, possibly a dacryoconarid that is turned on its axis or a cyst, is filled with microspar and is mantled by bladed calcite crystals (Plane-polarized light. Scale bar = 100 µm); **D**–MSEEL-58/59 (7,824.08 ft) a micron-scale view of a fossil (ff) that is filled with sparry calcite (scc), similar to the example highlighted in Figure 3.5C (Secondary electron detector. Scale bar = 10 µm).

EGSP WV-7 (WV7)

The Cherry Valley is represented by recrystallized bedded limestones and crystalline carbonates that are dominantly composed of calcite in the WV7 core (Fig. 3.6). Due to poor condition of the core, vertically bounding mudstones were not photographed or sampled. This Cherry Valley interval is thin in comparison with other cores in this study, and includes thinly bedded mudstones. Though SWIR results were inconclusive, as they erroneously detected siderite, XRD confirmed a predominantly calcite composition.

Wackestones and Packstones

Four samples in the WV7 core are characterized as either a wackestone (2) or packstone (2) between the depths of 6,615.17 and 6,615.83 feet. These rocks are texturally similar and can be distinguished only by fossil content (Fig. 3.7A/B/D). The matrices are mainly composed of calcite based on petrography and compositional analyses. A nonlaminated microtexture is characteristic in both samples as diagenesis has largely rendered depositional fabrics unrecognizable, though depositional bedding planes are apparent at low magnifications. These textures are largely overprinted by diagenesis at higher magnification as the matrices are recrystallized or neomorphosed to hypidiotopic, equigranular microspar.

Calcite is the predominant diagenetic mineral in the wackestones and packstones. Fossil tests commonly feature equant calcite growth on the interior and exterior with a drusy calcite or ferroan calcite (Fig. 3.7A) fill. Minor dolomite and barite (Fig. 3.7A) cements are generally associated with fossils. Pyrite is typically associated with organic material which is mostly observed as highly degraded, fine, amorphous kerogen that is disseminated throughout the matrix.

Dacryoconarids (*Nowakia*; Fig. 3.7B) are the primary fossil type. In fewer instances, fecal pellets and collapsed, organic-walled cysts are observed. Nondescript fragments, which are disseminated along bedding throughout the rocks, are likely dacryoconarids.

Crystalline carbonate

One sample taken at 6,616.08 feet in the WV7 core is characterized as a crystalline carbonate with a microsparitic texture, though the lack of recognizable depositional fabric may be due to neomorphism of a micritic, calcareous mudstone rather than diagenetic overprinting. The matrix of this interval is predominantly composed of calcite based on petrography and compositional analyses. A nonlaminated texture is observed as bedforms are not strongly preserved within the xenotopic, inequigranular microspar matrix (Fig. 3.7C).

Calcite is the predominant diagenetic mineral in these two samples. Minor ferroan calcite is generally associated with fossils or crystallized within fossils cysts that are walled by organic material (Fig. 3.7C). Collophane, organic residue, and pyrite fills select cysts. Pyrite is typically associated with organic material which is mostly observed as highly degraded, fine, amorphous kerogen that is disseminated throughout the matrix.

Nondescript fossil fragments and collapsed, organic-walled cysts are the only identifiable fossils. Fossils are highly recrystallized and commonly feature circumgranular, bladed or equant calcite growth (Fig. 3.7C). Ferroan calcite is commonly associated with more robust fossils such as crinoid or trilobite fragments.

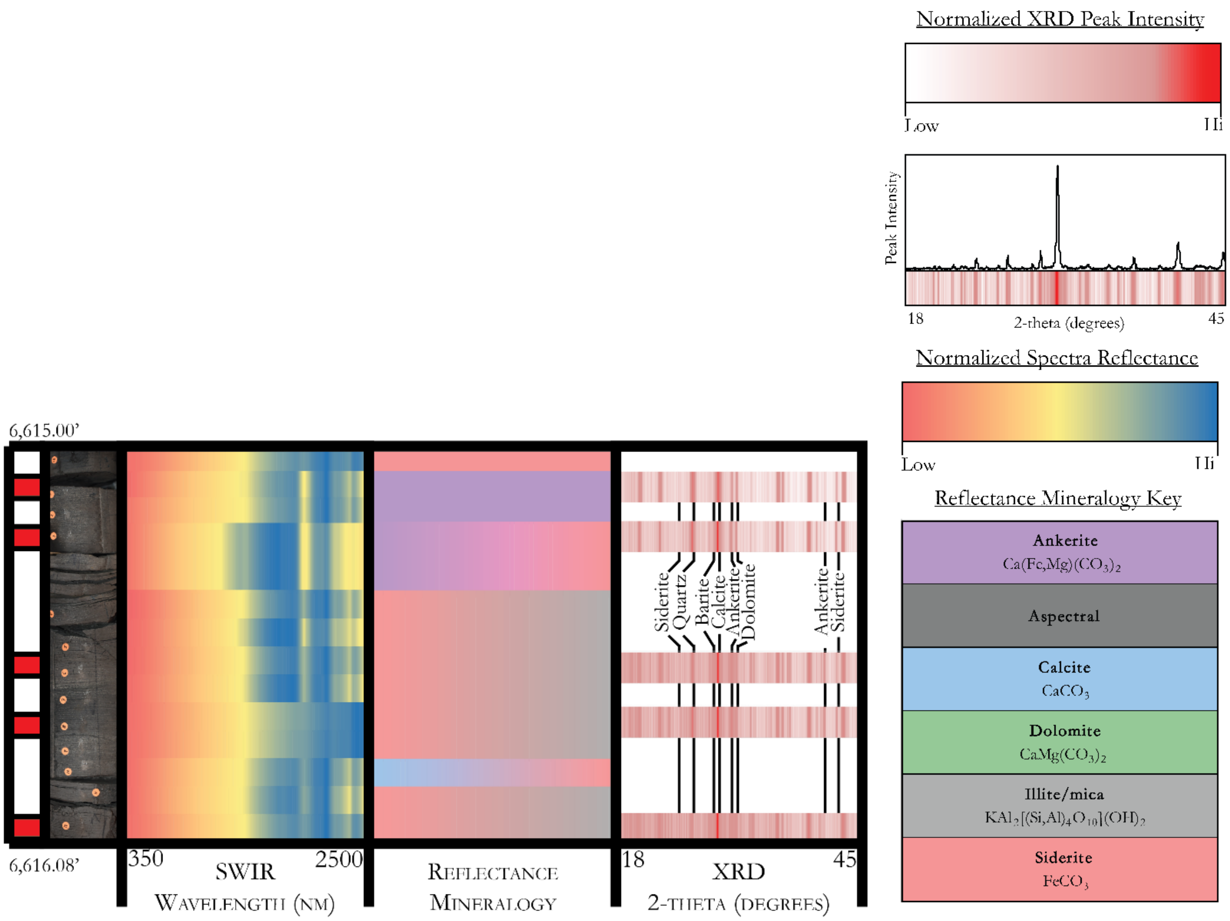

Figure 3.6: Compositional results for the WV7 core. The observed sector is dominated by calcite, corresponding to the Cherry Valley carbonates. Vertically bounding mudstones are not pictured due to deterioration of the core. Note the position in feet of the top and bottom of the core interval studied. The red bars at far left represent a sampled interval. Columns of data include: left column are core photographs; second column from left are raw SWIR data; second column from right is SWIR-based automated mineralogy; right column shows mineralogy based on XRD.

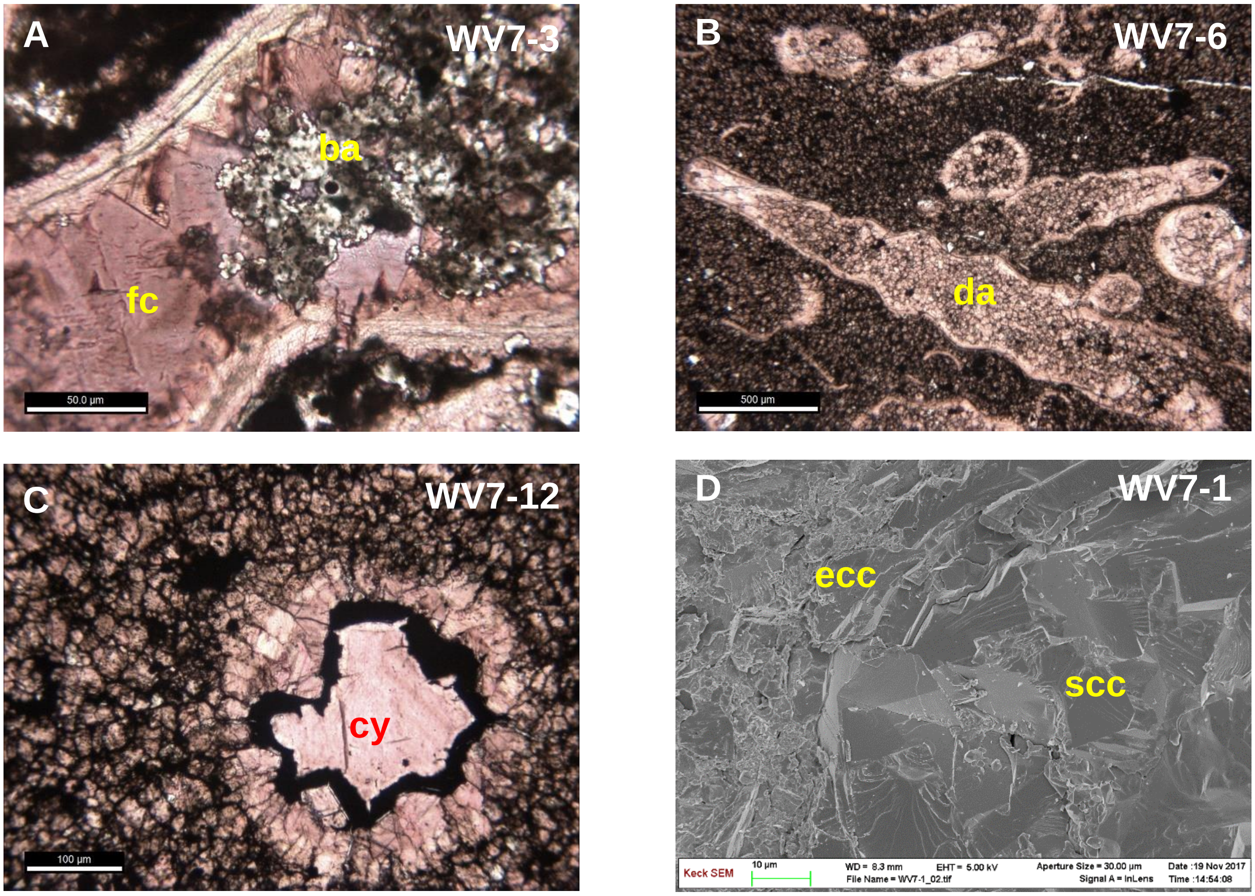

Figure 3.7: WV7 core petrologic images: **A**–WV7-3 (6,615.33 ft) a fossil is filled with various diagenetic phases including ferroan calcite (fc) and barite (ba) (Plane-polarized light. Scale bar = 50 µm); **B**–WV7-6 (6,615.67 ft) dacryoconarids (da) are the dominant fossil type in the WV7 core (Plane-polarized light. Scale bar = 500 µm); **C**–WV7-12 (6,616.08 ft) a collapsed, organic-walled cysts (cy), likely algal, has a sparry calcite interior that is separated from the matrix by an organic wall. Diagenetic, bladed calcite is crystallized on its surface (Plane-polarized light. Scale bar = 100 µm); **D**– WV7-1 (6,615.17 ft) a fossil rimmed with equant calcite (ecc) filled by sparry calcite (scc) (Secondary electron detector. Scale bar = 2 µm).

PENNSYLVANIA

St. Whipkey #1

The WHIP core includes two distinct limestone intervals that make up the Cherry Valley carbonates, as well as interbedded mudstones (Fig. 3.8). The upper portion of the Cherry Valley comprises crystalline carbonates with calcareous mudstones at its base. Calcite is the dominant mineral as determined by XRD, and a poorly reflective surface likely lends to inaccurate siderite-rich SWIR results.

Crystalline carbonates

Three samples between the depths of 7,868.58 and 7,870.75 feet in the WHIP core are characterized as crystalline carbonates with a microsparitic texture (Fig. 3.9A/B). The matrices of these crystalline carbonates are predominantly composed of calcite based on petrography and compositional analyses. A nonlaminated texture is characteristic of all samples as diagenesis has largely rendered depositional fabrics unrecognizable. The matrices are recrystallized or neomorphosed to xenotopic, inequigranular microspar (Fig. 3.9D).

The diagenetic mineral assemblage includes recrystallized calcite with lesser amounts of ferroan calcite, barite, and dolomite. These minor cements are typically crystallized within cysts that are walled by organic material, though no trends in either morphology or mineralogy are apparent. Subvertical calcite-filled fractures are common and the calcite may be ferroan (Fig. 3.9B). Irregular, anastomosing, organic-filled stylolites propagate parallel to bedding in all samples and are generally associated with agglomerated baroque dolomite. Pyrite is typically associated with organic material which is mostly observed as highly degraded, fine, amorphous kerogen that is disseminated throughout the matrix.

All samples contain a significant number of fossils, though identification and precise quantification is made difficult by diagenesis. Collapsed, organic-walled cysts are likely algal and are the best-preserved fossils. Other nondescript fossil fragments are apparent and not identifiable.

Argillaceous mudstones

Two samples have been characterized as argillaceous mudstones with fossiliferous, organic, and pyritic variants. The matrices of these mudstones are primarily composed of illitic clay minerals based on their petrography. A well-laminated texture is present in both rocks, with laminae commonly defined by detrital phyllosilicates, fossil fragments, and organic particles and stringers. Minor diagenetic cement is predominantly composed of calcite. Variable amounts of calcite, ferroan calcite, and dolomite exist in select portions of the rock and are generally associated with fossils. Elevated pyrite content is attributed to the higher abundance of organic material. Minor quartz silt is disseminated throughout the mudstone.

The fossil assemblage comprises dacryoconarids, nondescript fragments, collapsed organic-walled cysts, and phosphatic bone fragments. Organic material fills select fossil tests that have not been fully filled with calcite.

Calcareous and calcareous/argillaceous mudstone

Two samples at the bottom of the studied interval, at depths 7,872.25 feet and 7872.67 feet, are characterized as calcareous and calcareous/argillaceous mudstones, respectively. Despite an elevated clay component in the upper sample, both rocks share lithological similarities. These moderately well-laminated mudstones are cemented by calcite to varying degrees. Equant calcite, ferroan calcite, dolomite, and collophane fill fossils tests (Fig. 3.9C). Minor barite cement may be associated with select fossils. Dolomite rhombohedra are disseminated throughout the matrix.

Fossils include dacryoconarids (*Nowakia*) as well as nondescript fragments and phosphatic bone fragments. Organic particles and stringers are not uncommon in this sample and are generally associated with framboidal pyrite.

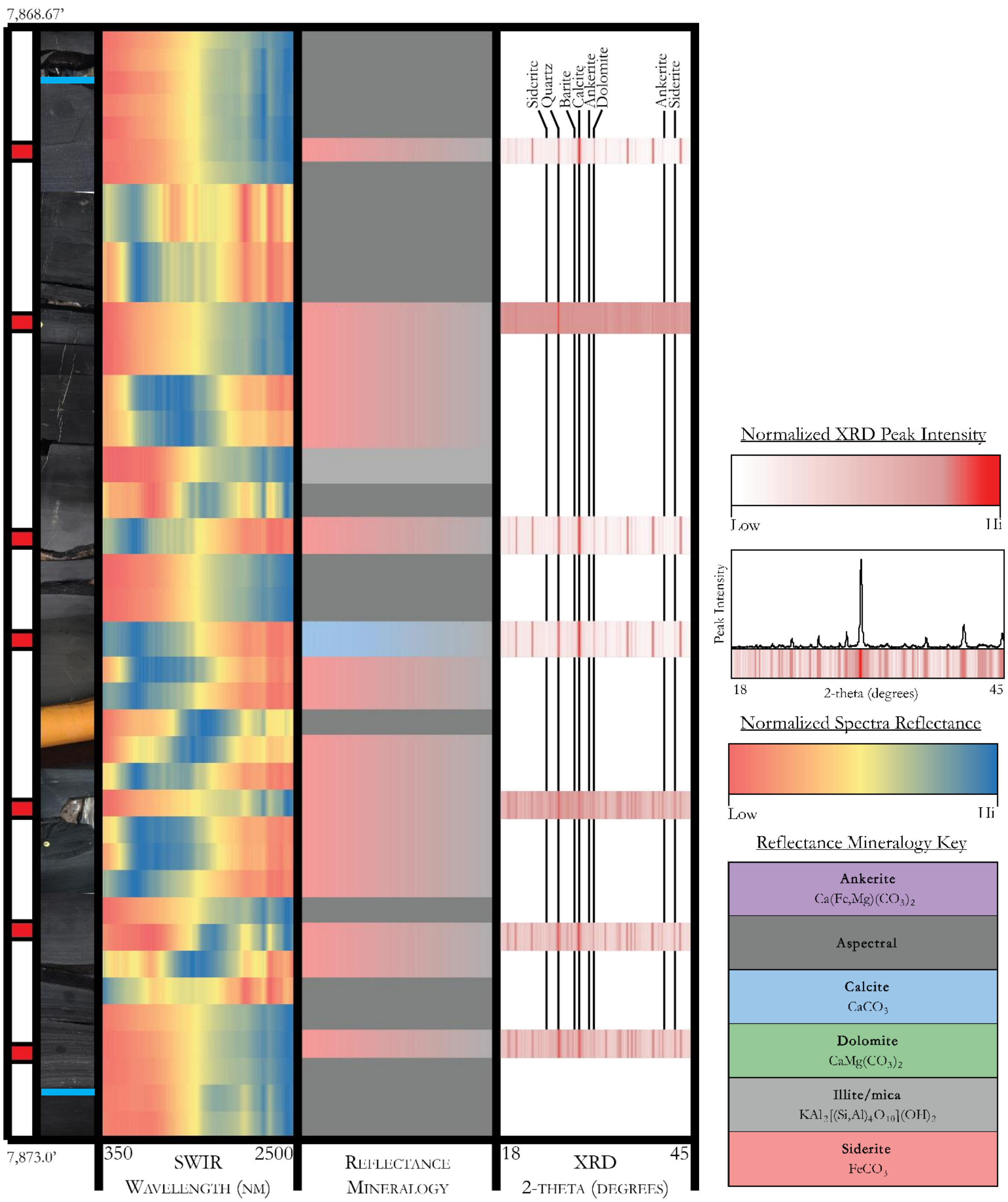

Figure 3.8: Compositional results for the WHIP core. The central sector is dominated by calcite, corresponding to the Cherry Valley carbonates (between blue lines), whereas the top and bottom intervals are dominated by clay-rich mudstones. Note the position in feet of the top and bottom of the core interval studied. The red bars at far left represent a sampled interval. Columns of data include: left column are core photographs; second column from left are raw SWIR data; second column from right is SWIR-based automated mineralogy; right column shows mineralogy based on XRD.

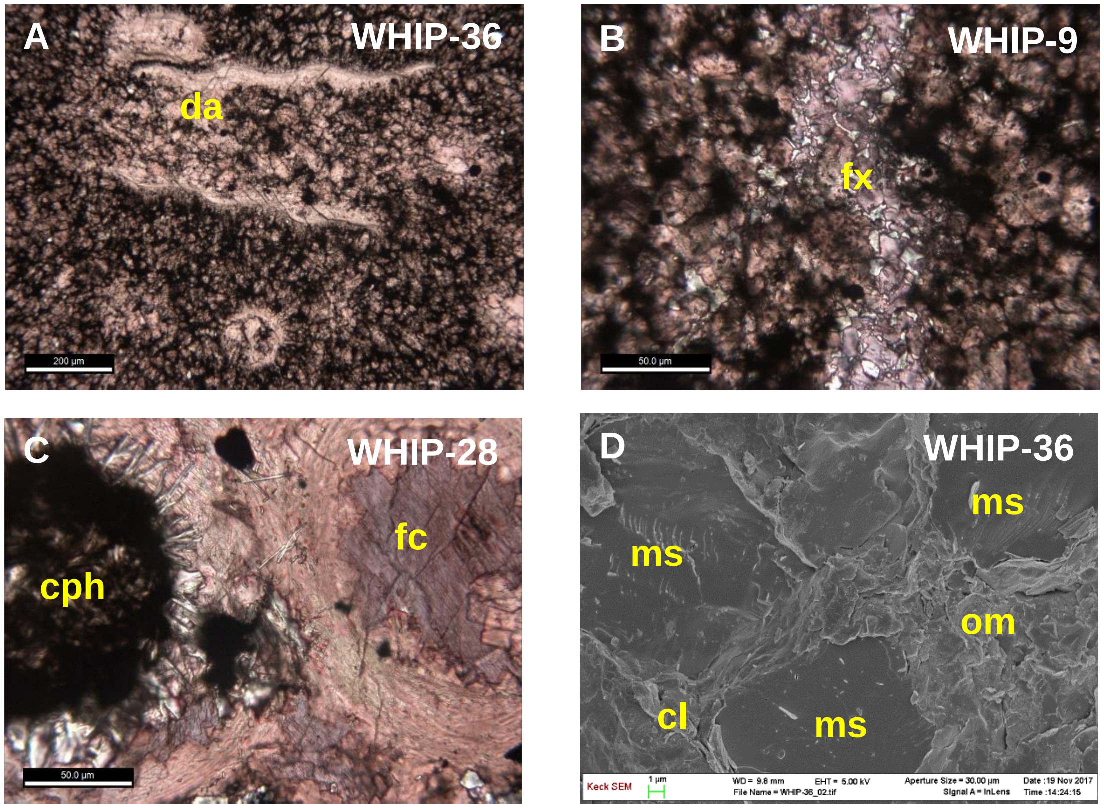

Figure 3.9: WHIP core petrologic images: **A**–WHIP 36 (7,868.58 ft) a partial fossil of dacryoconarid that is filled with microspar and rimmed with bladed or equant calcite (Plane-polarized light. Scale bar = 200 µm); **B**–WHIP-9 (7,870.50 ft) subvertical fracture that is healed by ferroan calcite, as evidenced by the purple stain (Plane-polarized light. Scale bar = 100 µm); **C**–WHIP-28 (7,872.67 ft) fossil tests are occluded by several mineral phases including ferroan calcite (fc) and collophane (cph) (Plane-polarized light. Scale bar = 100 µm); **D**–WHIP-36 (7,868.58 ft) clay minerals (cl) and organic material (om) fills the spaces between matrix microspar (ms) (Secondary electron detector. Scale bar = 1 µm).

Bald Eagle 2015 (BE15)

The BE15 core includes primarily calcareous mudstones that make up the Cherry Valley carbonates. Calcite is the dominant mineral, as captured by XRD, and includes a significant amount of ankeritic dolomite, as determined by SWIR (Fig. 3.9). The Cherry valley is continuous, with insignificant interbedded mudstones, and neomorphism has affected this core than others in the study. Although the BE15 is the shallowest well, no evidence of meteoric water infiltration is apparent.

Calcareous/dolomitic mudstones

Seven samples in the BE15 core are characterized as calcareous/dolomitic mudstones with fossiliferous and silty varieties (Fig 3.11 A/C/D). These samples have compositional mixed matrices of calcite and dolomite, with minor amounts of clay minerals. Although bedding horizons are apparent by the alignment of fossils and silty laminae, diagenesis renders the microtexture to be weakly laminated. Detrital quartz silt and micas are between 15-25% and grains range in size from very fine to fine. Calcite is the dominant cementing mineral while dolomite is a comparatively minor constituent. Though clay minerals are present in the matrices of these rocks, calcite and dolomite cementation controls the resultant rock fabric. Other diagenetic mineralization includes barite, ferroan calcite, and ferroan dolomite or ankerite. In addition to acting as a cement, dolomite rhombohedra are crystallized throughout the matrix.

Dacryoconarids (*Styliolina* and *Viriatellina*; Fig 3.11A/D) and nondescript shell or skeletal fragments comprise the majority of fossil content. Fewer specimens of conodonts, brachiopods, collapsed algal cysts, possible crinoids, and bivalves are present. Fossil tests are commonly filled with calcite, dolomite, or ferroan calcite (Fig 3.11C).

Argillaceous mudstones

Two samples are characterized as argillaceous mudstones in the BE15 core, one (BE-15, 335.00 feet) that is stratigraphically above the Cherry Valley Limestone in the Oatka Creek Member and the other, an argillaceous/dolomitic mudstone (BE15-54, 339.13 feet), is below in the Union Springs Member. The lower depth includes the nodular and dolomitic variants. The matrices are primarily composed of illitic clay minerals based on its petrography, although minor dolomite and calcite cementation are present in select portions of the rock. The rock is moderately well laminated by the alignment of detrital grains and micas and fossil fragments. Equant calcite is crystallized on the interiors of fossil tests that have not been crushed. In select tests that have not been fully occluded by diagenetic calcite, barite may fill the remainder. Minor sphalerite is noted in this rock, which may imply a hydrothermal component. Dolomite rhombohedra are disseminated through the clay-rich matrix. Notably, the lower argillaceous mudstone includes barite nodules that are fractured.

A majority of observed fossils are nondescript fragments, though several collapsed, organic-walled cysts and phosphatic fragments, likely bone fragments or conodonts, are noted in the lower the argillaceous mudstone.

Crystalline carbonate

One samples 337.25 feet in the BE15 core is characterized as crystalline carbonates with a microsparitic texture (Fig 3.11B). The matrix of this rock is predominantly composed of calcite based on petrography and compositional analyses. A nonlaminated texture is characteristic as diagenesis has largely rendered depositional fabrics unrecognizable. The matrices are recrystallized or neomorphosed to xenotopic, inequigranular microspar.

The diagenetic mineral assemblage includes recrystallized calcite with lesser amounts of ferroan calcite, barite, and dolomite (Fig 3.11C). These minor cements are typically crystallized within cysts that are walled by organic material. Trace amounts of barite may be replaced by ferroan calcite. Pyrite is typically associated with organic material which is mostly observed as highly degraded, fine, amorphous kerogen that is disseminated throughout the matrix.

A diverse assemblage of fossils includes dacryoconarids (*Styliolina*), crinoids, brachiopods, and collapsed, organic-walled cysts. Other nondescript fossil fragments are apparent and not identifiable.

Figure 3.10 (following facing pages): Compositional results for the BE15 core. The central sector is dominated by calcite, corresponding to the Cherry Valley carbonates (between blue lines), whereas the top and bottom intervals are dominated by clay-rich mudstones. Note the position in feet of the top and bottom of the core interval studied. The red bars at far left represent a sampled interval. Columns of data include: left column are core photographs; second column from left are raw SWIR data; second column from right is SWIR-based automated mineralogy; right column shows mineralogy based on XRD.

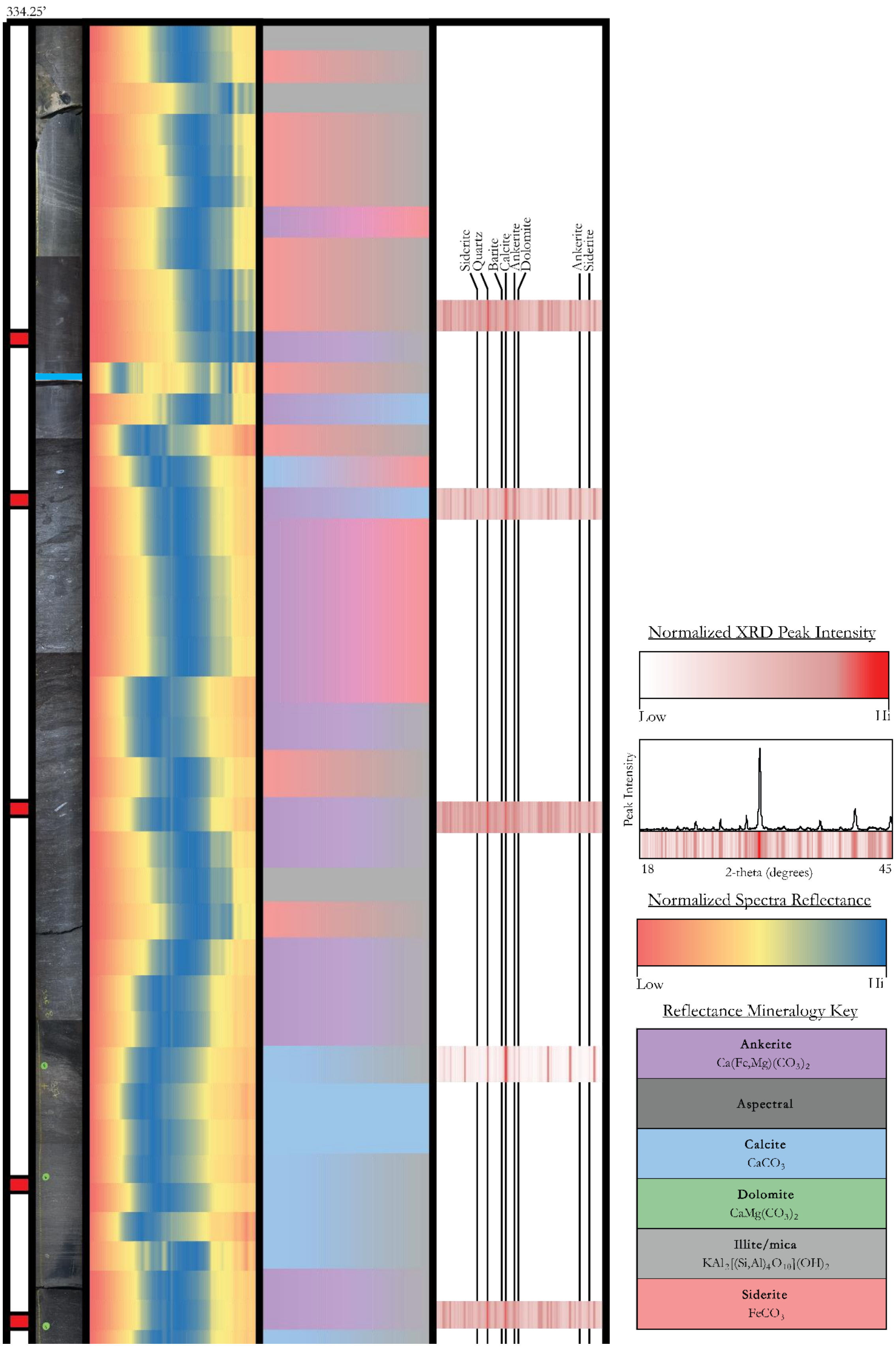
334.25'
Siderite
Quartz
Barite
Calcite
Ankerite
Dolomite
Ankerite
Siderite
Normalized XRD Peak Intensity
Low
Hi
Peak Intensity
18
2-theta (degrees)
45
Normalized Spectra Reflectance
Low
Hi
Reflectance Mineralogy Key
Ankerite
Ca(Fe,Mg)(CO3)2
Aspectral
Calcite
CaCO3
Dolomite
CaMg(CO3)2
Illite/mica
KAl2[(Si,Al)4O10](OH)2
Siderite
FeCO3

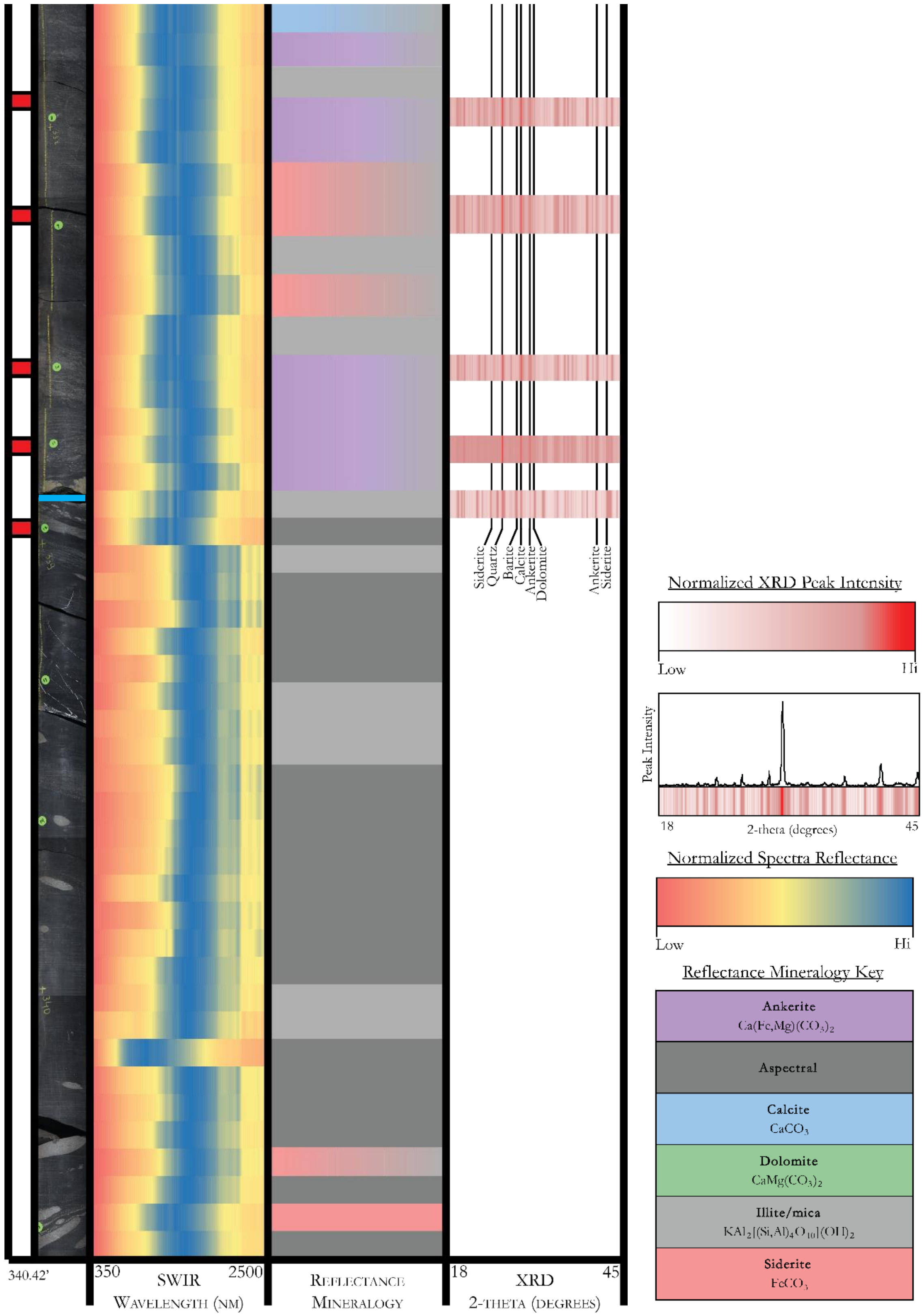

340.42'
350
SWIR
2500
Wavelength (nm)
Reflectance
Mineralogy
18
XRD
45
2-theta (degrees)
Siderite
Quartz
Barite
Calcite
Ankerite
Dolomite
Ankerite
Siderite
Normalized XRD Peak Intensity
Low
Hi
Peak Intensity
18
2-theta (degrees)
45
Normalized Spectra Reflectance
Low
Hi
Reflectance Mineralogy Key
Ankerite
Ca(Fe,Mg)(CO3)2
Aspectral
Calcite
CaCO3
Dolomite
CaMg(CO3)2
Illite/mica
KAl2[(Si,Al)4O10](OH)2
Siderite
FeCO3

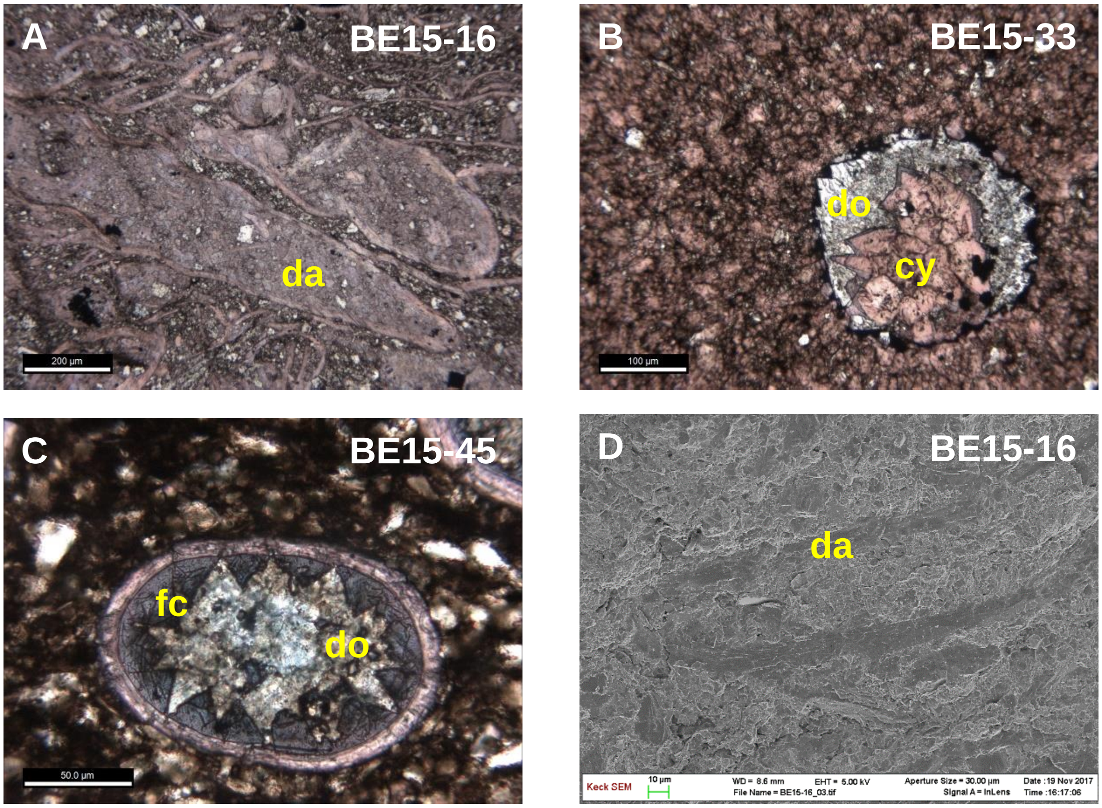

Figure 3.11: BE15 core petrologic images: **A**–BE15-16 (335.50 ft) dacryoconarids (da), including *Viriatellina*, are well preserved in the BE15 well and are filled with ferroan calcite (Plane-polarized light. Scale bar = 200 µm); **B**–BE15-33 (337.25 ft) the interiors of some cysts (cy) include a dolomite (do) fill that reinforces a rectilinear morphology (Plane-polarized light. Scale bar = 100 µm); **C**–BE15-45 (338.25 ft) equant ferroan calcite (fc) mineralization is followed up dolomitization (do) within the interior of this fossil, likely an algal cyst (Plane-polarized light. Scale bar = 100 µm); **D**–BE15-16 (335.50 ft) little distinguishes the calcite fill from the calcite-cemented matrix surrounding this dacryoconarid (da) at SEM scale (Secondary electron detector. Scale bar = 10 µm).

NEW YORK

Strong #1 (TCC)

The Cherry Valley carbonates in the TCC core are the most texturally and compositionally heterogenous interval in this study. XRD and SWIR compositions outline a framework of bedded limestones and crystalline carbonates, calcareous and argillaceous mudstones, and crystalline dolomites (Fig. 3.12). The upper portion is dominated by bedded limestones and calcareous mudstones and the bottom of the interval is noted for nodules hosted within interbedded mudstones, as observed in core.

Crystalline carbonates

Nine samples between 4,185.83 and 4,189.21 feet in the TCC core are characterized as crystalline carbonates with a microsparitic texture. Eight samples are in the Cherry Valley Member, with the single sample being a concretion immediately below in the Bakoven Member at the Cherry Valley Member interface. The matrices of the crystalline carbonates are predominantly composed of calcite based on petrography and compositional analyses. These rocks are typically nonlaminated, due to diagenetic overprinting of most depositional fabrics, and exhibit a microsparitic matrix texture. Several samples have a felted texture where bladed barite is either crystallized or has been subsequently replaced by calcite. Of all lithologies in the TCC core, the crystalline carbonates exhibit the most variability, in terms of compositional or textural heterogeneity, between individual samples.

The diagenetic mineral assemblage includes recrystallized calcite with lesser amounts of ferroan calcite, barite, and dolomite (Fig. 3.12D). Dolomite acts as a significant cement in portions of select samples, particularly in Sample 10-TCC2 at 4,186.71 feet where it is immediately below an interval of crystalline dolomites, or may be irregularly crystallized as rhombohedra. Subvertical or bedding-parallel, calcite- or ferroan calcite-filled fractures are common. Irregular, anastomosing, organic-filled stylolites propagate in some intervals. Pyrite is typically associated with organic material which is mostly observed as highly degraded, fine, amorphous kerogen that is disseminated throughout the matrix and coats microspar in some samples.

All samples contain a significant number of fossils, though identification and precise quantification is commonly made difficult by diagenesis. The fossil assemblage comprises crinoid stems and plates, ostracods, brachiopods, bivalves, dacryoconarids (*Nowakia, Viriatella,* and *Styliolina*), and collapsed, organic-walled cysts. Other nondescript fossil fragments are apparent and not identifiable.

Argillaceous mudstones

Nine samples have been characterized as argillaceous mudstones with fossiliferous, organic, and pyritic variants. Two of the samples are located within the interpreted Cherry Valley Member, acting as a matrix to calcareous concretions, while the remaining seven are in the underlying Bakoven Member of the Union Springs Formation. The matrices of these mudstones are primarily composed of illitic clay minerals based on their petrography. These rocks are generally weakly to well-laminated, with laminae commonly defined by detrital phyllosilicates, fossil fragments, and organic particles and stringers. Minor diagenetic cement is predominantly composed of calcite, some of which is microsparitic when located within nodules. Notably, minor sphalerite is crystallized within fractures at the Cherry Valley Member-Bakoven Member interface. Variable amounts of calcite, ferroan calcite, and dolomite exist in select portions of the rock and are generally associated with fossils which are mostly dacryoconarid or shell fragments. Less common fossils include organic-walled cysts, phosphatic bone fragments, and algal mats. Elevated pyrite content is attributed to the higher abundance of organic material. Minor quartz silt is disseminated throughout the mudstone.

Calcareous/argillaceous, calcareous/dolomitic, and calcareous mudstones

Seven samples in the TCC core are characterized as variants of calcareous mudstones (Fig. 3.12A/C). Four samples are calcareous/argillaceous mudstones, two are calcareous mudstones, and one is a calcareous/dolomitic mudstone. Two of these mudstones are in the overlying East Berne Member and the remaining five are in the Cherry Valley Member. These samples are either calcite-dominated rocks or have compositional mixed matrices of calcite and clays or dolomite. Bedding horizons are distinguished by aligned fossils and silty laminae, lending to weakly to moderately well-laminated textures. Detrital quartz silt and micas is less than 10-15% and grains range in size from very fine to fine. Calcite is the dominant cementing mineral while dolomite is a comparatively minor constituent. Though clay minerals are present in the matrices of these rocks, calcite and dolomite cementation controls the resultant rock fabric. In calcareous/argillaceous mudstones, depositional clay minerals are a compositionally and texturally controlling influence. Other diagenetic mineralization includes barite (Fig. 3.12A), which may be replaced by calcite and exhibit a felted texture (Fig. 3.12C), ferroan calcite (Fig. 3.12A), and ferroan dolomite or ankerite. In addition to acting as a cement, dolomite rhombohedra are crystallized throughout the matrix.

Dacryoconarids (*Styliolina* and *Viriatellina*) and nondescript shell or skeletal fragments comprise the majority of fossil content. Fewer specimens of larger, more robust fossils fragments may be from bivalves and ostracods, and phosphatic bone fragments. Fossil tests are commonly filled with calcite, dolomite, or ferroan calcite

Wackestones and packstones

Five samples in the TCC core are characterized as a bedded limestone, which include wackestones or packstones, in the Cherry Valley carbonates (Fig. 3.13). The matrices of these limestones reflect many similarities with the crystalline carbonates, particularly the microsparitic samples, though they display distinct textural characteristics that suggest a less advanced degree of recrystallization. They are predominantly composed of calcite based on petrography and compositional analyses, with minor amounts of dolomite and barite. A poorly laminated texture is characteristic of these rocks, depending on the degree of recrystallization of matrix calcite.

The diagenetic mineral assemblage includes recrystallized calcite with lesser amounts of ferroan calcite, barite, and dolomite. These minor cements are typically crystallized within fossils. Subvertical calcite-filled fractures and irregular, anastomosing, organic-filled stylolites are common and the calcite is homogenized with surrounding matrix calcite. Pyrite is typically associated with organic material which is mostly observed as highly degraded, fine, amorphous kerogen that is disseminated throughout the matrix.

All samples contain a significant number of fossils, though identification and precise quantification is commonly made difficult by diagenesis. Crinoid stems and plates, ostracods, brachiopods, bivalves, and dacryoconarids (*Nowakia* and *Styliolina*) occur. Collapsed, organic-walled cysts are likely algal and are the best-preserved fossils. Other nondescript fossil fragments are apparent, yet not identifiable.

Crystalline dolomites

Two samples, at depths 4,186.21 and 4,186.42 feet, are characterized as crystalline dolomites (Fig. 3.12B). Both samples are primarily composed of ferroan dolomite (or ankerite) with minor amounts of calcite, barite, and ferroan calcite. Recrystallization lends to nonlaminated texture, resulting in massive, sparry dolomite as well as dolomite microspar. These textures are likely due to depositional fabrics such as fossil material (sparry dolomite) and micrite (dolomite microspar). Remnant barite is replaced by dolomite. Dissolution of dolomite is occluded by calcite, likely representing a late stage of diagenesis. Conodonts are the only identifiable fossil observed.

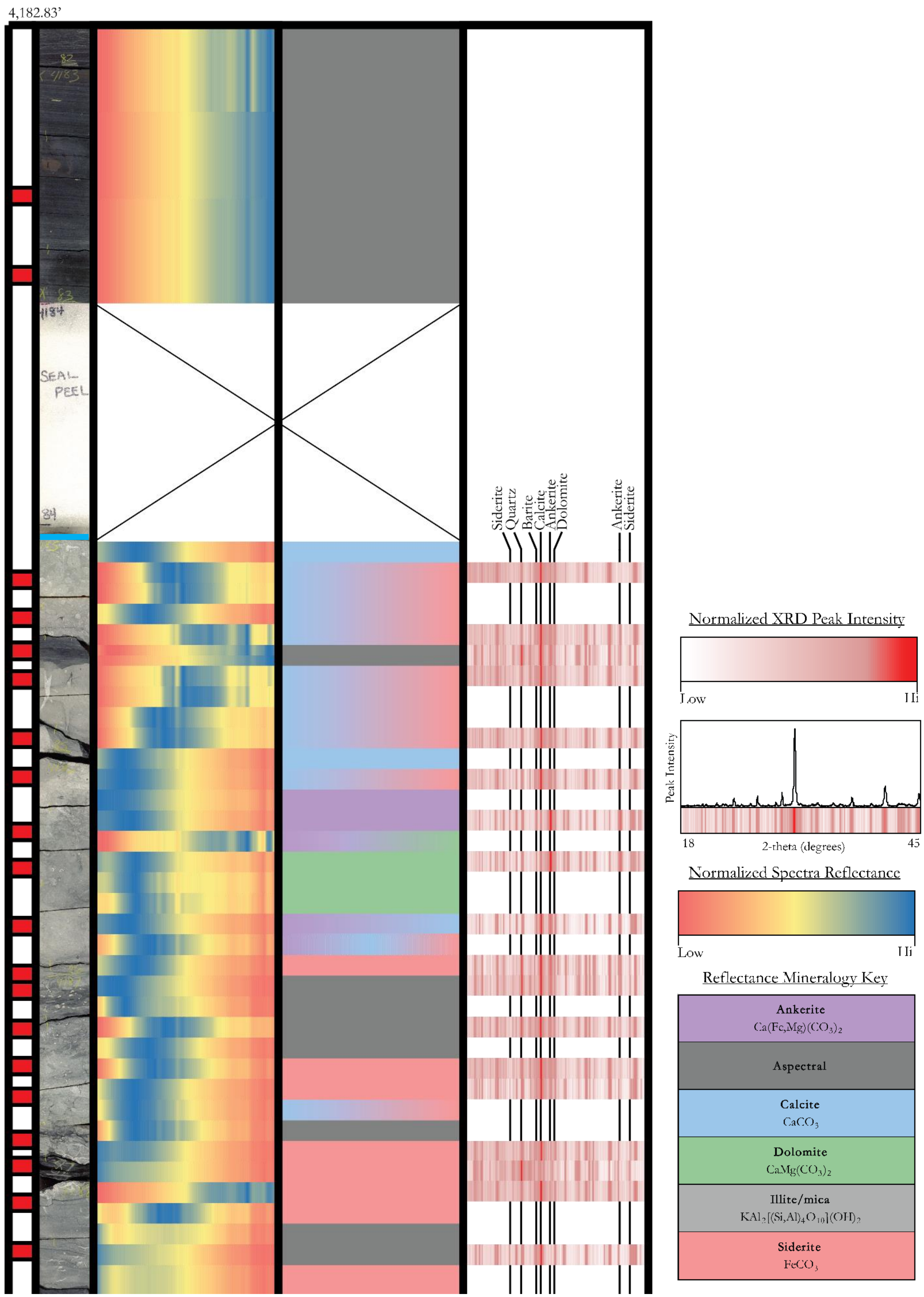
4,182.83'
82
4183
83
4184
SEAL
PEEL
84
Siderite
Quartz
Barite
Calcite
Ankerite
Dolomite
Ankerite
Siderite
Normalized XRD Peak Intensity
Low
Hi
Peak Intensity
18
2-theta (degrees)
45
Normalized Spectra Reflectance
Low
Hi
Reflectance Mineralogy Key
Ankerite
Ca(Fe,Mg)(CO3)2
Aspectral
Calcite
CaCO3
Dolomite
CaMg(CO3)2
Illite/mica
KAl2[(Si,Al)4O10](OH)2
Siderite
FeCO3

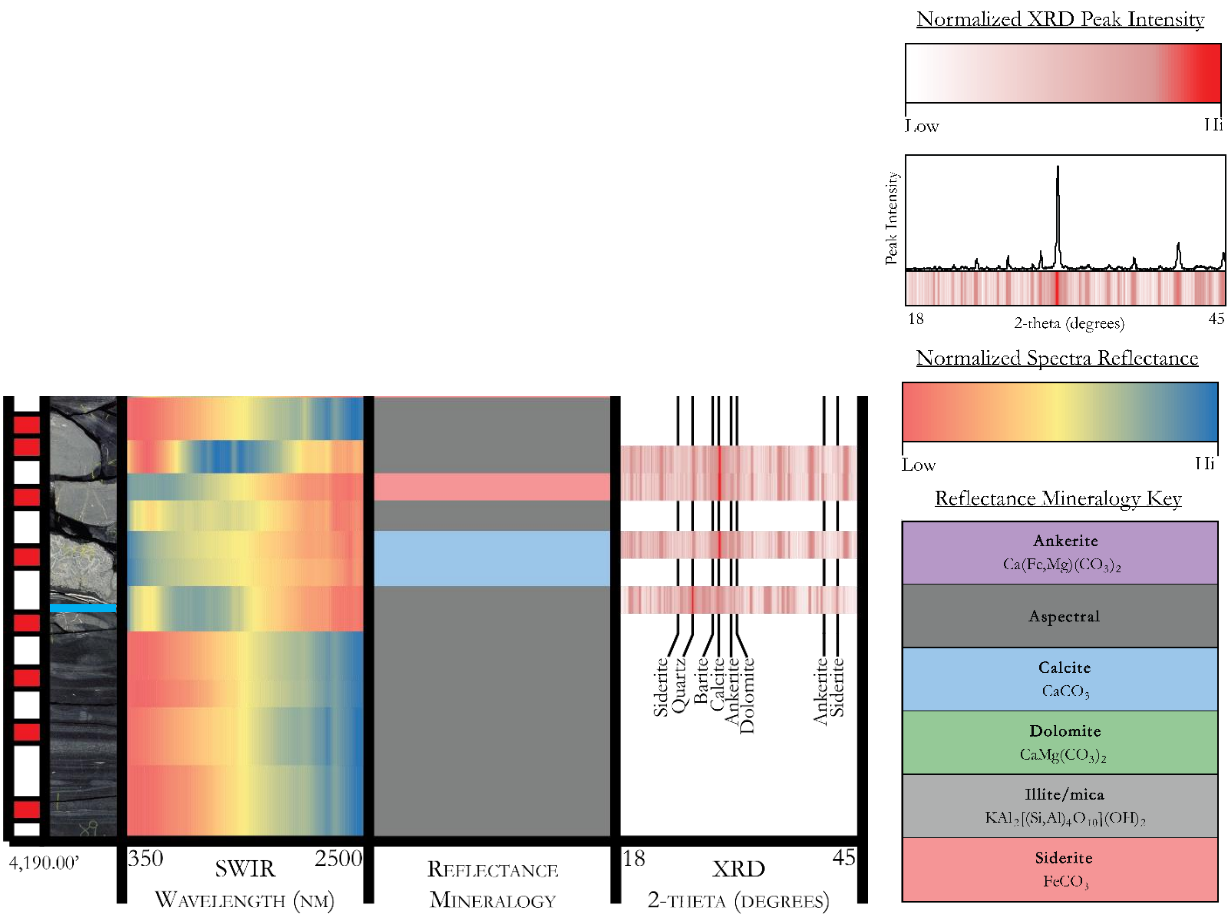

Figure 3.12 (continued from facing page): Compositional results for the TCC core. The central sector is dominated by calcite, corresponding to the Cherry Valley carbonates (between blue lines), whereas the top and bottom intervals are dominated by clay-rich mudstones. Contact between overlying mudstone and Cherry Valley was not recovered during coring. Note the position in feet of the top and bottom of the core interval studied. The red bars at far left represent a sampled interval. Columns of data include: left column are core photographs; second column from left are raw SWIR data; second column from right is SWIR-based automated mineralogy; right column shows mineralogy based on XRD).

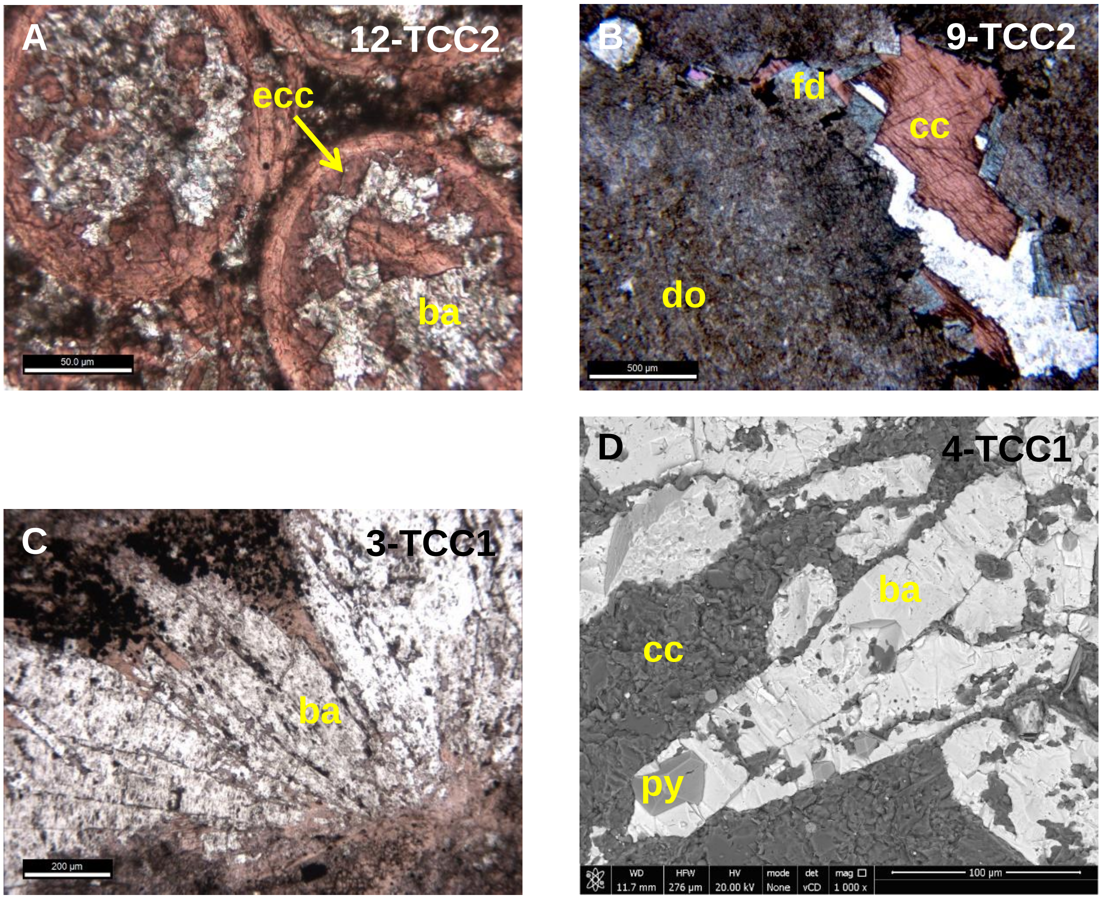

Figure 3.13: TCC core petrologic images: **A**–12-TCC2 (4,187.08 ft) a fossil test is filled with a primary stage of equant calcite (ecc) followed by barite (ba) (Plane-polarized light. Scale bar = 50 µm); **B**–9-TCC2 (4,186.42 ft) one interval has been thoroughly dolomitized (do) and includes zones that feature pores, which have developed due to dissolution, that are filled with ferroan dolomite (fd) and calcite (cc) (Plane-polarized light. Scale bar = 500 µm); **C**–3-TCC1 (4,187.25 ft) radial growths of bladed barite (ba) are a common diagenetic feature and may be partially or entirely replaced by calcite (Plane-polarized light. Scale bar = 200 µm); **D**–4-TCC1 (4,188.25 ft) another view of the morphology of barite blades (ba) and their relationship with a calcareous matrix (Backscatter electron detector. Scale bar = 100 µm).

EGSP NY-4 / Valley Vista View (NY4)

The Cherry Valley carbonates are represented by calcite-rich limestones, as determined by XRD and SWIR analyses, in the NY4 core (Fig. 3.14). These carbonates are compositionally homogenous with few components that have not been calcitized including dolomites. The interval is continuous and does not feature interbedded mudstones, as has been evident in other cores.

Wackestones and packstone

Eight samples are characterized as bedded limestones, which include wackestones and packstones, with a microsparitic variant in the NY4 core (Fig. 3.15A/C). These rocks are texturally similar and are distinguished by fossil content. The matrices are mainly composed of calcite based on petrography and compositional analyses. A poorly laminated microtexture is preserved as diagenesis has largely overprinted depositional fabrics, though depositional horizons are distinguished observed by the alignments of fossil material. These textures are largely overprinted at higher magnification as the matrices are recrystallized to equigranular and xenotopic or hypidiotopic microspar. Poikilotopic fabrics may be present in sparry portions.

Calcite is the predominant diagenetic mineral in the wackestones and packstones. Fossil tests commonly feature equant or bladed calcite growth on the interior and exterior with a drusy calcite (Fig. 3.15A/C), dolomite, or pyrite fill. Minor dolomite cement or rhombohedra are a common diagenetic constituent. Pyrite is typically associated with organic material which is mostly observed as highly degraded, fine, amorphous kerogen that is disseminated throughout the matrix. Calcite-filled fractures intersect one another at 45-degree angles. Irregular, anastomosing stylolites are filled with organic material and clay minerals.

Dacryoconarids (*Styliolina*; Fig. 3.15A) and collapsed, organic-walled cysts (Fig. 3.15C) are the primary fossil types as well as nondescript fragments. The NY4 core includes a higher number of nondescript, disaggregated fossils than other cores.

Crystalline carbonates

Two samples at the depths of 3,844.70 and 3,844.95 feet in the NY4 core are characterized as crystalline carbonates with a microsparitic texture (Fig. 3.15B/D). The matrices of these crystalline carbonates are predominantly composed of calcite based on petrography and compositional analyses. The textures in these rocks are nonlaminated as diagenesis has overprinted depositional fabrics. The matrices are recrystallized to xenotopic, inequigranular microspar.

Calcite is the dominant diagenetic mineral at these intervals. Minor dolomite cement and disseminated rhombohedra (Fig. 3.15D) occur. In addition to the neomorphosed, microsparitic calcite matrix, fossils typically have bladed or equant calcite growths or sparry calcite fill. A felted texture, comprising blades of diagenetic calcite, suggest a stage of barite growth during early diagenesis that has since been replaced by calcite (Fig. 3.15B). Healed, millimeter-scale fractures, filled with calcite, propagate parallel to bedding (Fig. 3.15B). Subvertical, irregular, anastomosing stylolites are common and filled with organic material, framboidal pyrite, and clay minerals. Dacryoconarids and collapsed, organic-walled cysts are the primary fossil types as well as nondescript fragments.

Figure 3.14 (following facing pages): Compositional results for the NY4 core. The bottom two-thirds of the pictured core is dominated by calcite, corresponding to the Cherry Valley carbonates, whereas the top interval is dominated by clay-rich mudstones (not sampled). Underlying mudstones are not pictured. Contact between overlying mudstone and Cherry Valley was not recovered during coring. Note the position in feet of the top and bottom of the core interval studied. The red bars at far left represent a sampled interval. Columns of data include: left column are core photographs; second column from left are raw SWIR data; second column from right is SWIR-based automated mineralogy; right column shows mineralogy based on XRD).

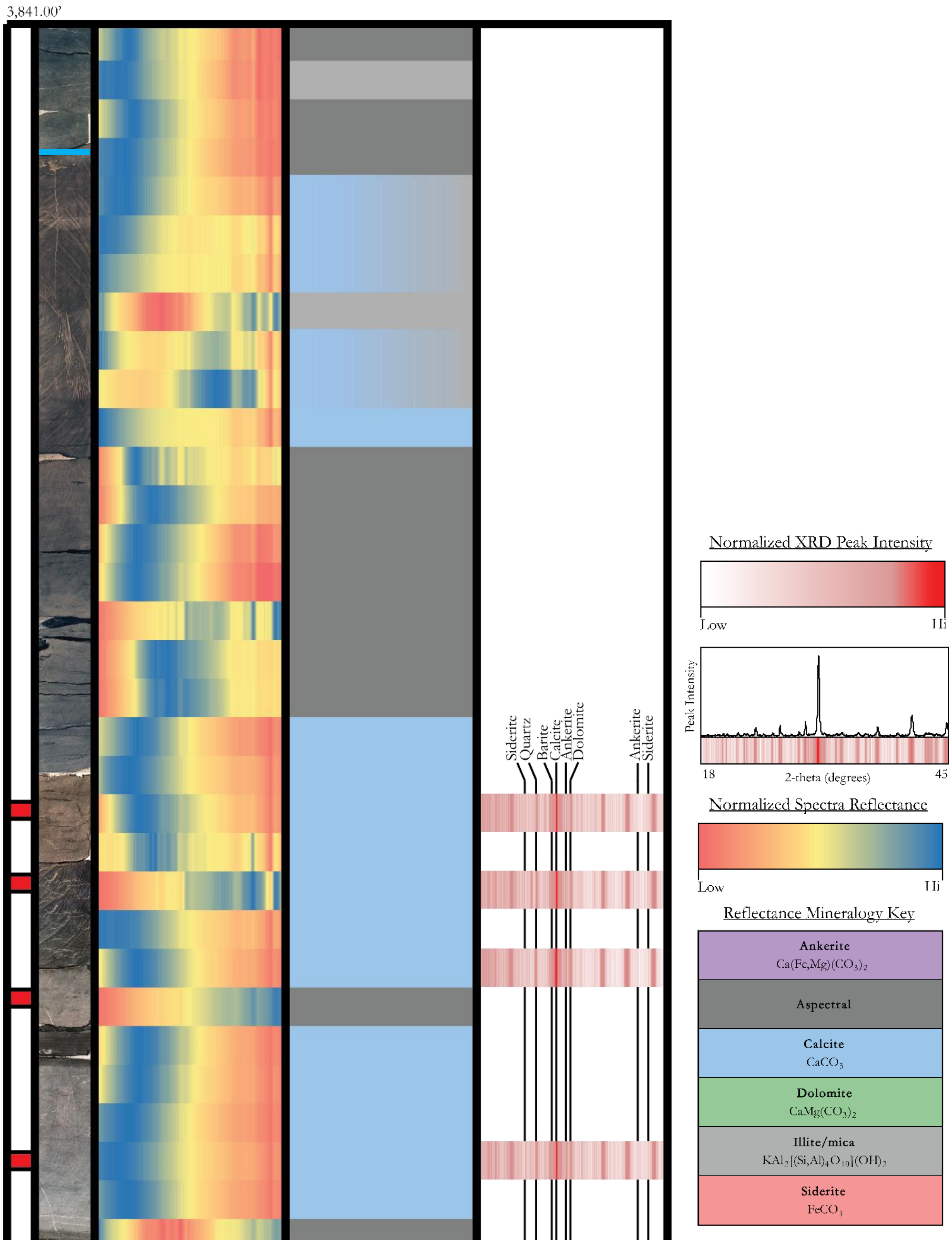
3,841.00'
Siderite
Quartz
Barite
Calcite
Ankerite
Dolomite
Ankerite
Siderite
Normalized XRD Peak Intensity
Low
Hi
Peak Intensity
18
2-theta (degrees)
45
Normalized Spectra Reflectance
Low
Hi
Reflectance Mineralogy Key
Ankerite
Ca(Fe,Mg)(CO3)2
Aspectral
Calcite
CaCO3
Dolomite
CaMg(CO3)2
Illite/mica
KAl2[(Si,Al)4O10](OH)2
Siderite
FeCO3

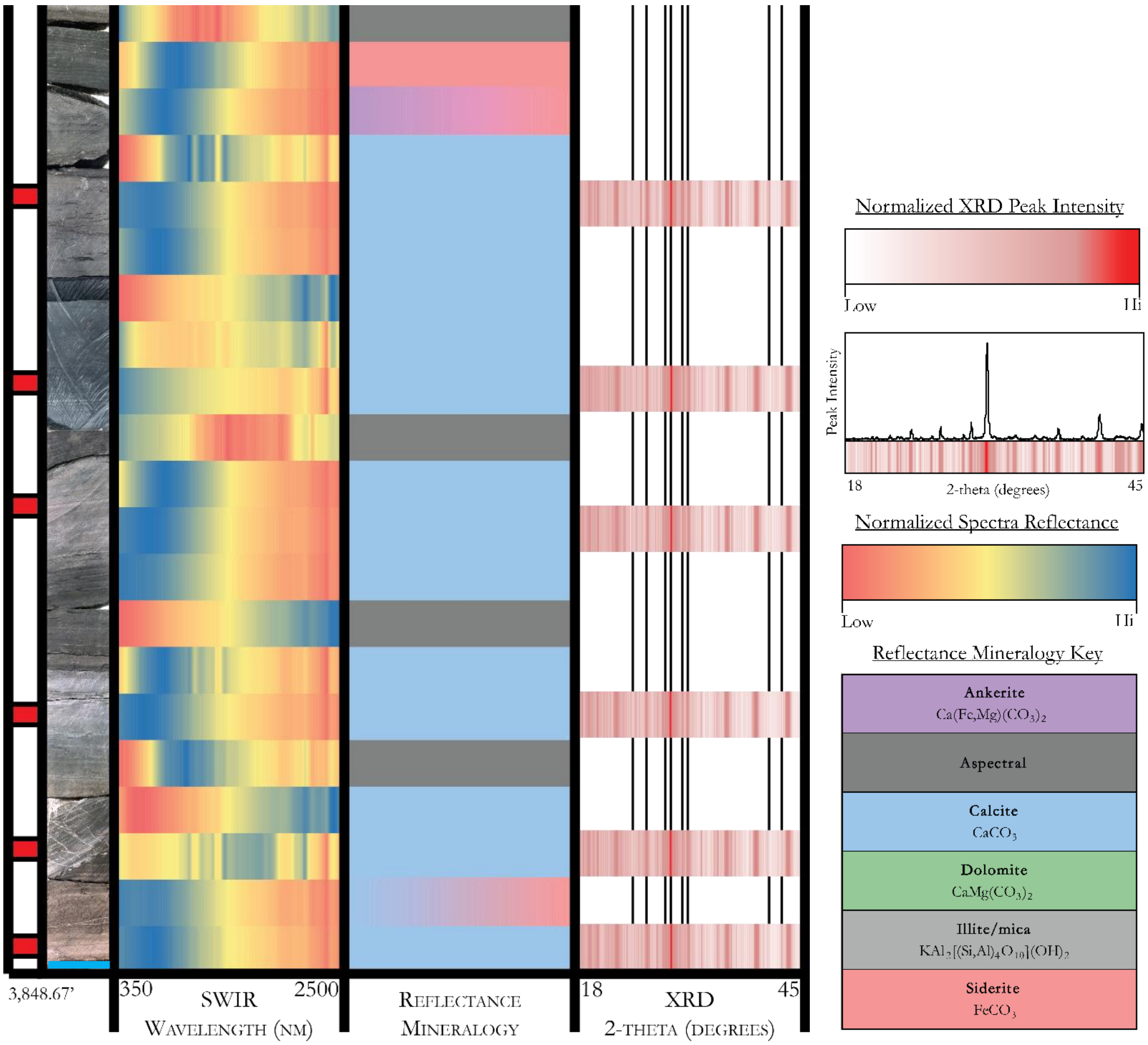
3,848.67'
350
SWIR
2500
WAVELENGTH (NM)
REFLECTANCE
MINERALOGY
18
XRD
45
2-THETA (DEGREES)
Normalized XRD Peak Intensity
Low
Hi
Peak Intensity
18
2-theta (degrees)
45
Normalized Spectra Reflectance
Low
Hi
Reflectance Mineralogy Key
Ankerite
Ca(Fe,Mg)(CO3)2
Aspectral
Calcite
CaCO3
Dolomite
CaMg(CO3)2
Illite/mica
KAl2[(Si,Al)4O10](OH)2
Siderite
FeCO3

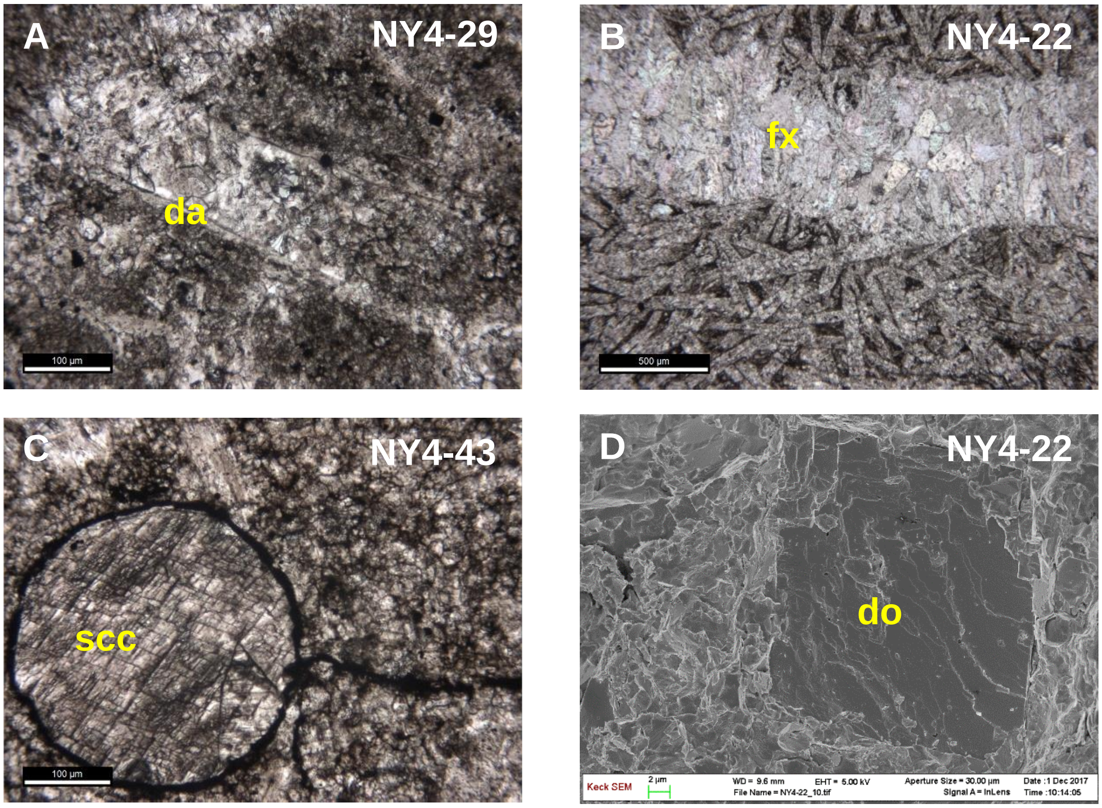

Figure 3.15: NY4 core petrologic images **A**–NY4-29 (3,845.50 ft) dacryoconarids (da) and other fossils are typically filled with sparry calcite while the matrix is recrystallized to microspar (Plane-polarized light. Scale bar = 100 µm); **B**–NY4-22 (3,844.70 ft) a pervasive felted texture, likely the result of nodular barite blades that are subsequently replaced by calcite, is interrupted by septarian-style fractures (fx) (Plane-polarized light. Scale bar = 500 µm); **C**–NY4-43 (3,847.33 ft) an organic-walled cyst is preserved by sparry calcite fill, indicating early diagenetic mineralization (Plane-polarized light. Scale bar = 100 µm); **D**–NY4-22 (3,844.70 ft) dolomite rhombohedra (do) are disseminated through much of the NY4 core, though it does not occur as a cement as seen in other wells (Secondary electron detector. Scale bar = 2 µm).

Beaver Meadow 1 (BMC)

The BMC core features the Cherry Valley carbonates in distinct limestone packages that are separated by interbedded mudstones, as seen in core and compositional analyses (Fig. 3.16). Less advanced neomorphism has protected depositional textures and fabrics better than other cores, with bedded limestones largely making up the Cherry Valley.

Wackestones and packstones

Eight samples are characterized as bedded limestones, including wackestones and packstones, with a microsparitic variant in the BMC core between 1,902.58 and 1,906.17 feet (Fig. 3.17 A/C). These rocks are texturally similar and can be only distinguished by fossil content. The matrices are mainly composed of calcite based on petrography and compositional analyses. At low resolution (e.g., Fig. 3.17A), depositional horizons are distinguished by the alignments, or lack thereof, of fossil material. At higher magnification, depositional textures are largely overprinted by recrystallized or neomorphosed xenotopic microspar. The result is a poorly laminated microtexture due to diagenetic overprinting depositional fabrics.

Calcite is the predominant diagenetic mineral in the wackestones and packstones. Fossil tests commonly feature equant or bladed calcite growth on the interior and exterior with a drusy calcite, dolomite, or pyrite fill. Minor dolomite cement or rhombohedra (Fig. 3.17C) are a common diagenetic constituent. Pyrite is typically associated with organic material which is mostly observed as highly degraded, fine, amorphous kerogen that is disseminated throughout the matrix.

Dacryoconarids (*Styliolina*; Fig. 3.17D) are the primary fossil type as well as nondescript fragments. Select intervals include trilobites (Fig. 3.17A), crinoids, phosphatic bone fragments, and stromatoporoids. Collapsed, organic-walled cysts are observed. In upper wackestones, carbonate allochems resemble algal mat structures.

Calcareous mudstones

Two samples in the BMC core are characterized as calcareous mudstones with fossiliferous modifiers. The calcareous mudstones are located outside of the Cherry Valley Member, at the top (East Berne Member of the Oatka Creek Formation) and bottom (Bakoven Member of the Union Springs Formation) of the sampled interval. These rocks are moderately laminated with fossil fragments defining the bedding plane.

Calcite is the primary diagenetic mineral, particularly within fossiliferous intervals, and is the primary matrix material. Clay minerals make up a negligible proportion of the mudstone matrix. Minor dolomite cements and rhombohedra are disseminated throughout the rocks. The fossil assemblage includes dacryoconarids (*Viriatellina*), conodonts, algal mat structures, and nondescript fragments.

Crystalline carbonates

Two samples between the depths of 1,906.50 and 1,906.75 feet in the BMC core are characterized as crystalline carbonates with a microsparitic texture (Fig. 3.17B). The matrices of these crystalline carbonates are predominantly composed of calcite based on petrography and compositional analyses. The textures in these rocks are nonlaminated as calcite diagenesis has largely rendered depositional fabrics unrecognizable. The matrices are recrystallized to xenotopic, equigranular microspar.

Calcite is the dominant diagenetic mineral at these intervals. Minor dolomite cement is typically associated with fossil fill. In addition to the neomorphosed, microsparitic calcite matrix, fossils typically have bladed or equant calcite growths (Fig. 3.17B) or sparry calcite fill. Subvertical, irregular, anastomosing stylolites are common and filled with organic material, framboidal pyrite, and clay minerals. A diverse fossil assemblage includes dacryoconarids (*Styliolina*), crinoids, stromatoporoids, ostracods, trilobites, and nondescript fragments.

Argillaceous mudstone

One sample at 1,900 feet, within the East Berne Member, is classified as an organic, argillaceous mudstone. This sample is characterized by an elevated organic content that renders much of this rock's thin section to be opaque. Minor amounts of quartz silt and dolomite rhombohedra speckle the matrix.

Figure 3.16 (following facing pages): Compositional results for the Beaver Meadows core. The upper portion of the core is dominated by calcite, corresponding to the Cherry Valley carbonates, whereas the top and bottom intervals are dominated by clay-rich mudstones. Note the position in feet of the top and bottom of the core interval studied. The red bars at far left represent a sampled interval. Columns of data include: left column are core photographs; second column from left are raw SWIR data; second column from right is SWIR-based automated mineralogy; right column shows mineralogy based on XRD.

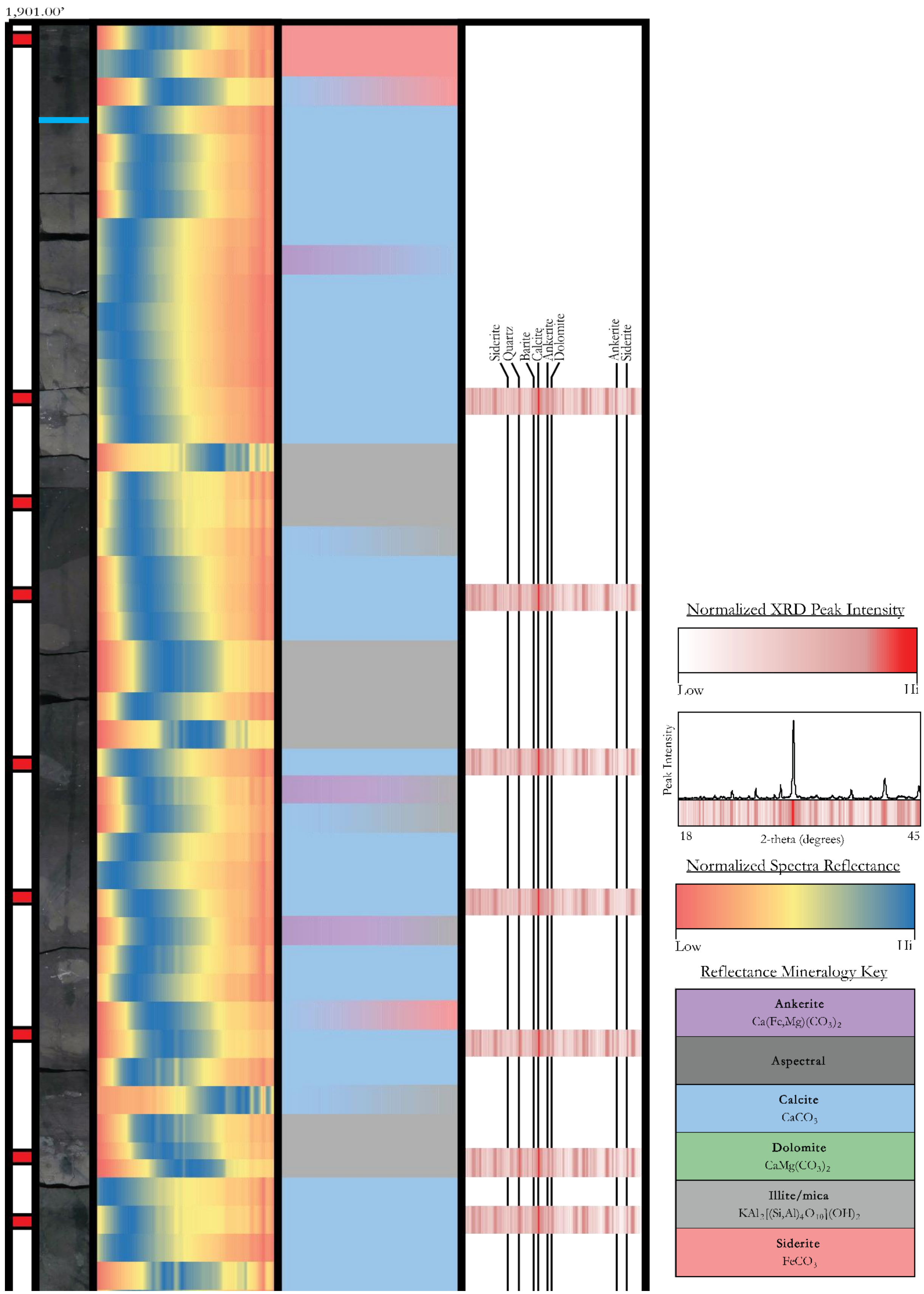
1,901.00'
Siderite
Quartz
Barite
Calcite
Ankerite
Dolomite
Ankerite
Siderite
Normalized XRD Peak Intensity
Low
Hi
Peak Intensity
18
2-theta (degrees)
45
Normalized Spectra Reflectance
Low
Hi
Reflectance Mineralogy Key
Ankerite
Ca(Fe,Mg)(CO3)2
Aspectral
Calcite
CaCO3
Dolomite
CaMg(CO3)2
Illite/mica
KAl2[(Si,Al)4O10](OH)2
Siderite
FeCO3

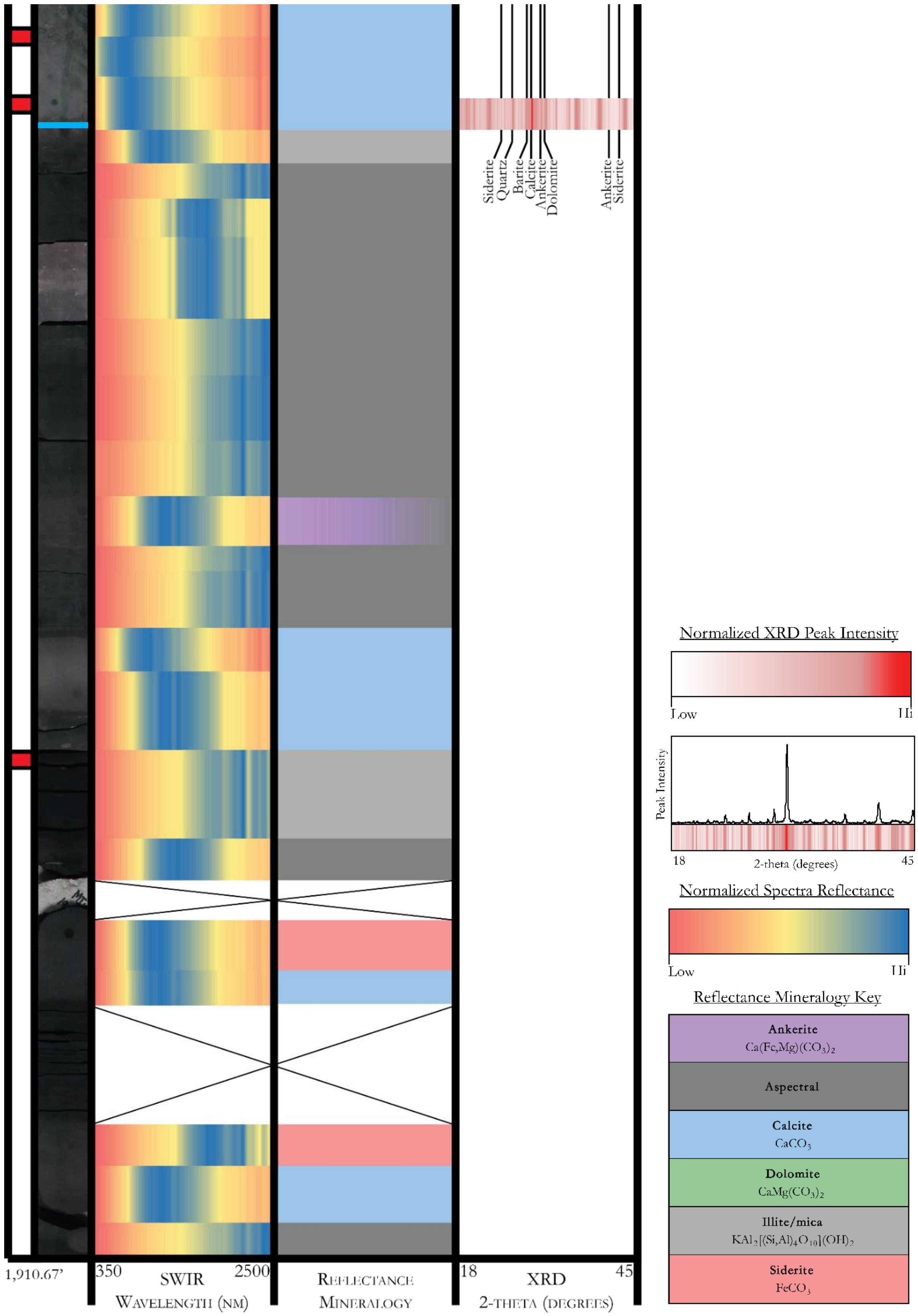
Siderite
Quartz
Barite
Calcite
Ankerite
Dolomite
Ankerite
Siderite
1,910.67'
350
SWIR
2500
Wavelength (nm)
Reflectance
Mineralogy
18
XRD
45
2-theta (degrees)
Normalized XRD Peak Intensity
Low
Hi
Peak Intensity
18
2-theta (degrees)
45
Normalized Spectra Reflectance
Low
Hi
Reflectance Mineralogy Key
Ankerite
$Ca(Fe,Mg)(CO_3)_2$
Aspectral
Calcite
$CaCO_3$
Dolomite
$CaMg(CO_3)_2$
Illite/mica
$KAl_2[(Si,Al)_4O_{10}](OH)_2$
Siderite
$FeCO_3$

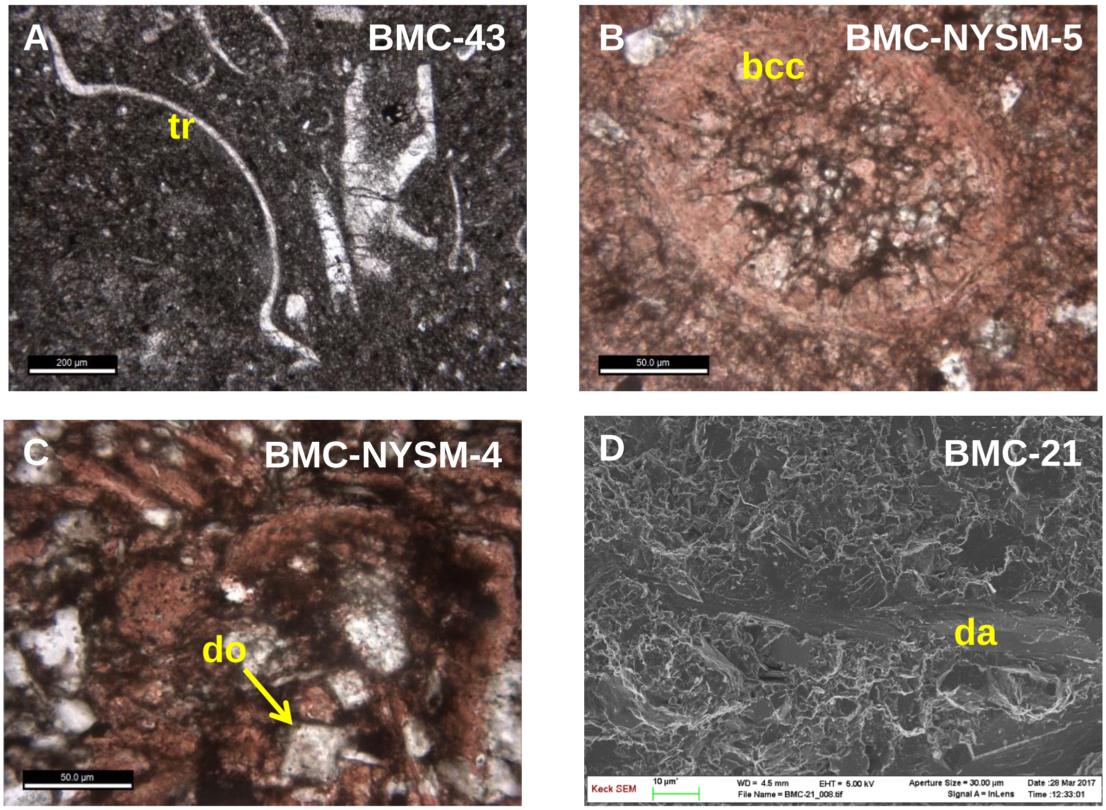

Figure 3.17: BMC core petrologic images **A**–BMC-43 (1,906.17 ft) the cross section of a trilobite is preserved within the microsparitic matrix of this wackestone (Plane-polarized light. Scale bar = 200 µm); **B**–BMC-NYSM-5 (1,906.50 ft) bladed calcite crystallizes on the interior of fossil tests which may be algal cysts (Plane-polarized light. Scale bar = 50 µm); **C**–BMC-NYSM-4 (1,903.00 ft) dolomite rhombohedra are common and disseminated through much of the BMC core (Plane-polarized light. Scale bar = 50 µm); **D**–BMC-21 (1,903.50 ft) dacryoconarids are common throughout the sampled interval and may be filled with sparry or microsparitic calcite (Secondary electron detector. Scale bar = 10 µm).

STABLE ISOTOPE GEOCHEMISTRY

Carbon and oxygen isotope ratios (‰, VPDB) were tested for 80 individual samples (i.e., not including "sister" analyses), between the eight cores from West Virginia (GOFF, MSEEL, WV7), Pennsylvania (WHIP, BE15), and New York (TCC, NY4, BMC). Specific locations of analyzed samples are available in Appendix I. Among all analyses, $\delta^{13}C_{VPDB}$ values range from -15.36 to -0.08 ‰ and $\delta^{18}O_{VPDB}$ values from -0.76 to -11.31 ‰. These results are summarized in Table 3.2 and Figures 3.18 and 3.19.

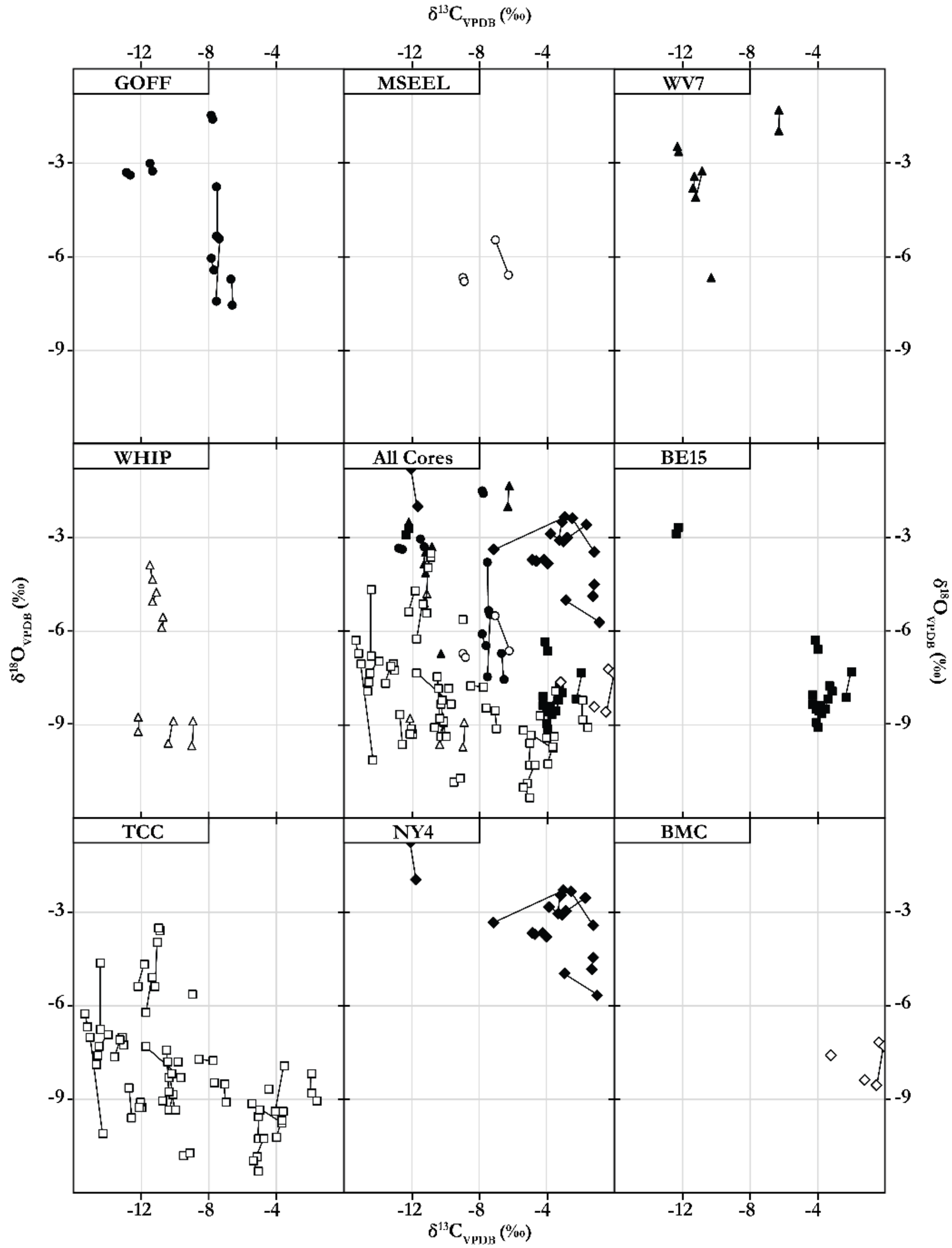

Figure 3.18: Data for the stable isotope ratios of the Cherry Valley limestones. Each core is displayed individually and is marked with a distinct symbol. All cores are displayed together at center. "Sister" samples from each depth are tied together with a bar.

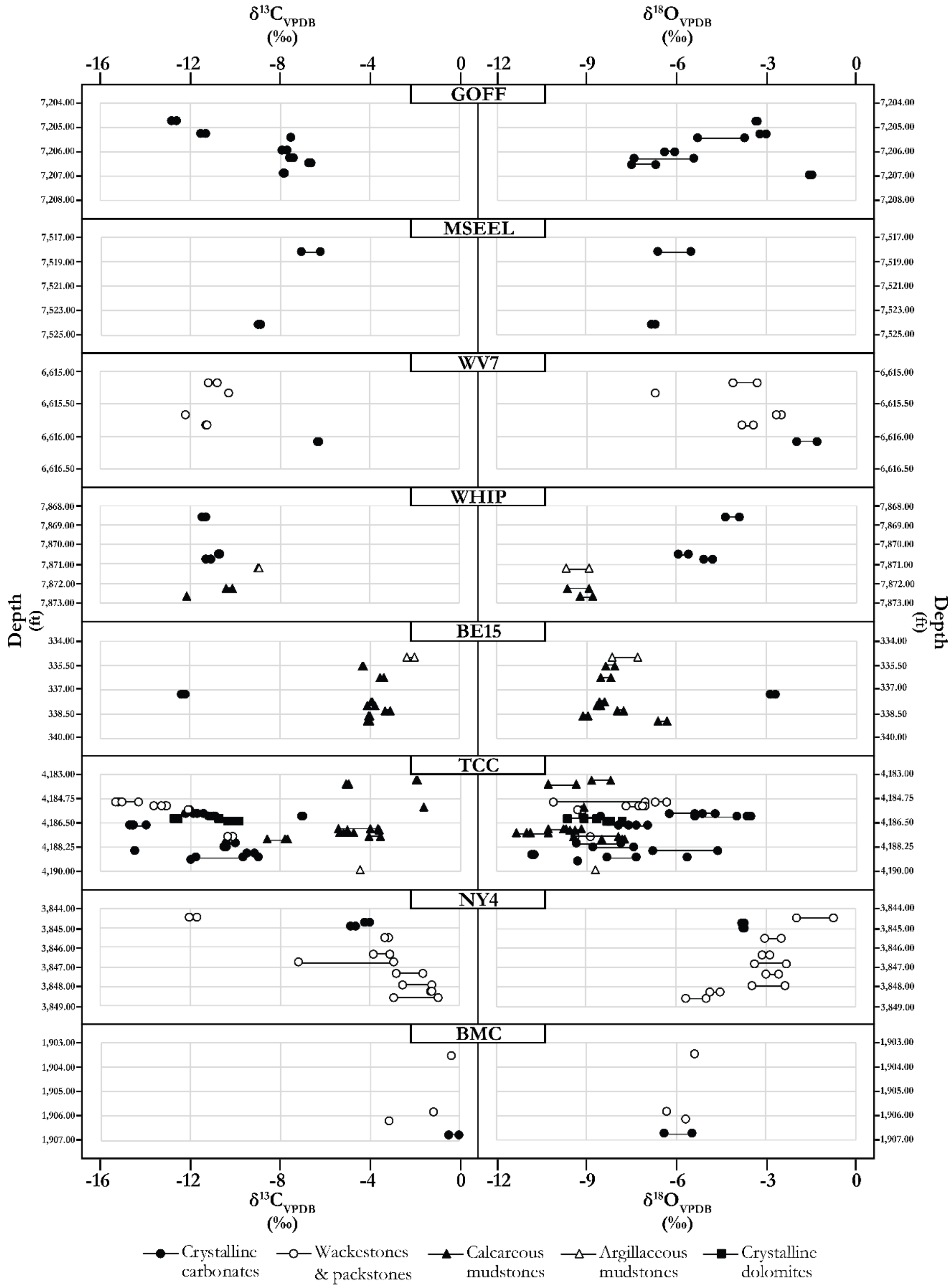

Figure 3.19: $\delta^{13}C$ and $\delta^{18}O$ values at their respective depths in all cores and designated by lithology. Paired samples for each depth are tied together with a bar.

Variance of isotopic values in each core are largely dependent on lithology (Fig. 3.19), namely between mudstones ($n = 24$) and limestones ($n = 52$), inclusive of wackestones, packstones, and crystalline carbonates (Fig. 3.20). The range of $\delta^{13}C$ and $\delta^{18}O$ is similar between bedded limestones (wackestones and packstones) and crystalline carbonates which are interpreted to be more highly altered. The $\delta^{18}O$ values in limestones are heavier (mean = -5.49 ‰; $\sigma = 2.40$ ‰) than mudstones (mean = -8.86 ‰; $\sigma = 1.06$ ‰). The $\delta^{13}C$ values show an opposite trend, as limestones are lighter (mean = -8.93 ‰; $\sigma = 4.17$ ‰) than mudstones (mean = -5.07 ‰; $\sigma = 2.65$ ‰). Samples with significant dolomite content display weaker covariance between carbon and oxygen isotope values. Limestones with elevated dolomite (Table 3.1; $n = 10$), including crystalline dolomites and samples denoted as "dolomitic", are isotopically lighter in both $\delta^{13}C$ (mean = -12.90 ‰; $\sigma = 1.75$ ‰) and $\delta^{18}O$ (mean = -7.70 ‰; $\sigma = 1.34$ ‰) than dolomite-poor rocks ($n = 46$; $\delta^{13}C$ mean = -8.25 ‰; $\sigma = 3.97$ ‰ and $\delta^{18}O$ mean = -5.19 ‰; $\sigma = 2.38$ ‰).

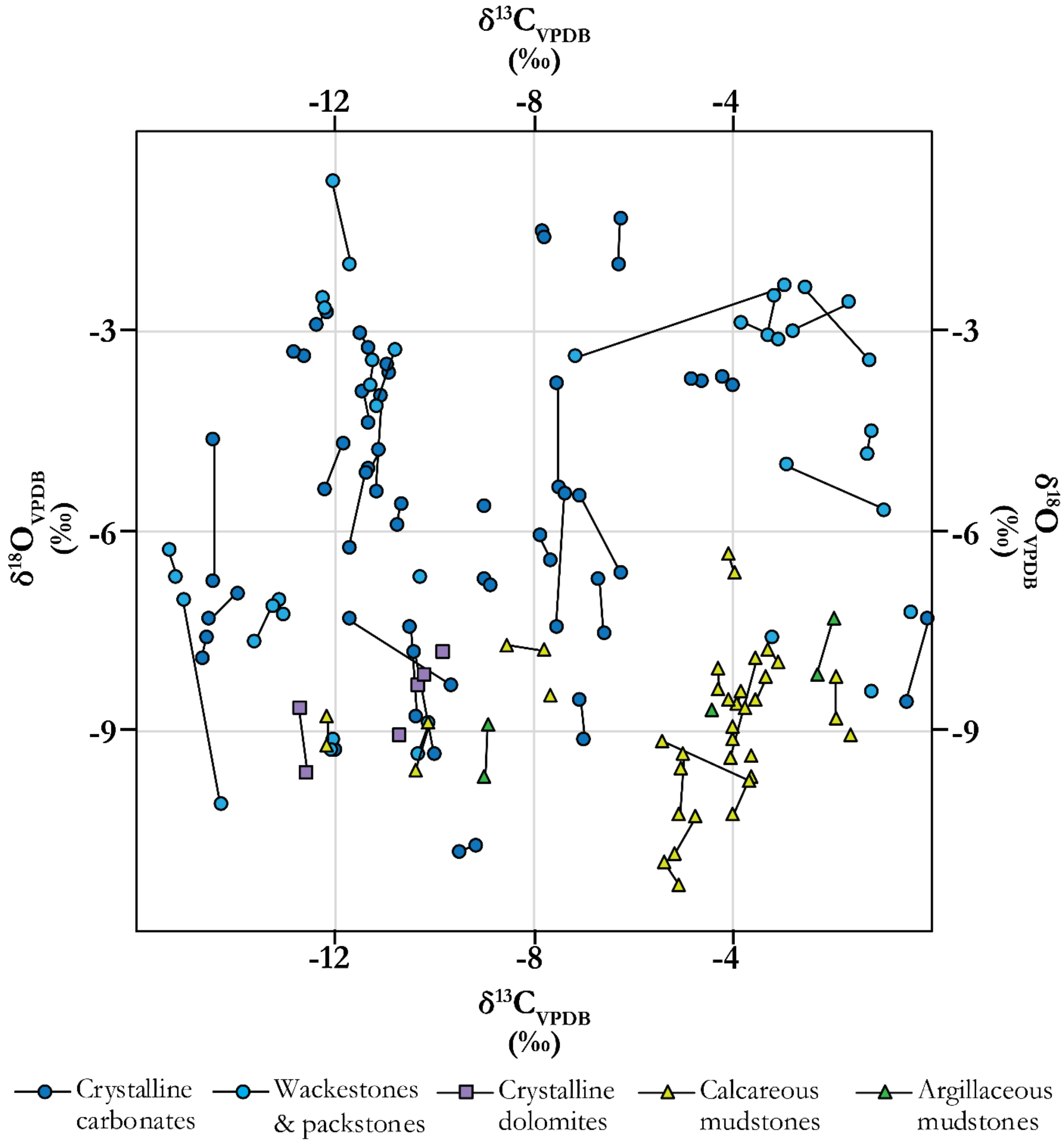

Figure 3.20: Comparison of stable-isotope ratios and lithology of all studied samples. Paired samples for each depth are tied together with a bar.

The TCC core is the most sampled (n = 37) and well understood due to its role as a pilot well to the study, and it most tightly constrains the relationship between isotopic composition and lithology (Figs. 3.21 and 3.22). The $\delta^{13}C$ of limestones (wackestones, packstones, crystalline carbonates, and crystalline dolomites) progressively grows heavier with increasing depth. Conversely, mudstones (calcareous and argillaceous varieties) have progressively lighter $\delta^{13}C$ with depth. Any minor trends in oxygen isotope ratios for either lithologic group are not considered statistically significant. Though the range of isotopic compositions is generally unique to each core, these trends are generally present in all sampled lithologies (Fig. 3.20).

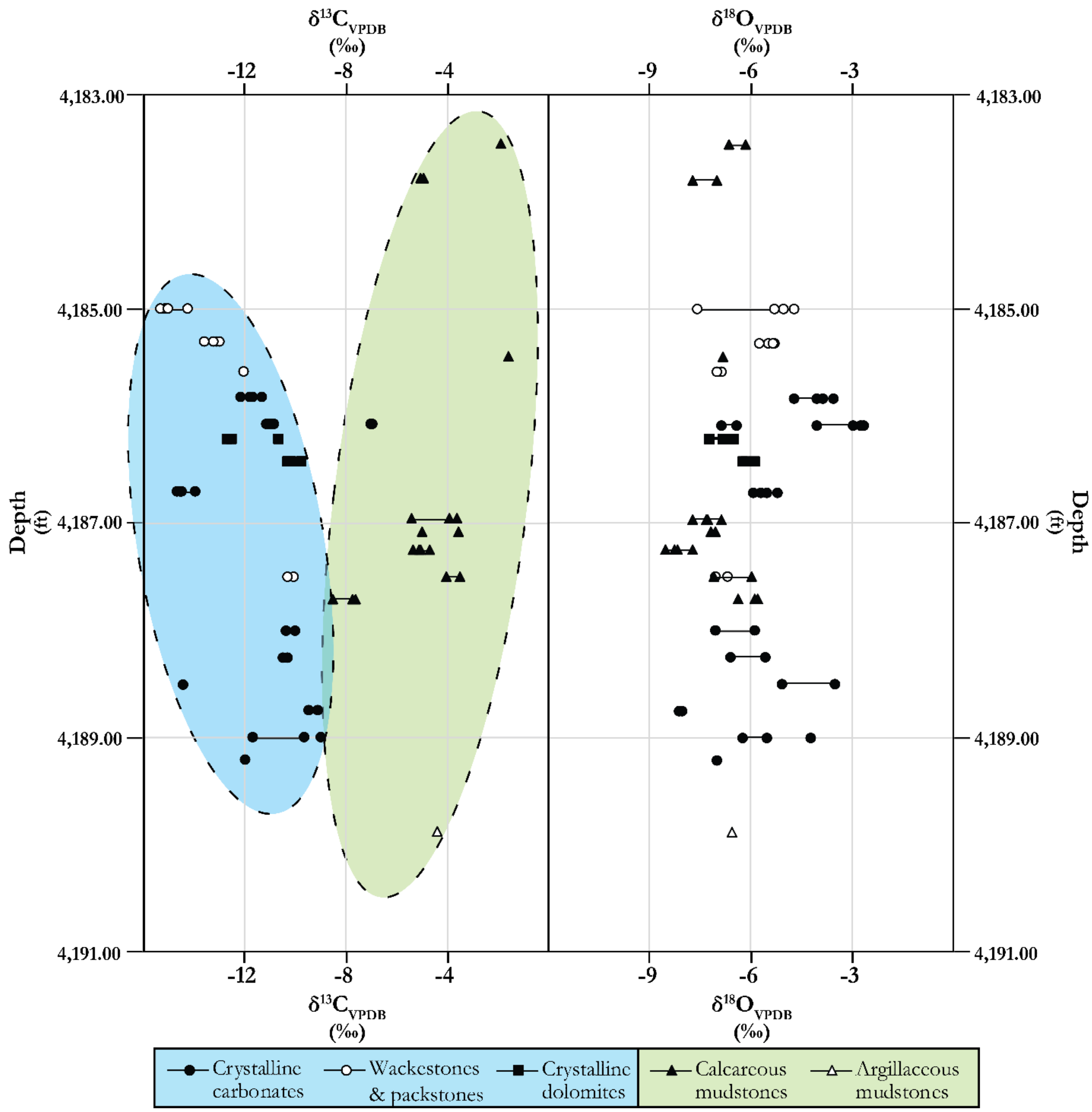

Figure 3.21: $\delta^{13}C$ and $\delta^{18}O$ values in the TCC cores are highlighted due to the number of samples. Trends in the carbonate isotopes in limestones (blue, including crystalline carbonates and bedded limestones) and mudstones (green) are highlighted. Paired samples for each depth are tied together with a bar.

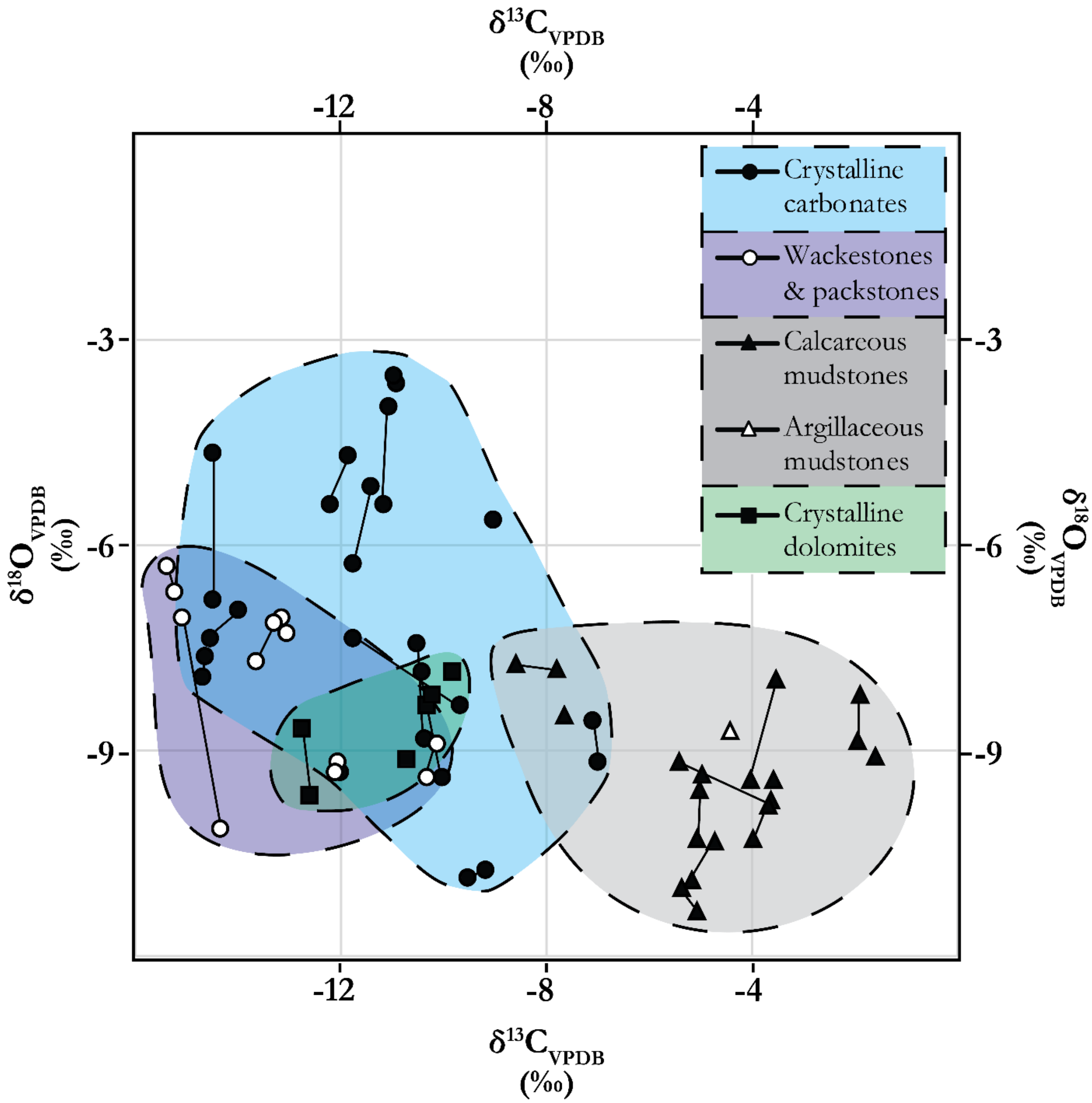

Figure 3.22: Lithologies in the TCC core show preferential grouping in stable isotope composition. Limestones, including crystalline carbonates, bedded limestones, and crystalline dolomite, contrast strongly with mudstones without including depth as a factor. Paired samples for each depth are tied together with a bar.

Spatial variations in isotopic composition in limestones, including wackestones, packstones, crystalline carbonates, and crystalline dolomites, occur perpendicular to the generally southwest-to-northeast trending axis of the Appalachian orogenic front (Fig.

3.23). Carbon and oxygen isotope compositions are progressively heavier from southeast (proximal – $\delta^{13}C$ mean = -10.12 ‰; σ = 3.58 ‰ and $\delta^{18}O$ mean = -6.85 ‰; σ = 2.11 ‰) to northwest (distal – $\delta^{13}C$ mean = -5.92 ‰; σ = 4.07 ‰ and $\delta^{18}O$ mean = -3.31 ‰; σ = 1.25 ‰).

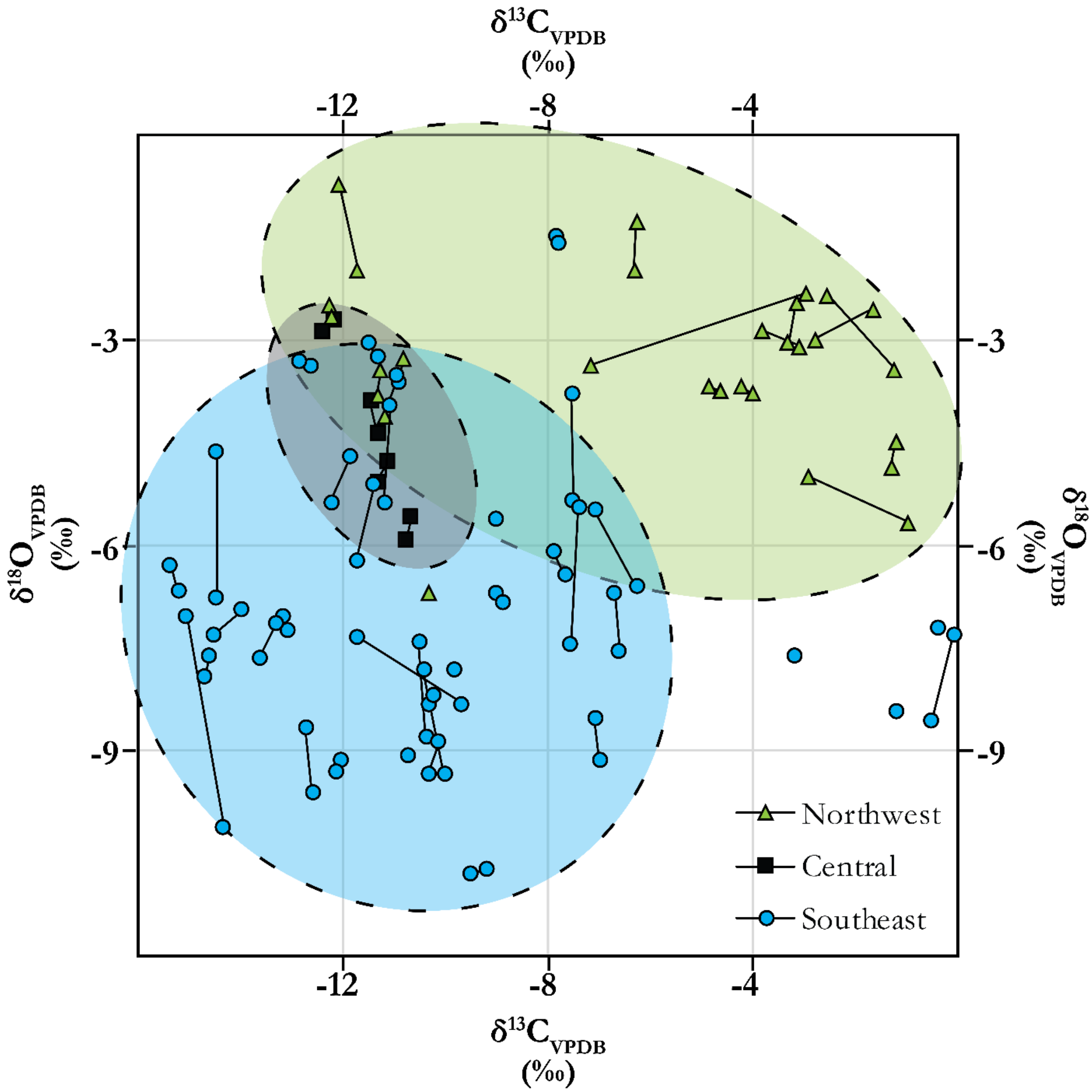

Figure 3.23: Comparison of stable-isotope ratios in limestones (wackestones, packstones, and crystalline carbonates) and their position respective to the Appalachian orogenic axis. Spatial groups trendline indicates the generalized separation of isotopic compositions between limestones in the most distal (northwest – green grouping) cores, the central cores (gray grouping) that were studied and those more proximal (southeast – blue grouping). The WHIP and BE15 cores are considered central and lay within the transition of isotopic values between the distal (WV7/NY4) and proximal (GOFF/MSEEL/TCC/BMC) cores. Paired samples for each depth are tied together with a bar.

Textural heterogeneity affects isotopic compositions in limestones that include wackestones, packstones, crystalline carbonates, and crystalline dolomites (Fig. 3.24). Generally, samples that are "microsparitic" are heavier in carbon (mean = -7.61 ‰; σ = 4.19 ‰) and oxygen (mean = -4.72 ‰; σ = 2.32 ‰) isotope ratios as opposed to limestones that possess micritic or sparitic matrices ($\delta^{13}C$ mean = -12.11 ‰; σ = 2.12 ‰ and $\delta^{18}O$ mean = -7.27 ‰; σ = 1.80 ‰). A smaller subset of rocks with a "felted" texture, implying an earlier diagenetic stage of likely bladed barite crystallization that has subsequently been mostly replaced by calcite, has distinct ranges of carbon (mean = -8.14 ‰; σ = 3.02 ‰) and oxygen (mean = -6.32 ‰; σ = 2.25 ‰) compositions.

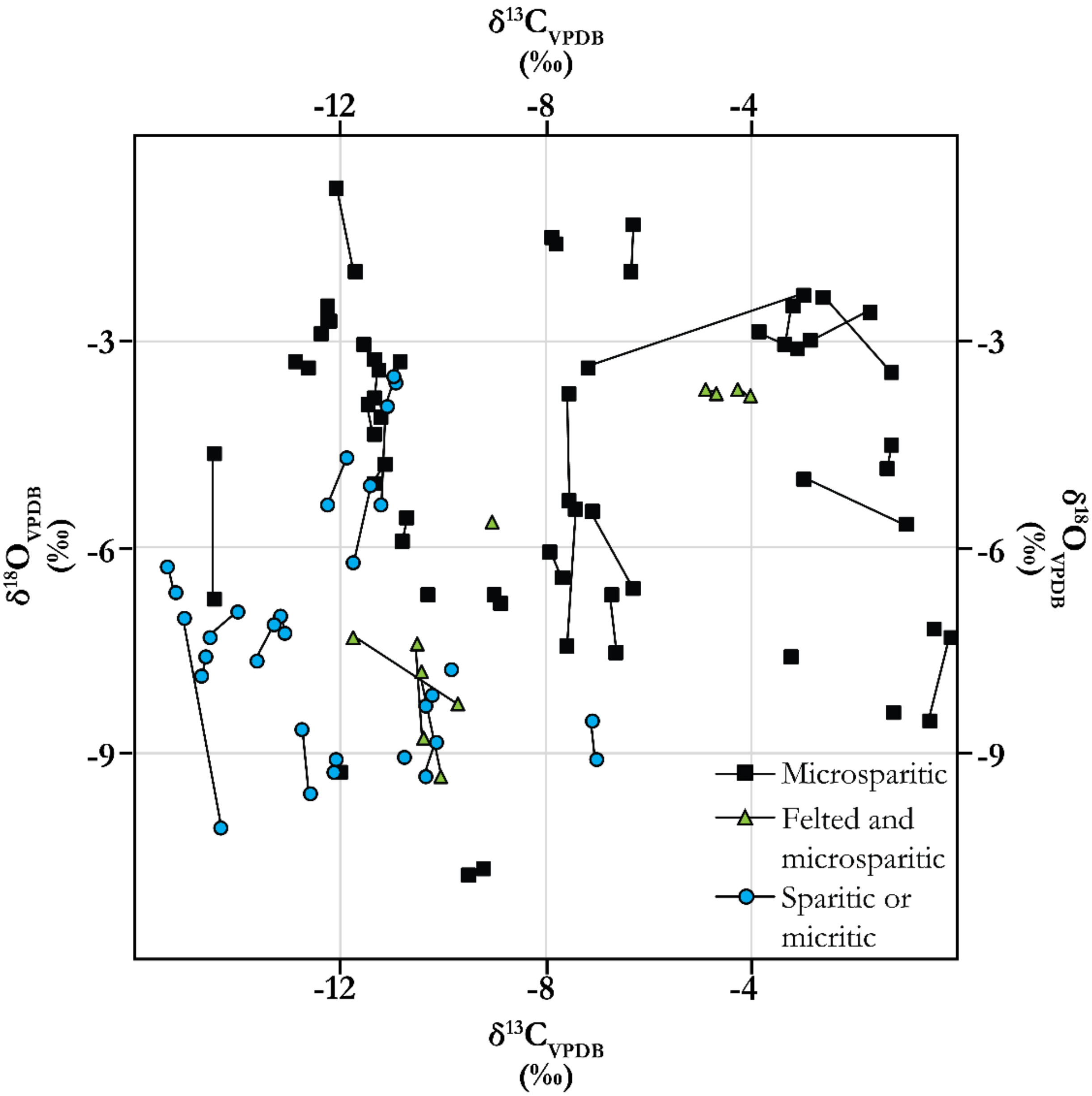

Figure 3.24: Stable isotope ratios of limestones are compared according to textural characteristics. Generally, sparitic or micritic textures represent the lowest degree of neomorphism whereas microsparitic and felted textures are interpreted as more advanced stages of recrystallization.

Thermal covariance, as determined by interpolating Conodont Alteration Index (CAI) data from Repetski et al (2011), is best displayed by carbon isotope ratios of mudstones in the sample suite (Fig. 3.25). In samples that are interpreted to have been exposed to conditions consistent with CAI values of 2.5 – 3.0, carbon isotope ratios have a mean of -10.46 ‰ with a standard deviation of 1.44; in samples with CAI values of 3.0 – 3.5, the mean is -4.64 ‰ with a standard deviation of 1.81; and in samples with CAI values of 3.5 – 4.0, the mean is -3.62 ‰ with a standard deviation of 0.67.

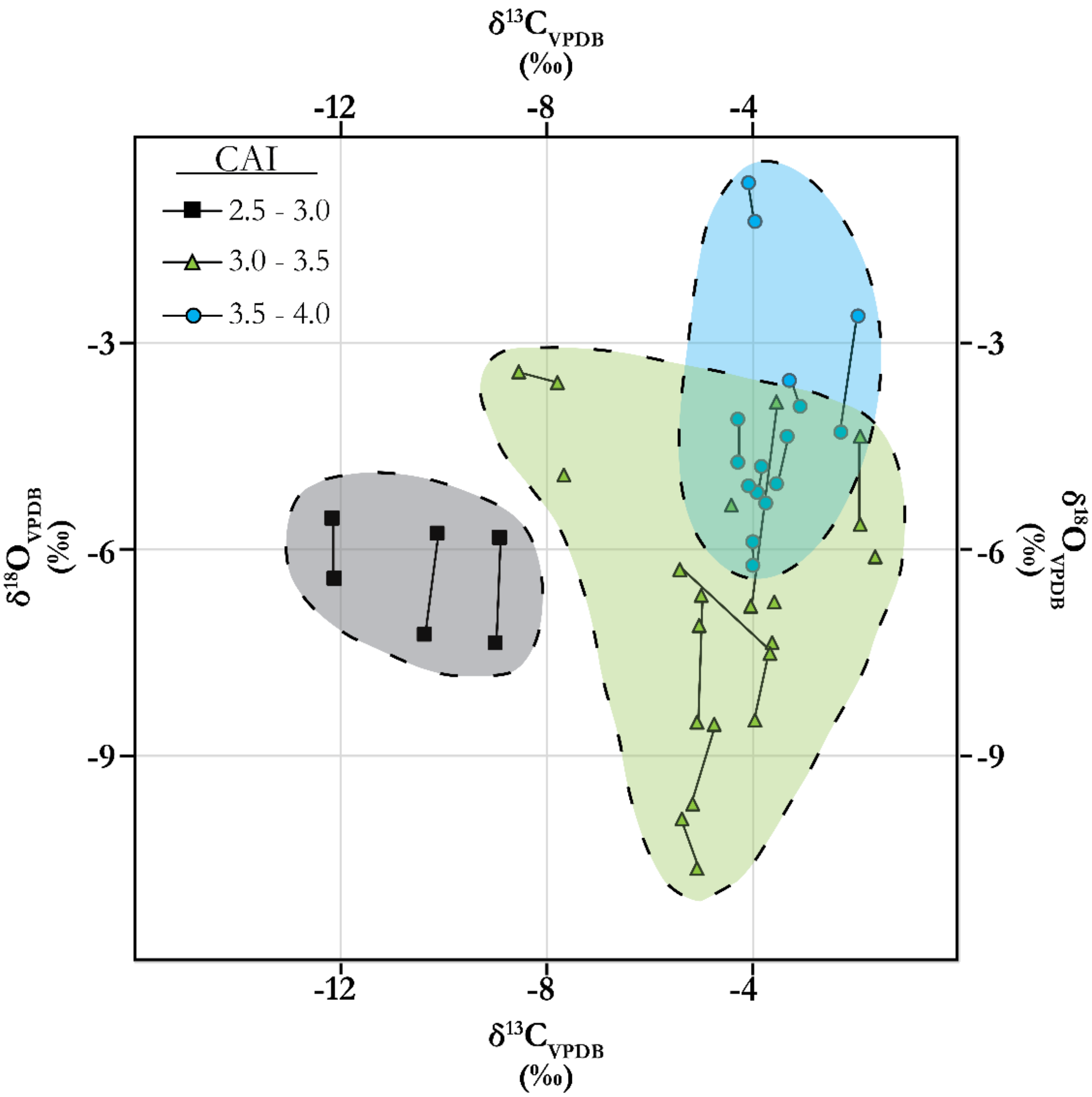

Figure 3.25: Stable-isotope grouping of mudstones based on an interpolated model of thermal alternation, as determined by Conodont Alteration Index (CAI). An interpolated model CAI, based on previously published oil and gas well data (Repetski et al., 2008), in the Appalachian basin was used to generalize zones of thermal maturation.

Table 3.2: Stable carbon and oxygen isotope ratios from selected samples from cores in West Virginia, Pennsylvania, and New York.

Sample ID	Depth (ft)	Sample A				Sample B			
		$\delta^{13}C_{VPDB}$ (‰)	$\delta^{13}C$ S.D.	$\delta^{18}O_{VPDB}$ (‰)	$\delta^{18}D$ S.D.	$\delta^{13}C_{VPDB}$ (‰)	$\delta^{13}C$ S.D.	$\delta^{18}O_{VPDB}$ (‰)	$\delta^{18}D$ S.D.
GOFF-10/11-1	7,204.75	-12.63	0.034	-3.37	0.274	-12.86	0.034	-3.30	0.274
GOFF-17-1	7,205.25	-11.51	0.034	-3.03	0.274	-11.33	0.034	-3.26	0.274
GOFF-19/20-1	7,205.42	-7.52	0.034	-5.33	0.274	-7.54	0.034	-3.77	0.274
GOFF-26/27-1	7,205.96	-7.67	0.034	-6.44	0.274	-7.89	0.034	-6.07	0.274
GOFF-31/32-1	7,206.25	-7.56	0.034	-7.43	0.274	-7.40	0.034	-5.45	0.274
GOFF-35/36-1	7,206.50	-6.60	0.034	-7.54	0.274	-6.70	0.034	-6.71	0.274
GOFF-39/40-1	7,206.92	-7.85	0.034	-1.49	0.274	-7.80	0.034	-1.58	0.274
MSEEL-15-1	7,518.17	-7.09	0.034	-5.48	0.274	-6.26	0.034	-6.61	0.274
MSEEL-58/59-1	7,524.08	-9.01	0.034	-6.70	0.274	-8.88	0.034	-6.81	0.274
WV7-1-1	6,615.17	-10.82	0.034	-3.29	0.274	-11.19	0.034	-4.11	0.274
WV7-3-1	6,615.33	-10.30	0.034	-6.68	0.274	N/A			
WV7-6-1	6,615.67	-12.24	0.034	-2.49	0.274	-12.23	0.034	-2.65	0.274
WV7-8-1	6,615.83	-11.32	0.034	-3.81	0.274	-11.26	0.034	-3.43	0.274
WV7-12-1	6,616.08	-6.31	0.034	-1.99	0.274	-6.27	0.034	-1.29	0.274
WHIP-36-1	7,868.58	-11.34	0.034	-4.36	0.274	-11.46	0.034	-3.90	0.274
WHIP-3-1	7,869.83	N/A				N/A			
WHIP-9-1	7,870.50	-10.77	0.138	-5.91	0.366	-10.68	0.034	-5.58	0.274
WHIP-12-1	7,870.75	-11.33	0.034	-5.07	0.274	-11.12	0.034	-4.78	0.274
WHIP-17-1	7,871.25	-9.00	0.034	-9.67	0.274	-8.93	0.034	-8.90	0.274
WHIP-23-1	7,872.25	-10.12	0.034	-8.88	0.274	-10.39	0.034	-9.60	0.274
WHIP-28-1	7,872.67	-12.16	0.034	-9.21	0.274	-12.18	0.034	-8.77	0.274

Table 3.2 (cont.): Stable carbon and oxygen isotope ratios from selected samples from cores in West Virginia, Pennsylvania, and New York.

Sample ID	Depth (ft)	Sample A				Sample B			
		$\delta^{13}C_{VPDB}$ (‰)	$\delta^{13}C$ S.D.	$\delta^{18}O_{VPDB}$ (‰)	$\delta^{18}D$ S.D.	$\delta^{13}C_{VPDB}$ (‰)	$\delta^{13}C$ S.D.	$\delta^{18}O_{VPDB}$ (‰)	$\delta^{18}D$ S.D.
BE15-10-1	335.00	-1.99	0.142	-7.30	0.247	-2.32	0.142	-8.14	0.247
BE15-16-1	335.50	-4.31	0.142	-8.05	0.247	-4.29	0.142	-8.36	0.247
BE15-23-1	336.25	-3.34	0.142	-8.18	0.247	-3.54	0.142	-8.52	0.247
BE15-33-1	337.25	-12.19	0.142	-2.70	0.247	-12.38	0.142	-2.89	0.247
BE15-38-1	337.70	-3.92	0.142	-8.58	0.247	-3.85	0.142	-8.40	0.247
BE15-42-1	338.00	-3.76	0.142	-8.66	0.247	-4.09	0.142	-8.54	0.247
BE15-45-1	338.25	-3.11	0.142	-7.95	0.247	-3.29	0.142	-7.76	0.247
BE15-49-1	338.60	-4.03	0.142	-8.94	0.247	-4.00	0.142	-9.11	0.247
BE15-52-1	338.95	-4.11	0.034	-6.33	0.274	-3.99	0.034	-6.61	0.274
BE15-54-1	339.13	N/A				N/A			
1-TCC2-1	4,183.46	-1.94	0.150	-8.17	0.281	-1.95	0.150	-8.82	0.281
2-TCC2-1	4,183.79	-5.00	0.159	-9.33	0.452	-5.08	0.150	-10.26	0.281
2-TCC1-1	4,185.00	-15.21	0.184	-6.67	0.414	-15.36	0.184	-6.28	0.414
2-TCC1-2	4,185.00	-15.05	0.184	-7.03	0.414	-14.32	0.455	-10.10	0.307
3-TCC2-1	4,185.31	-13.15	0.159	-7.02	0.452	-13.07	0.159	-7.25	0.452
3-TCC2-2	4,185.31	-13.62	0.159	-7.65	0.452	-13.28	0.159	-7.12	0.452
4-TCC2-1	4,185.44	N/A				-1.65	0.150	-9.05	0.281
5-TCC2-1	4,185.58	-12.06	0.159	-9.11	0.452	-12.11	0.159	-9.28	0.452
6-TCC2-1	4,185.83	-11.86	0.159	-4.68	0.452	-12.22	0.159	-5.37	0.452
6-TCC2-2	4,185.83	-11.73	0.150	-6.23	0.281	-11.40	0.159	-5.11	0.452
7-TCC2-1	4,186.08	-10.92	0.159	-3.61	0.452	-10.95	0.159	-3.50	0.452
7-TCC2-2	4,186.08	-11.18	0.159	-5.39	0.452	-11.08	0.159	-3.95	0.452
7-TCC2-3	4,186.08	-7.09	0.159	-8.53	0.452	-7.01	0.159	-9.11	0.452

Table 3.2 (cont.): Stable carbon and oxygen isotope ratios from selected samples from cores in West Virginia, Pennsylvania, and New York.

Sample ID	Depth (ft)	Sample A				Sample B			
		$\delta^{13}C_{VPDB}$ (‰)	$\delta^{13}C$ S.D.	$\delta^{18}O_{VPDB}$ (‰)	$\delta^{18}D$ S.D.	$\delta^{13}C_{VPDB}$ (‰)	$\delta^{13}C$ S.D.	$\delta^{18}O_{VPDB}$ (‰)	$\delta^{18}D$ S.D.
8-TCC2-1	4,186.21	-12.73	0.159	-8.65	0.452	-12.58	0.159	-9.61	0.452
8-TCC2-2	4,186.21	-10.72	0.159	-9.07	0.452	N/A			
9-TCC2-1	4,186.42	-9.83	0.150	-7.80	0.281	N/A			
9-TCC2-2	4,186.42	-10.34	0.150	-8.31	0.281	-10.21	0.150	-8.17	0.281
10-TCC2-1	4,186.71	-13.98	0.150	-6.93	0.281	-14.53	0.150	-7.31	0.281
10-TCC2-2	4,186.71	-14.69	0.150	-7.90	0.281	-14.61	0.150	-7.60	0.281
11-TCC2-1	4,186.96	-5.43	0.150	-9.14	0.281	-3.68	0.150	-9.74	0.281
11-TCC2-2	4,186.96	-3.99	0.184	-10.24	0.414	-3.66	0.150	-9.67	0.281
12-TCC2-1	4,187.08	-3.62	0.142	-9.37	0.247	N/A			
12-TCC2-2	4,187.08	-5.04	0.184	-9.54	0.414	N/A			
3-TCC1-1	4,187.25	-5.19	0.455	-10.84	0.307	-4.75	0.455	-10.27	0.307
3-TCC1-2	4,187.25	-5.08	0.455	-11.31	0.307	-5.39	0.455	-10.96	0.307
13-TCC2-1	4,187.33	N/A				N/A			
14-TCC2-1	4,187.50	-4.06	0.184	-9.40	0.414	-3.54	0.184	-7.92	0.414
14-TCC2-2	4,187.50	-10.13	0.455	-8.86	0.307	-10.35	0.455	-9.34	0.307
15-TCC2-1	4,187.71	-7.67	0.142	-8.45	0.247	N/A			
15-TCC2-2	4,187.71	-8.57	0.184	-7.71	0.414	-7.79	0.184	-7.78	0.414
16-TCC2-1	4,187.83	N/A				N/A			
17-TCC2-1	4,188.00	-10.43	0.184	-7.82	0.414	-10.03	0.455	-9.34	0.307
4-TCC1-1	4,188.25	-10.38	0.142	-8.78	0.247	-10.51	0.184	-7.42	0.414
4-TCC1-2	4,188.25	N/A				N/A			
18-TCC2-1	4,188.50	-14.46	0.455	-6.76	0.307	-14.46	0.138	-4.63	0.366
18-TCC2-2	4,188.50	N/A				N/A			

Table 3.2 (cont.): Stable carbon and oxygen isotope ratios from selected samples from cores in West Virginia, Pennsylvania, and New York.

Sample ID	Depth (ft)	Sample A				Sample B			
		$\delta^{13}C_{VPDB}$ (‰)	$\delta^{13}C$ S.D.	$\delta^{18}O_{VPDB}$ (‰)	$\delta^{18}D$ S.D.	$\delta^{13}C_{VPDB}$ (‰)	$\delta^{13}C$ S.D.	$\delta^{18}O_{VPDB}$ (‰)	$\delta^{18}D$ S.D.
19-TCC2-1	4,188.75	-9.51	0.455	-10.80	0.307	-9.18	0.455	-10.71	0.307
6-TCC1-1	4,189.00	-11.74	0.455	-7.32	0.307	-9.68	0.455	-8.30	0.307
6-TCC1-2	4,189.00	-9.02	0.184	-5.62	0.414	N/A			
20-TCC2-1	4,189.21	N/A				N/A			
20-TCC2-2	4,189.21	N/A				-12.00	0.455	-9.28	0.307
21-TCC2-1	4,189.42	N/A				N/A			
22-TCC2-1	4,189.88	N/A				-4.44	0.184	-8.68	0.414
NY4-20-1	3,844.45	-12.07	0.034	-0.76	0.274	-11.71	0.034	-1.98	0.274
NY4-22-1	3,844.70	-3.99	0.034	-3.80	0.274	-4.23	0.138	-3.69	0.366
NY4-24-1	3,844.95	-4.65	0.138	-3.74	0.366	-4.86	0.138	-3.70	0.366
NY4-29-1	3,845.50	-3.17	0.138	-2.48	0.366	-3.31	0.138	-3.04	0.366
NY4-35-1	3,846.36	-3.84	0.138	-2.86	0.366	-3.08	0.797	-3.11	0.470
NY4-39-1	3,846.78	-2.95	0.797	-2.32	0.470	-7.16	0.797	-3.37	0.470
NY4-43-1	3,847.33	-1.66	0.797	-2.56	0.470	-2.81	0.797	-2.99	0.470
NY4-47-1	3,847.92	-1.25	0.797	-3.44	0.470	-2.56	0.797	-2.35	0.470
NY4-50-1	3,848.25	-1.31	0.797	-4.85	0.470	-1.23	0.797	-4.50	0.470
NY4-52-1	3,848.58	-0.96	0.797	-5.67	0.470	-2.94	0.797	-5.00	0.470
BMC-13-1	1,902.58	N/A				N/A			
BMC-21-1	1,903.50	-0.41	0.034	-7.21	0.274	N/A			
BMC-26-1	1,904.25	N/A				N/A			
BMC-30-1	1,904.75	N/A				N/A			
BMC-35-1	1,905.33	N/A				N/A			

Table 3.2 (cont.): Stable carbon and oxygen isotope ratios from selected samples from cores in West Virginia, Pennsylvania, and New York.

Sample ID	Depth (ft)	Sample A				Sample B			
		$\delta^{13}C_{VPDB}$ (‰)	$\delta^{13}C$ S.D.	$\delta^{18}O_{VPDB}$ (‰)	$\delta^{18}D$ S.D.	$\delta^{13}C_{VPDB}$ (‰)	$\delta^{13}C$ S.D.	$\delta^{18}O_{VPDB}$ (‰)	$\delta^{18}D$ S.D.
BMC-40-1	1,905.83	-1.20	0.184	-8.41	0.414	N/A			
BMC-43-1	1,906.17	-3.21	0.034	-7.60	0.274	N/A			
BMC-48-1	1,906.75	-0.08	0.034	-7.31	0.274	-0.51	0.034	-8.55	0.274

CHAPTER FOUR : DISCUSSION

DEPOSITIONAL FACIES AND COMPARISON OF BASIN-WIDE PETROLOGIC CHARACTERISTICS

Depositional environments and mechanisms of the Cherry Valley carbonates are difficult to discern due to diagenetic alteration of original textures and compositions. Previous studies describe these limestones as open marine carbonates, in water as deep as other 150 m or more (Ettensohn, 1985; Sageman et al., 2003), that were deposited throughout the basin in the continued absence of significant siliciclastic input (Anderson et al., 1988; Griffing and Ver Straeten, 1991; Ver Straeten, 2007; Ver Straeten et al., 1994). Although this study ultimately agrees with earlier conclusions, this work demonstrates more clearly the links between primary depositional conditions and the final rock. As discussed below, early diagenesis on the seafloor was controlled directly by depositional facies, such that carbonate or barite nodules formed in specific primary sedimentary facies prior to overall lithification. These eogenetic nodules controlled subsequent diagenetic facies as burial progressed.

The Cherry Valley carbonates and adjacent mudstones represent changing ocean-bottom conditions and relative hiatuses in siliciclastic deposition. Using the Chestnut Street outcrop (and New York state stratigraphic naming convention) of the Cherry Valley carbonates to illustrate a depositional history (Fig. 4.1), the general depositional sequence of the Cherry Valley carbonates is: (1) deposition of mudstones, likely calcareous or micritic, in which algal cysts are abundant (Bakoven Member of

Union Springs, Fig. 4.1, TCC below 4,189.00 ft) (2) hiatus in siliciclastic deposition, allowing for the formation of eogenetic carbonate or barite nodules in bedded limestones or calcareous mudstones (Hurley Member of the Oatka Creek Formation, Fig. 4.1, TCC depths 4,187.83 - 4,189.00 ft); (3) deposition of bedded limestones, including carbonate mudstones, wackestones, and packstones (bottom of the Cherry Valley Member of the Oatka Creek Formation, Fig. 4.1, TCC depths 4,186.08 - 4,187.83 ft), and renewed interbedded, organic-rich, argillaceous mudstones; (4) further deposition of fossiliferous mudstones; (5) hiatus in siliciclastic deposition, leading to an upper-bounding carbonate or barite nodule facies (top of the Cherry Valley Member, Fig. 4.1, TCC depths 4,185.00 - 4186.08 ft) prior to (6) deposition of the organic-rich, argillaceous mudstones (East Berne Member of the Oatka Creek Formation, Fig. 4.1, TCC above 4,185.00 ft). These depositional environment intervals correspond to the stratigraphic names as follows. The basal mudstone (1) and its nodules (2) form the upper part of the Bakoven member of the Union Springs Formation. The bedded limestones (3) mudstone (4) and upper nodules (5) constitute the Cherry Valley Member itself. The capping argillaceous mudstones (6) constitute the Oatka Creek Formation (or equivalent). This sequence is summarized in Figure 4.2.

Figure 4.1: Outcrop photograph at Cherry Valley, New York, showing the representative sequence of the Bakoven Member of the Union Springs Formation (Bak) and the Hurley (Hur), Cherry Valley (CVM), and East Berne (EB) Members of the Oatka Creek Formation. These units are correlated to the TCC core (right). Data columns in the core are explained in Figure 3.12.

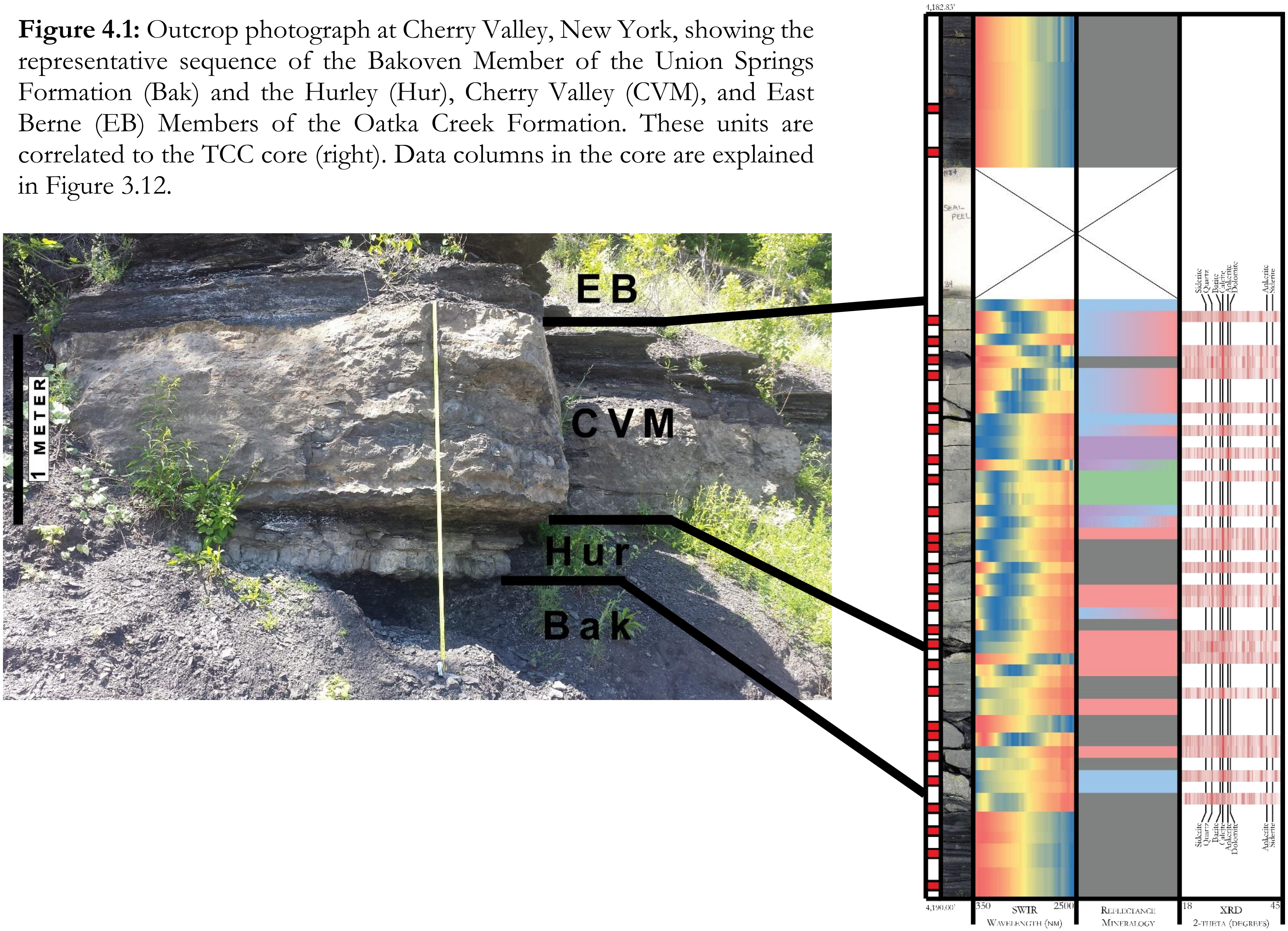

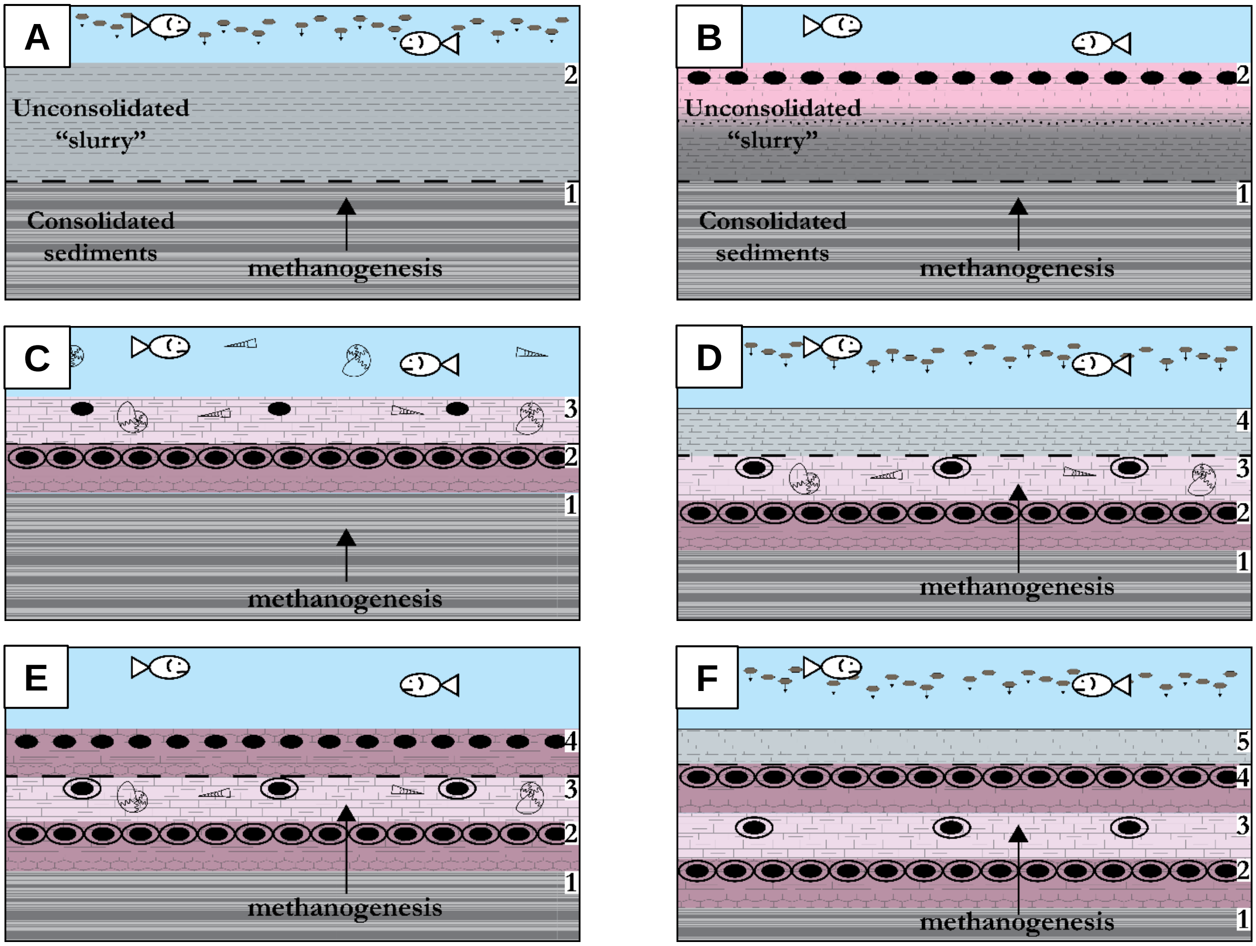

Figure 4.2: The depositional model of the Cherry Valley carbonates, including early diagenetic evolution of nodules in the unlithified sediments. Numbered beds are equivalent from one animation to the next, showing how diagenesis shaped lithology. The dashed line represents a transition from unconsolidated slurry or deposits to consolidated sediments. **A**–deposition of mudstones; **B**–hiatus in siliciclastic deposition, allowing for the formation of eogenetic carbonate or barite nodules; **C**–deposition of bedded limestones; **D**–further deposition of fossiliferous mudstones; **E**–hiatus in siliciclastic deposition, leading to an upper-bounding carbonate or barite nodule facies; **F**–deposition of the organic-rich, argillaceous mudstones.

The Purcell Limestone, which is another nodular bed in the Marcellus, has historically been interpreted as equivalent to the Cherry Valley carbonates in Pennsylvania and West Virginia (Kohl et al., 2014; Lash and Engelder, 2011). This study treats the two as distinctly separate units, as log responses in the Marcellus typically include two discrete low-gamma zones: one within the upper mudstone unit (interpreted here as the Purcell Limestone) and another at the interface between the upper and lower mudstones (interpreted here as the true Cherry Valley carbonates; Fig. 1.7). Little petrologic information is available for the Purcell Limestone, and outcrop descriptions are limited (Engelder et al., 2011) The type section of the Purcell Limestone was described by Cate (1963) who suggested the name be used informally. It is possible that both beds, if not equivalent, developed nodules under similar conditions.

Based on all the cores studied, a shared characteristic of the Cherry Valley carbonates is the described depositional sequence and the occurrence (or absence in the BE15 core) of methanogenic nodules which reflect changing ocean-bottom conditions and relative hiatuses in siliciclastic deposition. These nodules form in sediments near the sediment-water interface when calcium carbonate is precipitated from oversaturated waters pore waters that result from oxidation of organic material by sulfate reduction (Bojanowski et al., 2014). Although heavily altered, sedimentary fabrics and relict fossils reveal that these nodules from both nodular facies were deposited as mudstones with similar depositional characteristics as the unaltered, organic-rich mudstones of the Marcellus subgroup. Notably, the nodular facies contain abundant algal cysts (Fig. 4.3A) which are the dominant source of organic material in economically important intervals (Obermajer et al., 1997). Further complicating the interpretation, bedded limestones (wackestones and packstones, Fig. 4.3B), which have been recrystallized, have also likely undergone nodularization. An overlap in petrographic properties between nodules and neomorphosed limestones, however, make it unsuitable to discern the two diagenetic textures. Therefore, the crystalline carbonate lithology does not exclusively lend itself to either depositional facies (mudstone or bedded limestone). Alternatively, these same lithologies do not necessarily equate to nodule formation. The Cherry Valley nodules, though partially flattened by compaction, are concentric and are depleted in ^{13}C (Lash, 2015), and they grew as a result of oxidizing organic matter under anoxic conditions in the underlying organic-rich sediments of the Union Springs Formation (Bojanowski, 2009). Development of micritic, bedded limestones in an open marine setting signals a pause in siliciclastic input prior to deposition of the upper Marcellus mudstones (Anderson et al., 1988; Majewski, 2003; Zatoń et al., 2011).

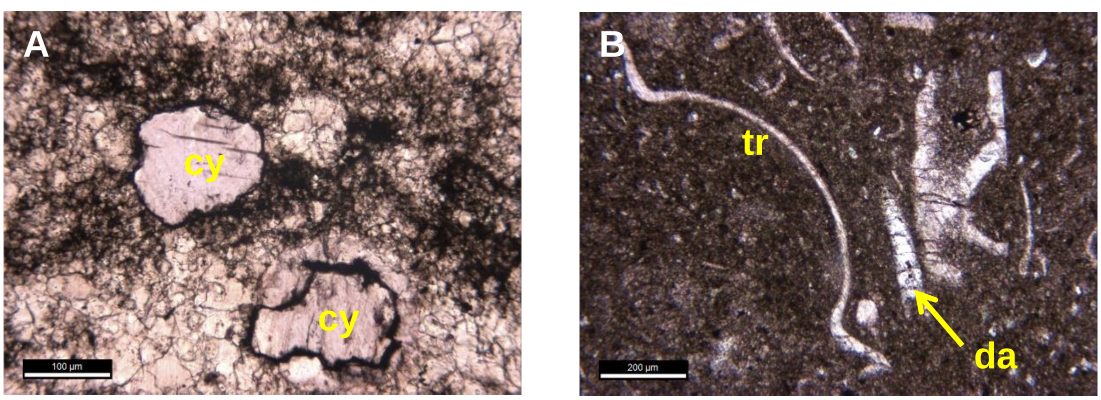

Figure 4.3: Examples of nodular (**A**) and bedded limestone (**B**) facies. Abundant algal cysts are typical of the nodular facies (cy) in all portions of the basin, particularly at the tops and bottoms of the Cherry Valley carbonates. Pelagic fauna, including dacryoconarids (da) or trilobites (tr), are representative of the bedded limestone facies.

Depositional facies description of southwestern cores:

In cores in the southwestern region, the Cherry Valley is dominated by the upper nodular limestone and the lower nodular limestone, with little evidence of an intermediate bedded limestone that comprises pelagic fauna. However, these bedded limestones are well represented in the MSEEL core, which is the best preserved and most recently drilled core, and which also includes basal and upper-bounding nodules. Bedded limestones are the dominant lithology in the upper portion of the sampled interval in the WV7 core that is underlain by a basal nodule. Geophysical logs (Fig. 1.7), which were unavailable at the time of sampling, suggest the upward continuance of a low resistivity zone in the WV7 core. Nodular facies are dominant in both GOFF and WHIP wells, with high confidence that a bedded limestone facies is absent from these cores. Both WHIP and WV7 cores are located north of the GOFF and MSEEL cores and the lack of the limestones may simply imply regional variations of depositional conditions.

Depositional facies description of central core:

Facies descriptions of the Cherry Valley Member from the central Appalachian Basin are based on the BE15 core from central Pennsylvania. Overlying a basal calcareous and pyritic nodular facies that was observed in core but not sampled for thin section, in vertical succession, are: (1) a calcareous mudstone facies which includes dacryoconarids, fragments of algal mats, crinoids, and conodonts, and is partially cemented by diagenetic dolomite; (2) a microsparitic crystalline carbonate that was likely a bedded limestone at deposition; (3) a calcareous mudstone facies that is partially cemented by dolomite. These basal and upper-bounding calcareous mudstone facies represent the nodular facies from other portions of the basin.

Wang (2014) studied the Cherry Valley Member in two cores (Bald Eagle 2009 and Snow Shoe) in central Pennsylvania (Fig. 2). A similar vertical sequence of depositional facies in these cores were observed, including: (1) a basal, nodular, calcareous mudstone; (2) a wackestone; and (3) a silty, calcareous mudstone. Notably, the Bald Eagle 2009 and Snow Shoe cores have elevated detrital silt content compared to the BE15. The proximity to a sediment source may be influence the occurrence of nodules.

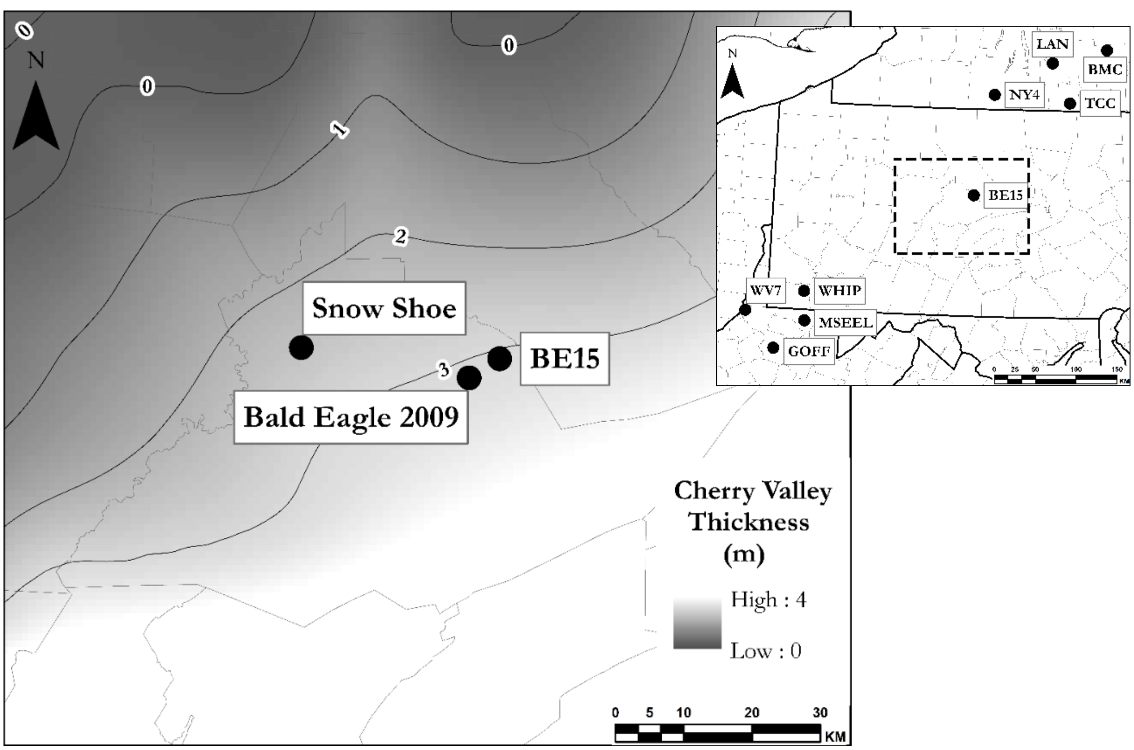

Figure 4.4: Locations of cores in central Pennsylvania, including two that were part of a previous study (Wang, 2014).

Depositional facies description of northeastern cores:

Depositional facies from the Cherry Valley Member in New York display more textural and compositional heterogeneity than those studied in West Virginia and Pennsylvania. The BMC and NY4 cores follow a similar sequence of facies, with upper and lower nodular facies with an intervening bedded limestone. The sequence of facies in the NY4 and BMC cores is: (1) a basal, calcareous nodular facies; (2) a bedded limestone facies that is predominantly composed of dacryoconarids, trilobites, and crinoids; and (3) a calcareous, nodular facies. The TCC core has experienced a divergent diagenetic history that obscures its depositional origins more than for the other cores. The sequence of facies of the TCC, from the uppermost Union Springs through 5 ft of Cherry Valley, is: (1) a barite and calcareous nodular facies with interbedded, organic-rich mudstones; (2) a baritic, calcareous mudstone facies; (3) a calcareous, nodular facies; and (4) a bedded limestone facies. The top of the Cherry Valley Member was not recovered during drilling; therefore, the lack of core may explain the absence of an observed upper, nodular facies.

SIGNIFICANT DIAGENETIC FEATURES

Syngenetic/eogenetic processes

Micritization

Because of diagenetic alteration, original micrite and its texture are no longer present. Micritization processes include autochthonous or biologically induced micrite, allochthonous or deposited micrite, or pseudomicrite or diagenetic micrite. The Cherry

Valley carbonates, which were deposited in deeper waters across the Appalachian Basin, likely consisted of allochthonous micrite that was sourced by the disintegration of pelagic fauna during deposition.

Nodules

Textures associated with carbonate (Fig. 4.5A) or barite nodules (Fig. 4.5B/C) are common throughout all cores. The nodules are typically highlighted by pervasive microspar that has overprinted depositional fabrics. Carbonate nodules are most common in the studied rocks and include heavily recrystallized fossils. Barite nodules, which are highlighted by bladed crystals, are less common and are partially to entirely replaced by calcite.

Dolomite rhombohedra

Organogenic dolomite develops as a result of bacterial sulfate reduction and continued methanogenesis in the organic-rich sediments of the Marcellus mudstones (Howe et al., 2016; Mazzullo, 2000; Scholle and Ulmer-Scholle, 2003). Disseminated, organogenic dolomite rhombohedra (Fig. 4.5D and 4E) are crystallized within the matrices in mudstones and within select fossils

Prismatic calcite crystals and void-filling cements

In many rocks, cementation of fossils preserves the original morphology of the fossil prior to compact. Prismatic or bladed calcite crystals (Fig.4.5 F/G) grow into the interiors or away from the exteriors of fossil tests. Generally adjacent to prismatic crystals, sparry or single-crystal calcite (Fig. 4.5H) and dolomite or, less commonly, barite or pyrite (Fig. 4.5I) occlude fossil tests or voids.

Mesogenetic/telogenetic processes

Fractures

Fractures (Fig. 4.5J/K) of various orientations are common throughout the Cherry Valley carbonates. They are filled with calcite and commonly propagate through larger rock components, such as fossils, while wrapping around more competent features such as quartz silt. Due to the two-dimensional constraints of thin section and SEM analysis, it is likely that fractures are more numerous in these rocks than visual inspection can estimate.

Pressure solution features

Pressure-solution features, such as stylolites (Fig. 4.5L), are a common feature throughout the Cherry Valley carbonates. These features are a result of chemical compaction that postdates mechanical compaction and produce irregular, suture-like contacts that are produced under pressure by differential vertical movement. Stylolitization typically involves a reduction in porosity as it provides carbonate for burial cementation (Flügel, 2010; Wong and Oldershaw, 1981). In the Cherry Valley carbonates, stylolites are morphologically irregular and anastomosing, typically propagating around fossils or earlier diagenetic mineralization, and are filled with organic material and clay minerals. The stylolites exhibit orientations that range between horizontal or bedding-parallel to vertical. The timing of stylolitization is uncertain in relation to fracture propagation as petrographic analysis did not capture the interaction between these two events.

Organic material

Organic material is disseminated throughout the Cherry Valley carbonates, particularly in more clay-rich intervals. While the amount of organic material is not comparable to other, more economically viable mudstones of the Marcellus, hydrocarbon migration through the Cherry Valley carbonates is apparent by the kerigenous staining or residue left on matrix materials such as microspar. Less commonly, organic particles or solids are in place. Framboidal pyrite is typically associated with organic material.

Blocky, recrystallized carbonate cements

Burial cements include calcite and dolomite. Blocky calcite cement is the product of prolonged neomorphism rather than singular events. It is an advanced indication of neomorphosed calcite or replaces previous diagenetic phases (Fig. 4.5M). Dolomites (Fig. 4.5N) were only observed in the TCC core and are distinguished by compositional analyses as well as thin section staining.

Exhumation

Dedolomitization

In select cases, dolomite rhombohedra are calcitized (Fig. 4.5O). Other diagenetic phases are also replaced by this calcite stage.

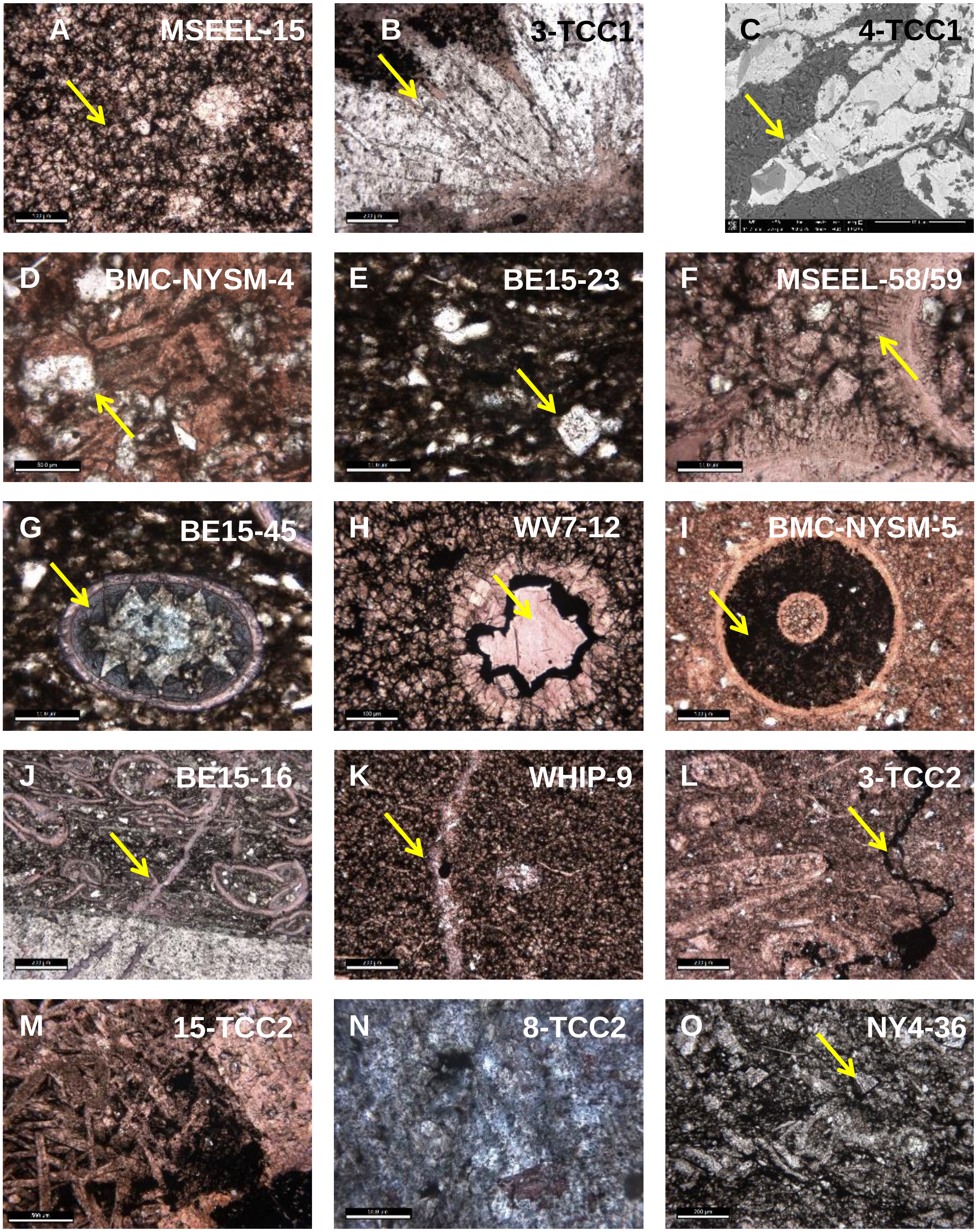

Figure 4.5: Example photomicrographs of representative features for a given paragenetic stage (in rows). Arrows point to the dominant feature highlighted by the photo. See text and individual sample descriptions in Appendix A for more information.

PARAGENESIS OF THE CHERRY VALLEY CARBONATES

Petrographic and geochemical analyses of the Cherry Valley carbonates define a general paragenesis of core material comprising eogenetic, mesogenetic, and telogenetic alterations. The observed paragenetic sequence is based on textural and compositional relationships according to cross-cutting relationships for qualitative chronological classification. Figure 4.6 represents the paragenetic sequence on a relative timescale, as eogenesis occurs in a short period compared to meso- and telogenesis (Fig. 4.7).

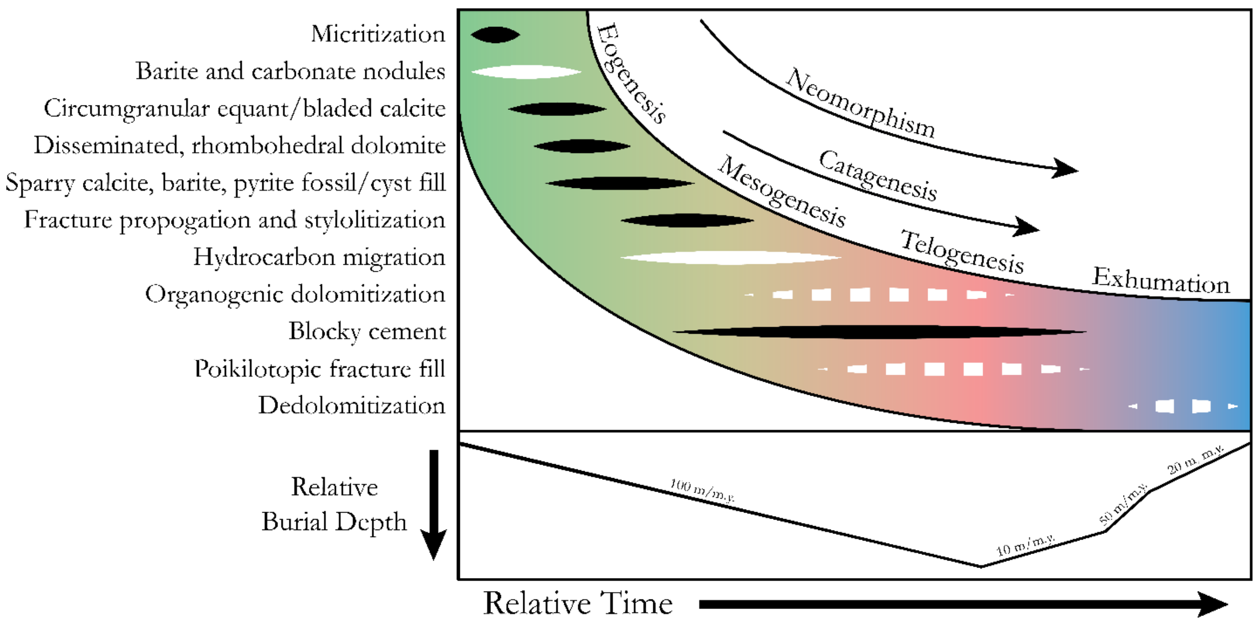

Figure 4.6: Paragenetic relationships are based on petrographic and compositional data. The upper part of the diagram shows relative temporal stages of diagenetic processes and authigenic mineralization in the Cherry Valley carbonates. Bar width represents the extent of each process, dashed bars represent uncertainty, and white bars represent the absence of a process in at least one core. Colors represent relative transitions from early (green, eogenetic), intermediate- (yellow, mesogenetic), and late-stage (red, telogenetic) burial diagenesis, as well as alteration associated with exhumation (blue). The lower part of the diagram shows relative burial history that reflects burial or exhumation rates of Pennsylvanian strata in the Appalachian Basin (from Reed et al., 2005).

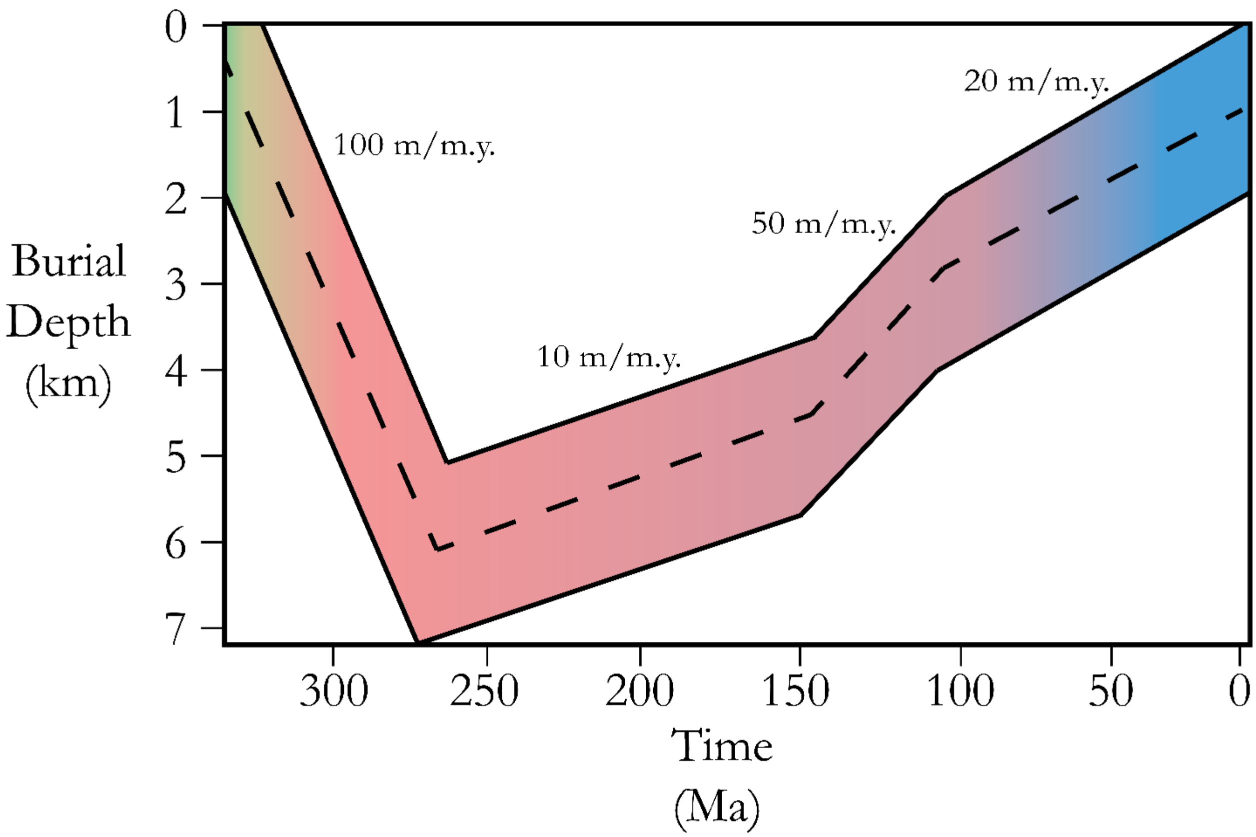

Figure 4.7: The paragenetic sequence shown on a linear timeline, highlighting the comparatively short period of eogenetic (green) alteration as opposed to mesogenesis (yellow) and telogenesis (red). Blue represents exhumation as the Marcellus approached the surface. The dotted line shows burial and exhumation rates (from Reed et al., 2005).

Shortly after deposition, diagenesis began with eogenetic alteration and progressed through the following stages:

(1) Development of diagenetic micrite in calcareous mudstones and bedded limestones (Fig. 4.8A);

(2) Barite and carbonate nodule formation (Fig. 4.8B)), except in BE15 where nodules are absent;

(3) Crystallization of equant or bladed carbonate on the interiors and exteriors of fossils (Fig. 4.8C). The ions needed for these stages of alteration and cementation were sourced by recrystallization of abundant fossils and depositional micrite. Circumgranular carbonate growth occurs near the surface-water interface and prior to compaction (Flügel, 2010; Scholle and Ulmer-Scholle, 2003);

(4) Organogenic dolomite (Fig. 4.8D) develops as a result of bacterial sulfate reduction and continued methanogenesis in the organic-rich sediments of the Marcellus mudstones (Howe et al., 2016; Mazzullo, 2000; Scholle and Ulmer-Scholle, 2003). Disseminated, organogenic dolomite rhombohedra (Fig. 4.6-4a and 4b) are crystallized within the matrices in mudstones and within select fossils;

(5) Precipitation of pore-filling minerals (Fig. 4.8E), including sparry calcite or dolomite, barite, and pyrite, fill fossil tests and algal cysts to preserve their original morphology (Flügel, 2010; Scholle and Ulmer-Scholle, 2003). Carbonate phases in stages 3-5 are commonly ferroan, further signifying a reducing ocean-bottom environment (Choquette and James, 1987). As burial progressed, the compaction and lithification of Marcellus sediments continued and neomorphism of the Cherry Valley carbonates shifted to mesogenetic alteration;

(6) Catagenesis of in situ organic material occurred in surrounding rock, and subsequent mobilization of liquid hydrocarbons via fractures and stylolites (Fig.

4.8F) then permeated through the Cherry Valley carbonates. Those mobilized hydrocarbons produced thin coatings of kerigenous residue on matrix constituents, namely matrix microspar. The introduction of hydrocarbons may have arrested prograding neomorphism and inhibited further recrystallization of microspar (Choquette and James, 1987; Laudon, 1996). This stage may have occurred during the Jurassic, resulting in basin-wide joint sets (Engelder et al., 2009). Though the timing of these fractures is well constrained, catagenesis had been ongoing since the late Paleozoic;

(7) The progress of many rocks in the Cherry Valley carbonates through burial diagenesis is marked by calcite recrystallization and pore space occlusion (Fig. 4.8G). This stage represents a transition to telogenetic alteration. In select regions of the basin, burial dolomitization (Fig. 4.8H) resulted in anhedral, crystalline dolomites. This category of dolomite is crystallized under different diagenetic conditions than previously developed organogenic dolomite. This dolomite was the product of compactional dewatering of the bounding, organic-rich mudstones (Flügel, 2010; Mazzullo, 2000; Scholle and Ulmer-Scholle, 2003). A high proportion of illite to smectite in these mudstones (Hosterman and Whitlow, 1983) that resulted from advanced diagenetic conversion from smectite to illite, particularly in the northeastern region (Engle and Rowan, 2014), is likely the source of Mg^{2+}-rich fluids. Saddle or baroque dolomite (Fig. 4.6-7a) is

associated with organic-filled stylolites in select cores. Additional burial alteration includes pore-reducing, blocky calcite and fracture fill, including the development of poikilotopic calcite textures in some fractures. Barite nodules may have been replaced by calcite during this stage (Fig. 4.6-7c);

(8) Alteration associated with exhumation is associated with dedolomitizing textures in calcite (Fig. 4.8I). This dedolomitization is interpreted to be the consequence of interaction of meteoric groundwater with the Cherry Valley carbonates, and marks the most recent stage of diagenesis.

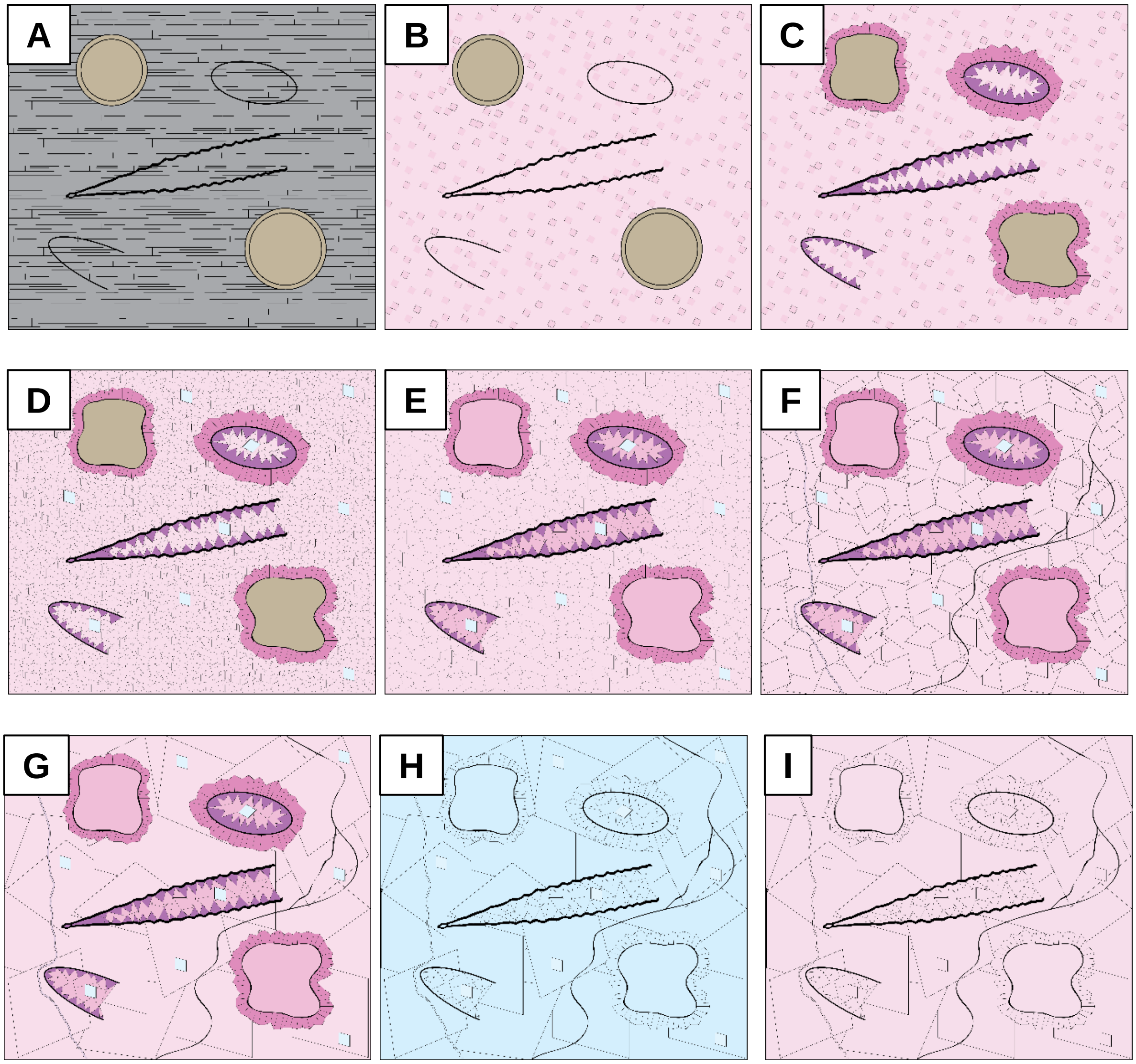

Figure 4.8: Cartoons of each step through the paragenetic sequence of the Cherry Valley carbonates in chronological order. Note, the increase in rhombohedral size in the background represents neomorphism. **A**–deposition and micritization; **B**–nodule formation and initial matrix calcite recrystallization; **C**–prismatic or bladed calcite crystallizes on the surfaces of fossils and cysts; **D**–crystallization of dolomite rhombohedra; E**–**fossils and cysts are filled with cements; **F**–fracturing and stylolitization; **G**–prolonged neomorphism results in recrystallized matrix, but coatings of hydrocarbons generated by catagenesis restricts neomorphism; **H**–if conditions are appropriate, burial dolomitization; I–dedolomitization if meteoric waters infiltrate the formation.

In areas where nodules have not formed in the Cherry Valley carbonates, such as BE15, there remains mudstones that vertically bound the bedded limestones. Paragenesis in these rocks includes eogenetic stages, including early diagenetic calcite crystallization within fossils, but pervasive cementation is not present in these mudstones. Rather, these rocks represent what the nodular facies may have originally been as they better preserve depositional fabrics.

GEOCHEMICAL SIGNALS OF PALEOENVIRONMENT AND DIAGENESIS

Depending upon the ocean-bottom redox conditions during deposition of the Cherry Valley carbonates, differing diagenetic pathways would be expected. Specifically, the development of carbonate or barite nodules shortly after deposition controls subsequent alteration. Stable carbon and oxygen isotopes provide insightful tracers of formation conditions as well as lithology.

Isotopic compositions of Cherry Valley carbonates do not reflect those of Eifelian brachiopods in unaltered marine carbonates from the Devonian which range from 0.0 to +3.0 ‰ $\delta^{13}C$ and -3.4 to -2.7 ‰ $\delta^{18}O$ (Fig. 4.9; van Geldern et al., 2006). Unaltered specimens of dacryoconarids from the Union Springs Formation and Oatka Creek Formation in New York range between 0 and 1.2 ‰ $\delta^{13}C$, which is within the accepted range of Devonian-age marine carbonates, and -8.0 to -5.7 ‰ $\delta^{18}O$ (Frappier et al., 2015). A lighter oxygen isotope composition in planktonic dacryoconarids than benthic brachiopods may be explained by the relatively warmer upper water column habitat of the planktonic dacryoconarids. Lynch-Stieglitz et al. (1999) provide an example of this expression in benthic microorganisms of environmental variations in a water column. They determined that $\delta^{18}O$ decreased with depth by a magnitude of 2 to 3 ‰ between the surface water and 800 m depth in the modern ocean adjacent to the Florida Keys and to the Little Bahama Banks.

Within the Cherry Valley member of the Marcellus subgroup, data represented here show that limestones (including wackestones, packstones, and crystalline carbonates) and mudstones are significantly lighter in both $\delta^{13}C$ and $\delta^{18}O$ than typical Devonian marine carbonates (0.0 to +3.0 ‰ $\delta^{13}C$ and -3.4 to -2.7 ‰ $\delta^{18}O$). The average $\delta^{18}O$ values in limestones from all cores are heavier (mean = -5.49 ‰; σ = 2.40 ‰) than mudstones (mean = -8.86 ‰; σ = 1.06 ‰). The $\delta^{13}C$ values are inversely related, as the carbonate minerals in limestones are lighter (mean = -8.93 ‰; σ = 4.17 ‰) than those in mudstones (mean = -5.07 ‰; σ = 2.65 ‰).

Methanogenic nodules that form in deep-marine mudstones within the shallow subsurface of the sulfate reduction zone form carbonates with depleted isotopic ratios (Bojanowski et al., 2014). These types of nodules are well documented in Devonian shales, including the Marcellus (Dix and Mullins, 1987; Siegel et al., 1987; Lash and Blood, 2004; Lash, 2016). In addition to petrographic evidence, the isotopic compositions of the Cherry Valley carbonates suggest a methanogenic source of the carbonates for these rocks. The carbon and oxygen isotope compositions of nodular limestones likely ranged between -15 and -25 ‰ $\delta^{13}C$ and -2 and 0‰ $\delta^{18}O$ VPDB as they precipitated from carbon dioxide produced by organic sulfate reduction in the loose sediments not far below the sediment-water interface (Fig. 4.9; Irwin et al., 1977). The precipitated calcite was sourced by porewater bicarbonate, which was derived from degradation of organic matter (Bojanowski et al., 2014; Irwin et al., 1977). Although original porewater compositions are no longer available, select nodules were tested for isotopic variance from center to rim (See TCC samples 6-TCC2 and 7-TCC2 in Appendix I) with no apparent change, and petrographic evidence suggests diagenetic influence that post-dated the methanogenic nodule formation would likely homogenize isotopic compositions in the nodules. To explain similarly depleted ^{13}C in the bedded limestones as in crystalline carbonates (Fig. 3.14), which are largely interpreted as nodular limestones, this methanogenic bicarbonate may have also been the source during micritization. Alternatively, if the nodular carbonate and bedded limestone originated with differing isotopic compositions, then fluid transfer of diagenetic calcite has equilibrated the carbon isotope signal between the two observed lithologies. Diagenetic cements, including these eogenetic calcite phases, are depleted in ^{18}O and reflect increased temperatures of the precipitating waters (Choquette and James, 1987).

Barite nodules, of which barite may be sourced by intraformational ashes such as the Tioga Ash Bed (Lovering and Van Heyl, 1989), are associated with high $\delta^{34}S$ values and result from a lower sedimentation rate and commensurate enhanced microbial sulfate reduction (Zhou et al., 2016). Lash (2016) outlines that these barite nodules likely formed as a result of substantial kinetic fractionation of ^{34}S that was aided by low seawater sulfate recharge rates as well as upward delivery of barium and methane.

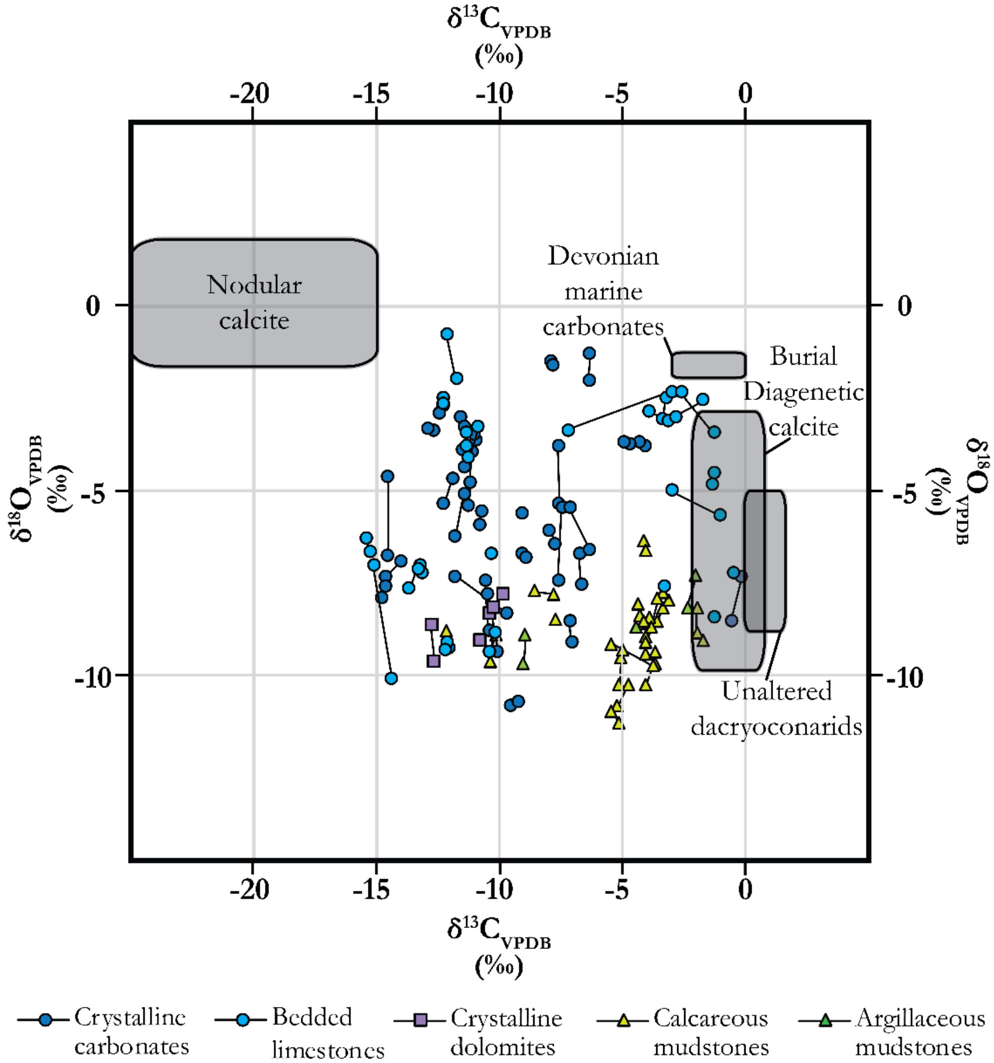

Figure 4.9: Isotopic compositions of Cherry Valley nodular and bedded limestones relative to independent data sets. Cases illustrated in gray boxes represent ancient methanogenetic calcite nodules (Irwin et al., 1977), generalized isotopic ranges for burial diagenetic calcite (Choquette and James, 1987), unaltered dacryoconarids of the Marcellus subgroup (Frappier et al., 2015), and Devonian global marine carbonates (van Geldern et al., 2006).

The observed isotopic compositions of Cherry Valley carbonates are not uniform from one part of the basin to another, and each core has a unique isotopic signature (Fig. 3.26). Generally, the $\delta^{13}C$ values of carbonate minerals in each core show higher variance among facies than do $\delta^{18}O$ values; the O isotopes of carbonate minerals are equilibrated across lithologies. This characteristic is most easily distinguished in the TCC core for which more numerous carbonate samples show lithological trends in $\delta^{13}C$ ratios whereas $\delta^{18}O$ is comparatively constant (Fig. 3.20). The $\delta^{13}C$ values of TCC lithologies starkly contrast because carbon isotopes within bedded limestones and those within crystalline carbonates, which are largely nodules, have not been subjected to temperature-dependent fractionation during recrystallization. This preservation of isotopic identity may have been due possibly to a decrease in porosity and permeability during burial. Unlike in TCC where mudstones and carbonate ^{18}O has homogenized, in some cores (e.g., WHIP and BE15, Fig. 3.19) the ^{18}O has been effectively shielded from equilibration across lithologies, possibly due to dissimilar fluid interaction because of petrophysical constraints. Given this difference in isotopic compositions between lithologies, a scenario can be hypothesized in which the carbonate materials in micritized mudstones, such as dacryoconarids, were better insulated from eogenetic signals that may enrich $\delta^{18}O$ ratios in crystalline carbonates or bedded limestones.

Eogenetic to mesogenetic phases of cementation, including coarser calcite spar or rhombic dolomite, are systematically crystallized with $\delta^{18}O$ ratios that range between

-8 to -3 ‰ and $\delta^{13}C$ ratios between -2 and 1 ‰ (Choquette and James, 1987). These isotopic compositions of diagenetic calcite provide a mechanism for the current transitional compositions in Cherry Valley nodular limestones, as carbon isotope compositions are enriched and oxygen carbon isotope ratios are depleted (Fig. 4.9).

The NY4 and BMC cores are the most northeastern wells in the study and are isotopically distinct from the rest of the sampled material. Limestones in the NY4 and BMC are significantly heavier than those in the rest of cores, with average $\delta^{13}C$ ratios of -2.53 ‰ (σ = 1.57 ‰) compared to -10.63 ‰ (σ = 2.69 ‰) and average $\delta^{18}O$ ratios of -3.91 ‰ (σ = 2.02 ‰) compared to -6.00 ‰ (σ = 2.36 ‰). Although isotopically distinctive, they comprise a similar depositional sequence as the Cherry Valley carbonates elsewhere in the basin including the presence of overlying and underlying, organic-rich mudstones. Two likely explanations exist for this trend: (1) the carbonates retained the isotopic signature of Devonian sea water at the time of deposition; or (2) meteoric groundwater has interacted with the Cherry Valley carbonates in the shallower wells (2,000 – 4,000 ft) of southern New York. In NY4 and BMC, textures of all diagenetic stages are present though the composition has largely been recrystallized by a late-stage calcite phase. Notably, these rocks in NY4 and BMC appear petrographically alike to others in the Cherry Valley that are interpreted to be nodular. The isotopic signature, however, more accurately reflects that of Devonian sea water than of methanogenic carbonate. The more likely scenario is that groundwater has infiltrated the formation. Dedolomitization textures are most present in these wells. Early diagenetic features, such as circumgranular, bladed or equant calcite and bladed barite nodules, are compositionally indistinguishable from one another as they have been recrystallized by a singular calcite phase. Karst features are well developed in underlying carbonates in central and western New York, namely the Middle Devonian Onondaga Limestone and Upper Silurian Akron-Bertie Formation, that allow permeation of meteoric waters into the subsurface (Reddy and Kappel, 2010). Although recent surface processes may not be directly responsible for the observed meteoric diagenesis, they provide one option to explain this variance in isotopic compositions. Other shallow wells, namely BE15 and TCC, do not exhibit these same dedolomitization characteristics.

CONTEXTUAL SYNTHESIS OF DEPOSITIONAL, DIAGENETIC, AND GEOCHEMICAL INSIGHTS

The Cherry Valley carbonates present a unique opportunity to integrate textural and compositional heterogeneity into a spatially organized geologic history. These carbonates are distinct in both spatial distribution and stratigraphic position, and a complex diagenetic relationship with their bounding, organic-rich mudstones presents a chance to add to the highly studied Marcellus "shale". Whereas siliciclastic deposition is dependent on base level and on local variations sediment supply, the Cherry Valley carbonates prominently represent a simultaneous, basin-wide, diagenetic response that reflects ocean-bottom conditions as well as its traditionally described pelagic limestone deposits.

It is most apparent that although recrystallization masks the origins of the Cherry Valley carbonates, it also aids in diagnosing how diagenetic facies are controlled by depositional conditions. Specifically, alteration associated with meso- to telogenetic processes is dependent upon nodule formation, or lack thereof, in either mudstones or bedded limestones. In one instance, calcareous mudstones host methanogenic nodules which evolved to be so extensive that they are subsequently considered crystalline carbonates. In the other instance, bottom-water conditions or continued siliciclastic input inhibited the growth of nodules in these depositionally equivalent rocks. The formation of nodules controls later-stage diagenesis which includes pore-reducing cementation or dolomitization whereas the original laminated texture may be preserved in the event that nodules do not form. Compositionally, calcite is the dominant diagenetic phase in either case, though nodule formation favors advanced neomorphism of microspar.

The geochemical signature of these carbonates is controlled by the growth of nodules. Initial isotopic compositions of nodules are depleted in ^{13}C, yet thereafter the nodules are progressively replaced by isotopically heavier diagenetic carbonates. Mudstones, on the other hand, predominantly maintain isotopic compositions closer to that of Devonian ocean water or to unaltered dacryoconarids. Planktonic dacryoconarids are the dominant source of calcite in these mudstones and preferentially built their shells with lighter oxygen (Frappier et al., 2015).

Considering the major features of the Marcellus, methanogenesis and catagenesis produced major changes expressed as the propagation of fractures and mobilization of hydrocarbons. Nevertheless, methanogenesis and catagenesis have an indeterminable effect on the isotopic compositions of these rocks. Other factors that may affect oxygen and carbon isotope compositions include the contribution of diagenetic dolomite or other minor carbonate minerals of variable content that have not been quantified. Due to the homogenization of isotopic compositions in nodular and bedded limestones, only mudstones display geochemical sensitivity to thermal conditions (Fig. 3.18) in the Cherry Valley carbonates. Increasing burial temperatures, as determined by Conodont Alteration Index, enriches isotopic compositions in mudstones as higher temperatures and increased pressures tend to promote diagenetic processes (Scholle and Ulmer-Scholle, 2003).

CHAPTER FIVE : CONCLUSIONS

The Cherry Valley carbonates are a thin, laterally continuous unit that consists of pelagic limestones and nodular carbonates and separate the upper and lower organic-rich mudstones of the Marcellus "shale". These carbonate units, formally described in New York State as the Cherry Valley Member of the Oatka Creek Formation, include a basal calcareous mudstone facies that hosts methanogenic nodules, an intermediate pelagic limestone that classically defines the Cherry Valley carbonates and includes cephalopods and dacryoconarids, and an upper-bounding calcareous mudstone facies that hosts methanogenic nodules.

Petrologic and geochemical evaluation of these carbonates indicates lithological and spatial relationships that are produced by a basin-wide diagenetic sequence in West Virginia, Pennsylvania, and New York. Specifically, the Cherry Valley carbonates reflect ocean-bottom conditions as the development of early diagenetic nodules control subsequent diagenetic pathways. The general diagenetic sequence for the Cherry Valley carbonates begins with (1) the development of micrite in the calcareous mudstones and bedded limestones that was followed by a hiatus of siliciclastic input, allowing for the (2) formation of methanogenetic nodules in the shallow subsurface of the sulfate reduction zone. Eogenetic cements largely consist of (3) equant or bladed calcite on fossil tests and (4) organogenetic dolomite rhombohedra that subsequently crystallized prior to compaction. (5) Pore-filling cements, specifically sparry carbonates, barite, and pyrite, occlude the remaining space within algal cysts and fossil tests, and preserved the morphologies of these fragile primary sedimentary materials. (6) As burial progressed, organic material in organic-rich mudstones matured to the point of mobilization via fractures and stylolites that permeated the matrices of the Cherry Valley carbonates. (7) Late stage cementation phases include continued calcite crystallization, and dolomitization in select regions, that effectively prohibited further fluid exchange within the Cherry Valley carbonates until (8) exhumation exposed the formation to dedolomitizing groundwaters.

These diagenetic stages control resultant isotopic compositions. A major finding is that the early formation of nodules in mudstones set in action differing geochemical responses to subsequent increases in pressure and temperature. Whereas nodular carbonates crystallize with lighter carbon isotope compositions (Irwin et al., 1977), subsequent diagenesis has enriched these limestones to a transitional isotopic composition (Choquette and James, 1987). In contrast, in calcareous mudstones that did not undergo nodule formation, isotopic compositions reflect thermal conditions that enrich $\delta^{13}C$ in carbonate minerals as temperature or pressure increased.

APPENDIX A: DETAILED PETROLOGIC ANALYSES

Example of Petrographic Descriptions

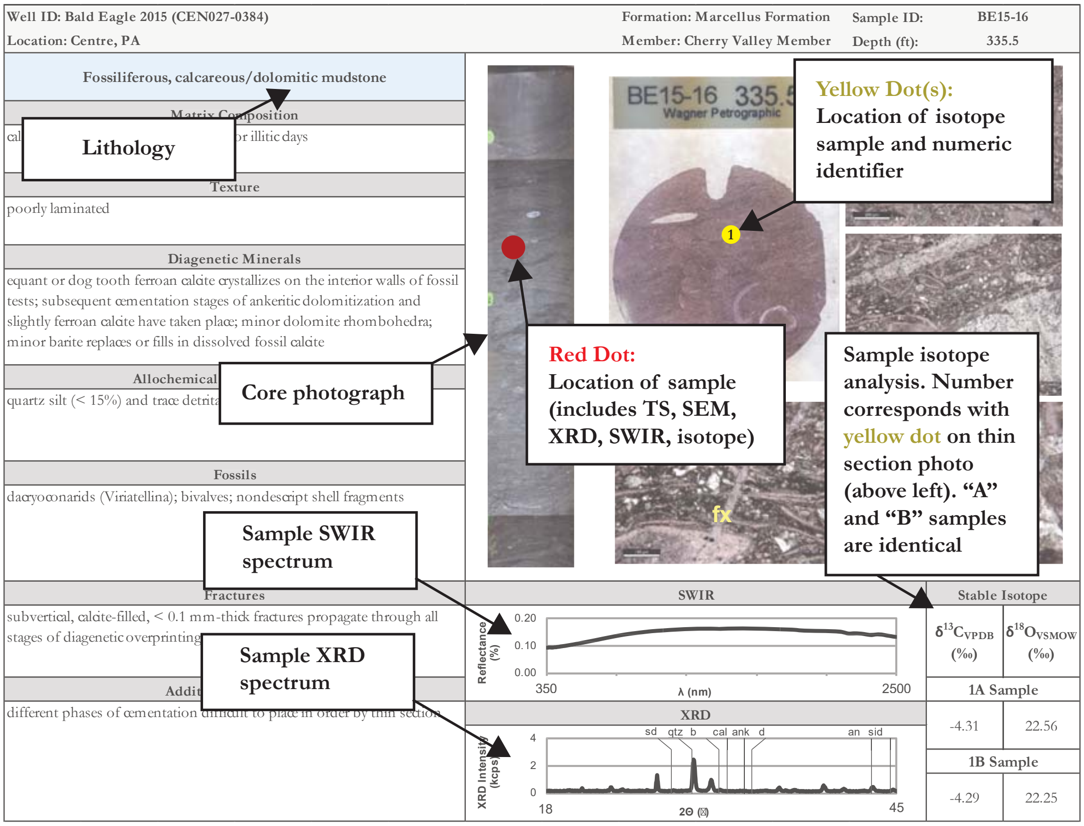

Explanation of annotations in TS/SEM descriptions

am	–	algal mat
ba	–	barite
bcc	–	bladed calcite
bf	–	phosphatic bone fragment
cc	–	calcite (generic)
ce	–	cephalopod
CH	–	chlorite
cl	–	clay minerals (generic)
co	–	conodont
cph	–	collophane (phosphate)
cr	–	crinoid
cy	–	cyst
da	–	dacryoconarid
do	–	dolomite
ecc	–	equant calcite
fc	–	ferroan calcite
fd	–	ferroan dolomite (ankeritic)
ff	–	nondescript fossil fragment
fx	–	fracture
ga	–	gastropod
ms	–	microspar
om	–	organic material (generic)
os	–	ostracod
py	–	pyrite
q	–	quartz
scc	–	single-crystal calcite
si	–	silica (generic)
sp	–	sphalerite
sy	–	stylolite
tr	–	trilobite
xpl	–	cross-polarized light photomicrograph

Well ID: Nathan Goff #55 (4703305106)	Formation: Marcellus Formation	Sample ID:	GOFF-10/11
Location: Harrison, WV	Member: Cherry Valley Limestone	Depth (ft):	7204.75

Microsparitic crystalline carbonate

Matrix Composition
calcite

Texture
nonlaminated; matrix is recrystallized to xenotopic, inequigranular microspar

Diagenetic Minerals
calcite is the dominant diagenetic mineral; matrix and fossils are homogenized by calcite recrystallization; barite cements select laminae and replaces select fossils; ferroan calcite associated with barite; collophane fills select fossils; minor dolomite rhombohedra; pyrite framboids disseminated throughout

Allochemical or Detrital Grains
trace quartz silt

Fossils
nondescript fossil fragments; collapsed organic-walled cysts

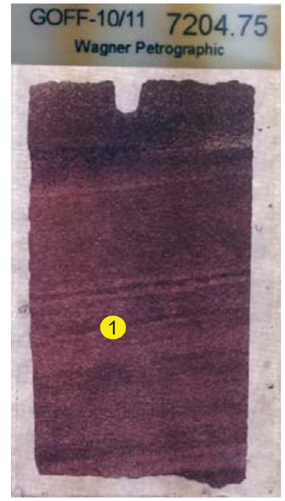

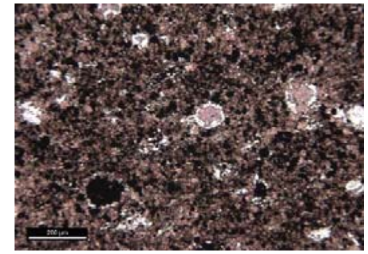

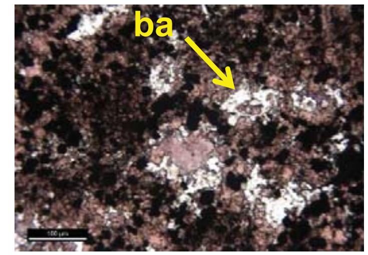

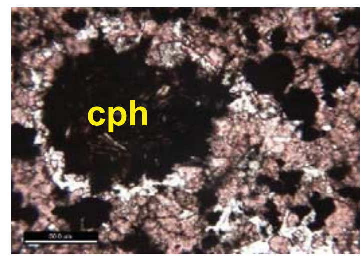

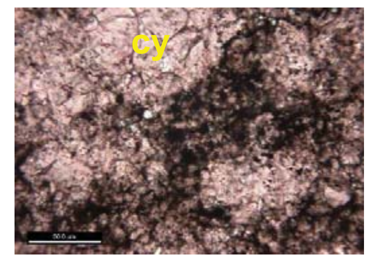

Fractures
irregular anastomosing stylolites propagate parallel to bedding

Additional Comments
minor organic material disseminated within matrix microspar

SWIR

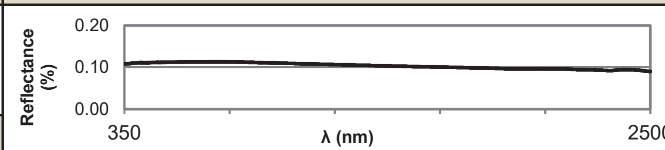

XRD

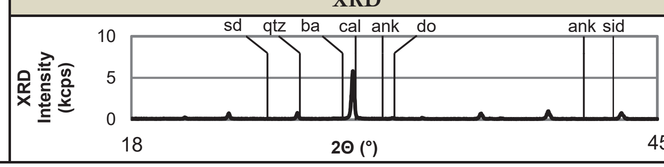

Stable Isotope

	$\delta^{13}C_{VPDB}$ (‰)	$\delta^{18}O_{VPDB}$ (‰)
1A Sample	-12.63	-3.37
1B Sample	-12.86	-3.30

Well ID: Nathan Goff #55 (4703305106)	**Formation: Marcellus Formation**	**Sample ID:**	**GOFF-10/11**
Location: Harrison, WV	**Member: Cherry Valley Limestone**	**Depth (ft):**	**7204.75**

Microsparitic crystalline carbonate

Matrix Composition and Microtexture

calcite recrystallization results in a microsparitic texture; clay minerals and degraded organic material fill areas between microspar

Diagenetic Minerals

calcite is the primary diagenetic mineral

Diagenetic Texture

neomorphism of calcite matrix, likely micritic in origin, gives the rock a massive or chunky appearance; select fossils include equant calcite overgrowths on their ridges

Pore Structure

clay and organic material admixed within microsparitic matrix, likely hosting nominal porosity

Depositional Fabric

diagenesis has destroyed a majority of depositional fabrics, as microspar growth has grown amidst what may have been a laminated, calcareous mudstone

Additional comments:

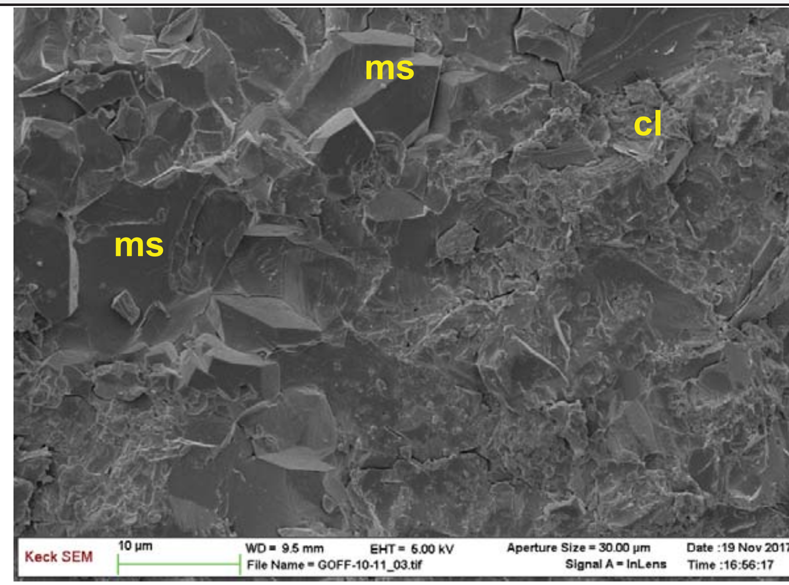

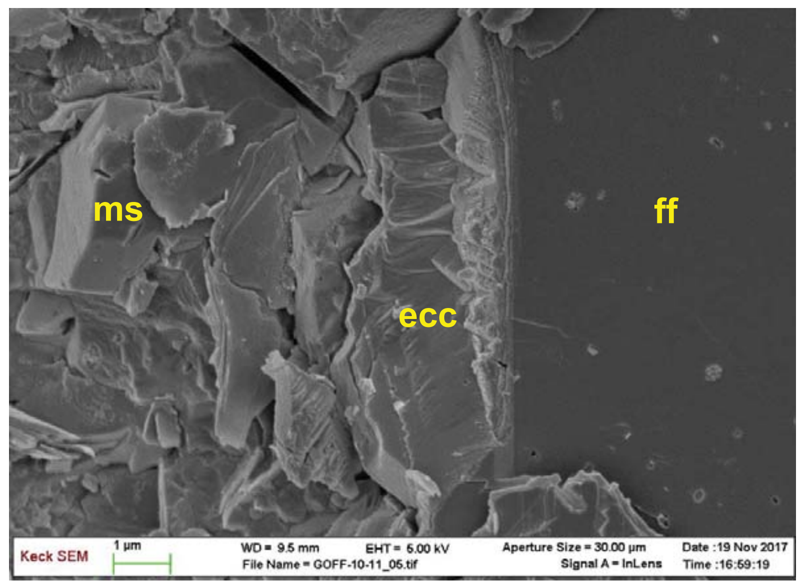

Well ID: Nathan Goff #55 (4703305106)	Formation: Marcellus Formation	Sample ID:	GOFF-17
Location: Harrison, WV	Member: Cherry Valley Limestone	Depth (ft):	7205.25

Microsparitic crystalline carbonate

Matrix Composition

calcite

Texture

nonlaminated; matrix is recrystallized to xenotopic, inequigranular microspar

Diagenetic Minerals

calcite is the dominant diagenetic mineral; matrix and fossils are homogenized by calcite recrystallization; ferroan calcite associated with barite; collophane fills select fossils; minor dolomite rhombohedra; pyrite framboids disseminated throughout

Allochemical or Detrital Grains

trace quartz silt

Fossils

nondescript fossil fragments; collapsed organic-walled cysts

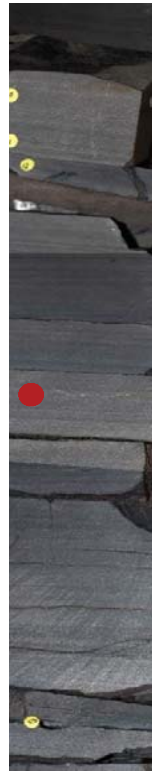

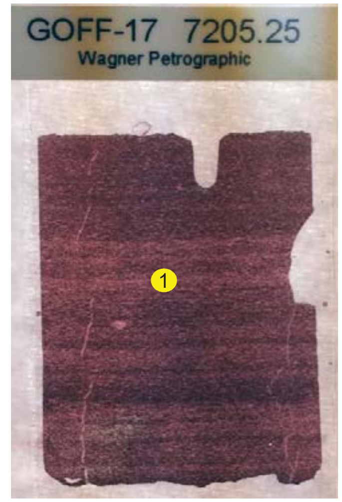

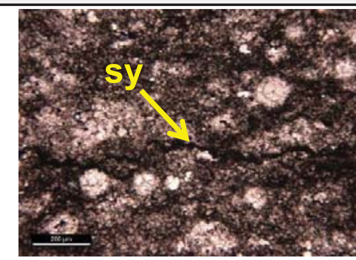

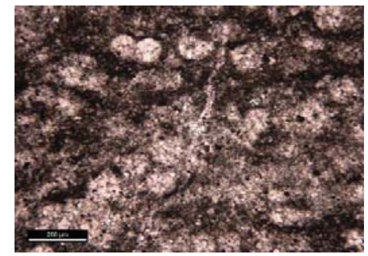

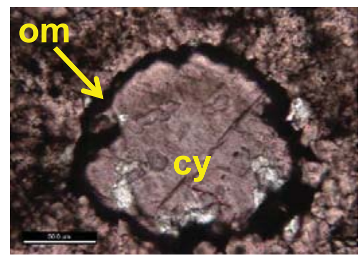

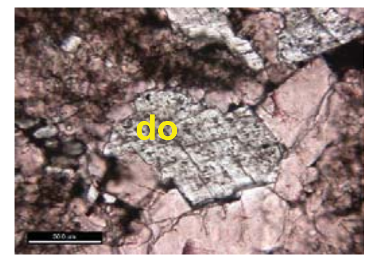

Fractures

vertical calcite-filled fractures are present throughout the thin section; en echelon subvertical fractures cross between vertical fractures; irregular anastomosing stylolites propagate parallel to bedding

Additional Comments

minor organic material disseminated within matrix microspar

SWIR

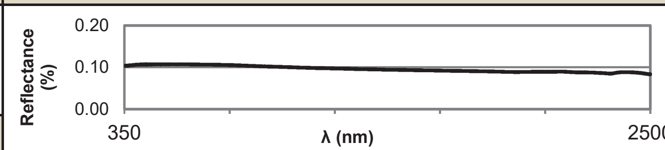

XRD

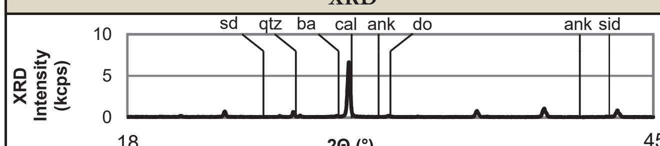

Stable Isotope

$\delta^{13}C_{VPDB}$ (‰)	$\delta^{18}O_{VPDB}$ (‰)
1A Sample	
-11.51	-3.03
1B Sample	
-11.33	-3.26

Well ID: Nathan Goff #55 (4703305106)	**Formation: Marcellus Formation**	**Sample ID:**	**GOFF-19/20**
Location: Harrison, WV	**Member: Cherry Valley Limestone**	**Depth (ft):**	**7205.42**

Microsparitic crystalline carbonate

Matrix Composition

calcite

Texture

nonlaminated; matrix is recrystallized to xenotopic, inequigranular microspar

Diagenetic Minerals

calcite is the dominant diagenetic mineral; matrix and fossils are homogenized by calcite recrystallization; ferroan calcite associated with barite; collophane fills select fossils; minor dolomite rhombohedra; pyrite framboids disseminated throughout; dolomite fills or crystallizes in association with stylolites

Allochemical or Detrital Grains

trace quartz silt

Fossils

nondescript fossil fragments; collapsed organic-walled cysts

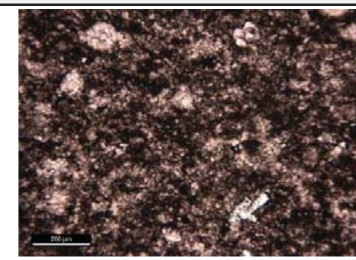

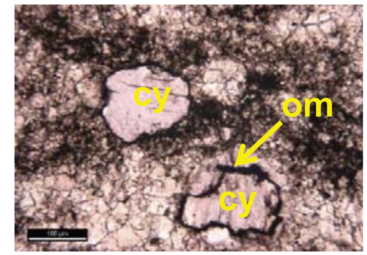

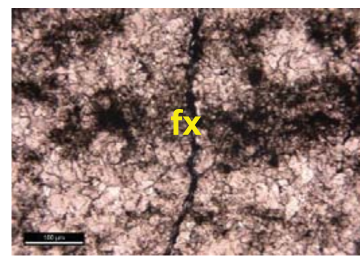

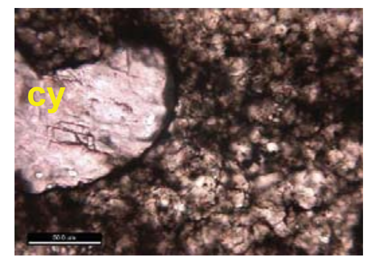

Fractures

subvertical organic-filled fractures; irregular anastomosing stylolites propagate parallel to bedding

Additional Comments

minor organic material disseminated within matrix microspar

SWIR

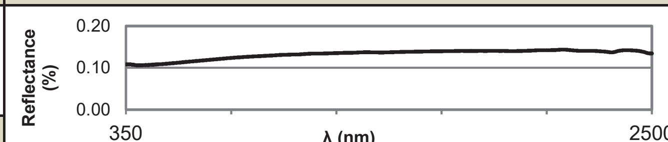

XRD

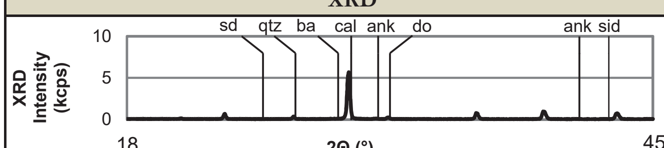

Stable Isotope

$\delta^{13}C_{VPDB}$ (‰)	$\delta^{18}O_{VPDB}$ (‰)
1A Sample	
-7.52	-5.33
1B Sample	
-7.54	-3.77

Well ID: Nathan Goff #55 (4703305106)	Formation: Marcellus Formation	Sample ID:	GOFF-19/20
Location: Harrison, WV	Member: Cherry Valley Limestone	Depth (ft):	7205.42

Microsparitic crystalline carbonate

Matrix Composition and Microtexture
calcite recrystallization results in a microsparitic texture; clay minerals and degraded organic material fill areas between microspar

Diagenetic Minerals
calcite is the primary diagenetic mineral; collophane, organic material, and pyrite fill select cyst tests

Diagenetic Texture
neomorphism of calcite matrix, likely micritic in origin, gives the rock a massive or chunky appearance; select fossils include equant calcite overgrowths on their ridges

Pore Structure
clay and organic material admixed within microsparitic matrix, likely hosting nominal porosity

Depositional Fabric
diagenesis has destroyed a majority of depositional fabrics, as microspar growth has grown amidst what may have been a laminated, calcareous mudstone

Additional comments:

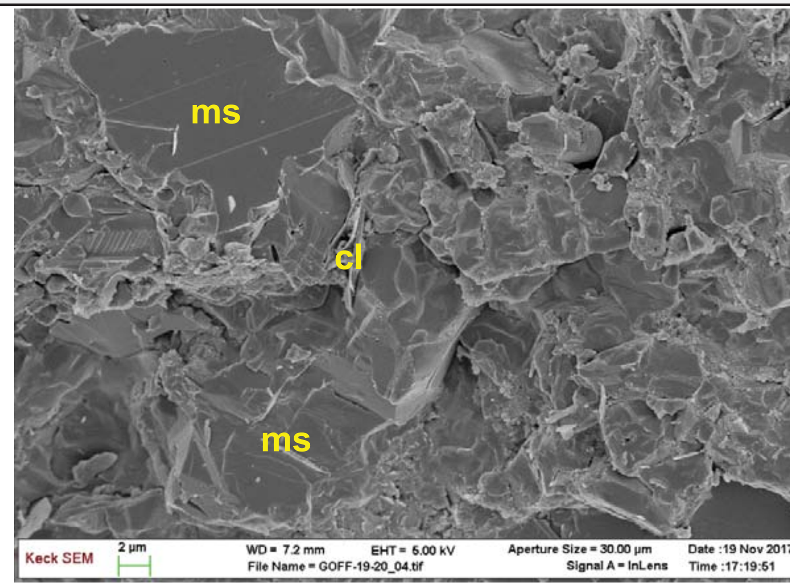

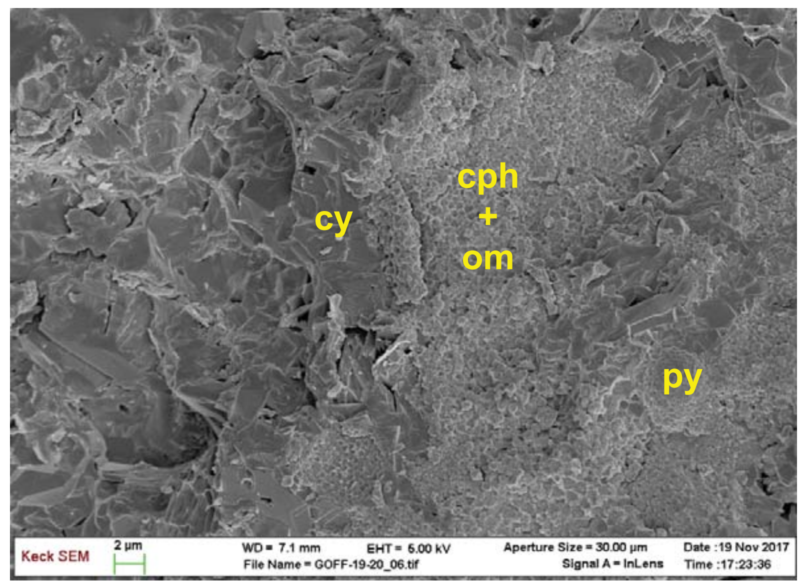

Well ID: Nathan Goff #55 (4703305106)	**Formation: Marcellus Formation**	**Sample ID:**	**GOFF-26/27**
Location: Harrison, WV	**Member: Cherry Valley Limestone**	**Depth (ft):**	**7205.96**

Microsparitic crystalline carbonate

Matrix Composition

calcite

Texture

nonlaminated; xenotopic, inequigranular microspar matrix

Diagenetic Minerals

calcite is the dominant diagenetic mineral; matrix and fossils are homogenized by calcite recrystallization; dolomite or ferroan calcite fills collapsed cysts; dolomite crystallizes along stylolites; minor barite

Allochemical or Detrital Grains

none

Fossils

nondescript fossil fragments; collapsed organic-walled cysts

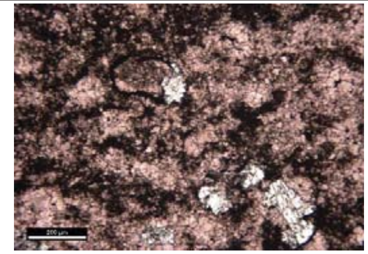

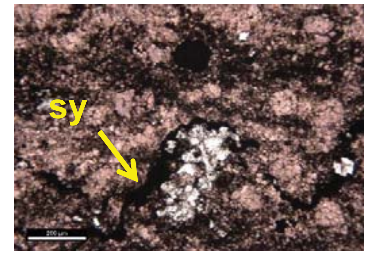

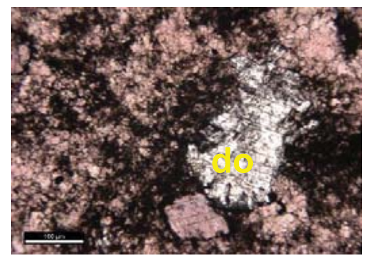

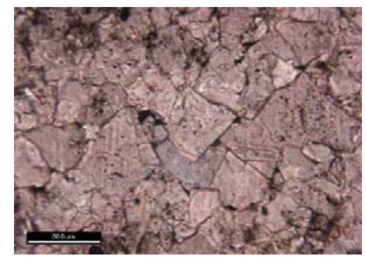

Fractures

irregular anastomosing stylolites propagate parallel to bedding

Additional Comments

organic material disseminated throughout microsparitic matrix

SWIR

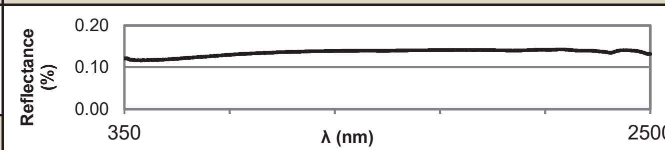

XRD

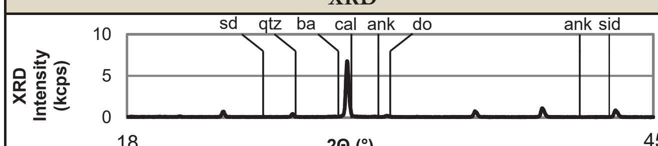

Stable Isotope

	$\delta^{13}C_{VPDB}$ (‰)	$\delta^{18}O_{VPDB}$ (‰)
1A Sample	-7.67	-6.44
1B Sample	-7.89	-6.07

Well ID: Nathan Goff #55 (4703305106)	Formation: Marcellus Formation	Sample ID:	GOFF-31/32
Location: Harrison, WV	Member: Cherry Valley Limestone	Depth (ft):	7206.25

Microsparitic crystalline carbonate

Matrix Composition

calcite

Texture

nonlaminated; xenotopic, inequigranular microspar matrix

Diagenetic Minerals

calcite is the dominant diagenetic mineral; matrix and fossils are homogenized by calcite recrystallization; dolomite or ferroan calcite fills collapsed cysts; dolomite crystallizes along stylolites; minor barite

Allochemical or Detrital Grains

none

Fossils

nondescript fossil fragments; collapsed organic-walled cysts

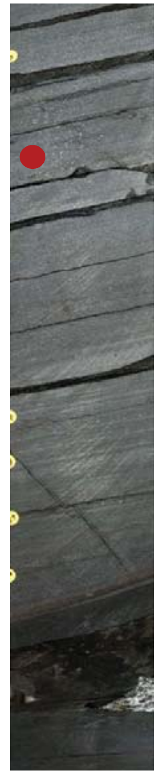

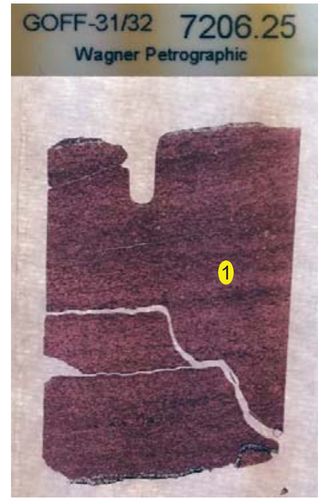

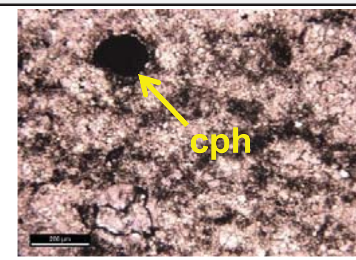

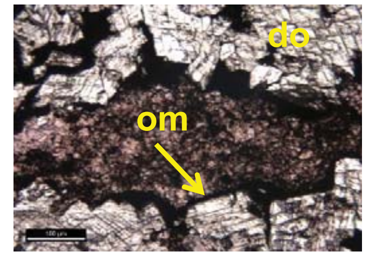

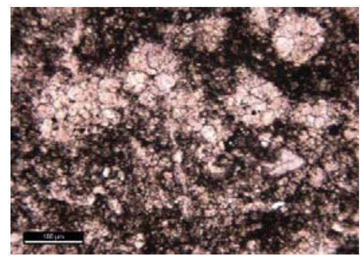

Fractures

irregular anastomosing stylolites propagate parallel to bedding; fracture or stylolite filled with organic residue or cement with dolomite crystallized within it

Additional Comments

organic material disseminated throughout microsparitic matrix

SWIR

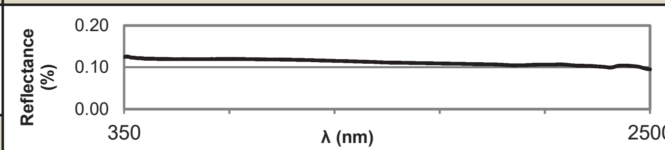

XRD

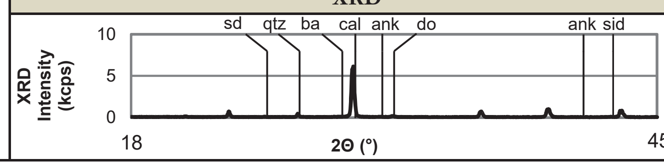

Stable Isotope

	$\delta^{13}C_{VPDB}$ (‰)	$\delta^{18}O_{VPDB}$ (‰)
1A Sample	-7.56	-7.43
1B Sample	-7.40	-5.45

Well ID: Nathan Goff #55 (4703305106)	Formation: Marcellus Formation	Sample ID:	GOFF-35/36
Location: Harrison, WV	Member: Cherry Valley Limestone	Depth (ft):	7206.50

Microsparitic crystalline carbonate

Matrix Composition

calcite

Texture

nonlaminated; xenotopic, inequigranular microspar matrix

Diagenetic Minerals

calcite is the dominant diagenetic mineral; matrix and fossils are homogenized by calcite recrystallization; dolomite, ferroan calcite, or collophane fills collapsed cysts; dolomite crystallizes along stylolites; minor barite

Allochemical or Detrital Grains

none

Fossils

nondescript fossil fragments; collapsed organic-walled cysts

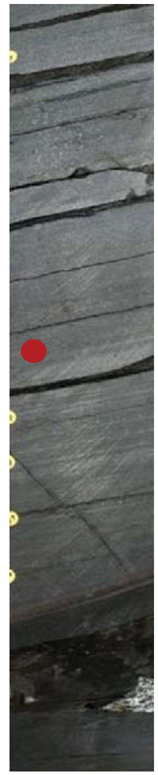

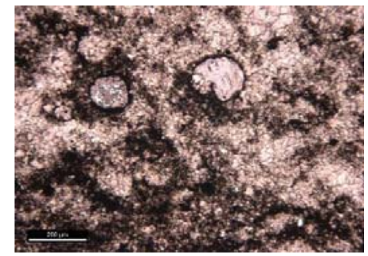

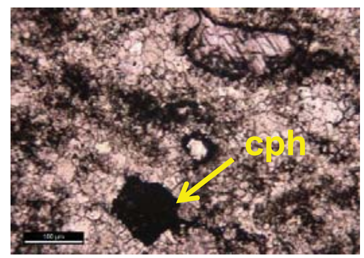

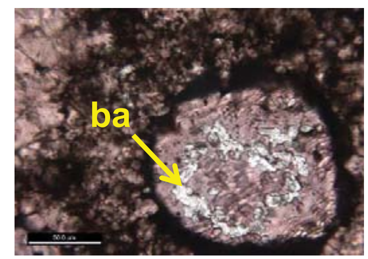

Fractures

fracture or stylolite filled with organic material nearly replaced by dolomite in entirety

Additional Comments

organic material disseminated throughout microsparitic matrix

SWIR

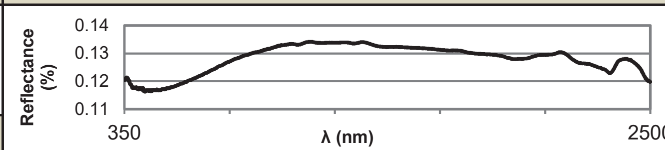

XRD

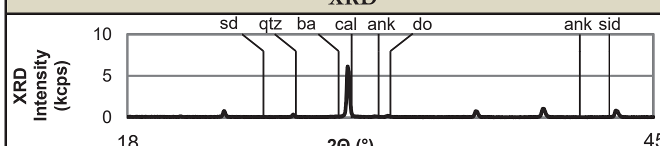

Stable Isotope

	$\delta^{13}C_{VPDB}$ (‰)	$\delta^{18}O_{VPDB}$ (‰)
1A Sample	-6.60	-7.54
1B Sample	-6.70	-6.71

Well ID: Nathan Goff #55 (4703305106)	Formation: Marcellus Formation	Sample ID:	GOFF-35/36
Location: Harrison, WV	Member: Cherry Valley Limestone	Depth (ft):	7206.50

Microsparitic crystalline carbonate

Matrix Composition and Microtexture

calcite recrystallization results in a microsparitic texture; clay minerals and degraded organic material fill areas between microspar

Diagenetic Minerals

calcite is the primary diagenetic mineral; pyrite generally associated with degraded organic material

Diagenetic Texture

neomorphism of calcite matrix, likely micritic in origin, gives the rock a massive or chunky appearance; select fossils include equant calcite overgrowths on their ridges

Pore Structure

clay and organic material admixed within microsparitic matrix, likely hosting nominal porosity

Depositional Fabric

diagenesis has destroyed a majority of depositional fabrics, as microspar growth has grown amidst what may have been a laminated, calcareous mudstone

Additional comments:

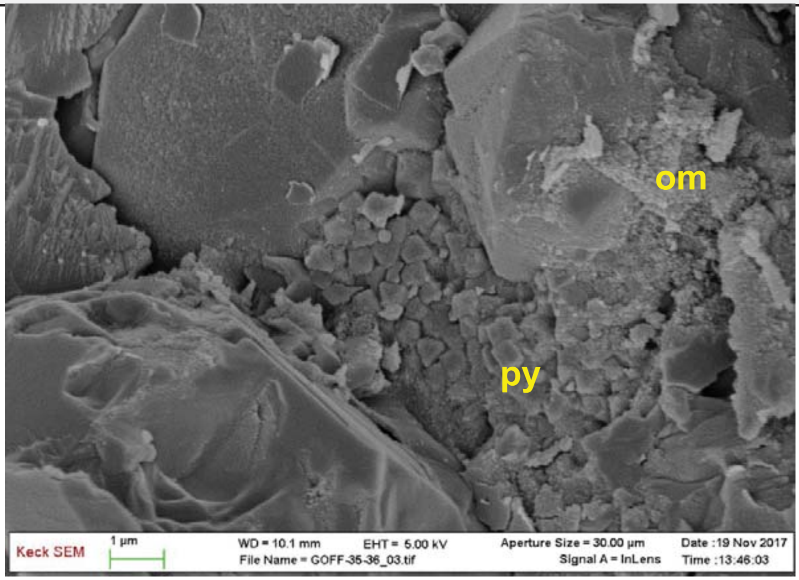

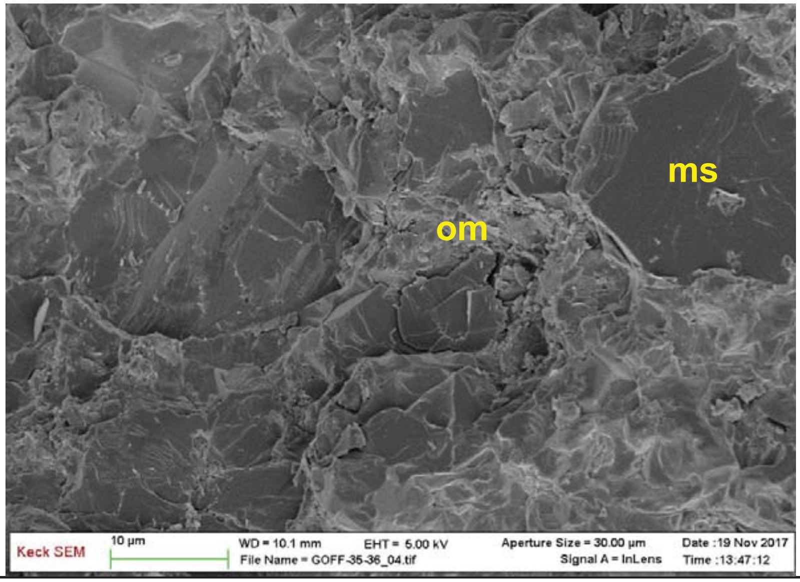

Well ID: Nathan Goff #55 (4703305106)	Formation: Marcellus Formation	Sample ID:	GOFF-39/40
Location: Harrison, WV	Member: Cherry Valley Limestone	Depth (ft):	7206.92

Microsparitic crystalline carbonate

Matrix Composition

calcite

Texture

nonlaminated; xenotopic, inequigranular microspar matrix

Diagenetic Minerals

calcite is the dominant diagenetic mineral; matrix and fossils are homogenized by calcite recrystallization; ferroan calcite or collophane fills collapsed cysts; dolomite crystallizes along stylolites; minor barite

Allochemical or Detrital Grains

none

Fossils

nondescript fossil fragments; collapsed organic-walled cysts

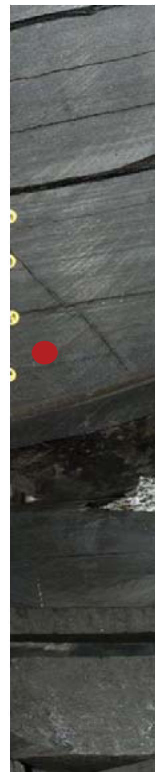

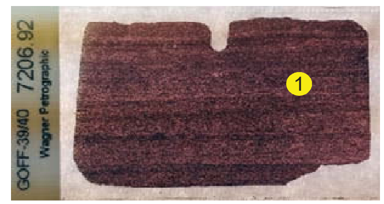

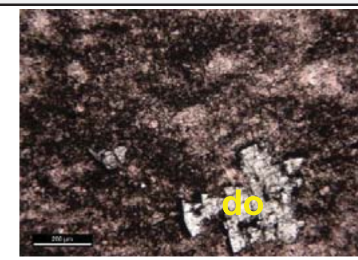

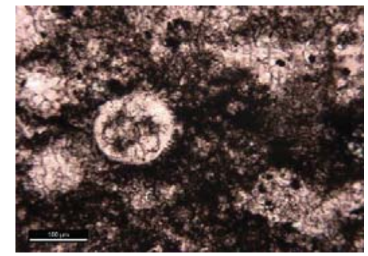

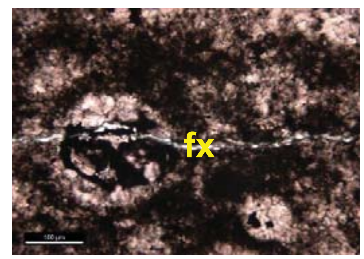

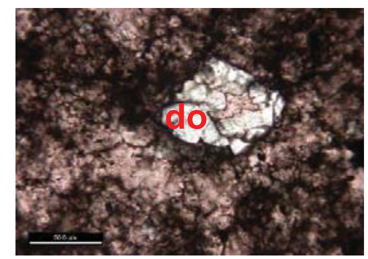

Fractures

hairline, calcite-filled fractures propagate parallel to bedding

Additional Comments

organic material disseminated throughout microsparitic matrix

SWIR

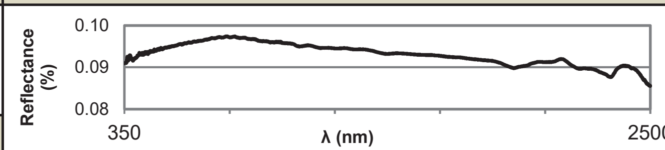

XRD

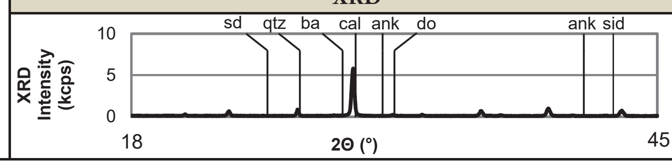

Stable Isotope

	$\delta^{13}C_{VPDB}$ (‰)	$\delta^{18}O_{VPDB}$ (‰)
1A Sample	-7.85	-1.49
1B Sample	7.80	-1.58

Well ID: MSEEL / MIP 3H (4706101707)	Formation: Marcellus Formation	Sample ID:	MSEEL-15
Location: Monongalia , WV	Member: Cherry Valley Limestone	Depth (ft):	7518.17

Microsparitic crystalline carbonate

Matrix Composition

calcite

Texture

nonlaminated; hypidiotopic, inequigranular microspar matrix

Diagenetic Minerals

calcite is the dominant diagenetic mineral; matrix and fossils are homogenized by calcite recrystallization; ferroan calcite or collophane fills collapsed cysts; dolomite crystallizes along stylolites; minor barite

Allochemical or Detrital Grains

none

Fossils

nondescript fossil fragments; collapsed organic-walled cysts

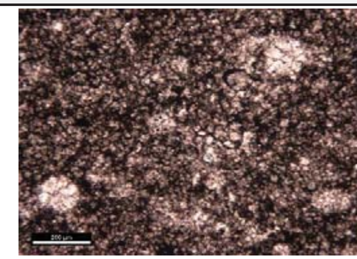

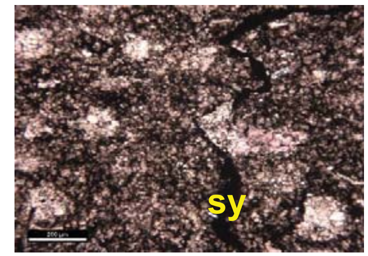

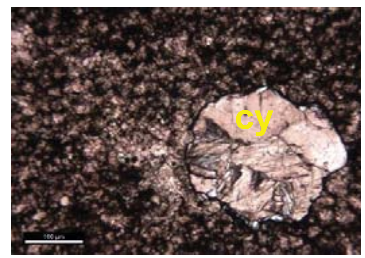

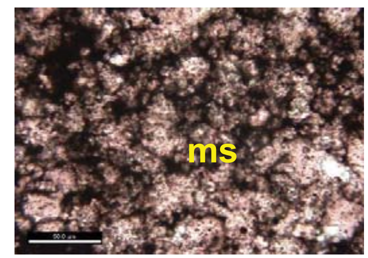

Fractures

vertical, irregular anastomosing stylolites filled with organic material

Additional Comments

organic material disseminated throughout microsparitic matrix

SWIR

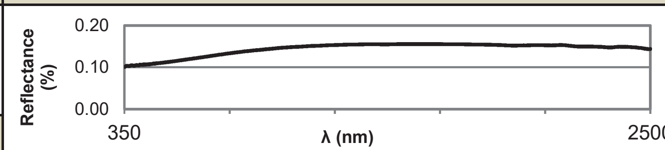

XRD

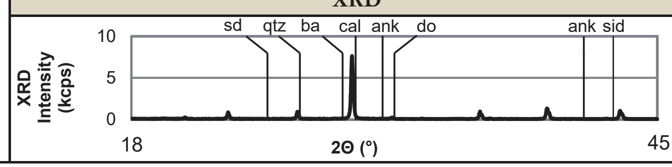

Stable Isotope

	$\delta^{13}C_{VPDB}$ (‰)	$\delta^{18}O_{VPDB}$ (‰)
1A Sample	-7.09	-5.48
1B Sample	-6.26	-6.61

Well ID: MSEEL / MIP 3H (4706101707)	Formation: Marcellus Formation	Sample ID:	MSEEL-15
Location: Monongalia , WV	Member: Cherry Valley Limestone	Depth (ft):	7518.17

Microsparitic crystalline carbonate

Matrix Composition and Microtexture

calcite recrystallization results in a microsparitic texture; clay minerals and degraded organic material fill areas between microspar

Diagenetic Minerals

calcite is the primary diagenetic mineral; minor pyrite associated with degraded organic material

Diagenetic Texture

neomorphism of calcite matrix, likely micritic in origin, gives the rock a massive or chunky appearance; select fossils include equant calcite overgrowths on their ridges

Pore Structure

clay and organic material admixed within microsparitic matrix, likely hosting nominal porosity

Depositional Fabric

diagenesis has destroyed most depositional fabrics, as microspar growth has grown amidst what may have been a laminated, calcareous mudstone

Additional comments:

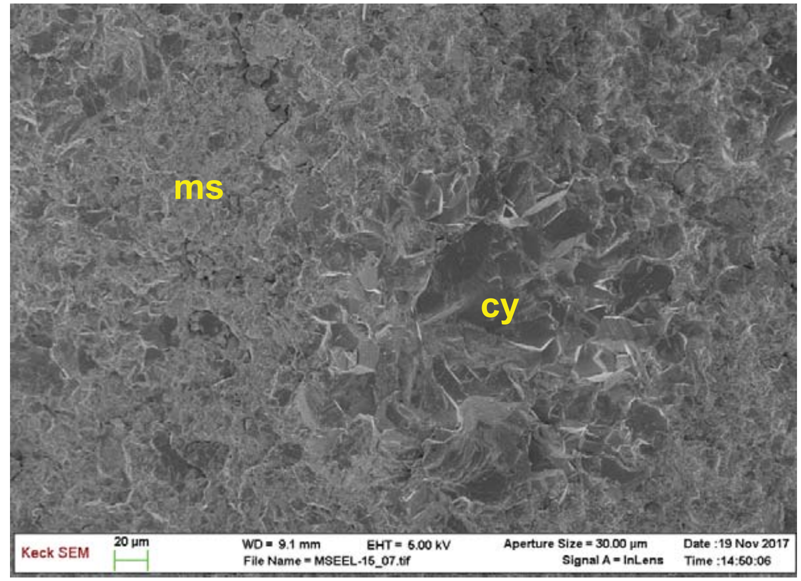

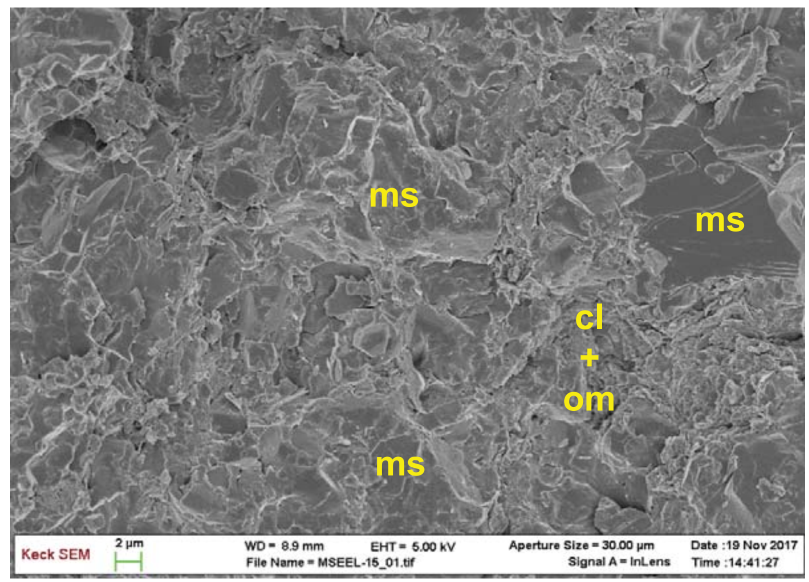

Well ID: MSEEL / MIP 3H (4706101707)	**Formation: Marcellus Formation**	**Sample ID:**	**MSEEL-58/59**
Location: Monongalia , WV	**Member: Cherry Valley Limestone**	**Depth (ft):**	**7524.08**

Microsparitic crystalline carbonate

Matrix Composition
calcite

Texture
nonlaminated; xenotopic, inequigranular microspar matrix

Diagenetic Minerals
calcite is the dominant diagenetic mineral; fossils are rimmed with circumgranular, equant or bladed calcite crystals; more robust fossils are composed of ferroan calcite

Allochemical or Detrital Grains
quartz silt (< 5%)

Fossils
dacryoconarids (Styliolina); gastropods; crinoids; ostracods; possible trilobites; nondescript fossil fragments; collapsed organic-walled cysts

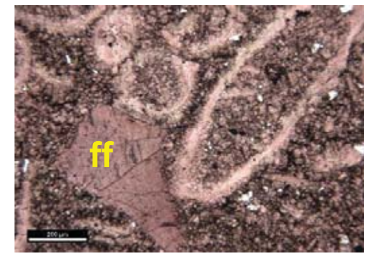

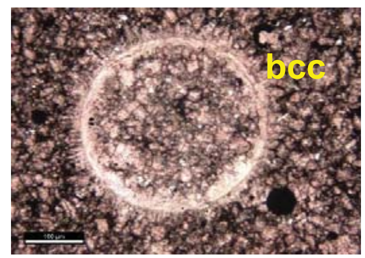

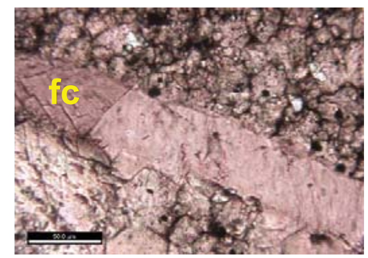

Fractures
vertical, organic-filled, irregular anastomosing stylolites

Additional Comments
organic material disseminated throughout microsparitic matrix

SWIR

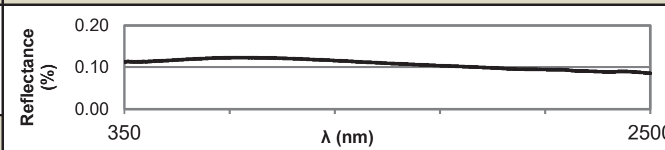

XRD

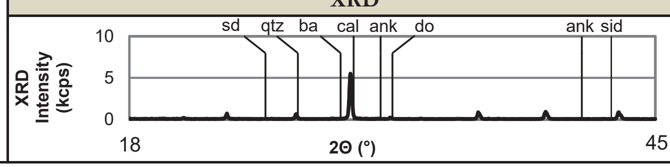

Stable Isotope

	$\delta^{13}C_{VPDB}$ (‰)	$\delta^{18}O_{VPDB}$ (‰)
1A Sample	-9.01	-6.70
1B Sample	-8.88	-6.81

Well ID: MSEEL / MIP 3H (4706101707)	Formation: Marcellus Formation	Sample ID:	MSEEL-58/59
Location: Monongalia , WV	Member: Cherry Valley Limestone	Depth (ft):	7524.08

Microsparitic crystalline carbonate

Matrix Composition and Microtexture

calcite recrystallization results in microsparitic microtexture

Diagenetic Minerals

calcite is the primary diagenetic mineral; minor pyrite

Diagenetic Texture

neomorphism of calcite matrix, which was likely micritic in origin, lends to a massive and chunky appearance; fossils typically feature a bladed or equant calcite overgrowths; fossil interiors are filled with microspar or single-crystal calcite

Pore Structure

porosity is likely restricted to equant pores that are hosted within the microspar matrix

Depositional Fabric

depositional fabrics are overprinted by recrystallization

Additional comments:

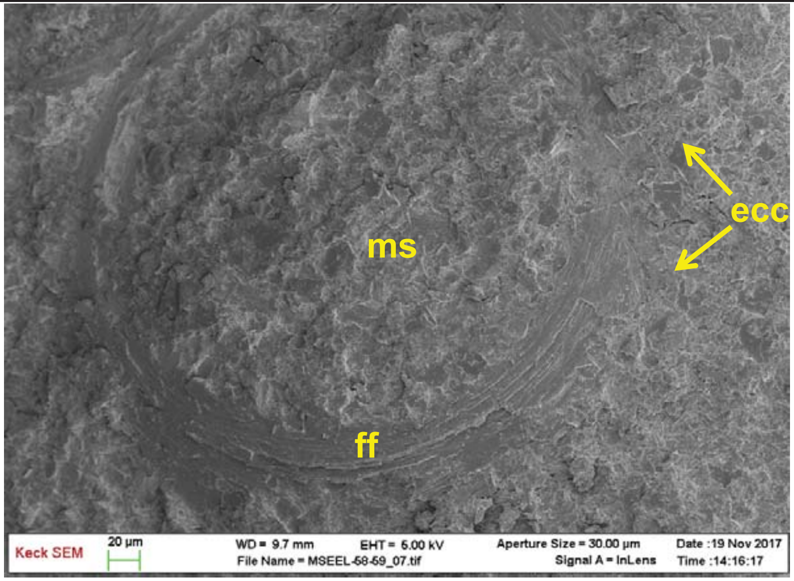

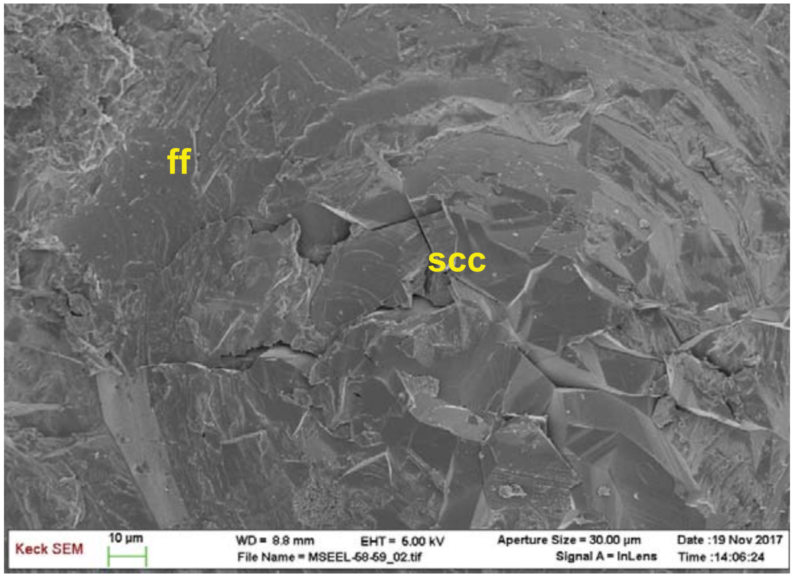

Well ID: EGSP WV-7 (4710300645)	Formation: Marcellus Formation	Sample ID:	WV7-1
Location: Wetzel, WV	Member: Cherry Valley Limestone	Depth (ft):	6615.17

Microsparitic packstone

Matrix Composition

calcite

Texture

poorly laminated; calcite is recrystallized to inequigranular, xenotopic microspar

Diagenetic Minerals

calcite is the primary diagenetic mineral; matrix calcite is neomorphosed to microspar; fossils are rimmed with equant calcite or ferroan calcite; minor dolomite cementation, primarily filling fossils; minor barite

Allochemical or Detrital Grains

trace quartz silt

Fossils

dacryoconarids (Nowakia); nondescript shell fragments

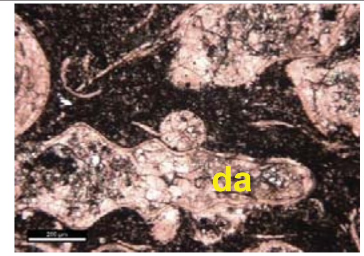

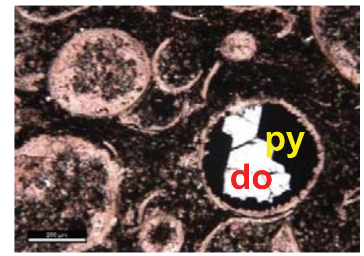

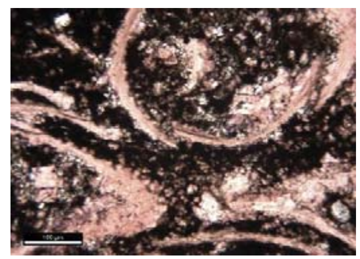

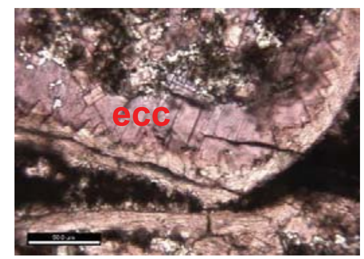

Fractures

none

Additional Comments

organic material disseminated throughout matrix microspar

SWIR

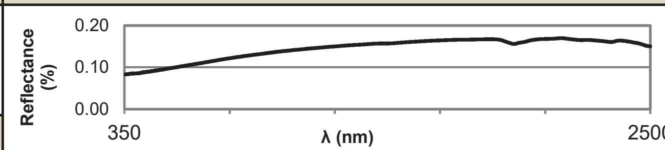

XRD

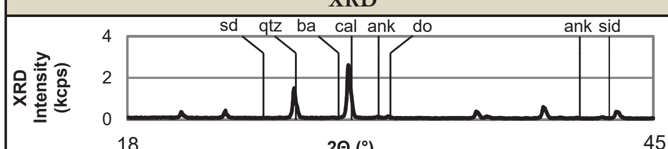

Stable Isotope

	$\delta^{13}C_{VPDB}$ (‰)	$\delta^{18}O_{VPDB}$ (‰)
1A Sample	-10.82	-3.29
1B Sample	-11.19	-4.11

Well ID: EGSP WV-7 (4710300645)	**Formation: Marcellus Formation**	**Sample ID:**	**WV7-1**
Location: Wetzel, WV	**Member: Cherry Valley Limestone**	**Depth (ft):**	**6615.17**

Microsparitic packstone

Matrix Composition and Microtexture

calcite recrystallization results in a microsparitic texture; clay minerals and degraded organic material fill areas between microspar

Diagenetic Minerals

calcite is the primary diagenetic mineral; organic material and pyrite fill select cyst tests

Diagenetic Texture

neomorphism of calcite matrix, likely micritic in origin, gives the rock a massive or chunky appearance; select fossils include equant calcite overgrowths; calcite fills most fossils, either as single-crystal calcite or microspar

Pore Structure

clay and organic material admixed within microsparitic matrix, likely hosting nominal porosity

Depositional Fabric

diagenesis has destroyed a majority of depositional fabrics, as microspar growth has grown amidst what may have been a laminated, fossiliferous, calcareous mudstone

Additional comments:

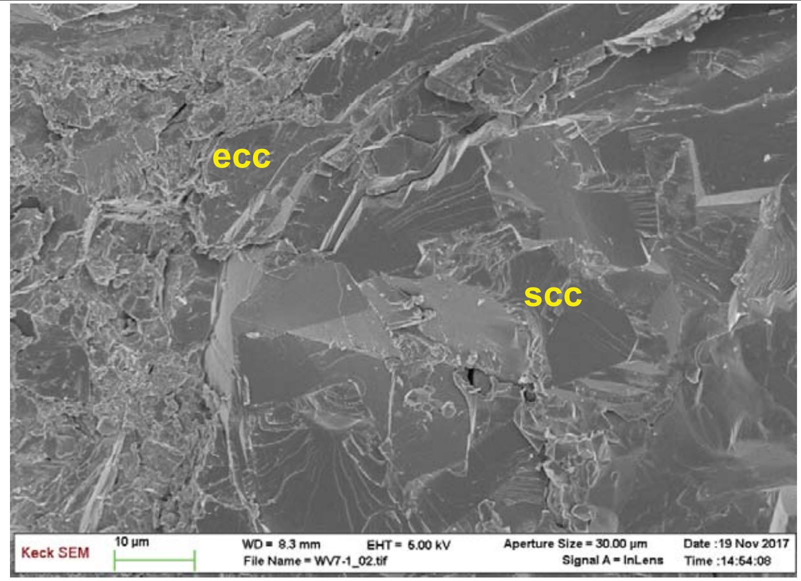

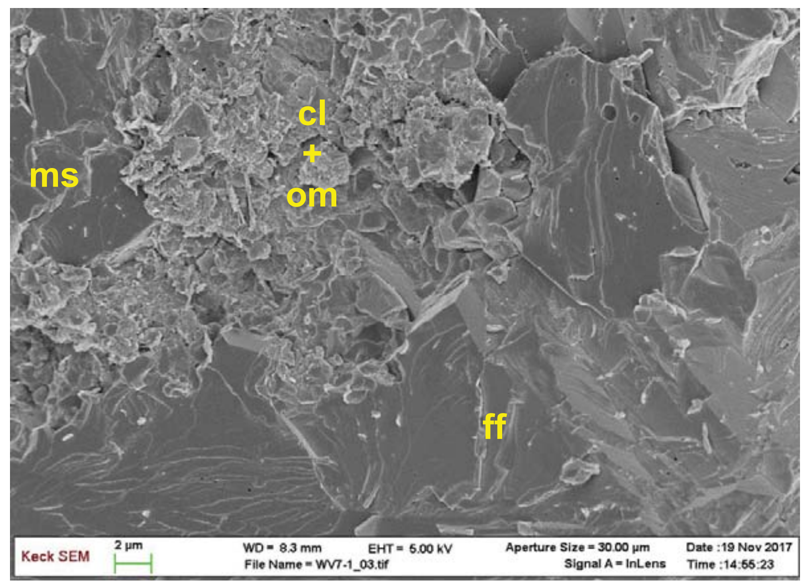

Well ID: EGSP WV-7 (4710300645)	Formation: Marcellus Formation	Sample ID:	WV7-3
Location: Wetzel, WV	Member: Cherry Valley Limestone	Depth (ft):	6615.33

Microsparitic packstone

Matrix Composition

calcite

Texture

poorly laminated; calcite is recrystallized to inequigranular, xenotopic microspar

Diagenetic Minerals

calcite is the primary diagenetic mineral; matrix calcite is neomorphosed to microspar; fossils are rimmed with equant calcite; sparry ferroan calcite fills select fossils; minor dolomite cementation, primarily filling fossils; minor barite

Allochemical or Detrital Grains

trace quartz silt

Fossils

dacryoconarids (Nowakia); nondescript shell fragments

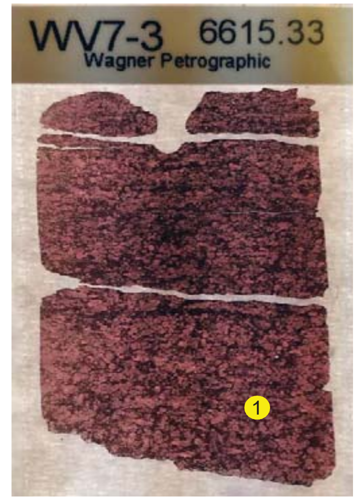

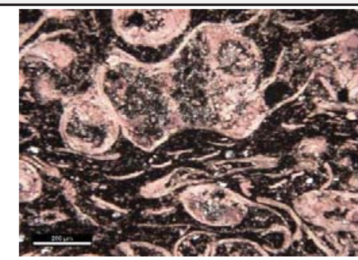

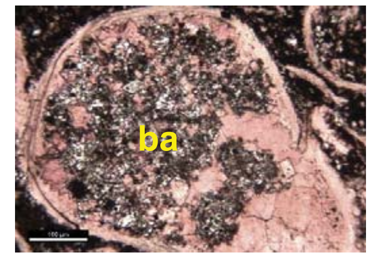

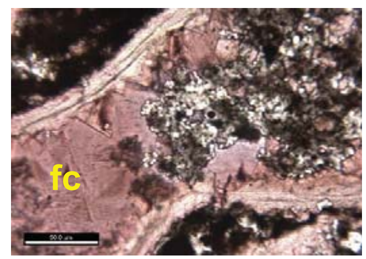

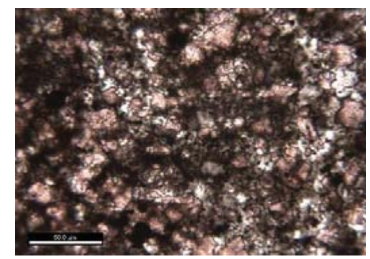

Fractures

none

Additional Comments

organic material disseminated throughout matrix microspar

SWIR

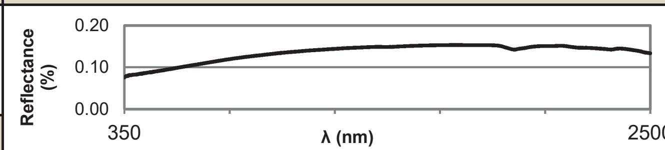

XRD

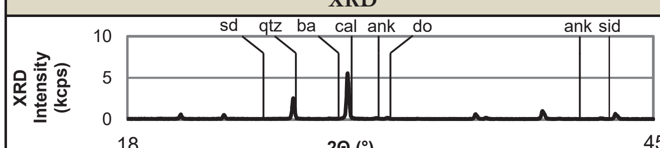

Stable Isotope

$\delta^{13}C_{VPDB}$ (‰)	$\delta^{18}O_{VPDB}$ (‰)
1A Sample	
-10.30	-6.68
1B Sample	
N/A	N/A

Well ID: EGSP WV-7 (4710300645)	Formation: Marcellus Formation	Sample ID:	WV7-6
Location: Wetzel, WV	Member: Cherry Valley Limestone	Depth (ft):	6615.67

Microsparitic wackestone

Matrix Composition

calcite

Texture

poorly laminated; calcite is recrystallized to equigranular, hypidiotopic microspar

Diagenetic Minerals

calcite is the primary diagenetic mineral; matrix calcite is neomorphosed to microspar; fossils are rimmed with equant to bladed calcite; sparry ferroan calcite fills select fossils; minor dolomite cementation, primarily filling fossils; minor barite; minor dolomite rhombohedra

Allochemical or Detrital Grains

trace quartz silt

Fossils

dacryoconarids (Nowakia); nondescript shell fragments; fecal pellets

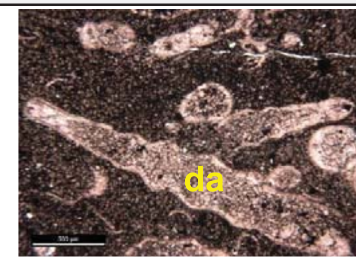

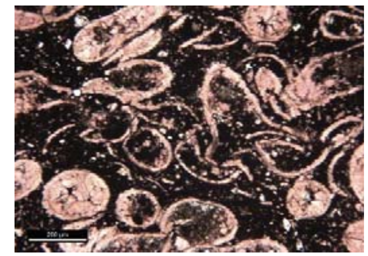

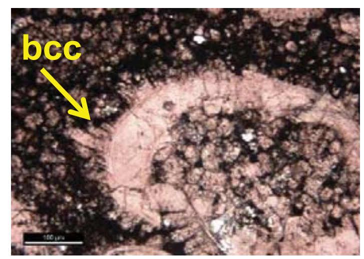

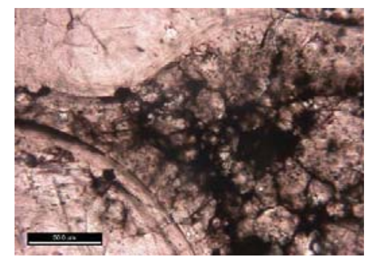

Fractures

organic residue cements fractures

Additional Comments

organic material disseminated throughout matrix microspar

SWIR

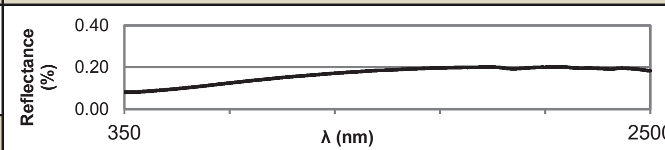

XRD

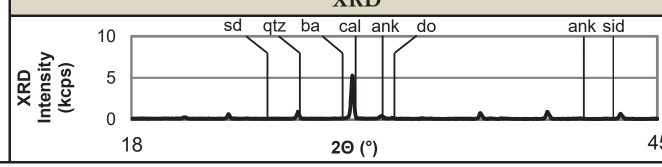

Stable Isotope

$\delta^{13}C_{VPDB}$ (‰)	$\delta^{18}O_{VPDB}$ (‰)
1A Sample	
-12.24	-2.49
1B Sample	
-12.23	-2.65

Well ID: EGSP WV-7 (4710300645)	**Formation: Marcellus Formation**	**Sample ID:**	**WV7-8**
Location: Wetzel, WV	**Member: Cherry Valley Limestone**	**Depth (ft):**	**6615.83**

Microsparitic wackestone

Matrix Composition

calcite

Texture

poorly laminated; calcite is recrystallized to equigranular, hypidiotopic microspar

Diagenetic Minerals

calcite is the primary diagenetic mineral; matrix calcite is neomorphosed to microspar; fossils are rimmed with equant to bladed calcite; sparry ferroan calcite fills select fossils; minor dolomite cementation, primarily filling fossils; minor barite; minor dolomite rhombohedra

Allochemical or Detrital Grains

trace quartz silt

Fossils

dacryoconarids (Nowakia and Styliolina); nondescript shell fragments; fecal pellets; collapsed organic-walled cysts

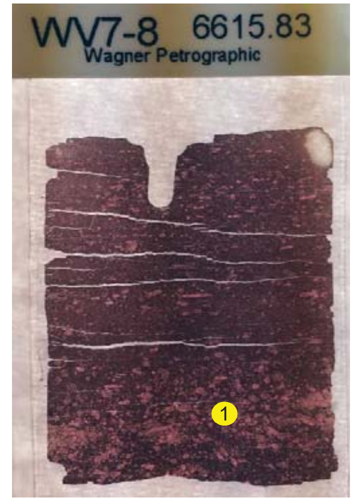

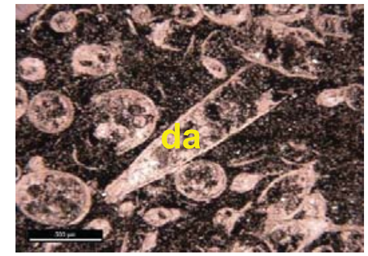

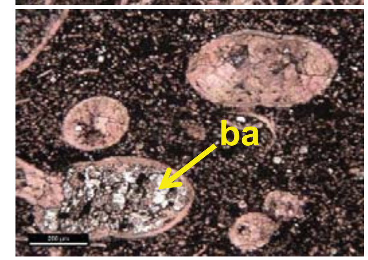

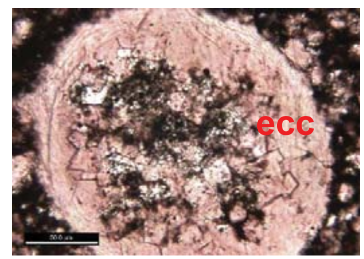

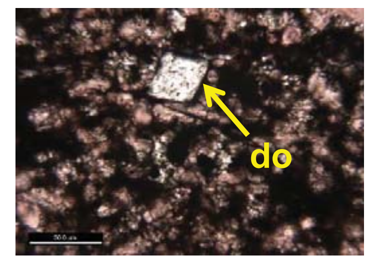

Fractures

none

Additional Comments

organic material disseminated throughout matrix microspar

SWIR

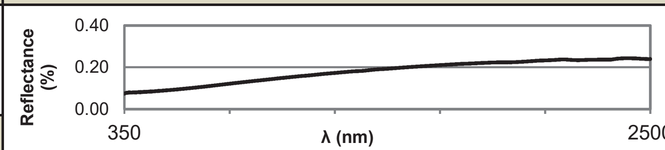

XRD

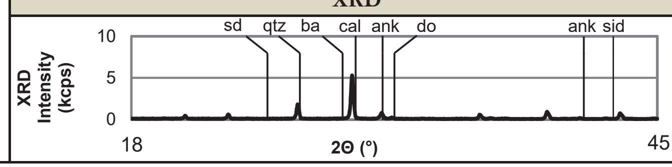

Stable Isotope

	$\delta^{13}C_{VPDB}$ (‰)	$\delta^{18}O_{VPDB}$ (‰)
1A Sample	-11.32	-3.81
1B Sample	-11.26	-3.43

Well ID: EGSP WV-7 (4710300645)	Formation: Marcellus Formation	Sample ID:	WV7-12
Location: Wetzel, WV	Member: Cherry Valley Limestone	Depth (ft):	6616.08

Microsparitic crystalline carbonate

Matrix Composition
calcite

Texture
nonlaminated; inequigranular, xenotopic microspar matrix

Diagenetic Minerals
calcite is the dominant diagenetic mineral; matrix is neomorphosed to microspar; fossils are filled with collophane, calcite, ferroan calcite, and pyrite; disseminated dolomite rhombohedra

Allochemical or Detrital Grains
trace quartz silt

Fossils
nondescript fossil fragments; collapsed organic-walled cysts

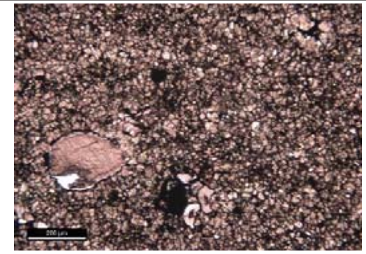

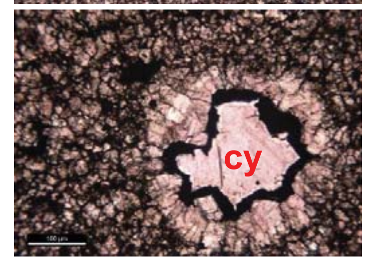

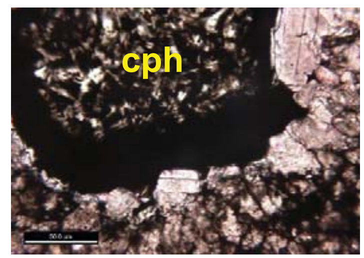

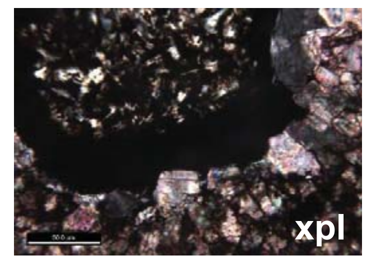

Fractures
none

Additional Comments
organic material disseminated through matrix microspar

SWIR

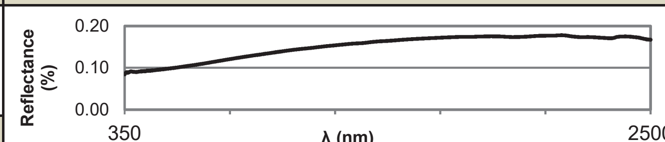

XRD

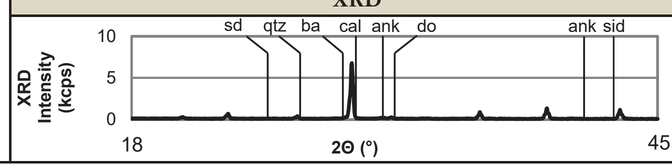

Stable Isotope

	$\delta^{13}C_{VPDB}$ (‰)	$\delta^{18}O_{VPDB}$ (‰)
1A Sample	-6.31	-1.99
1B Sample	-6.27	-1.29

Well ID: EGSP WV-7 (4710300645)	**Formation: Marcellus Formation**	**Sample ID:**	**WV7-12**
Location: Wetzel, WV	**Member: Cherry Valley Limestone**	**Depth (ft):**	**6616.08**

Microsparitic crystalline carbonate

Matrix Composition and Microtexture

calcite recrystallization results in a microsparitic texture; clay minerals and degraded organic material fill areas between microspar

Diagenetic Minerals

calcite is the primary diagenetic mineral; minor pyrite associated with degraded organic material; trace dolomite rhombohedra

Diagenetic Texture

neomorphism of calcite matrix, likely micritic in origin, gives the rock a massive or chunky appearance

Pore Structure

clay and organic material admixed within microsparitic matrix, likely hosting nominal porosity

Depositional Fabric

diagenesis has destroyed a majority of depositional fabrics, as microspar growth has grown amidst what may have been a laminated, calcareous mudstone

Additional comments:

fossils either not accurately represented in SEM sample or are not distinguishable from altered matrix

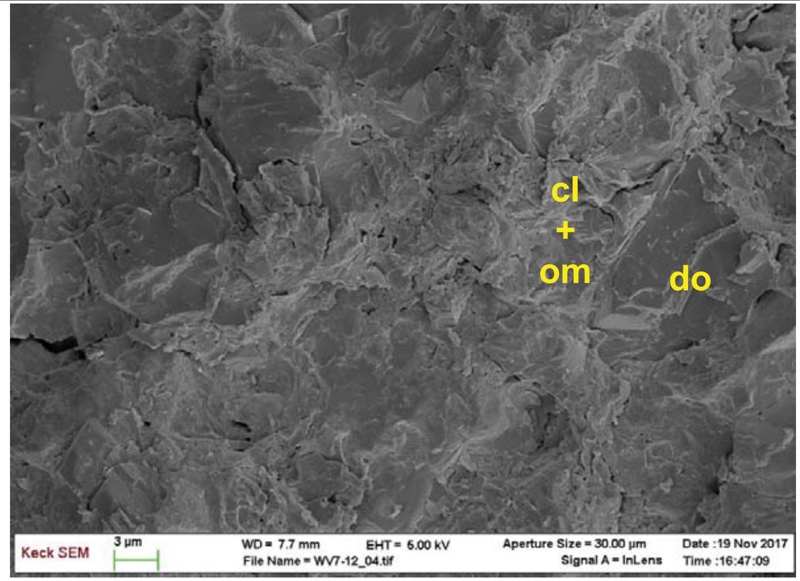

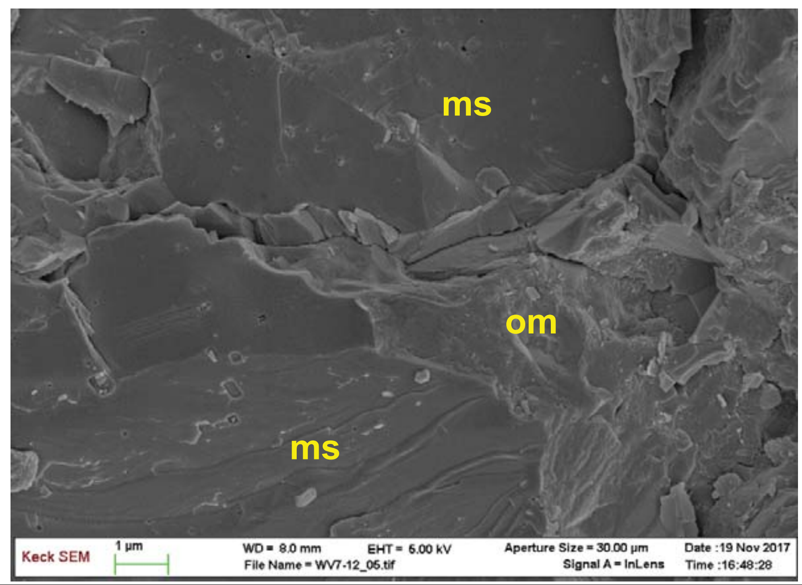

Well ID: St. Whipkey #1 (3705924715)	Formation: Marcellus Formation	Sample ID:	WHIP-36
Location: Greene, PA	Member: Cherry Valley Member	Depth (ft):	7868.58

Microsparitic crystalline carbonate

Matrix Composition

calcite

Texture

nonlaminated; calcite is recrystallized to hypidiotopic, equigranular microspar

Diagenetic Minerals

calcite is the dominant diagenetic mineral; a final stage of calcite neomorphism overprints depositional fabric and previous diagenetic phases; textural differences in calcite growth on the interior of fossil tests suggest a previous and since-overprinted calcite crystallization stage

Allochemical or Detrital Grains

none

Fossils

nondescript fossil or shell fragments; collapsed organic-walled cysts

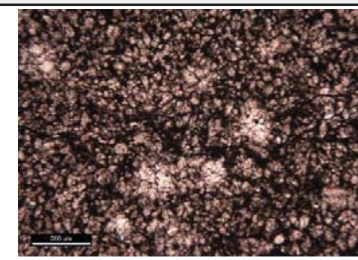

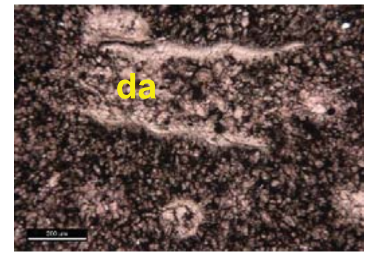

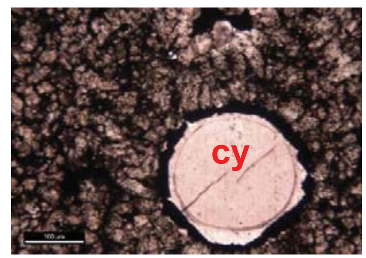

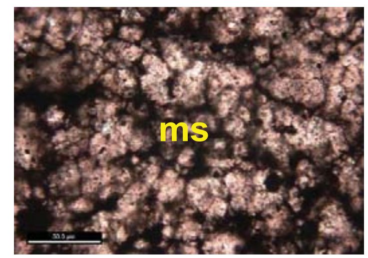

Fractures

none

Additional Comments

organic material disseminated between microspar crystals

SWIR

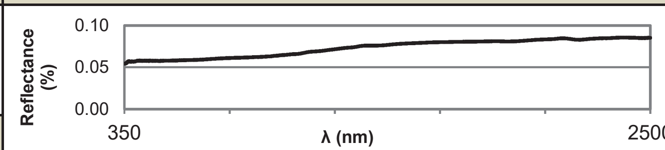

XRD

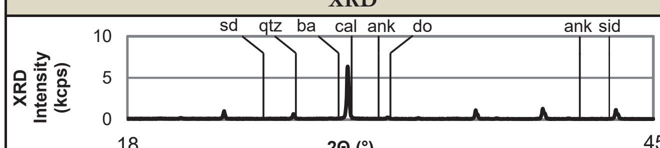

Stable Isotope

	$\delta^{13}C_{VPDB}$ (‰)	$\delta^{18}O_{VPDB}$ (‰)
1A Sample	-11.34	-4.36
1B Sample	-11.46	-3.90

Well ID: St. Whipkey #1 (3705924715)	Formation: Marcellus Formation	Sample ID:	WHIP-36
Location: Greene, PA	Member: Cherry Valley Member	Depth (ft):	7868.58

Microsparitic crystalline carbonate

Matrix Composition and Microtexture

calcite recrystallization results in a microsparitic texture; clay minerals and degraded organic material fill areas between microspar

Diagenetic Minerals

calcite is the primary diagenetic mineral

Diagenetic Texture

neomorphism of calcite matrix, likely micritic in origin, gives the rock a massive or chunky appearance; select fossils include equant calcite overgrowths on their ridges; cysts may be filled with single-crystal calcite

Pore Structure

clay and organic material admixed within microsparitic matrix, likely hosting nominal porosity

Depositional Fabric

diagenesis has destroyed a majority of depositional fabrics, as microspar growth has grown amidst what may have been a laminated, calcareous mudstone

Additional comments:

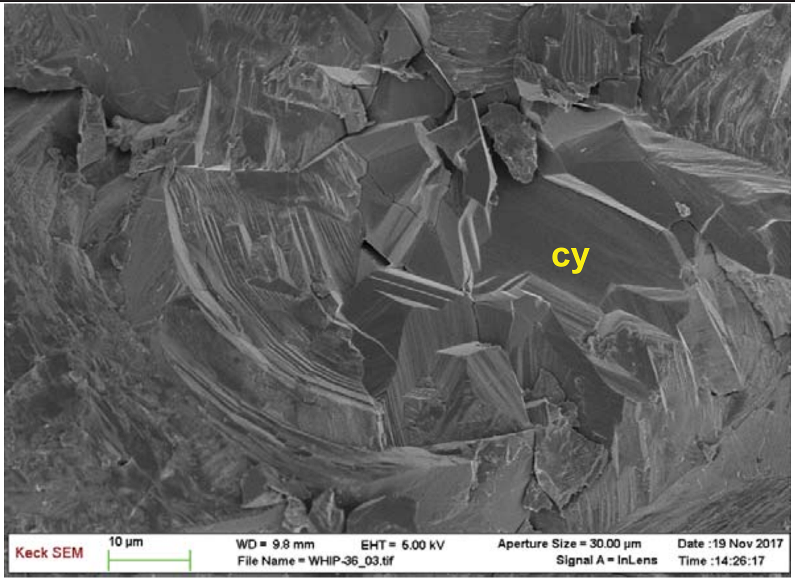

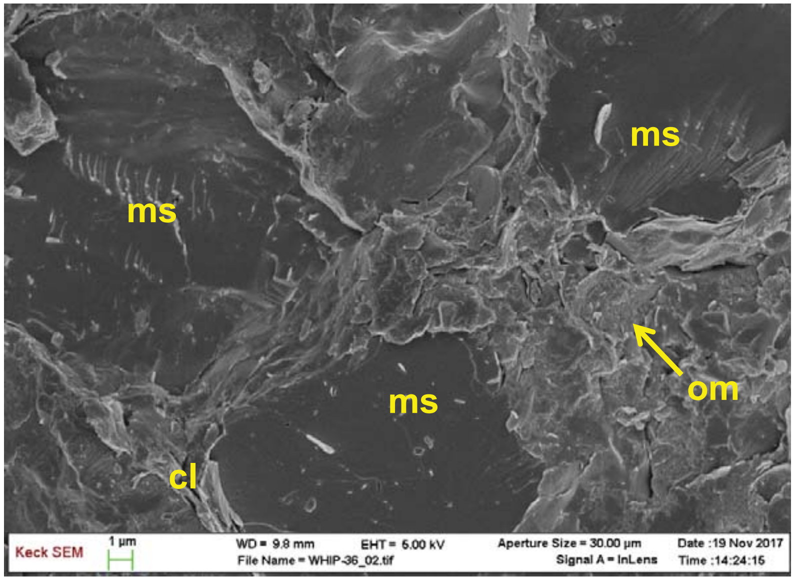

Well ID: St. Whipkey #1 (3705924715)	**Formation: Marcellus Formation**	**Sample ID:**	**WHIP-3**
Location: Greene, PA	**Member: Cherry Valley Member**	**Depth (ft):**	**7869.83**

Organic, pyritic, argillaceous mudstone

Matrix Composition
illitic clays

Texture
moderately well-laminated texture defined by detrital micas and organic particles

Diagenetic Minerals
illitization of clay-rich matrix; pyrite is associated with organic material

Allochemical or Detrital Grains
quartz silt (<10%), detrital micas, and silt-sized allochems are disseminated throughout the rock

Fossils
rare, nondescript fossil or shell fragments; collapsed organic-walled cysts

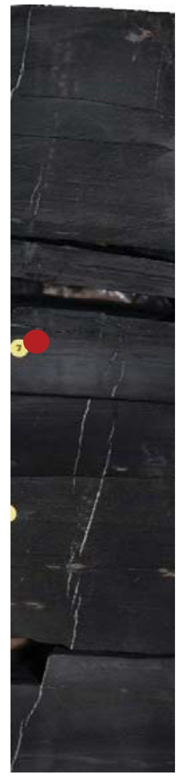

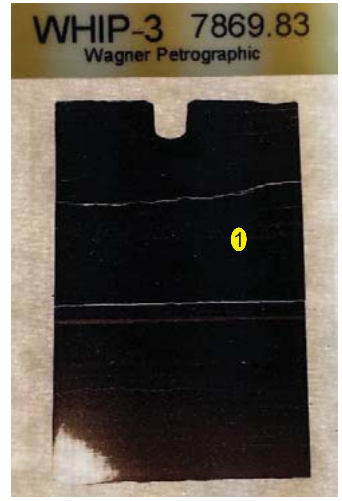

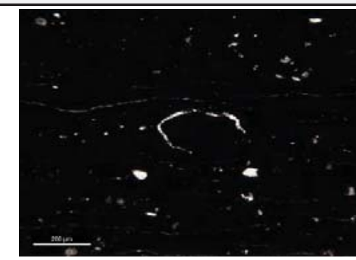

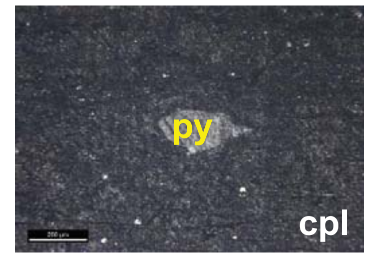

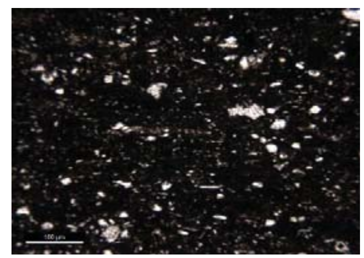

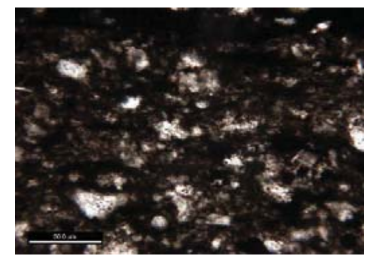

Fractures
none

Additional Comments

SWIR
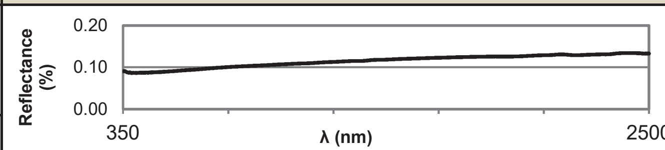

XRD
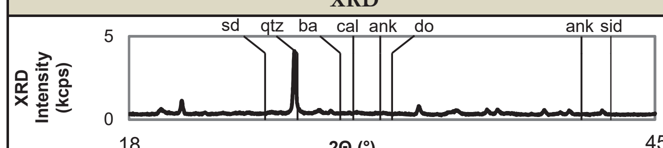

Stable Isotope

$\delta^{13}C_{VPDB}$ (‰)	$\delta^{18}O_{VPDB}$ (‰)
1A Sample	
N/A	N/A
1B Sample	
N/A	N/A

Well ID: St. Whipkey #1 (3705924715)	Formation: Marcellus Formation	Sample ID:	WHIP-9
Location: Greene, PA	Member: Cherry Valley Member	Depth (ft):	7870.50

Microsparitic crystalline carbonate

Matrix Composition

calcite

Texture

weakly laminated; depositional horizons hardly distinguishable; calcite is recrystallized to hypidiotopic and equigranular microspar

Diagenetic Minerals

calcite is the dominant diagenetic mineral; equant calcite rims the interiors of fossil tests; select fossils are filled with dolomite and barite; ferroan calcite and barite fill fractures

Allochemical or Detrital Grains

trace quartz silt

Fossils

nondescript dacryoconarids; nondescript fossil or shell fragments; collapsed organic-walled cysts

Fractures

en echelon set of subvertical fractures

Additional Comments

organic material disseminated within microsparitic matrix

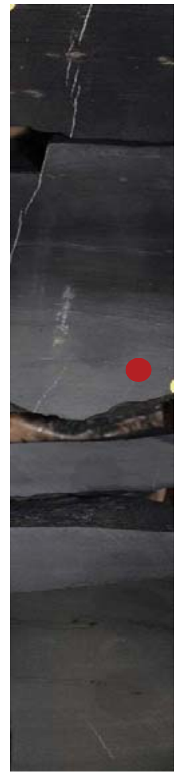

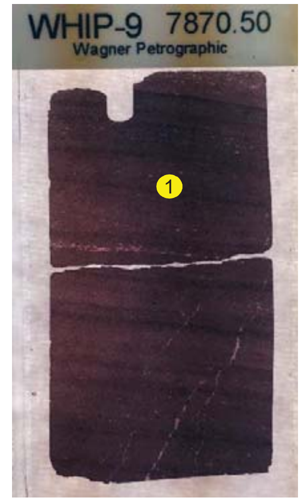

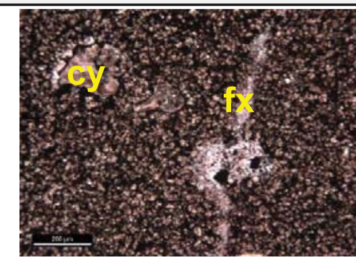

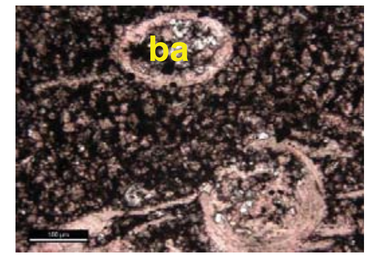

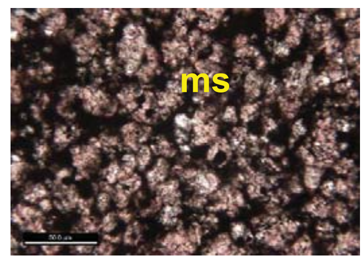

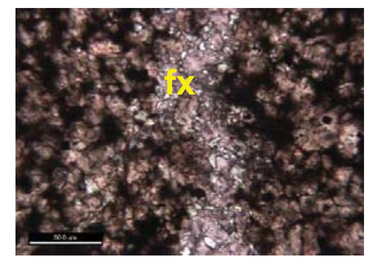

SWIR

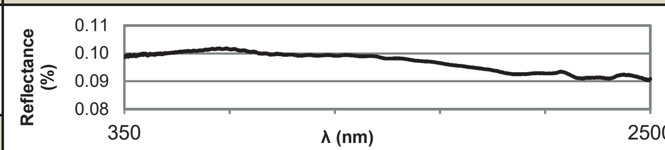

XRD

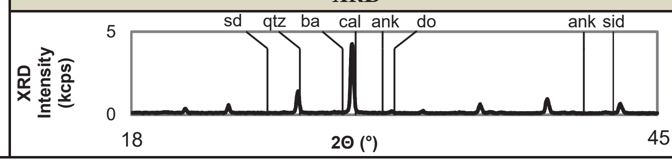

Stable Isotope

	$\delta^{13}C_{VPDB}$ (‰)	$\delta^{18}O_{VPDB}$ (‰)
1A Sample	-10.77	-5.91
1B Sample	-10.68	-5.58

Well ID: St. Whipkey #1 (3705924715)	Formation: Marcellus Formation	Sample ID:	WHIP-9
Location: Greene, PA	Member: Cherry Valley Member	Depth (ft):	7870.50

Microsparitic crystalline carbonate

Matrix Composition and Microtexture

calcite recrystallization results in a microsparitic texture; clay minerals and degraded organic material fill areas between microspar

Diagenetic Minerals

calcite is the primary diagenetic mineral

Diagenetic Texture

neomorphism of calcite matrix, likely micritic in origin, gives the rock a massive or chunky appearance; select fossils include equant calcite overgrowths on their ridges

Pore Structure

clay and organic material admixed within microsparitic matrix, likely hosting nominal porosity

Depositional Fabric

diagenesis has destroyed a majority of depositional fabrics, as microspar growth has grown amidst what may have been a laminated, calcareous mudstone

Additional comments:

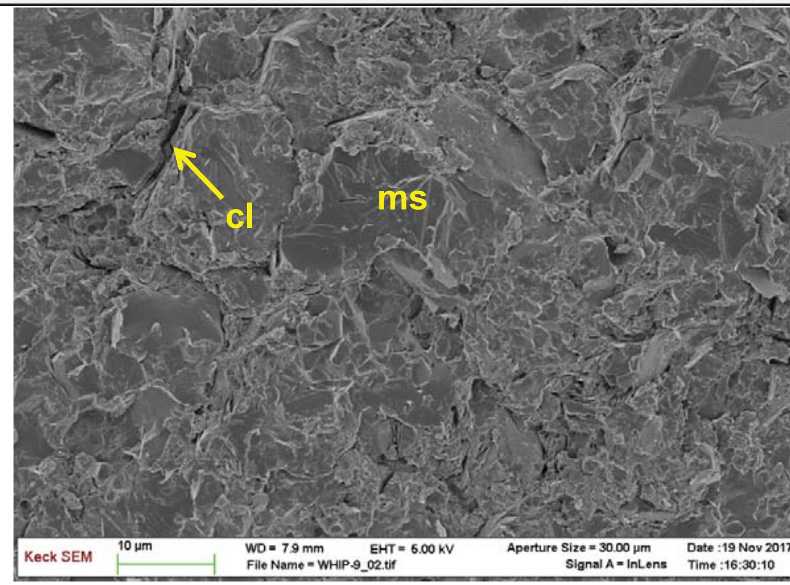

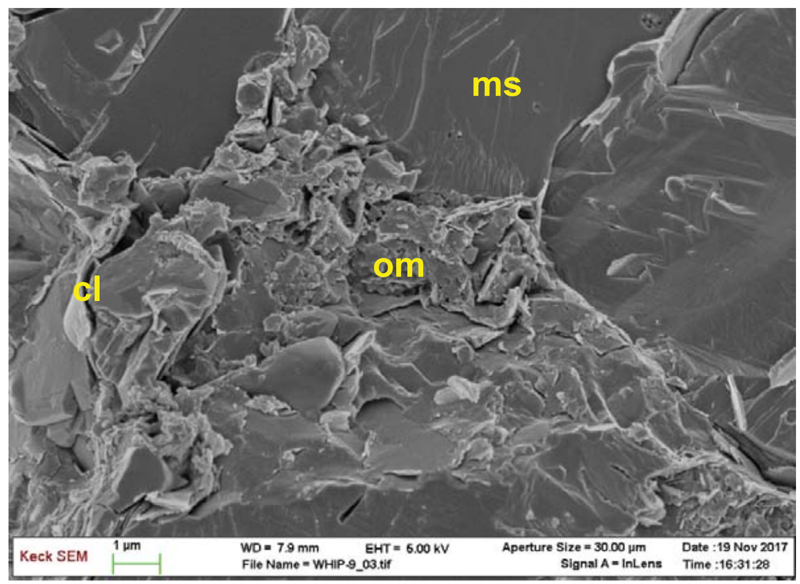

Well ID: St. Whipkey #1 (3705924715)	**Formation: Marcellus Formation**	**Sample ID:**	**WHIP-12**
Location: Greene, PA	**Member: Cherry Valley Member**	**Depth (ft):**	**7870.75**

Microsparitic crystalline carbonate

Matrix Composition

calcite

Texture

weakly laminated; depositional horizons hardly distinguishable; calcite is recrystallized to hypidiotopic and equigranular microspar

Diagenetic Minerals

calcite is the dominant diagenetic mineral; equant calcite or ferroan calcite rims the fossil tests; select fossils are filled with dolomite and barite; ferroan calcite and barite fill fractures

Allochemical or Detrital Grains

trace quartz silt

Fossils

nondescript dacryoconarids; nondescript fossil or shell fragments; collapsed organic-walled cysts

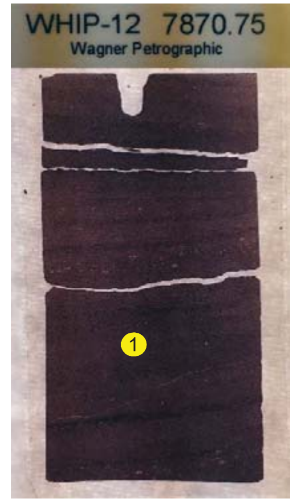

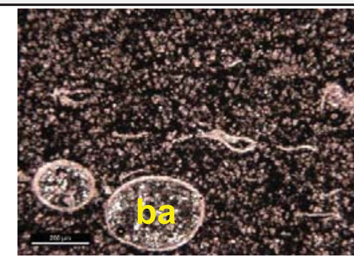

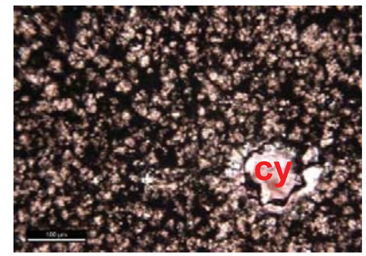

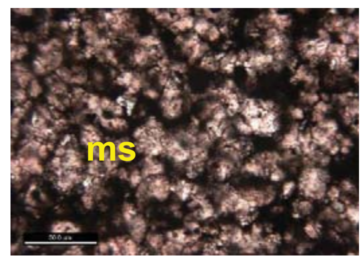

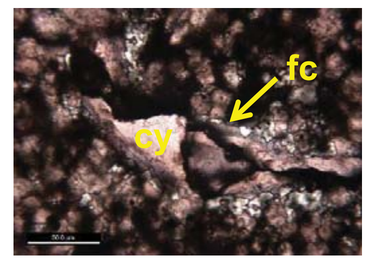

Fractures

en echelon set of subvertical fractures

Additional Comments

organic material disseminated within microsparitic matrix

SWIR

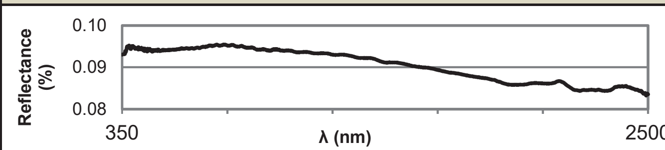

XRD

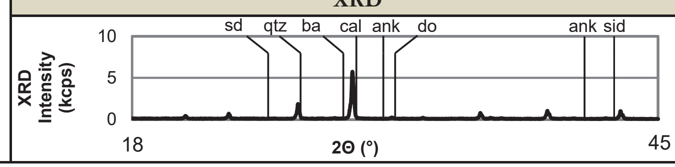

Stable Isotope

$\delta^{13}C_{VPDB}$ (‰)	$\delta^{18}O_{VPDB}$ (‰)
1A Sample	
-11.33	-5.07
1B Sample	
-11.12	-4.78

Well ID: St. Whipkey #1 (3705924715)	Formation: Marcellus Formation	Sample ID:	WHIP-17
Location: Greene, PA	Member: Cherry Valley Member	Depth (ft):	7871.25

Fossiliferous, organic, argillaceous mudstone

Matrix Composition

illitic clay minerals

Texture

well laminated; laminae defined by aligned fossils, organic particles, and detrital micas

Diagenetic Minerals

fossil-rich laminae are partially cemented by calcite; fossils are typically flattened, but the interiors of those that remained intact have eogenetic, equant calcite growth; some fossil tests are filled with organic material and associated framboidal pyrite; minor dolomite rhombohedra

Allochemical or Detrital Grains

quartz silt (< 10%) and detrital mica

Fossils

nondescript dacryoconarids; nondescript shell fragments; phosphatic bone fragments

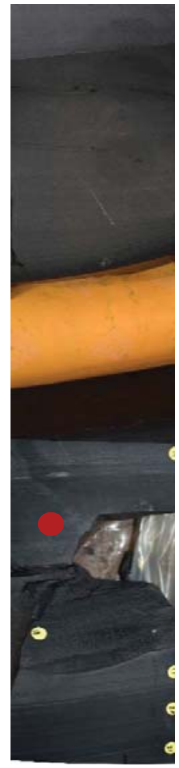

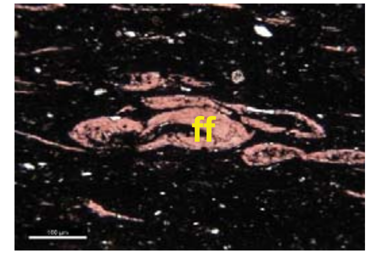

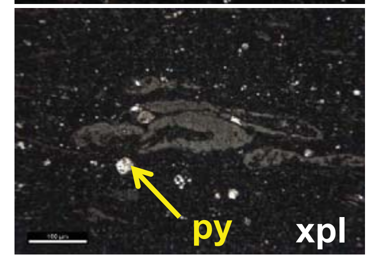

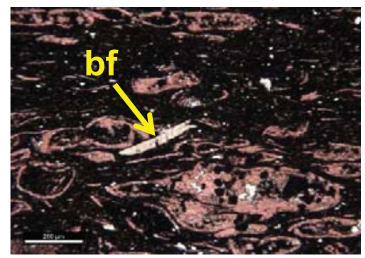

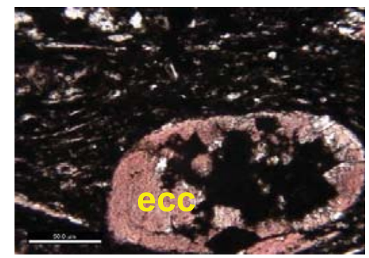

Fractures

none

Additional Comments

SWIR

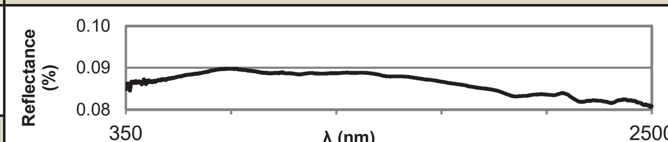

XRD

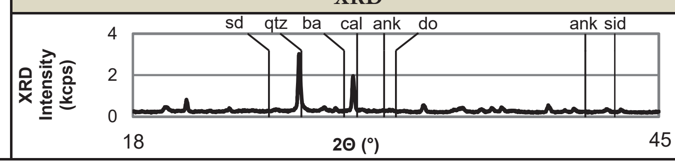

Stable Isotope

	$\delta^{13}C_{VPDB}$ (‰)	$\delta^{18}O_{VPDB}$ (‰)
1A Sample	-9.00	-9.67
1B Sample	-8.93	-8.90

Well ID: St. Whipkey #1 (3705924715)	Formation: Marcellus Formation	Sample ID:	WHIP-23
Location: Greene, PA	Member: Cherry Valley Member	Depth (ft):	7872.25

Fossiliferous, calcareous/argillaceous mudstone

Matrix Composition
calcite and illitic clays

Texture
moderately well-laminated

Diagenetic Minerals
calcite partially cements matrix, which was likely argillaceous in origin; equant calcite growth on interior of fossil tests; fossils filled with calcite, dolomite, and collophane; dolomite rhombohedra disseminated

Allochemical or Detrital Grains
quartz silt (< 15%) and detrital mica

Fossils
nondescript dacryoconarids; nondescript fossil fragments; phosphatic bone fragments

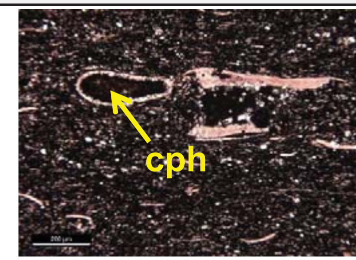

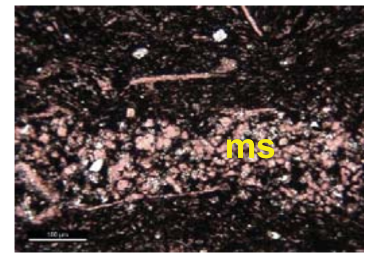

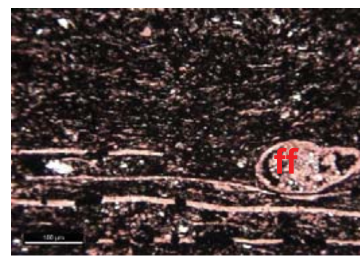

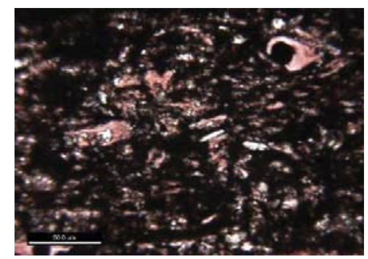

Fractures
none

Additional Comments
organic material fills select fossils

SWIR

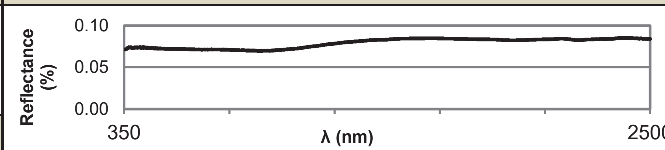

XRD

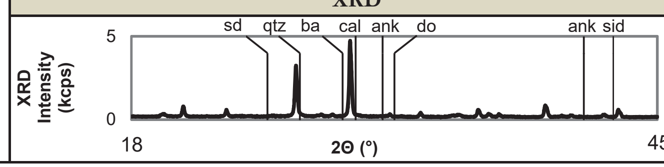

Stable Isotope

$\delta^{13}C_{VPDB}$ (‰)	$\delta^{18}O_{VPDB}$ (‰)
1A Sample	
-10.12	-8.88
1B Sample	
-10.39	-9.60

Well ID: St. Whipkey #1 (3705924715)	Formation: Marcellus Formation	Sample ID:	WHIP-28
Location: Greene, PA	Member: Cherry Valley Member	Depth (ft):	7872.67

Fossiliferous, calcareous mudstone

Matrix Composition

calcite

Texture

moderately well-laminated

Diagenetic Minerals

calcite cements matrix, which was likely argillaceous in origin; neomorphic aggradation gives matrix calcite a slightly grainy texture; equant calcite growth on interior of fossil tests; fossils filled with calcite, ferroan calcite, dolomite, and collophane; dolomite rhombohedra disseminated

Allochemical or Detrital Grains

quartz silt (< 5%) and detrital mica

Fossils

dacryoconarids (Nowakia); nondescript fossil fragments; phosphatic bone fragments

Fractures

none

Additional Comments

organic material fills select fossils

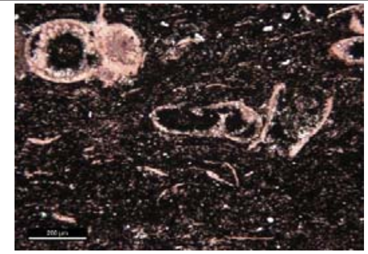

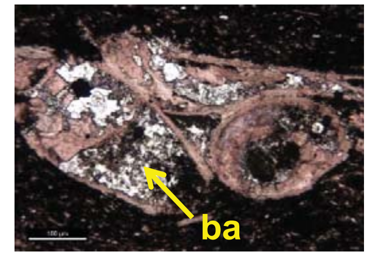

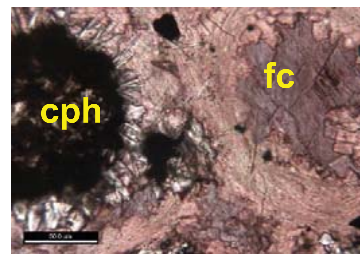

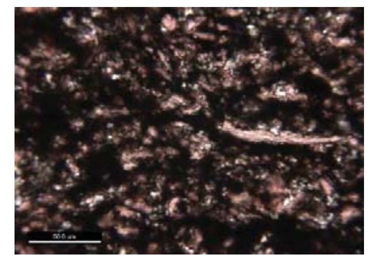

SWIR

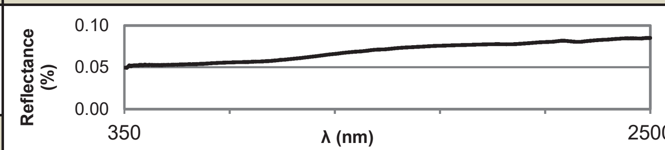

XRD

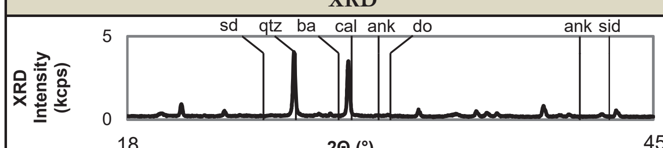

Stable Isotope

$\delta^{13}C_{VPDB}$ (‰)	$\delta^{18}O_{VPDB}$ (‰)
1A Sample	
-12.16	-9.21
1B Sample	
-12.18	-8.77

Well ID: St. Whipkey #1 (3705924715)	Formation: Marcellus Formation	Sample ID:	WHIP-28
Location: Greene, PA	Member: Cherry Valley Member	Depth (ft):	7872.67

Fossiliferous, calcareous mudstone

Matrix Composition and Microtexture

diagenetic calcite cements a clay-rich matrix

Diagenetic Minerals

calcite recrystallizes fossils and cements the matrix; minor pyrite is largely associated with organic material

Diagenetic Texture

interiors of fossils are filled with calcite; fossils are recrystallized and commonly display equant calcite overgrowths

Pore Structure

matrix-hosted porosity is observed within clay-rich portions as well as in equant pores in calcite cemented laminae

Depositional Fabric

the depositional surface is largely retained by the alignment of detrital clays and mica, though select portions or laminae are entirely cemented by calcite

Additional comments:

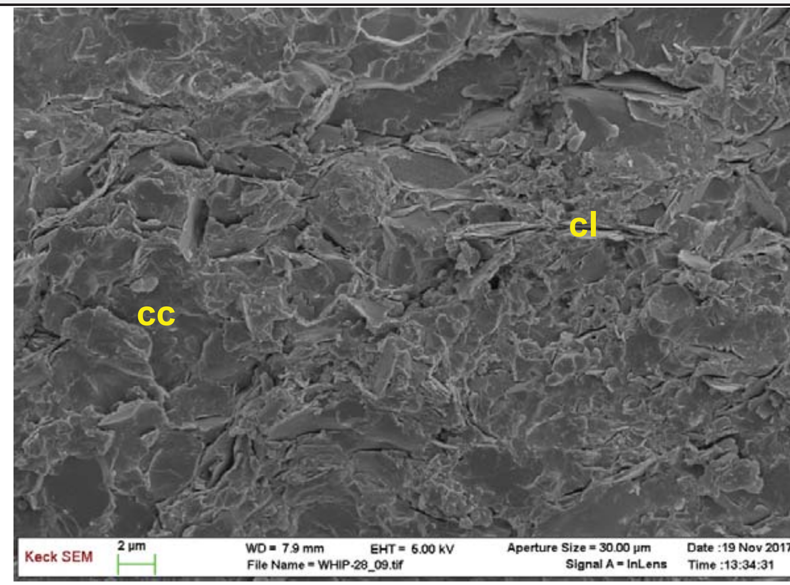

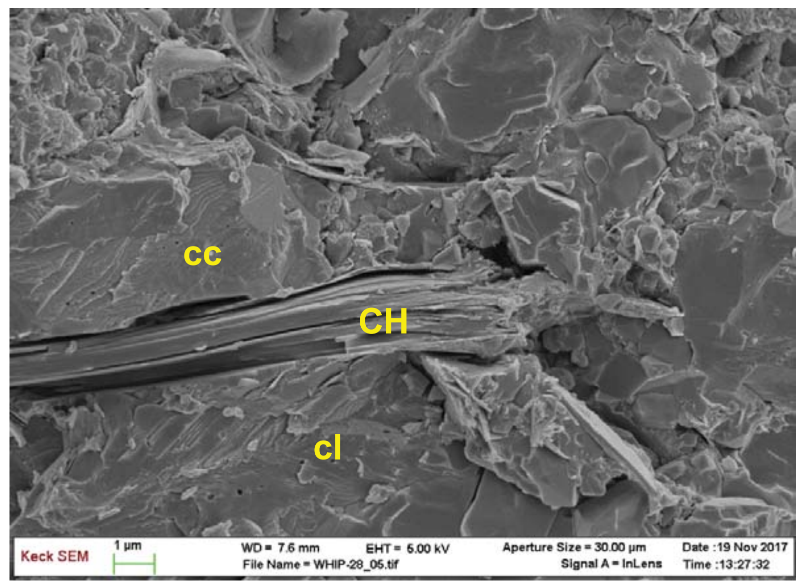

Well ID: Bald Eagle 2015 (CEN027-0384)	Formation: Marcellus Formation	Sample ID:	BE15-10
Location: Centre, PA	Member: Oatka Creek Member	Depth (ft):	335.00

Argillaceous mudstone

Matrix Composition

illitic clays with minor calcite cementation

Texture

moderately well laminated; bedding defined by aligned fossils, detrital micas, and organic particles

Diagenetic Minerals

equant or dog tooth ferroan calcite crystallizes on and partially occludes the interiors of fossil tests; remaining space is filled with dolomite; sphalerite is crystallized in select fossil tests; subtle haloes of calcite cement the clay matrix surrounding fossils; minor dolomite rhombohedra

Allochemical or Detrital Grains

quartz silt (< 15%) and detrital micas

Fossils

nondescript shell fragments

Fractures

none

Additional Comments

organic particles are disseminated through the matrix

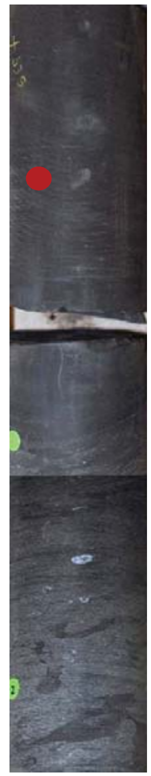

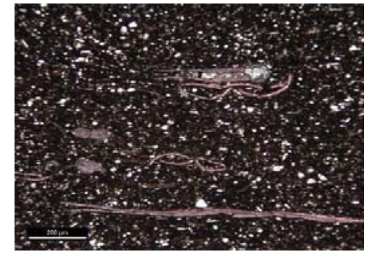

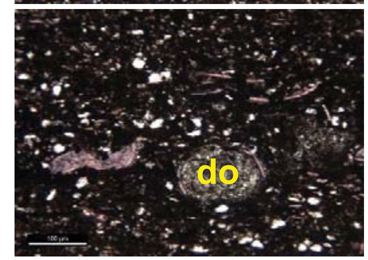

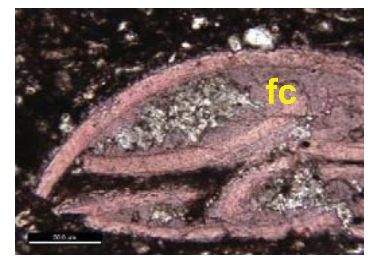

SWIR

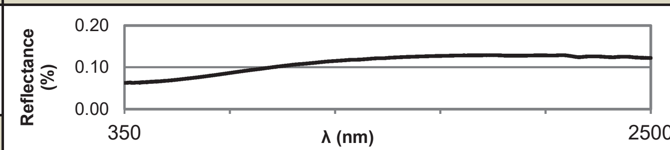

XRD

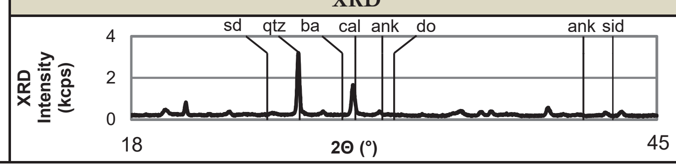

Stable Isotope

	$\delta^{13}C_{VPDB}$ (‰)	$\delta^{18}O_{VPDB}$ (‰)
1A Sample	-1.99	-7.30
1B Sample	-2.32	-8.14

Well ID: Bald Eagle 2015 (CEN027-0384)	**Formation: Marcellus Formation**	**Sample ID:**	**BE15-16**
Location: Centre, PA	**Member: Cherry Valley Member**	**Depth (ft):**	**335.50**

Fossiliferous, calcareous/dolomitic mudstone

Matrix Composition
calcite and ferroan dolomite with minor illitic clays

Texture
poorly laminated

Diagenetic Minerals
equant or dog tooth ferroan calcite crystallizes on the interior walls of fossil tests; subsequent cementation stages of ankeritic dolomitization and slightly ferroan calcite have taken place; minor dolomite rhombohedra; minor barite replaces or fills in dissolved fossil calcite

Allochemical or Detrital Grains
quartz silt (< 15%) and trace detrital micas

Fossils
dacryoconarids (Viriatellina); bivalves; nondescript shell fragments

Fractures
subvertical, calcite-filled, < 0.1 mm-thick fractures propagate through all stages of diagenetic overprinting

Additional Comments
different phases of cementation difficult to place in order by thin section

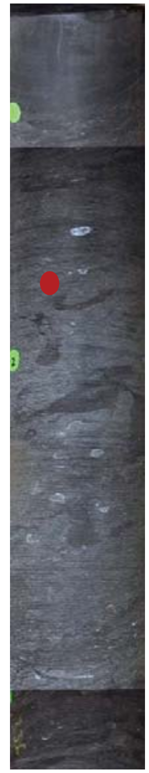

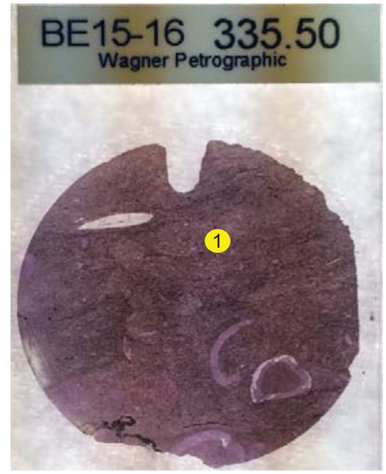

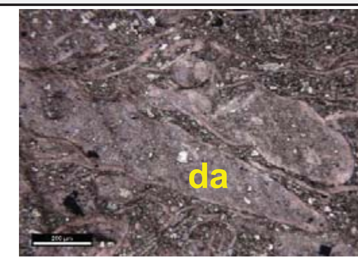

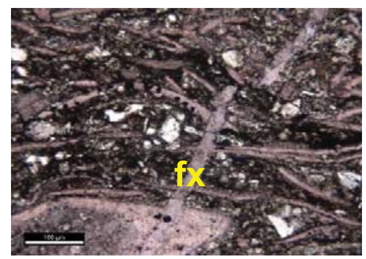

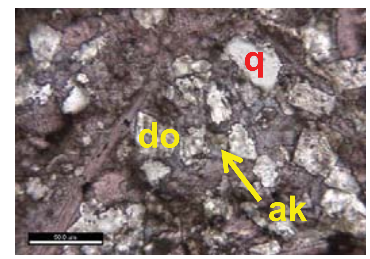

SWIR
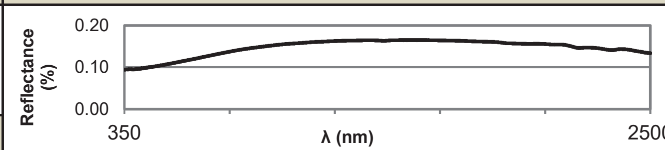

XRD
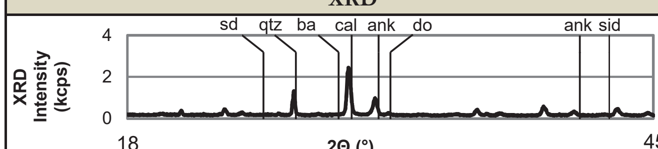

Stable Isotope

	$\delta^{13}C_{VPDB}$ (‰)	$\delta^{18}O_{VPDB}$ (‰)
1A Sample	-4.31	-8.05
1B Sample	-4.29	-8.36

Well ID: Bald Eagle 2015 (CEN027-0384)	Formation: Marcellus Formation	Sample ID:	BE15-16
Location: Centre, PA	Member: Cherry Valley Member	Depth (ft):	335.50

Fossiliferous, calcareous/dolomitic mudstone

Matrix Composition and Microtexture

calcite is the primary matrix component observed under SEM; dolomite, which is readily seen in thin section, is a minor constituent and is not easily distinguished by morphology at the micron scale

Diagenetic Minerals

calcite recrystallizes fossils and cements the matrix; minor dolomite rhombohedra are disseminated

Diagenetic Texture

interiors of fossils are filled with calcite or dolomite; fossils are recrystallized and commonly display calcite overgrowths

Pore Structure

equant pores are hosted within calcite cement

Depositional Fabric

clay minerals have been disrupted by calcite cementation, though the depositional horizon is generally still retained in portions of the rock that are muddier

Additional comments:

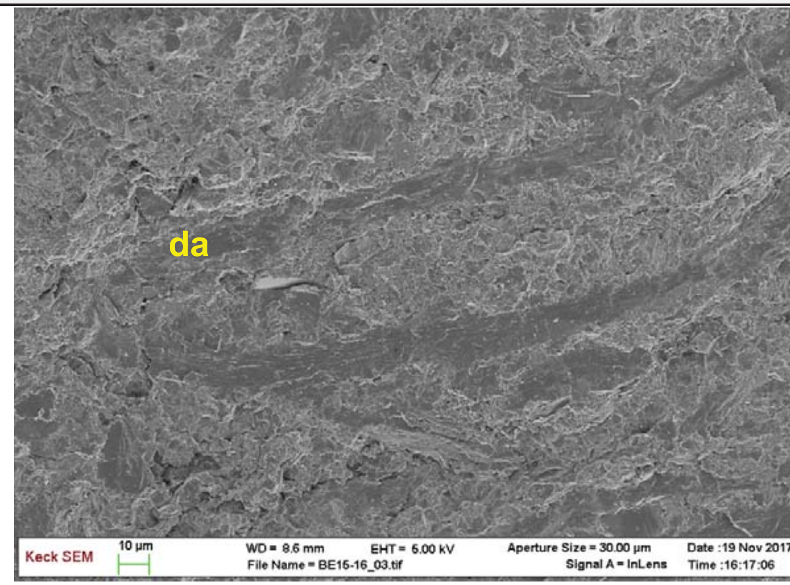

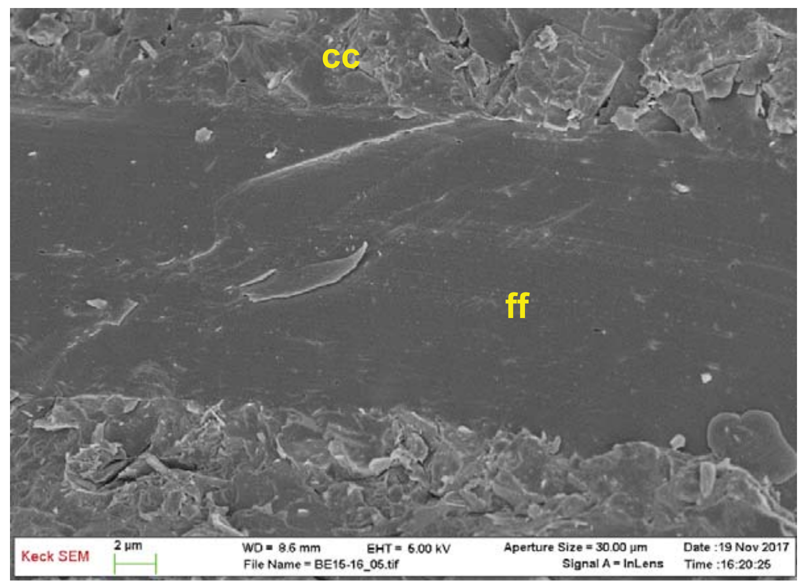

Well ID: Bald Eagle 2015 (CEN027-0384)	Formation: Marcellus Formation	Sample ID:	BE15-23
Location: Centre, PA	Member: Cherry Valley Member	Depth (ft):	336.25

Calcareous/dolomitic mudstone

Matrix Composition
calcite and ankeritic dolomite with minor illitic clays

Texture
poorly laminated

Diagenetic Minerals
argillaceous matrix cemented by ankeritic dolomite and calcite; equant or dog tooth ferroan calcite rims the interior of fossil tests; barite replaces select fossils; dolomite rhombohedra disseminated throughout; ankeritic dolomite preferentially cements silty lenses or laminae

Allochemical or Detrital Grains
quartz silt (< 20%)

Fossils
dacryoconarids (Styliolina); nondescript shell fragments; collapsed algal cysts; brachiopods; recrystallized, centimeter-scale fossils that resemble crinoids, though overprinting erases identifying features

Fractures
none

Additional Comments
minor organic content, mostly restricted to discrete particles

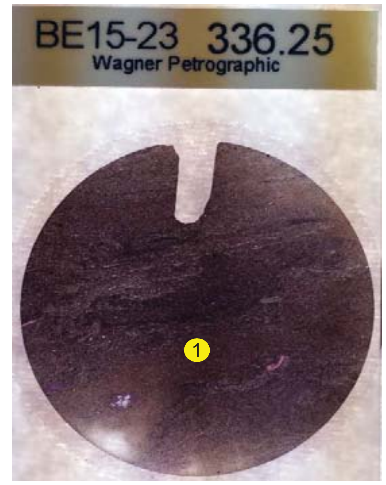

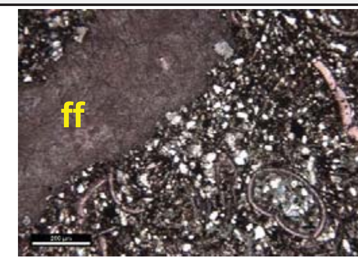

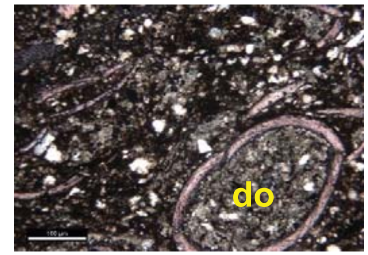

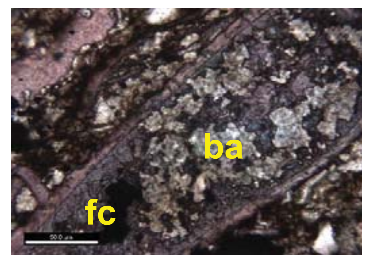

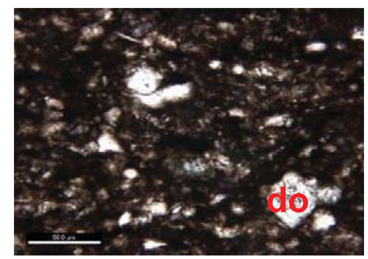

SWIR

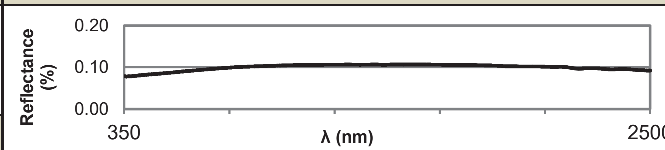

XRD

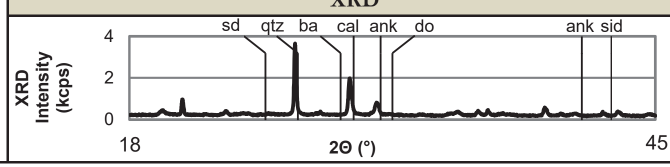

Stable Isotope

	$\delta^{13}C_{VPDB}$ (‰)	$\delta^{18}O_{VPDB}$ (‰)
1A Sample	-3.34	-8.18
1B Sample	-3.54	-8.52

Well ID: Bald Eagle 2015 (CEN027-0384)	Formation: Marcellus Formation	Sample ID:	BE15-33
Location: Centre, PA	Member: Cherry Valley Member	Depth (ft):	337.25

Microsparitic crystalline carbonate

Matrix Composition

calcite

Texture

nonlaminated; matrix calcite is recrystallized to xenotopic, inequigranular microspar

Diagenetic Minerals

calcite is the dominant diagenetic mineral; fossils are rimmed with equant calcite crystals; select fossils are replaced by dolomite; calcite in fossils that are rimmed by organic material are slightly ferroan; trace barite remains after ferroan calcite replacement

Allochemical or Detrital Grains

quartz silt (< 5%)

Fossils

dacryoconarids (Styliolina); crinoids; brachiopods; nondescript shell fragments; collapsed organic-walled cysts

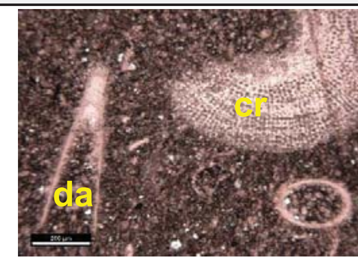

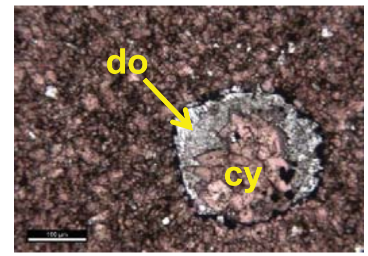

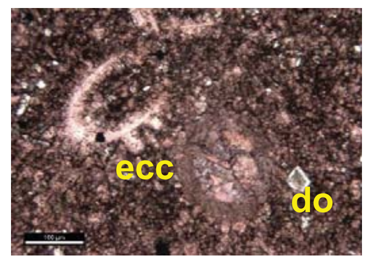

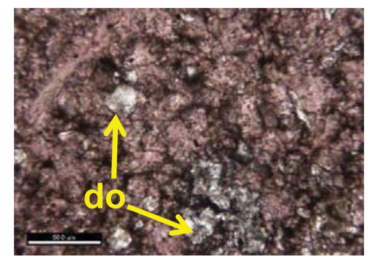

Fractures

none

Additional Comments

organic material lines select fossils

SWIR

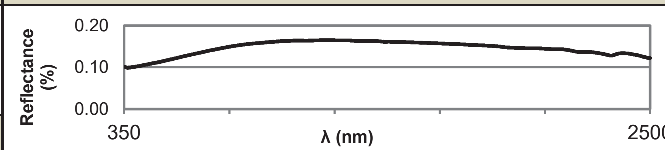

XRD

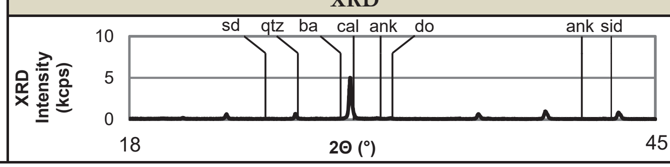

Stable Isotope

$\delta^{13}C_{VPDB}$ (‰)	$\delta^{18}O_{VPDB}$ (‰)
1A Sample	
-12.19	-2.70
1B Sample	
-12.38	-2.89

Well ID: Bald Eagle 2015 (CEN027-0384)	**Formation: Marcellus Formation**	**Sample ID:**	**BE15-33**
Location: Centre, PA	**Member: Cherry Valley Member**	**Depth (ft):**	**337.25**

Microsparitic crystalline carbonate

Matrix Composition and Microtexture

calcite recrystallization results in a microsparitic texture

Diagenetic Minerals

calcite is the primary diagenetic mineral; dolomite fills select cysts or is crystallized as cement or rhombohedra; minor pyrite

Diagenetic Texture

neomorphism of calcite matrix, likely micritic in origin, gives the rock a massive or chunky appearance; select fossils include equant calcite overgrowths on their ridges; select fossils are filled with framboidal pyrite and degraded organic material

Pore Structure

recrystallization occludes most pores; minor porosity likely associated with degradation of rare organic material

Depositional Fabric

diagenesis has overprinted all depositional fabrics

Additional comments:

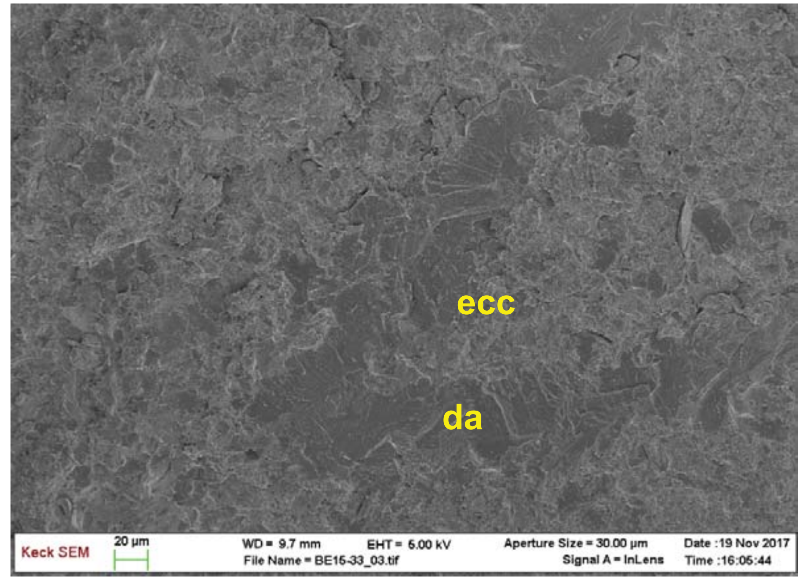

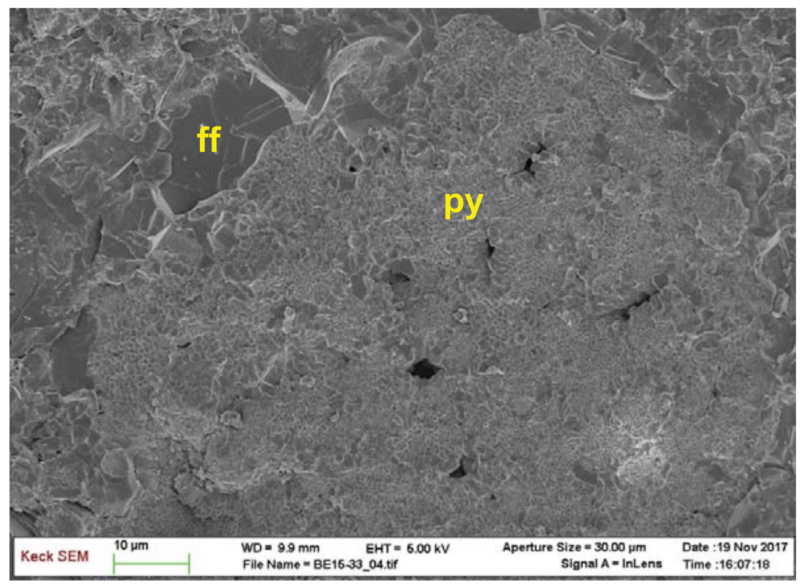

Well ID: Bald Eagle 2015 (CEN027-0384)	Formation: Marcellus Formation	Sample ID:	BE15-38
Location: Centre, PA	Member: Cherry Valley Member	Depth (ft):	337.70

Silty, calcareous/dolomitic mudstone

Matrix Composition

calcite and ankeritic dolomite with minor illitic clays

Texture

moderately well-laminated; bedding is defined by aligned fossil material, organic particles, and detrital micas

Diagenetic Minerals

equant ferroan calcite is crystallized on interiors of fossil tests; remaining pore space within fossil tests are filled with dolomite, barite, or pyrite; dolomite and ankerite rhombohedra disseminated throughout the rock

Allochemical or Detrital Grains

quartz silt (< 25%) and detrital micas

Fossils

dacryoconarids (Styliolina); nondescript shell or skeletal fragments

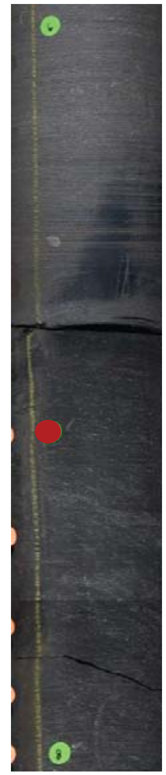

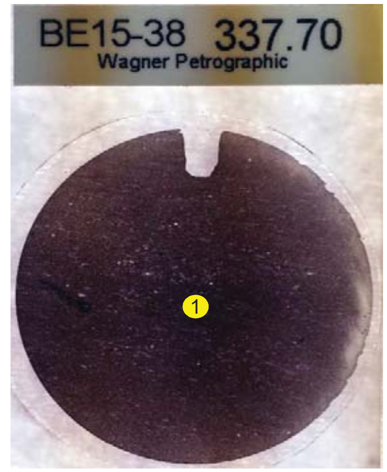

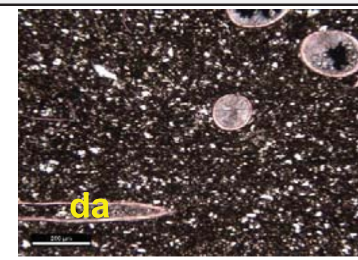

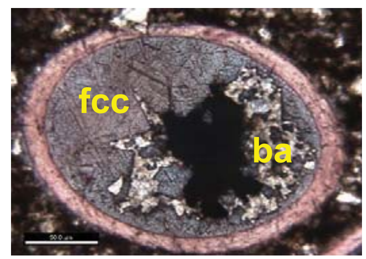

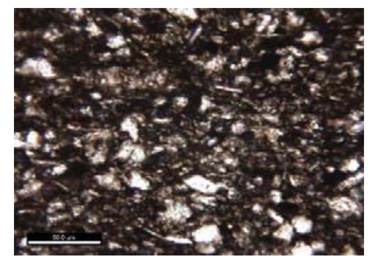

Fractures

none

Additional Comments

hydrocarbon staining or residues in select areas

SWIR

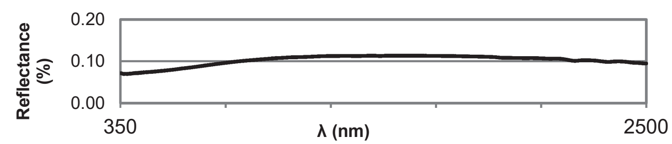

XRD

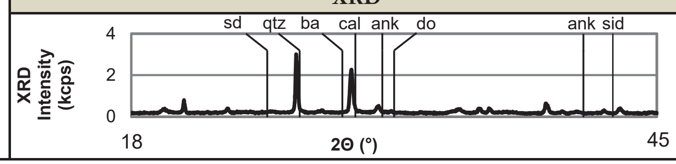

Stable Isotope

	$\delta^{13}C_{VPDB}$ (‰)	$\delta^{18}O_{VPDB}$ (‰)
1A Sample	-3.92	-8.58
1B Sample	-3.85	-8.40

Well ID: Bald Eagle 2015 (CEN027-0384)	Formation: Marcellus Formation	Sample ID:	BE15-42
Location: Centre, PA	Member: Cherry Valley Member	Depth (ft):	338.00

Calcareous/dolomitic mudstone

Matrix Composition
calcite and ankeritic dolomite with minor illitic clays

Texture
moderately well-laminated; bedding is defined by aligned fossil material, organic particles, and detrital micas

Diagenetic Minerals
equant ferroan calcite is crystallized on interiors of fossil tests; remaining pore space within fossil tests are filled with dolomite, barite, or pyrite; dolomite and ankerite rhombohedra disseminated throughout the rock

Allochemical or Detrital Grains
quartz silt (< 15%) and detrital micas

Fossils
dacryoconarids (Styliolina); crinoids; nondescript shell or skeletal fragments

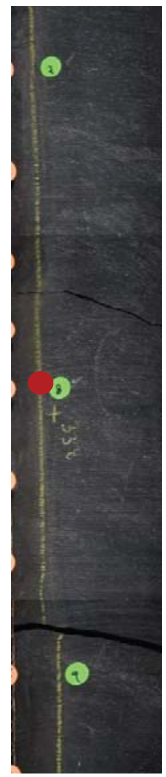

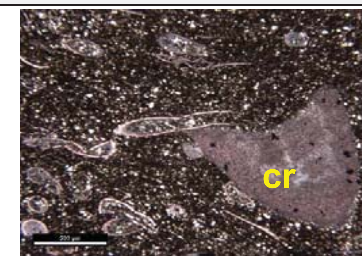

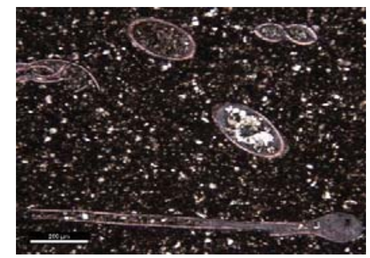

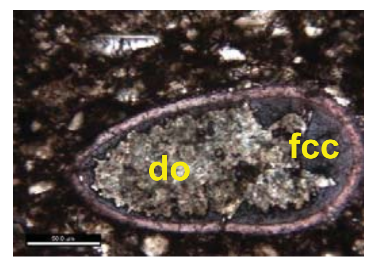

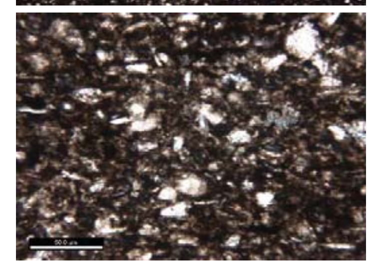

Fractures
none

Additional Comments
hydrocarbon staining or residues in select areas

SWIR

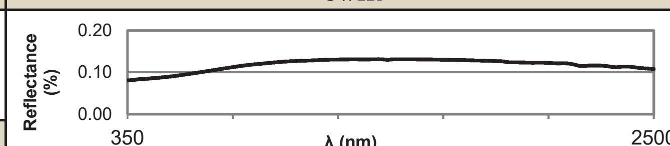

XRD

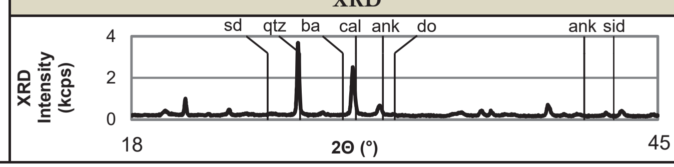

Stable Isotope

$\delta^{13}C_{VPDB}$ (‰)	$\delta^{18}O_{VPDB}$ (‰)
1A Sample	
-3.76	-8.66
1B Sample	
-4.09	-8.54

Well ID: Bald Eagle 2015 (CEN027-0384)	**Formation: Marcellus Formation**
Location: Centre, PA	**Member: Cherry Valley Member**
Sample ID:	**BE15-45**
Depth (ft):	**338.25**

Calcareous/dolomitic mudstone

Matrix Composition

calcite and ankeritic dolomite with minor illitic clays

Texture

moderately well-laminated; bedding is defined by aligned fossil material, organic particles, and detrital micas

Diagenetic Minerals

equant ferroan calcite is crystallized on interiors of fossil tests; remaining pore space within fossil tests are filled with dolomite, barite, or pyrite; dolomite and ankerite rhombohedra disseminated throughout the rock

Allochemical or Detrital Grains

quartz silt (< 20%) and detrital micas

Fossils

dacryoconarids (Styliolina); nondescript shell or skeletal fragments

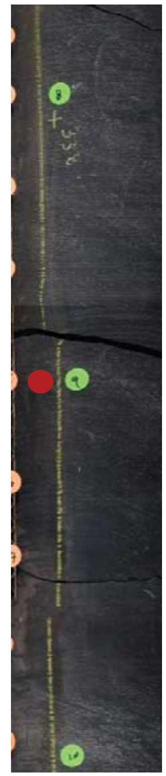

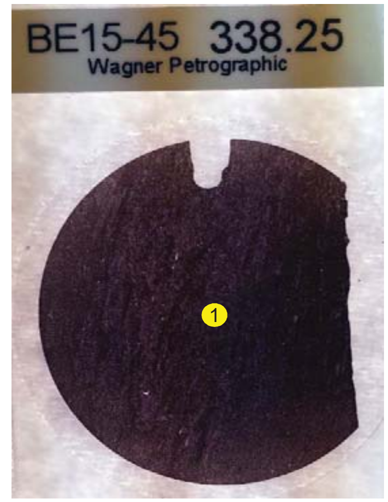

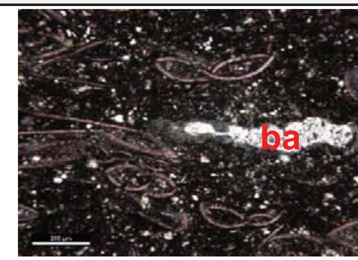

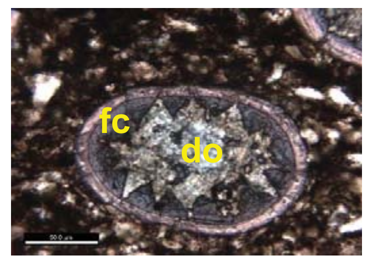

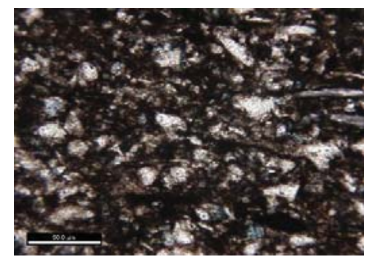

Fractures

none

Additional Comments

hydrocarbon staining or residues in select areas

SWIR

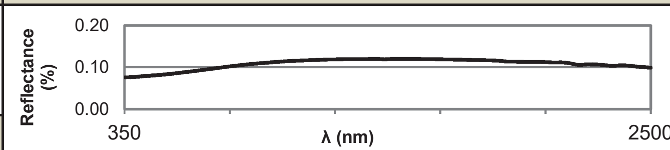

XRD

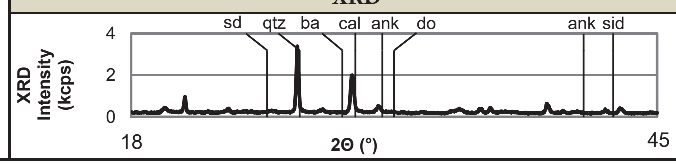

Stable Isotope

	$\delta^{13}C_{VPDB}$ (‰)	$\delta^{18}O_{VPDB}$ (‰)
1A Sample	-3.11	-7.95
1B Sample	-3.29	-7.76

Well ID: Bald Eagle 2015 (CEN027-0384)	Formation: Marcellus Formation	Sample ID:	BE15-49
Location: Centre, PA	Member: Cherry Valley Member	Depth (ft):	338.60

Fossiliferous, calcareous/dolomitic mudstone

Matrix Composition

calcite and ankeritic dolomite with minor illitic clays

Texture

moderately well-laminated; bedding is defined by aligned fossil material, organic particles, and detrital micas

Diagenetic Minerals

equant ferroan calcite is crystallized on interiors of fossil tests; remaining pore space within fossil tests are filled with dolomite, barite, or pyrite; dolomite and ankerite rhombohedra disseminated throughout the rock

Allochemical or Detrital Grains

quartz silt (< 20%) and detrital micas

Fossils

dacryoconarids (Styliolina and Viriatellina); nondescript shell or skeletal fragments; conodonts; algal mat structures recrystallized by ankerite and barite

Fractures

none

Additional Comments

hydrocarbon staining or residues in select areas

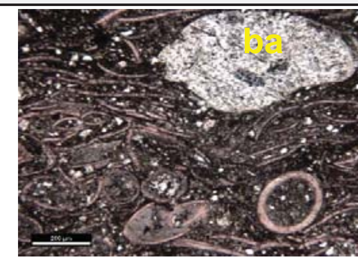

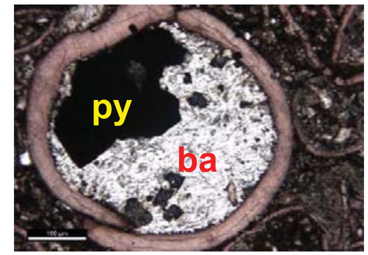

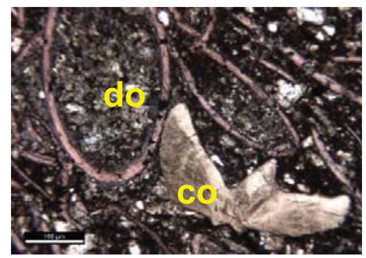

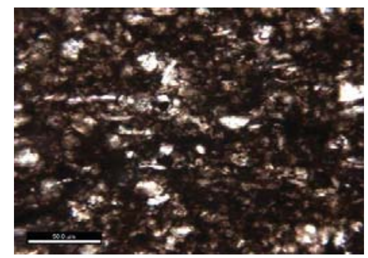

SWIR

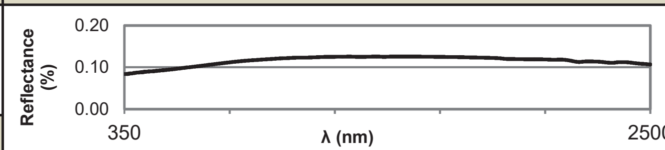

XRD

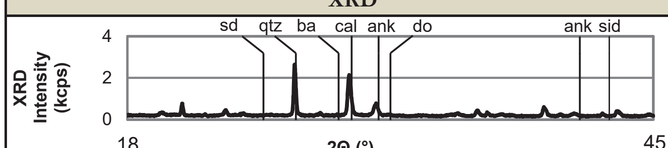

Stable Isotope

$\delta^{13}C_{VPDB}$ (‰)	$\delta^{18}O_{VPDB}$ (‰)
1A Sample	
-4.03	-8.94
1B Sample	
-4.00	-9.11

Well ID: Bald Eagle 2015 (CEN027-0384)	Formation: Marcellus Formation	Sample ID:	BE15-49
Location: Centre, PA	Member: Cherry Valley Member	Depth (ft):	338.60

Fossiliferous, calcareous/dolomitic mudstone

Matrix Composition and Microtexture

calcite is the primary matrix component observed under SEM; dolomite, which is readily seen in thin section, is a minor constituent and is not easily distinguished by morphology at the micron scale

Diagenetic Minerals

calcite recrystallizes fossils and cements the matrix; minor dolomite rhombohedra are disseminated; crystallization of select dolomites is apparently interrupted, possibly by mobilization of hydrocarbons which coat their surfaces

Diagenetic Texture

interiors of fossils are filled with calcite or dolomite; fossils are recrystallized and commonly display calcite overgrowths

Pore Structure

equant pores are hosted within calcite cement

Depositional Fabric

clay minerals have been disrupted by calcite cementation; detritus is tightly cemented by carbonate cements

Additional comments:

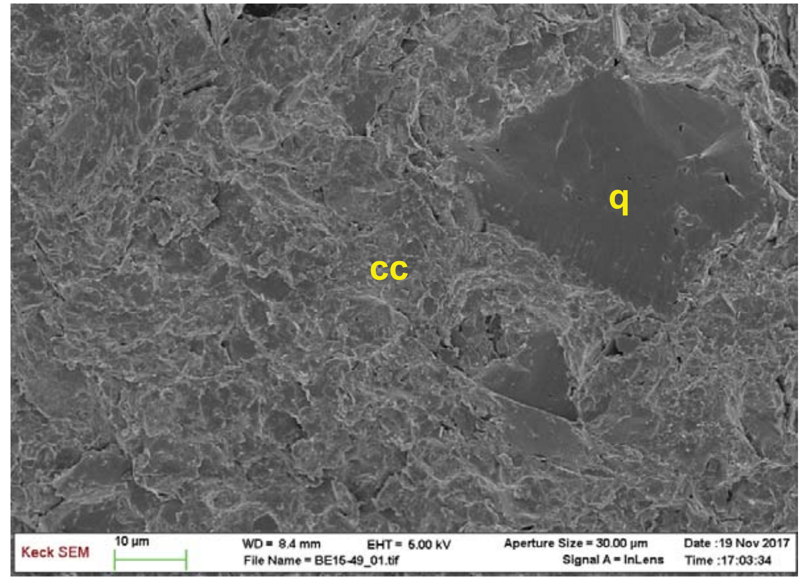

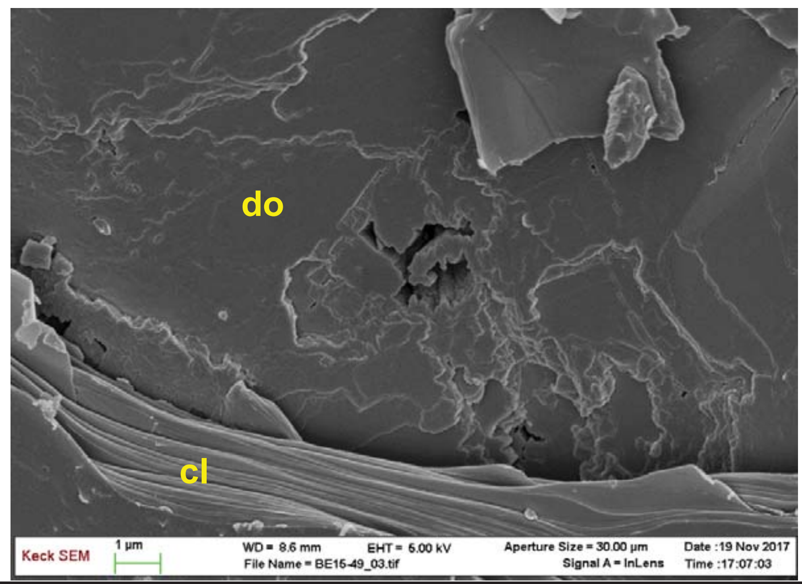

Well ID: Bald Eagle 2015 (CEN027-0384)	**Formation: Marcellus Formation**	**Sample ID:**	**BE15-52**
Location: Centre, PA	**Member: Union Springs Member**	**Depth (ft):**	**338.95**

Calcareous/dolomitic mudstone

Matrix Composition

calcite and ankeritic dolomite with minor illitic clays

Texture

moderately well-laminated, though algal mat structures lend to a chaotic texture in select portions

Diagenetic Minerals

equant ferroan calcite is crystallized on interiors of fossil tests; remaining pore space within fossil tests are filled with dolomite, barite, or pyrite; dolomite and ankerite rhombohedra disseminated throughout the rock

Allochemical or Detrital Grains

quartz silt (< 10%) and detrital micas

Fossils

dacryoconarids (Styliolina); nondescript shell or skeletal fragments; conodonts; algal mat structures recrystallized by ankerite and barite; collapsed organic-walled cysts

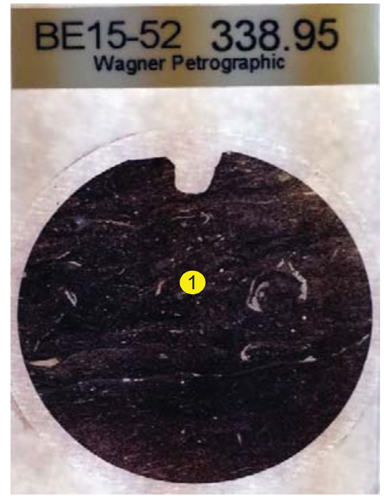

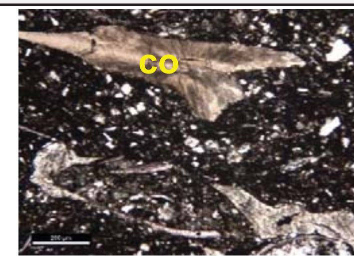

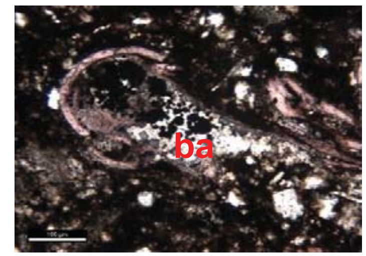

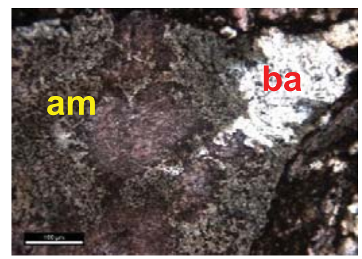

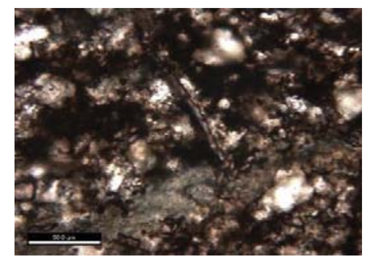

Fractures

none

Additional Comments

elevated organic content has rendered this rock more opaque from hydrocarbon staining

SWIR

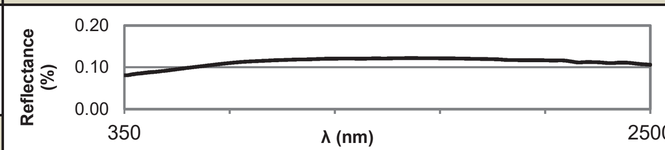

XRD

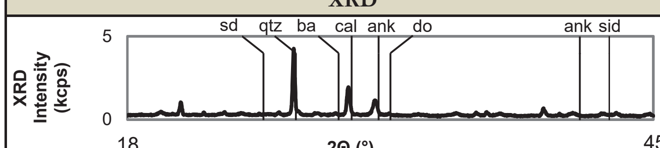

Stable Isotope

	$\delta^{13}C_{VPDB}$ (‰)	$\delta^{18}O_{VPDB}$ (‰)
1A Sample	-4.11	-6.33
1B Sample	-3.99	-6.61

Well ID: Bald Eagle 2015 (CEN027-0384)	Formation: Marcellus Formation	Sample ID:	BE15-54
Location: Centre, PA	Member: Union Springs Member	Depth (ft):	339.13

Nodular, dolomitic, argillaceous mudstone

Matrix Composition

illitic clays with minor calcite and dolomite cements

Texture

moderately well-laminated; nodules grow along bedding planes

Diagenetic Minerals

early nodular growth of felted barite; fractures within nodule filled with barite, but with a different crystalline texture; smaller nodules composed of bladed barite; mudstone above nodule is largely uncemented; dolomite partially cements lower mudstone

Allochemical or Detrital Grains

quartz silt (< 15%) and detrital micas

Fossils

nondescript shell fragments; conodonts or phosphatic bone fragments; collapsed organic-walled cysts

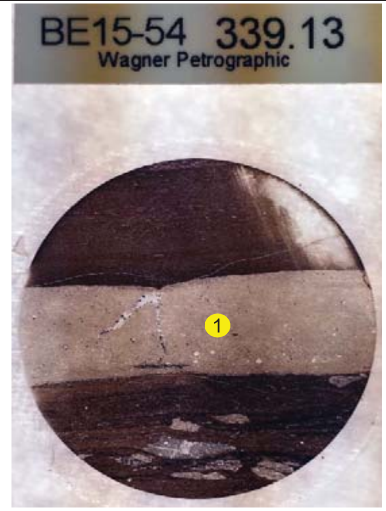

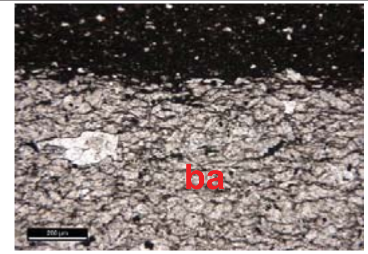

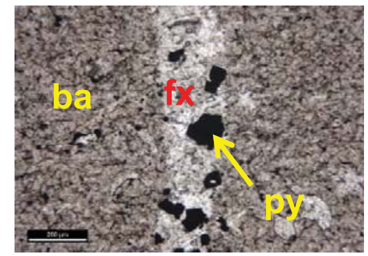

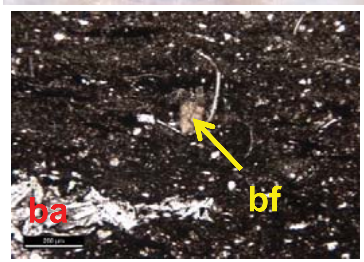

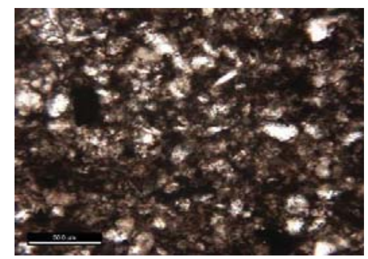

Fractures

millimeter-wide fractures within the nodules

Additional Comments

organic-rich stringers or lenses, primarily in the mudstones below the nodule

SWIR

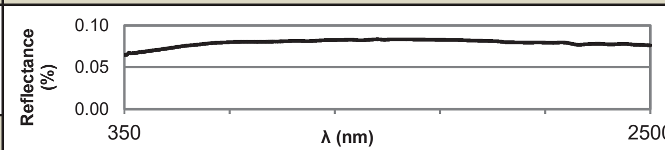

XRD

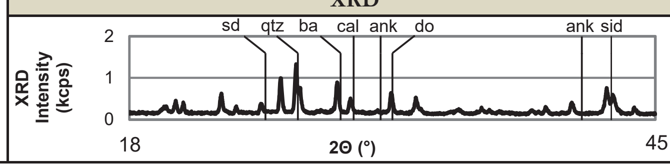

Stable Isotope

	$\delta^{13}C_{VPDB}$ (‰)	$\delta^{18}O_{VPDB}$ (‰)
1A Sample	N/A	N/A
1B Sample	N/A	N/A

Well ID: Strong #1 (31107264660000)	**Formation: Oatka Creek Formation**	**Sample ID:**	**1-TCC2**
Location: Tioga, NY	**Member: East Berne Member**	**Depth (ft):**	**4183.46**

Fossiliferous, calcareous/argillaceous mudstone

Matrix Composition
mix of clay and calcite

Texture
mostly well-laminated texture, defined by aligned mica flakes, clay minerals in the matrix, and fossil fragments

Diagenetic Minerals
calcite cement is the dominant diagenetic mineral; uncommon dolomite rhombohedra are disseminated throughout the rock

Allochemical or Detrital Grains
dominantly silt-sized quartz disseminated throughout without preferential deposition

Fossils
elongate shell fragments define bedding planes; nondescript dacryoconarids; size of shell varies widely, with the larger fragments less broken up and maintaining the curved morphology

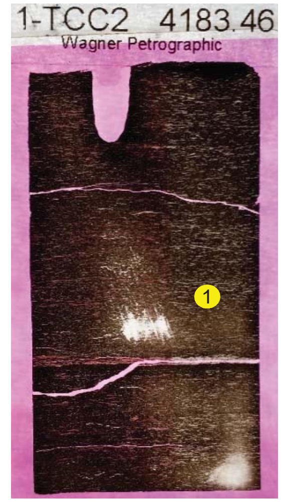

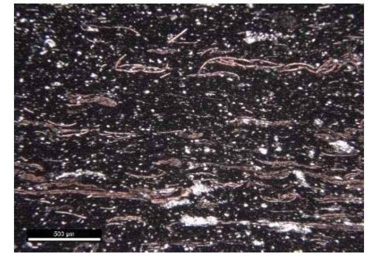

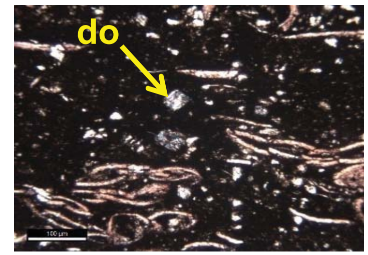

Fractures
none

Additional Comments
dark matrix, likely indicating significant disseminated kerigenous residue in the matrix; organic material outlines some detrital grains and fossils

SWIR

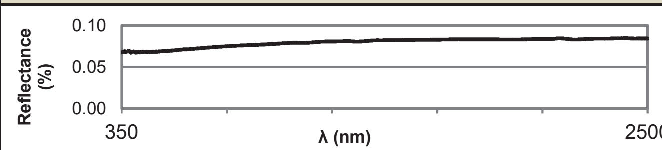

XRD
N/A

Stable Isotope

$\delta^{13}C_{VPDB}$ (‰)	$\delta^{18}O_{VPDB}$ (‰)
1A Sample	
-1.94	-8.17
1B Sample	
-1.95	-8.82

Well ID: Strong #1 (31107264660000)	Formation: Oatka Creek Formation	Sample ID:	2-TCC2
Location: Tioga, NY	Member: East Berne Member	Depth (ft):	4183.79

Fossiliferous, calcareous mudstone

Matrix Composition
mix of clay and calcite

Texture
mostly well-laminated texture defined by aligned dacryoconarids, clay minerals in the matrix, and fossil fragments

Diagenetic Minerals
matrix is highly cemented by calcite, giving it a pebbly appearance; dacryoconarids filled with calcite which may have more iron, judging by a slightly purple hue to the stain; sphalerite is crystallized randomly; rare dolomite rhombs disseminated, some of which have slightly ferroan rims

Allochemical or Detrital Grains
uncommon fine silt-sized quartz disseminated throughout without preferential deposition

Fossils
nondescript dacryoconarid shell fragments define bedding planes; size of shell varies widely, with the larger fragments less broken up and maintaining the curved morphology; uncommon fecal pellets

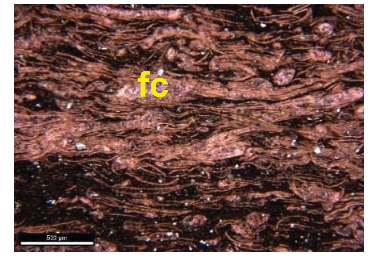

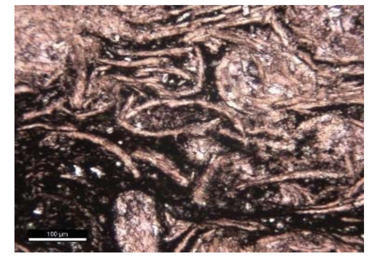

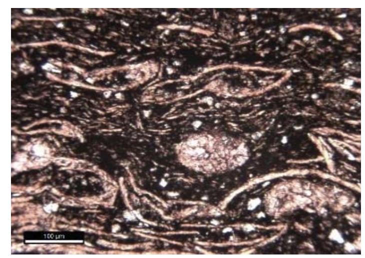

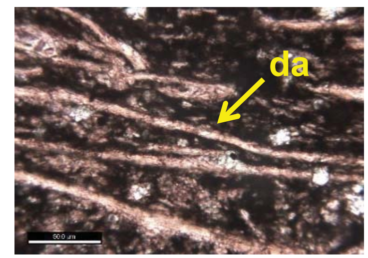

Fractures
pyrite and organic material associated with fracture

Additional Comments
dark matrix, likely indicating significant disseminated kerigenous residue in the matrix; organic material lines some detrital grains and fossils

SWIR

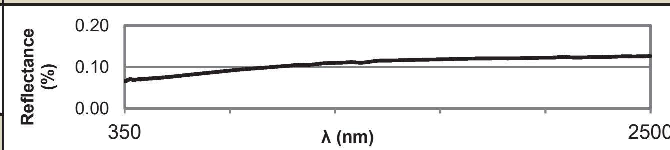

XRD
N/A

Stable Isotope

	$\delta^{13}C_{VPDB}$ (‰)	$\delta^{18}O_{VPDB}$ (‰)
1A Sample	-5.00	-9.33
1B Sample	-5.08	-10.26

Well ID: Strong #1 (31107264660000)	Formation: Oatka Creek Formation	Sample ID:	2-TCC1
Location: Tioga, NY	Member: Cherry Valley Member	Depth (ft):	4185.00

Packstone

Matrix Composition
calcite/micrite with minor clays; few discernable clays, mostly incorporated within the micritic matrix

Texture
poorly laminated, chaotic arrangement of fossils and sediments

Diagenetic Minerals
widespread calcite cementation/recrystallization; shell calcite = matrix calcite = fossil fill; dolomite fills center of the large gastropod at center

Allochemical or Detrital Grains
few, fine silt-sized quartz grains

Fossils
heavily recrystallized fossils; nautiloids or cephalopods; dacryoconarids (Nowakia and Styliolina); gastropods; nondescript shell fragments; bivalves; ostracods; phosphatic bone fragments; collapsed organic-walled cysts

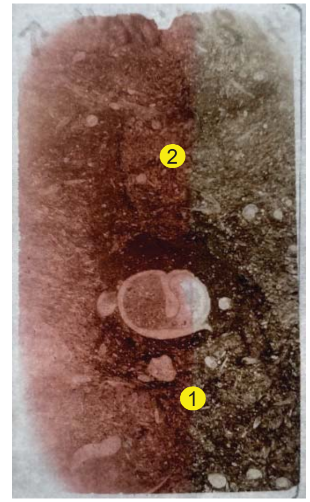

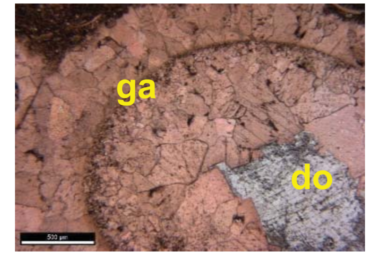

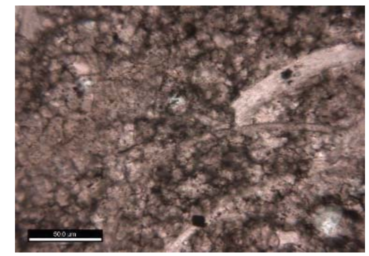

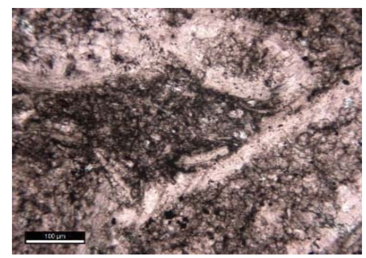

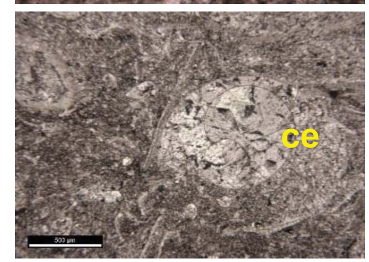

Fractures
subvertical fractures filled with organic material and pyrite

Additional Comments
organic material lines the rims of some fossil fragments; organic seams run vertically/perpendicular to bedding

SWIR

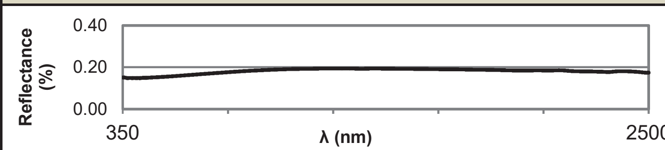

XRD

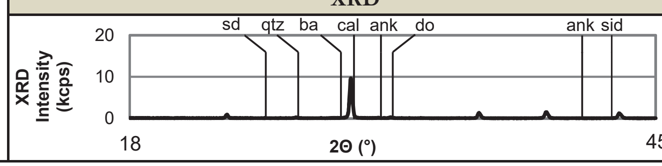

Stable Isotope (‰)

$\delta^{13}C_{VPDB}$	$\delta^{18}O_{VPDB}$
1A Sample	
-15.21	-6.67
1B Sample	
-15.36	-6.28
2A Sample	
-15.05	-7.03
2B Sample	
-14.32	-10.10

Well ID: Strong #1 (31107264660000)	Formation: Oatka Creek Formation	Sample ID:	2-TCC1
Location: Tioga, NY	Member: Cherry Valley Member	Depth (ft):	4185.00

Packstone

Matrix Composition and Microtexture

calcite cementation or recrystallization lends to a nonlaminated microtexture

Diagenetic Minerals

calcite is the most abundant diagenetic mineral; barite is crystallized in select portions of the calcareous matrix or as a replacement in fossils; minor dolomite rhombohedra are crystallized within the matrix; framboidal pyrite is associated with organic material

Diagenetic Texture and Fabric

neomorphism of micrite gives the matrix a homogenized or massive appearance; minor clays have been deformed and cemented; bladed barite crystals are replaced by calcite, as they were likely the result of an earlier diagenetic stage

Detrital Grains and Fossils

fossils are likely recrystallized based of their crystalline appearance, though are not compositionally distinct enough from calcite in the matrix; textural relationship between the matrix and detritus or fossils has largely been overprinted

Additional comments:

images are SE (top) and BSE (bottom) pair

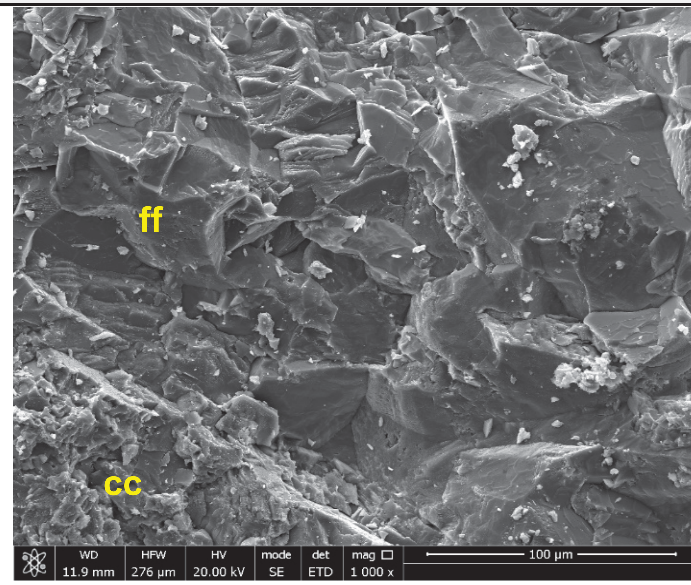

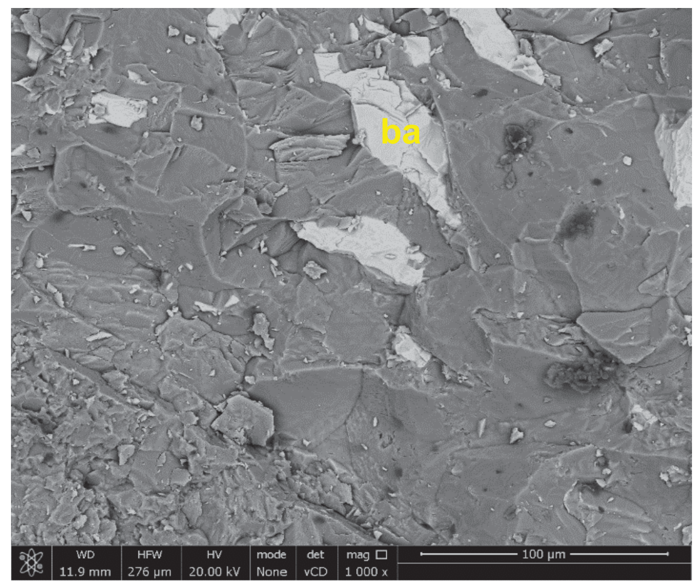

Well ID: Strong #1 (31107264660000)	Formation: Oatka Creek Formation	Sample ID:	3-TCC2
Location: Tioga, NY	Member: Cherry Valley Member	Depth (ft):	4185.31

Packstone

Matrix Composition

calcite/micrite with minor clays, likely illitic

Texture

poorly laminated

Diagenetic Minerals

calcite cementation/recrystallization throughout; some fossil shells are slightly ferroan; dolomite cement starts showing up near the bottom of the slide; calcite cement typically = fossil fill; parts of the gastropod shell are filled with barite; rare siderite

Allochemical or Detrital Grains

few very fine silt-sized quartz disseminated throughout

Fossils

dacryoconarids (Styliolina); larger fossil fragments likely bivalves or brachiopods; gastropod at bottom left; ostracods commonly intact; rare bone fragments

Fractures

organic-filled fractures typically oriented normal to bedding

Additional Comments

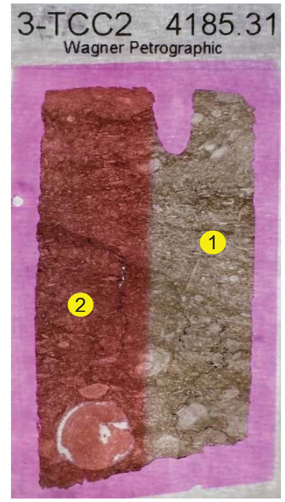

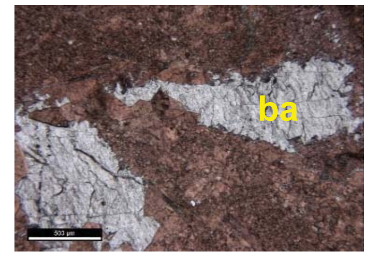

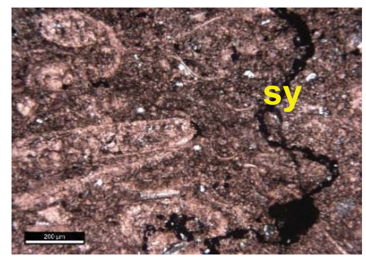

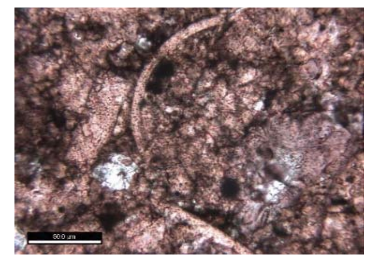

SWIR

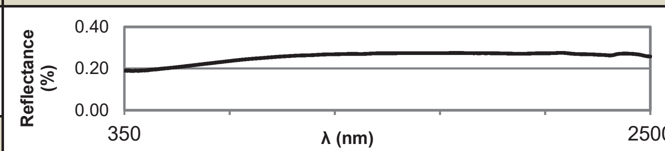

XRD

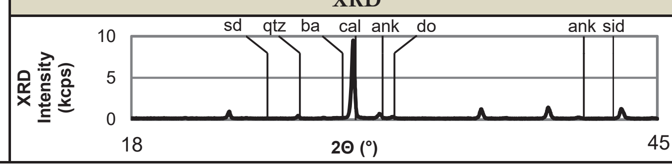

Stable Isotope (‰)

$\delta^{13}C_{VPDB}$	$\delta^{18}O_{VPDB}$
1A Sample	
-13.15	-7.02
1B Sample	
-13.07	-7.25
2A Sample	
-13.62	-7.65
2B Sample	
-13.28	-7.12

Well ID: Strong #1 (31107264660000)	Formation: Oatka Creek Formation	Sample ID:	3-TCC2
Location: Tioga, NY	Member: Cherry Valley Member	Depth (ft):	4185.31

Packstone

Matrix Composition and Microtexture

calcite cementation or recrystallization lends to a nonlaminated microtexture

Diagenetic Minerals

calcite is the most abundant diagenetic mineral; barite is crystallized in select portions of the calcareous matrix or as a replacement in fossils; minor dolomite rhombohedra are crystallized within the matrix; framboidal pyrite is associated with organic material

Diagenetic Texture and Fabric

neomorphism of micrite gives the matrix a homogenized or massive appearance; minor clays have been deformed and cemented; bladed barite crystals are replaced by calcite, as they were likely the result of an earlier diagenetic stage

Detrital Grains and Fossils

fossils are likely recrystallized based of their crystalline appearance, though are not compositionally distinct enough from calcite in the matrix; textural relationship between the matrix and detritus or fossils has largely been overprinted

Additional comments:

images are SE (top) and BSE (bottom) pair

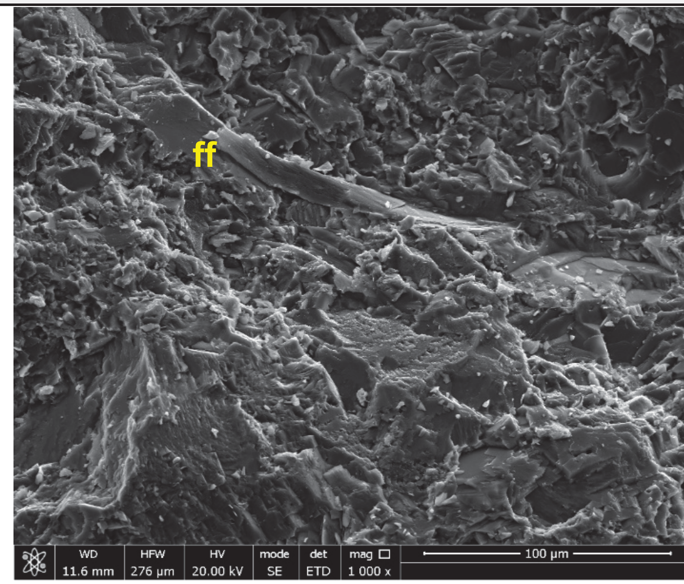

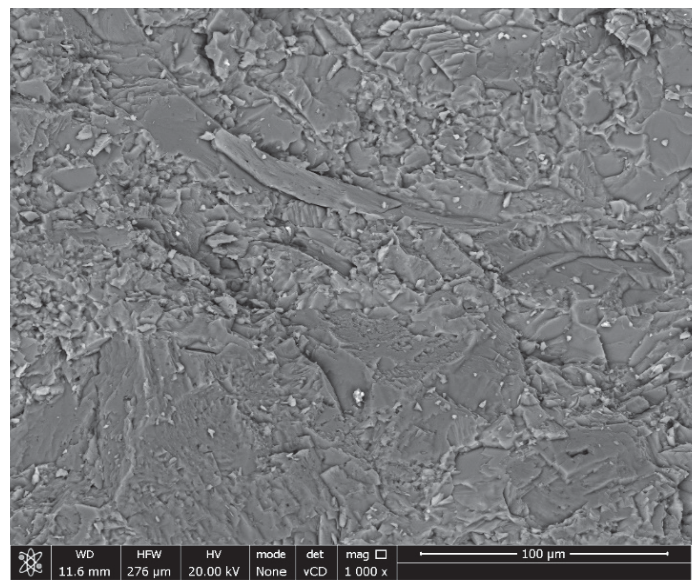

Well ID: Strong #1 (31107264660000)	**Formation: Oatka Creek Formation**	**Sample ID:**	**4-TCC2**
Location: Tioga, NY	**Member: Cherry Valley Member**	**Depth (ft):**	**4185.44**

Fossiliferous, calcareous/argillaceous mudstone

Matrix Composition
mostly illitic clays and organic material with calcite cement

Texture
well-laminated texture defined by aligned dacryoconarid shells, matrix clays and micas, and fossil fragments

Diagenetic Minerals
slight calcite overprint through much of the matrix; dolomite rhombohedra are distributed throughout the matrix, some with ferroan rims

Allochemical or Detrital Grains
very fine silt distributed throughout

Fossils
nondescript dacryoconarid shell fragments (rarely intact); few brachiopod fragments or other larger shells; phosphatic algal cysts

Fractures
organic material fills bedding-parallel fractures

Additional Comments
organic material widely disseminated throughout matrix clays

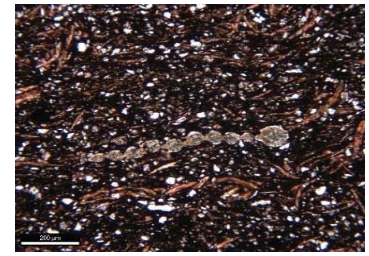

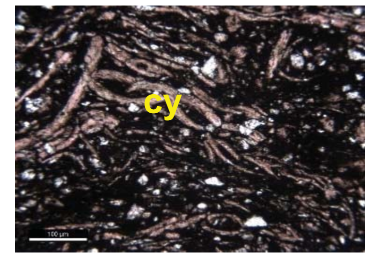

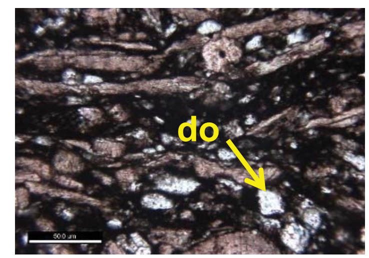

SWIR

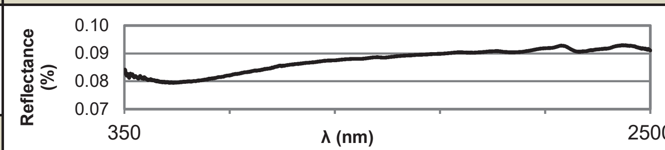

XRD

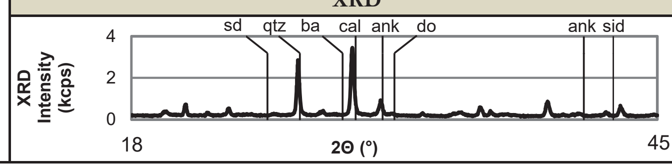

Stable Isotope

$\delta^{13}C_{VPDB}$ (‰)	$\delta^{18}O_{VPDB}$ (‰)
1A Sample	
N/A	N/A
1B Sample	
-1.65	-9.05

Well ID: Strong #1 (31107264660000)	**Formation: Oatka Creek Formation**	**Sample ID:**	**5-TCC2**
Location: Tioga, NY	**Member: Cherry Valley Member**	**Depth (ft):**	**4185.58**

Wackestone

Matrix Composition

calcite/micrite with minor clays

Texture

poorly laminated

Diagenetic Minerals

calcite in cement = shells = fossil fill, very well equilibrated; ferroan calcite fracture fill; some blotches of pyrite near top of slide; minor dolomite rhombs distributed randomly

Allochemical or Detrital Grains

very fine silt distributed throughout

Fossils

dacryoconarids (Styliolina); rare cephalopods; ostracods

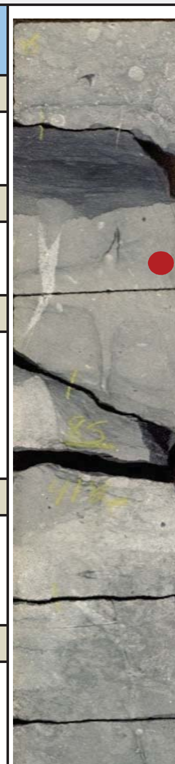

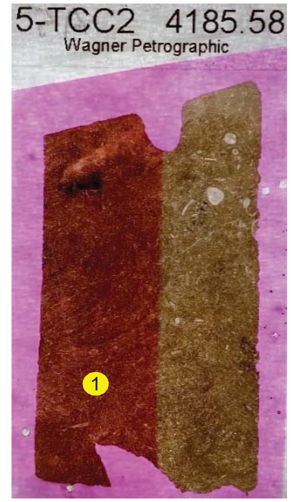

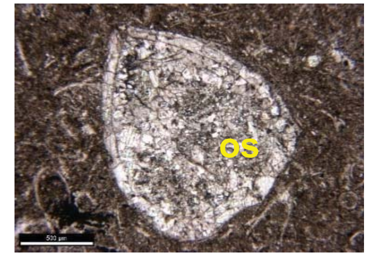

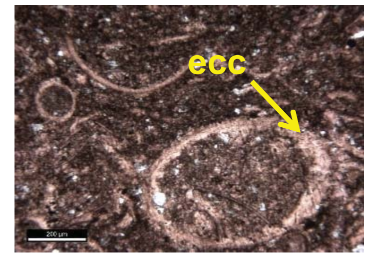

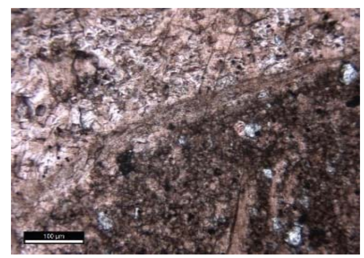

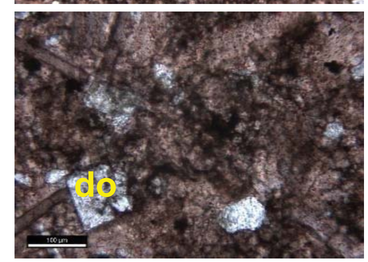

Fractures

healed ferroan calcite fracture runs vertical across thin section

Additional Comments

SWIR

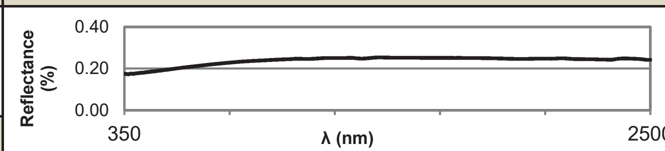

XRD

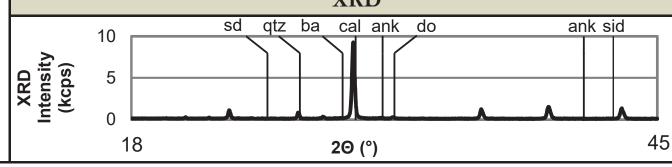

Stable Isotope

$\delta^{13}C_{VPDB}$ (‰)	$\delta^{18}O_{VPDB}$ (‰)
1A Sample	
-12.06	-9.11
1B Sample	
-12.11	-9.28

Well ID: Strong #1 (31107264660000)	Formation: Oatka Creek Formation	Sample ID:	5-TCC2
Location: Tioga, NY	Member: Cherry Valley Member	Depth (ft):	4185.58

Wackestone

Matrix Composition and Microtexture

calcite cementation or recrystallization lends to a nonlaminated microtexture

Diagenetic Minerals

calcite is the most abundant diagenetic mineral; minor dolomite rhombohedra are crystallized within the matrix; framboidal pyrite is associated with organic material; minor authigenic plagioclase

Diagenetic Texture and Fabric

neomorphism of micrite gives the matrix a homogenized or massive appearance; minor clays have been deformed and cemented

Detrital Grains and Fossils

fossils are likely recrystallized based of their crystalline appearance, though are not compositionally distinct enough from calcite in the matrix; textural relationship between the matrix and detritus or fossils has largely been overprinted

Additional comments:

images are SE (top) and BSE (bottom) pair

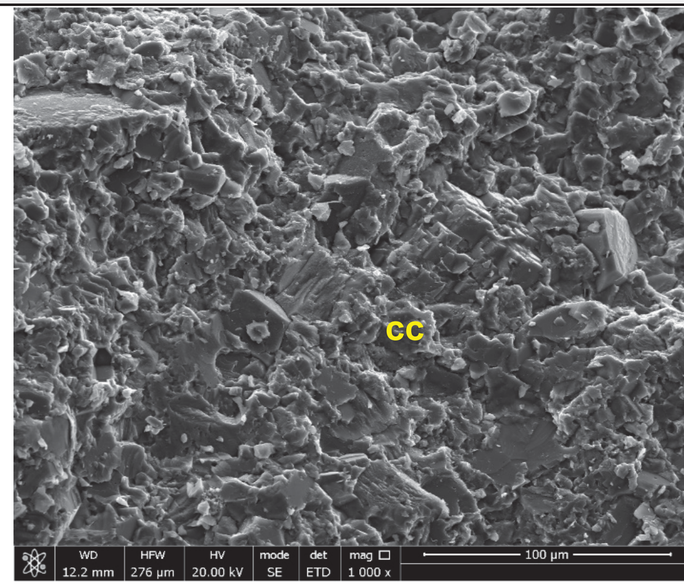

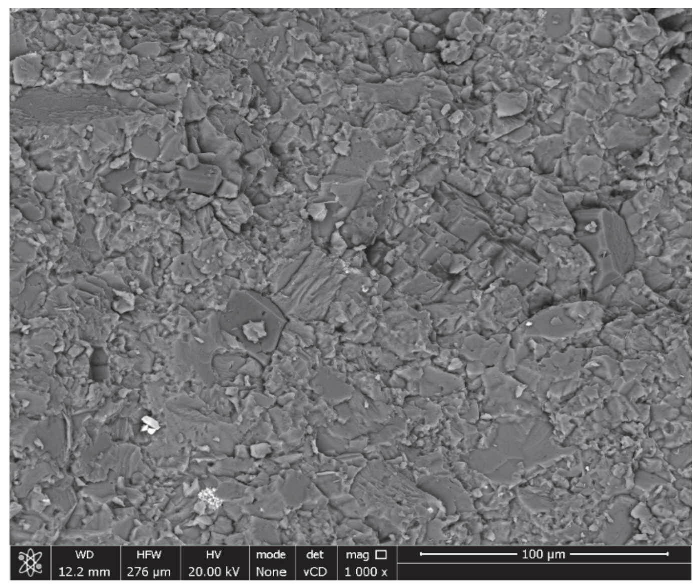

Well ID: Strong #1 (31107264660000)
Location: Tioga, NY
Formation: Oatka Creek Formation
Member: Cherry Valley Member
Sample ID: 6-TCC2
Depth (ft): 4185.83

Crystalline carbonate

Matrix Composition

calcite and ferroan calcite in the nodule; illitic clay in surrounding mudstone

Texture

chaotic arrangement within nodule; mudstone is well laminated and deformed by the nodule growth

Diagenetic Minerals

mudstone portion is cemented by dolomite with rare areas of ferroan dolomite; nodule is mostly finer grained sparite with coarser grained ferroan calcite cement; dolomite replaces select fossils and is rarely crystallized as a cement; pyrite mostly associated with OM in mudstone;

Allochemical or Detrital Grains

fine silt-sized quartz disseminated

Fossils

dacryoconarids fragments deposited along bedding in mudstone, chaotic and more intact in nodule; crinoid stems and plates, ostracods, dacryoconarids (Nowakia and Styliolina), brachiopod fragments, and bivalves in nodule area

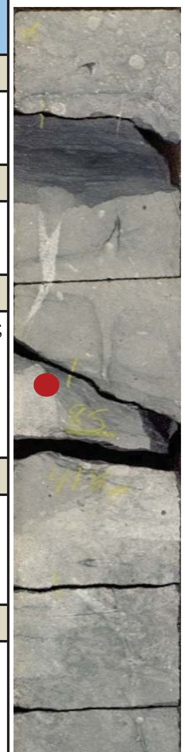

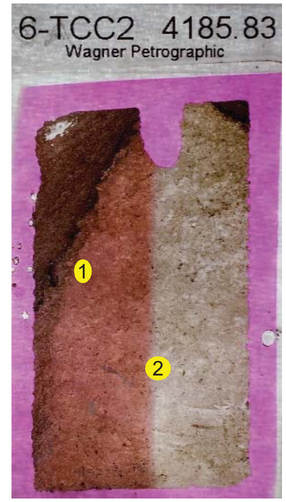

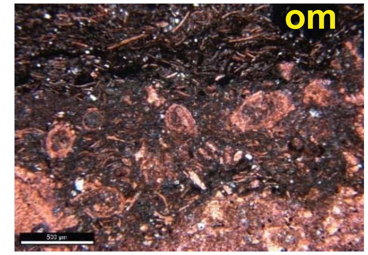

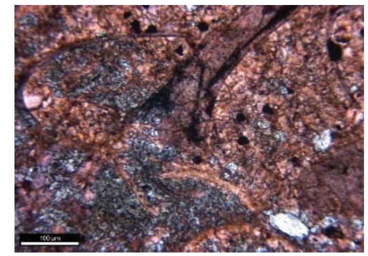

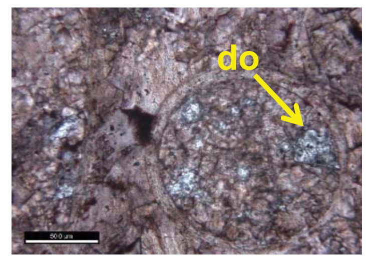

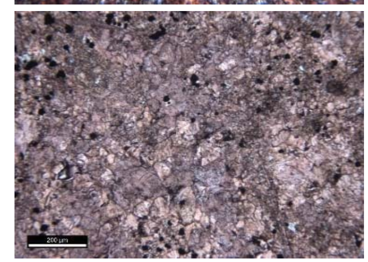

Fractures

slightly ferroan calcite fills a healed horizontal fracture that runs through mudstone and nodule

Additional Comments

patches of organic material mostly restricted to mudstone parts, especially right along the border with the nodule

SWIR

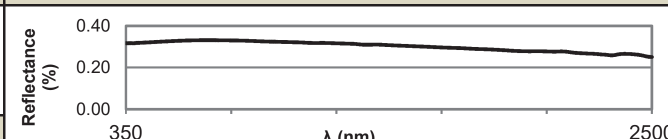

XRD

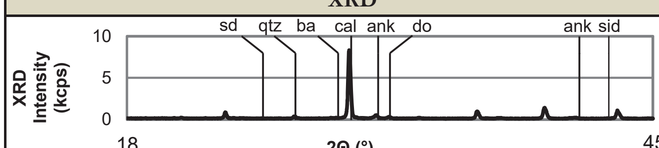

Stable Isotope (‰)

$\delta^{13}C_{VPDB}$	$\delta^{18}O_{VPDB}$
1A Sample	
-11.86	-4.68
1B Sample	
-12.22	-5.37
2A Sample	
-11.73	-6.23
2B Sample	
-11.40	-5.11

Well ID: Strong #1 (31107264660000)	**Formation: Oatka Creek Formation**	**Sample ID:**	**7-TCC2**
Location: Tioga, NY	**Member: Cherry Valley Member**	**Depth (ft):**	**4186.08**

Baritic crystalline carbonate

Matrix Composition

calcite, dolomite, and ferroan calcite in the nodule; dolomite and illitic clay in the mudstone

Texture

chaotic in nodule; well laminated and deformed by the nodule growth

Diagenetic Minerals

mudstone portion is cemented by dolomite with rare areas of ferroan dolomite; nodule is mostly finer-grained sparite with coarser grained ferroan calcite cement; barite replaces select fossils and is more common as a crystallized cement than its overlying nodule neighbor; minor barite

Allochemical or Detrital Grains

fine silt-sized quartz disseminated

Fossils

dacryoconarids fragments, though many intact, deposited along bedding in mudstone, chaotic and intact in nodule; ostracods, dacryoconarids (Viriatella and Nowakia), brachiopod fragments, and bivalves in nodule area

Fractures

slightly ferroan calcite fills a healed horizontal fracture that runs through mudstone and nodule

Additional Comments

patches of organic material mostly restricted to mudstone parts, especially right along the border with the nodule; pyrite mostly associated with organic material in mudstone

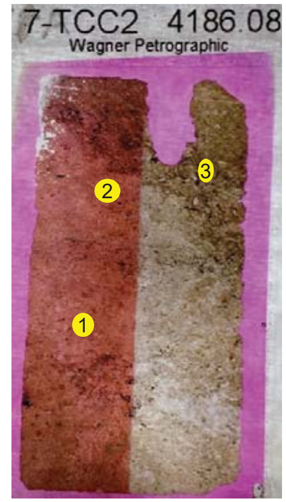

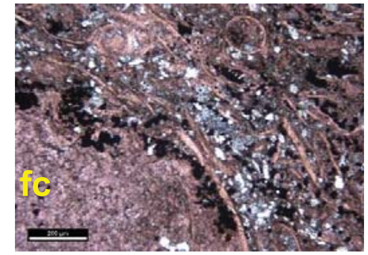

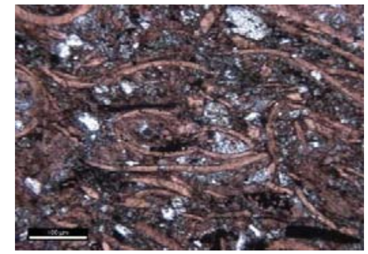

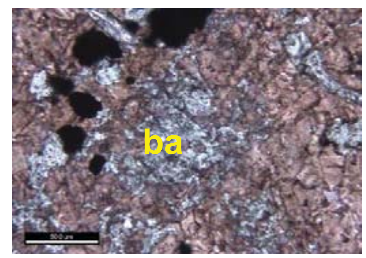

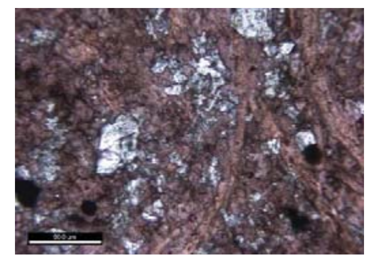

SWIR

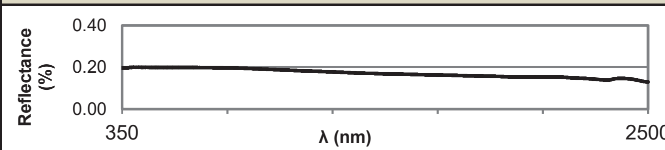

XRD

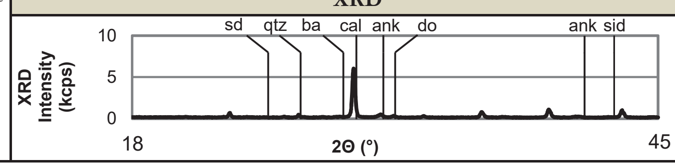

Stable Isotope (‰)

1 Sample (A | B)	
$\delta^{13}C_{VPDB}$	-10.92 | -10.95
$\delta^{18}O_{VPDB}$	-3.61 | -3.50
2 Sample (A | B)	
$\delta^{13}C_{VPDB}$	-11.18 | -11.08
$\delta^{18}O_{VPDB}$	-5.39 | -3.95
3 Sample (A | B)	
$\delta^{13}C_{VPDB}$	-7.09 | -7.01
$\delta^{18}O_{VPDB}$	-8.53 | -9.11

Well ID: Strong #1 (31107264660000)	Formation: Oatka Creek Formation	Sample ID:	7-TCC2
Location: Tioga, NY	Member: Cherry Valley Member	Depth (ft):	4186.08

Baritic crystalline carbonate

Matrix Composition and Microtexture

calcite recrystallization results in a crystalline, blocky microtexture

Diagenetic Minerals

calcite is the most abundant diagenetic mineral; barite is crystallized in select portions of the calcareous matrix or as a replacement in fossils; dolomite and ferroan dolomite cement select areas of the rock; framboidal pyrite is associated with organic material; minor authigenic clays

Diagenetic Texture and Fabric

neomorphism of micrite gives the matrix a homogenized or massive appearance; minor clays have been deformed and cemented; bladed barite crystals are replaced by calcite, as they were likely the result of an earlier diagenetic stage

Detrital Grains and Fossils

fossils are recrystallized and their morphology is largely lost; textural relationship between the matrix and detritus or fossils has largely been overprinted

Additional comments:

images are SE (top) and BSE (bottom) pair

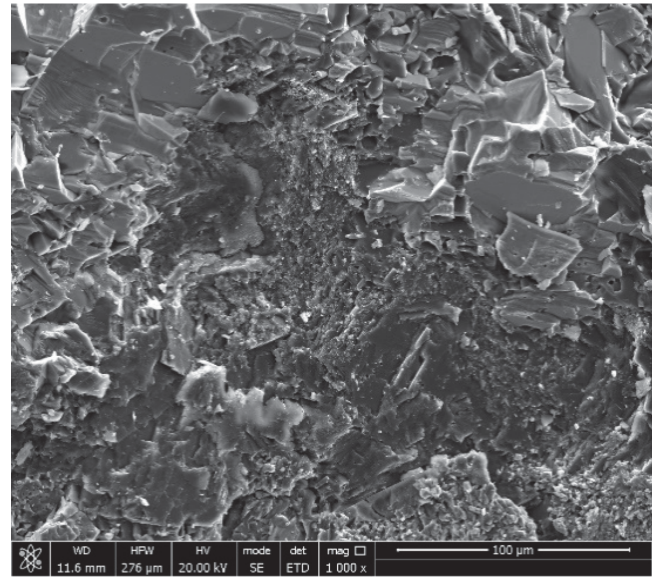

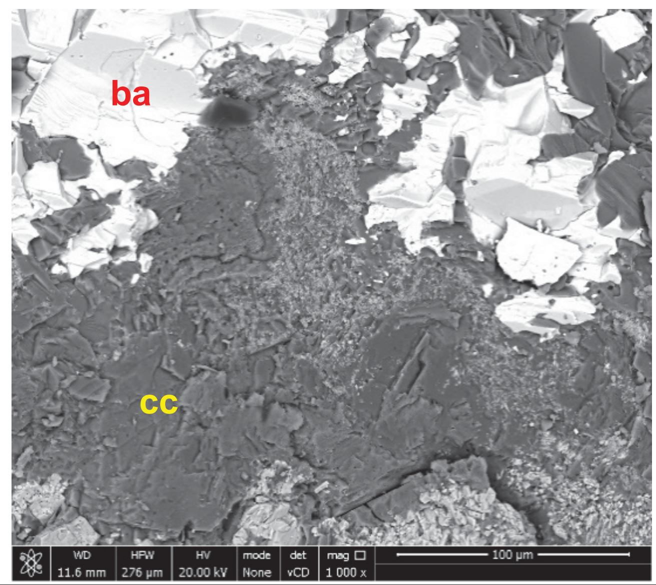

Well ID: Strong #1 (31107264660000)
Location: Tioga, NY
Formation: Oatka Creek Formation
Member: Cherry Valley Member
Sample ID: 8-TCC2
Depth (ft): 4186.21

Crystalline dolomite

Matrix Composition
dolomite microspar

Texture
non-laminated - recrystallization has completely erased fabric as shown by flipping the polars

Diagenetic Minerals
dolomite dominantly overprints the rock and all components within including fossils and matrix; slightly ferroan per blue hue; barite replaces some of the larger fossil fragments; original calcite remains as uncommon grains or protected fossil fill

Allochemical or Detrital Grains
few quartz silt grains

Fossils
unidentifiable shell fragments

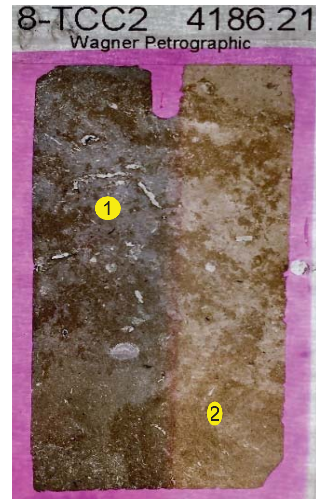

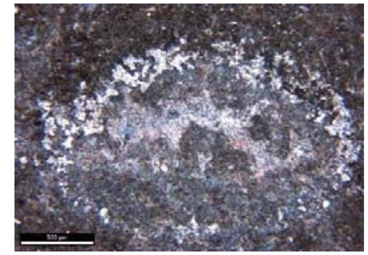

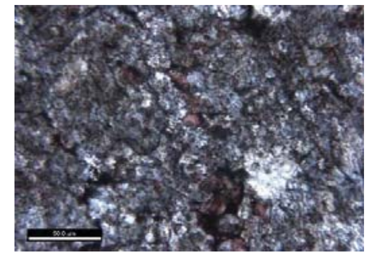

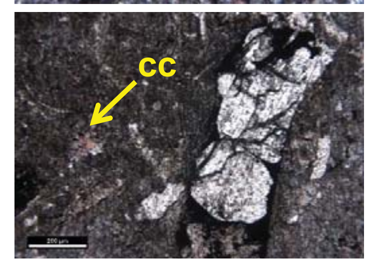

Fractures
none

Additional Comments
webby organic material; barite appears to have been dissolved away during sample prep as there are commonly holes associated with it;

SWIR

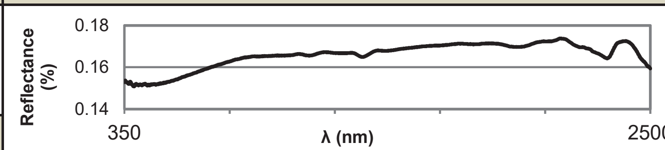

XRD

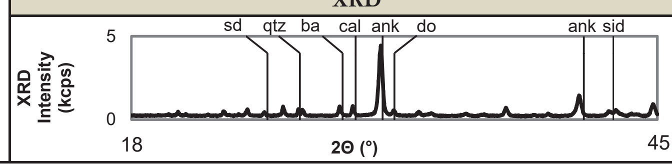

Stable Isotope (‰)

$\delta^{13}C_{VPDB}$	$\delta^{18}O_{VPDB}$
1A Sample	
-12.73	-8.65
1B Sample	
-12.58	-9.61
2A Sample	
-10.72	-9.07
2B Sample	
N/A	N/A

Well ID: Strong #1 (31107264660000)	**Formation: Oatka Creek Formation**	**Sample ID:**	**8-TCC2**
Location: Tioga, NY	**Member: Cherry Valley Member**	**Depth (ft):**	**4186.21**

Crystalline dolomite

Matrix Composition and Microtexture

dolomitization develops a coarsely crystalline or massive microtexture

Diagenetic Minerals

dolomite is the dominant diagenetic mineral; select portions of the sample include barite, which is partially replaced by dolomite; minor framboidal pyrite

Diagenetic Texture and Fabric

dolomite replacement of calcite destroys original depositional textures, creating a coarsely crystalline texture

Detrital Grains and Fossils

fossil morphology is rarely retained at the micron-scale and is largely distinguishable by the presence of barite which is mostly observed as fossil fill in thin section

Additional comments:

images are SE (top) and BSE (bottom) pair

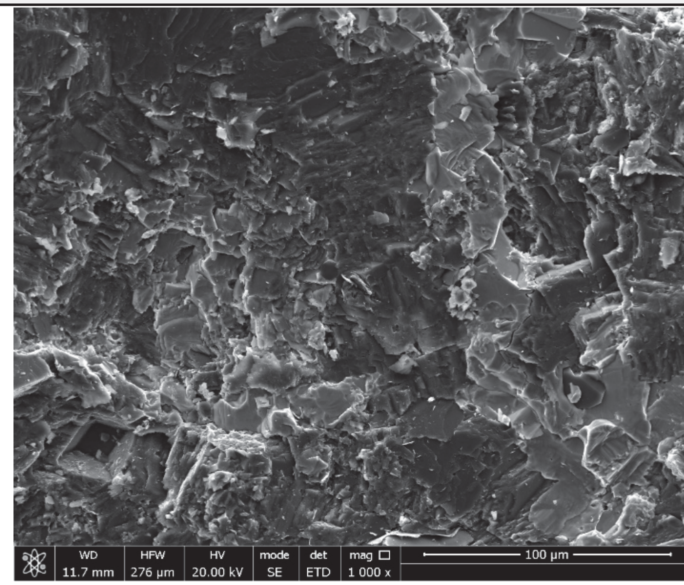

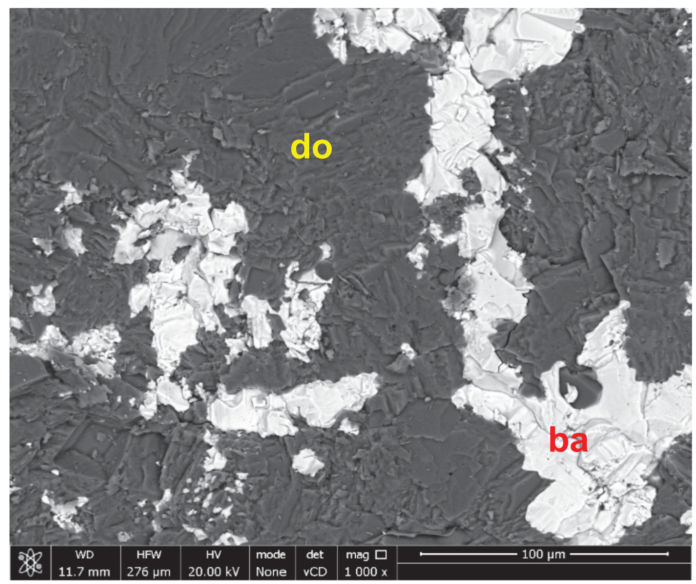

Well ID: Strong #1 (31107264660000)	Formation: Oatka Creek Formation	Sample ID:	9-TCC2
Location: Tioga, NY	Member: Cherry Valley Member	Depth (ft):	4186.42

Crystalline dolomite

Matrix Composition

dolomite microspar

Texture

non-laminated - recrystallization has completely erased fabric as shown by flipping the polars

Diagenetic Minerals

dolomite dominantly overprints the rock and all components within including fossils and matrix; slightly ferroan per blue hue; barite replaces some of the larger fossil fragments; little "original" calcite remains as little grains or protected fossil fills may still be calcite

Allochemical or Detrital Grains

few quartz silt grains

Fossils

unidentifiable shell fragments; conodonts

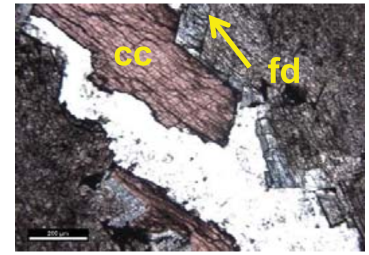

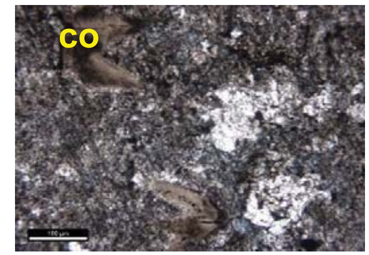

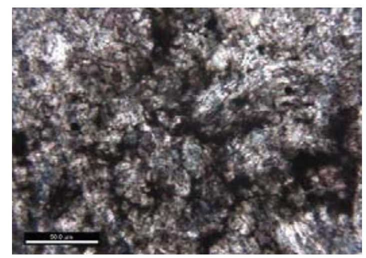

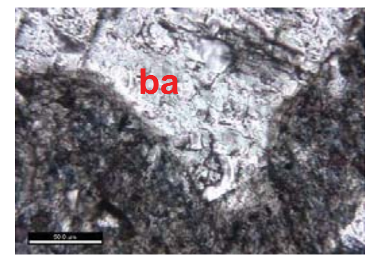

Fractures

vertical fracture healed by calcite

SWIR

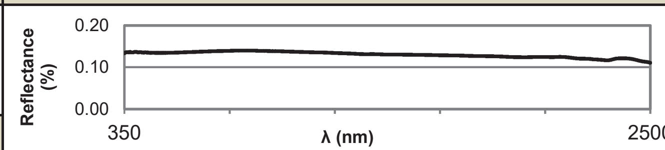

Additional Comments

webby organic material; barite appears to have been dissolved away during sample prep as there are commonly holes associated with it; difference between this sample and 8-TCC2 is the presence of an open pore that has separate instances of euhedral ferroan dolomite and calcite filling it

XRD

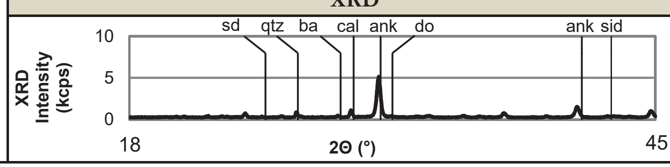

Stable Isotope (‰)

$\delta^{13}C_{VPDB}$	$\delta^{18}O_{VPDB}$
1A Sample	
-9.83	-7.80
1B Sample	
N/A	N/A
2A Sample	
-10.34	-8.31
2B Sample	
-10.21	-8.17

Well ID: Strong #1 (31107264660000)	Formation: Oatka Creek Formation	Sample ID:	9-TCC2
Location: Tioga, NY	Member: Cherry Valley Member	Depth (ft):	4186.42

Crystalline dolomite

Matrix Composition and Microtexture

dolomitization develops a coarsely crystalline or massive microtexture

Diagenetic Minerals

dolomite is the dominant diagenetic mineral; select portions of the sample include barite, which is partially replaced by dolomite; possible silica cement; minor framboidal pyrite associated with degraded organic material

Diagenetic Texture and Fabric

dolomite replacement of calcite destroys original depositional textures, creating a coarsely crystalline texture

Detrital Grains and Fossils

fossil morphology is rarely retained at the micron-scale and is largely distinguishable by the presence of barite which is mostly observed as fossil fill in thin section

Additional comments:

images are SE (top) and BSE (bottom) pair; phosphatic fragment likely a bone

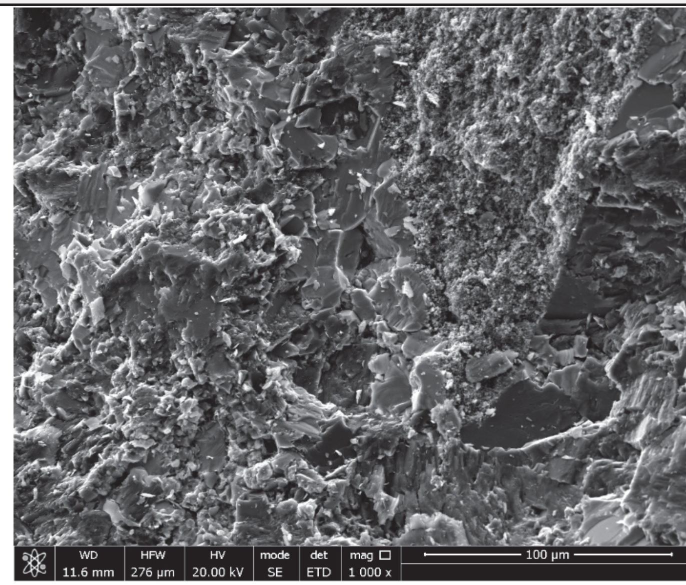

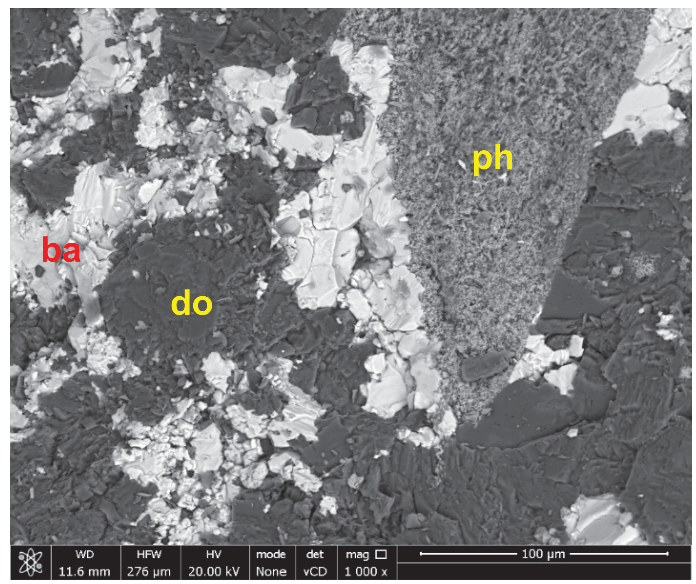

Well ID: Strong #1 (31107264660000)	Formation: Oatka Creek Formation	Sample ID:	10-TCC2
Location: Tioga, NY	Member: Cherry Valley Member	Depth (ft):	4186.71

Dolomitic crystalline carbonate

Matrix Composition
dolomite and calcite

Texture
weakly laminated - texture mostly overprinted by carbonate diagenesis

Diagenetic Minerals
calcite cement and fossil recrystallization is primary diagenetic process; dolomite is crystallized second to the calcite as a matrix cement and also replaces select fossils (though not nearly on the scale as the calcite); barite replaces select fossils, generally larger ones

Allochemical or Detrital Grains
uncommon quartz silt disseminated

Fossils
mostly shell fragments, ranging from thin bivalve or ostracod pieces to larger brachiopod or gastropod fragments; nondescript dacryoconarids

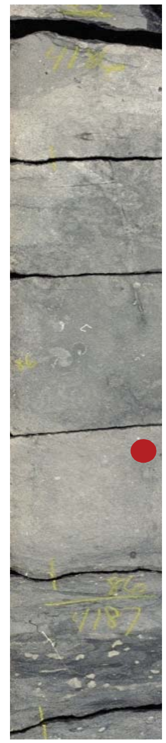

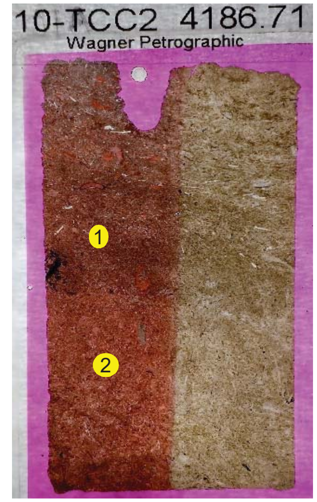

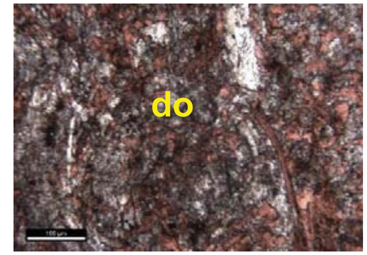

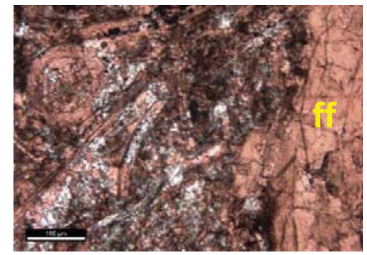

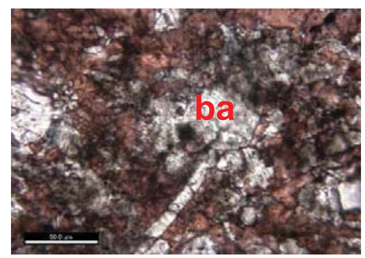

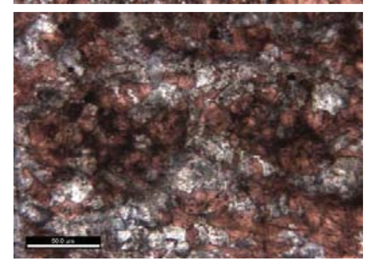

Fractures
none

Additional Comments
seemingly random splashes of organic material

SWIR

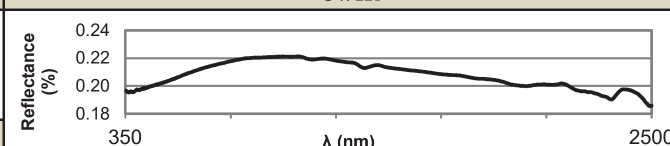

XRD

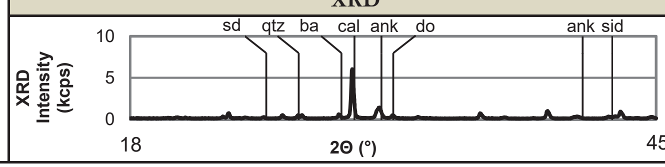

Stable Isotope (‰)

$\delta^{13}C_{VPDB}$	$\delta^{18}O_{VPDB}$
1A Sample	
-13.98	-6.93
1B Sample	
-14.53	-7.31
2A Sample	
-14.69	-7.90
2B Sample	
-14.61	-7.60

Well ID: Strong #1 (31107264660000)	Formation: Oatka Creek Formation	Sample ID:	10-TCC2
Location: Tioga, NY	Member: Cherry Valley Member	Depth (ft):	4186.71

Dolomitic crystalline carbonate

Matrix Composition and Microtexture

matrix is partially dolomitized

Diagenetic Minerals

dolomite is the dominant diagenetic mineral; select portions of the sample include barite, which is partially replaced by dolomite; possible silica cement; minor framboidal pyrite associated with degraded organic material

Diagenetic Texture and Fabric

dolomite replacement of calcite destroys original depositional textures, creating a coarsely crystalline texture

Detrital Grains and Fossils

fossil morphology is rarely retained at the micron-scale and is largely distinguishable by the presence of barite which is mostly observed as fossil fill in thin section

Additional comments:

images are SE (top) and BSE (bottom) pair

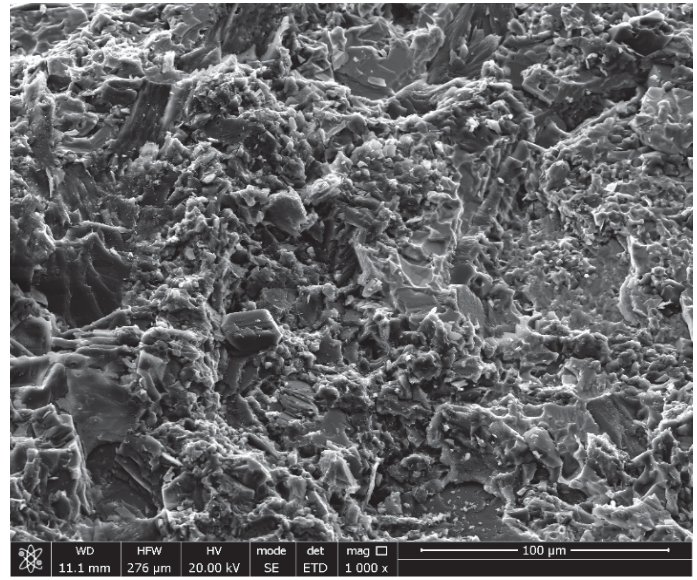

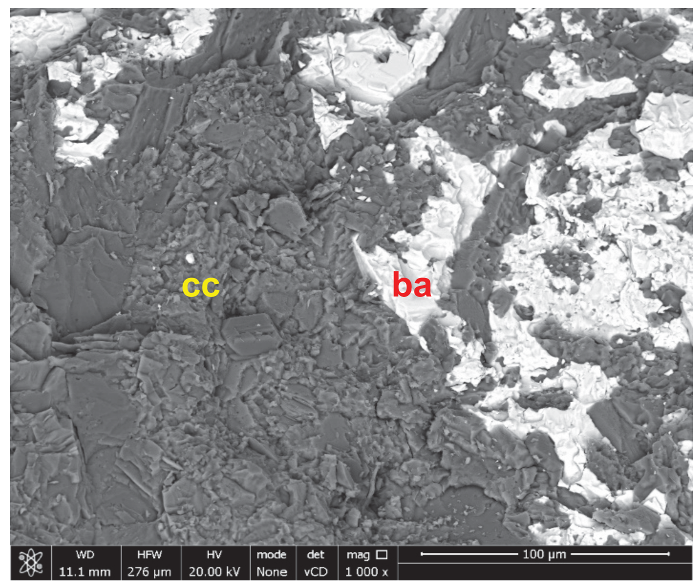

Well ID: Strong #1 (31107264660000)	Formation: Oatka Creek Formation	Sample ID: 11-TCC2
Location: Tioga, NY	Member: Cherry Valley Member	Depth (ft): 4186.96

Fossiliferous, dolomitic, calcareous/argillaceous mudstone

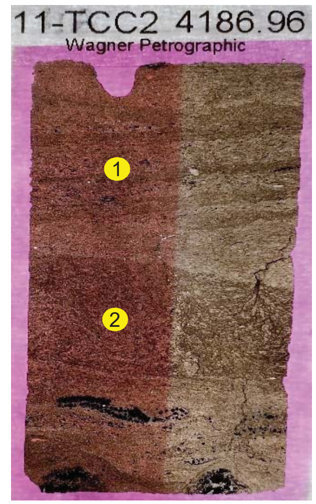

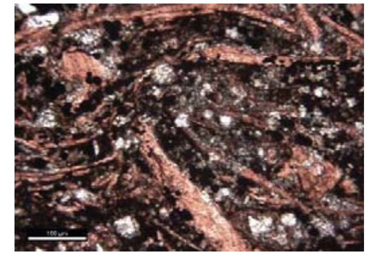

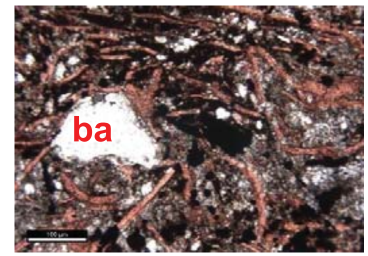

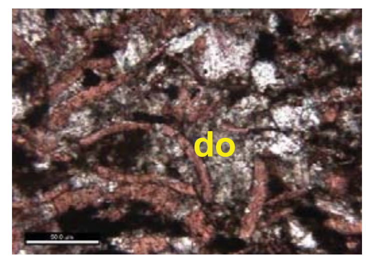

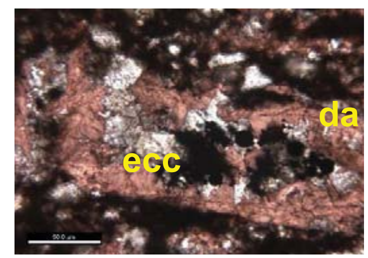

Matrix Composition

illitic clay, dolomite, and calcite

Texture

well-laminated, but highly cemented at finer scale

Diagenetic Minerals

fossiliferous mudstone cemented or recrystallized with dolomite; previous calcite cementation apparent prior to dolomitization; siderite; ferroan calcite associated with pyrite and organic material; dolomite rhombohedra disseminated throughout; some rhombs have ferroan dolomite rims or calcite cores

Allochemical or Detrital Grains

fossil fragments and higher amount of detrital silt than overlying samples.

Fossils

dacryoconarids (Viriatella) mostly with nondescript fossil fragments, perhaps bivalves or other shelly critters; several larger fragments may be ostracods; possible some bioturbation or concretion at the bottom

Fractures

none

Additional Comments

disseminated organic material with higher concentrations in select, clay-rich laminae.

SWIR

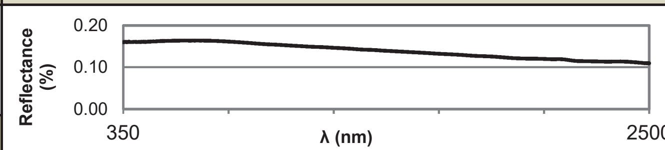

XRD

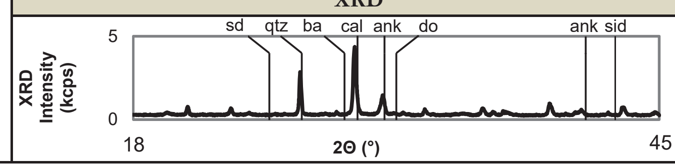

Stable Isotope (‰)

$\delta^{13}C_{VPDB}$	$\delta^{18}O_{VPDB}$
1A Sample	
-5.43	-9.14
1B Sample	
-3.68	-9.74
2A Sample	
-3.99	-10.24
2B Sample	
-3.66	-9.67

Well ID: Strong #1 (31107264660000)	**Formation: Oatka Creek Formation**	**Sample ID:**	**12-TCC2**
Location: Tioga, NY	**Member: Cherry Valley Member**	**Depth (ft):**	**4187.08**

Fossiliferous, dolomitic, calcareous/argillaceous mudstone

Matrix Composition

illitic clay, dolomite, and calcite

Texture

Well-laminated, but highly cemented at finer scale

Diagenetic Minerals

Fossiliferous mudstone cemented or recrystallized with dolomite; previous calcite cementation apparent prior to dolomitization; siderite; ferroan calcite commonly associated with pyrite and OM; dolomite rhombs disseminated throughout; some rhombs have ferroan dolomite rims or calcite cores

Allochemical or Detrital Grains

fossil fragments and higher amount of detrital silt than overlying samples.

Fossils

dacryoconarids (Viriatella) mostly with nondescript fossil fragments, perhaps bivalves or other shelly critters; several larger fragments may be ostracods; possible some bioturbation or concretion at the right

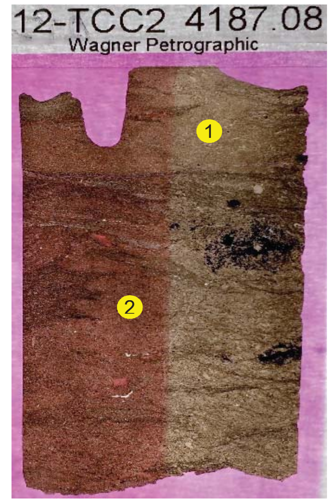

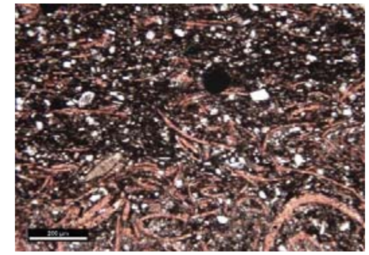

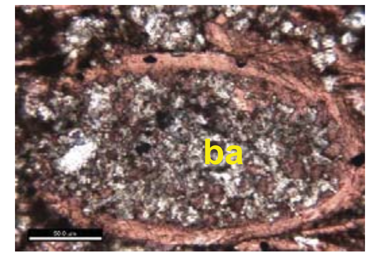

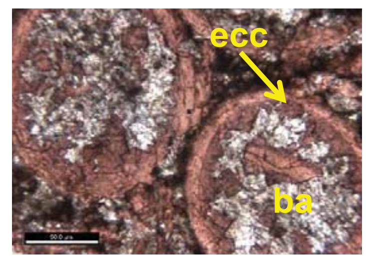

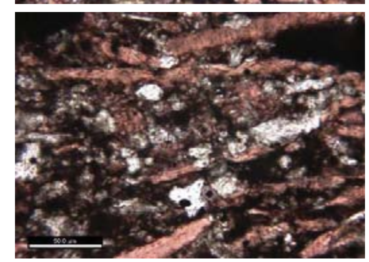

Fractures

ferroan calcite-healed fracture normal to bedding

Additional Comments

disseminated organic material with higher concentrations in select, clay-rich laminae.

SWIR

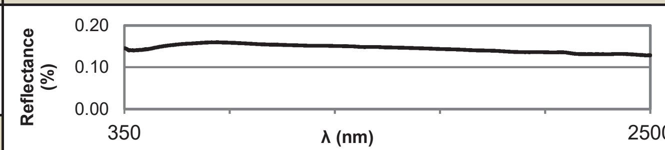

XRD

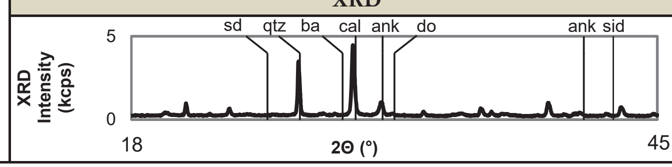

Stable Isotope (‰)

$\delta^{13}C_{VPDB}$	$\delta^{18}O_{VPDB}$
1A Sample	
-3.62	-9.37
1B Sample	
N/A	N/A
2A Sample	
-5.04	-9.54
2B Sample	
N/A	N/A

Well ID: Strong #1 (31107264660000)	Formation: Oatka Creek Formation	Sample ID:	12-TCC2
Location: Tioga, NY	Member: Cherry Valley Member	Depth (ft):	4187.08

Fossiliferous, dolomitic, calcareous/argillaceous mudstone

Matrix Composition and Microtexture

matrix is primarily calcite with minor dolomitic cements

Diagenetic Minerals

calcite and dolomite compose the micritic matrix; select portions of the sample include barite; minor framboidal pyrite associated with degraded organic material

Diagenetic Texture and Fabric

dolomite replacement of calcite destroys original depositional textures, creating a coarsely crystalline texture

Detrital Grains and Fossils

fossil fragments are recrystallized and typically include calcite overgrowths

Additional comments:

images are SE (top) and BSE (bottom) pair

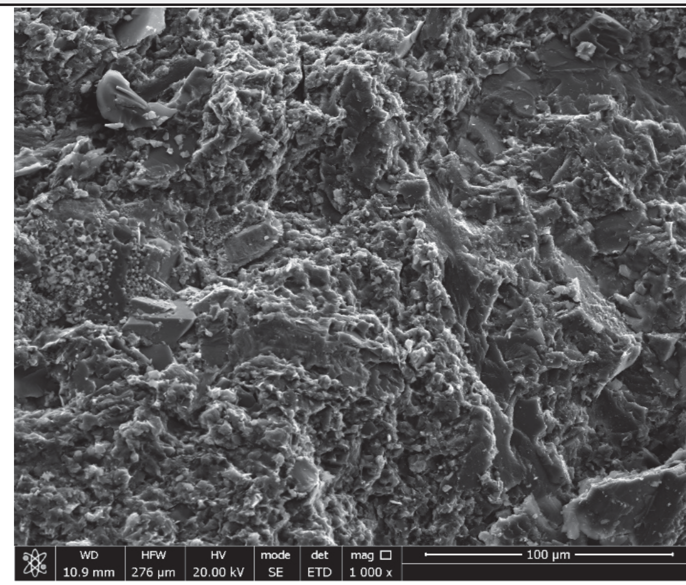

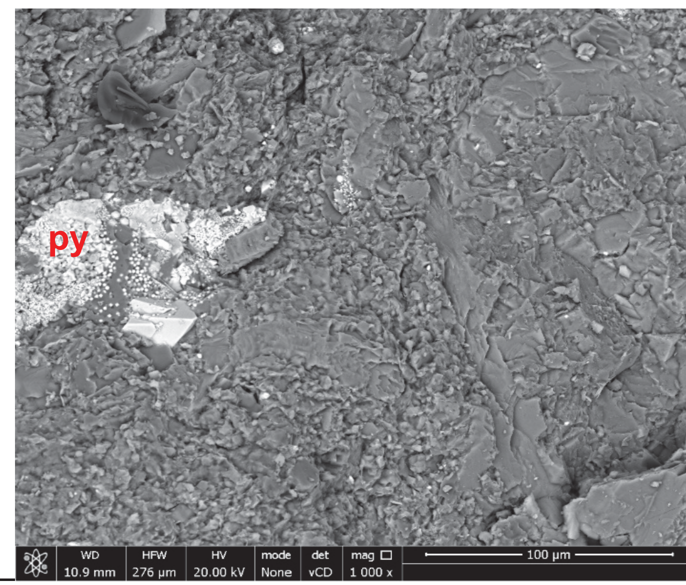

Well ID: Strong #1 (31107264660000)	Formation: Oatka Creek Formation	Sample ID:	3-TCC1
Location: Tioga, NY	Member: Cherry Valley Member	Depth (ft):	4187.25

Fossiliferous, baritic, calcareous mudstone

Matrix Composition

primarily calcite with likely some clays mixed in with the muddier portions

Texture

poorly laminated; original bedding was either uneven or it was disrupted by bioturbation or syngenetic deformation

Diagenetic Minerals

strongly overprinted by calcite recrystallization; some zones associated with burrowing are cemented by authigenic barite with some associated ferroan calcite; blocky calcite cement is pervasive throughout; relatively homogenous calcite composition

Allochemical or Detrital Grains

mostly quartz silt disseminated throughout

Fossils

dacryoconarids (Styliolina); nondescript, elongate shell fragments

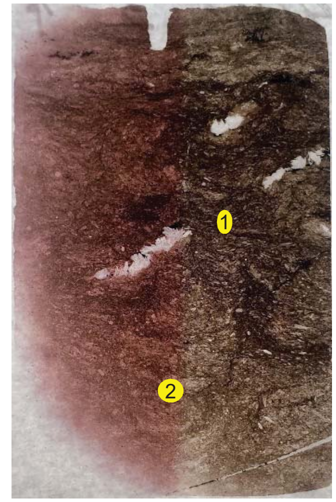

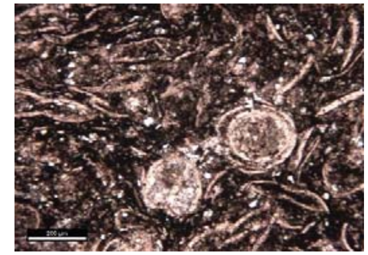

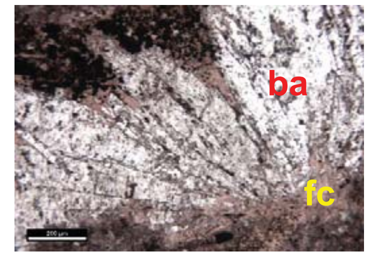

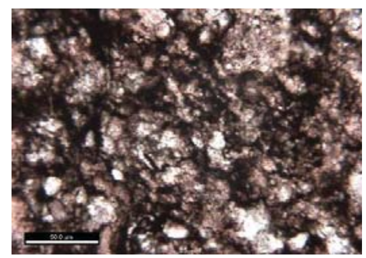

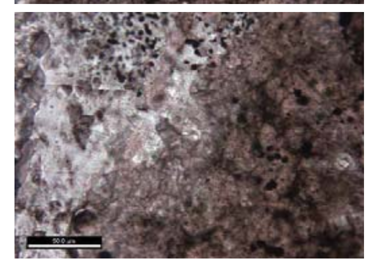

Fractures

several vertical, fluid-escape or pressure-solution structures contain organic material and clay

Additional Comments

organic material disseminated throughout the matrix as stringers or in seams

SWIR

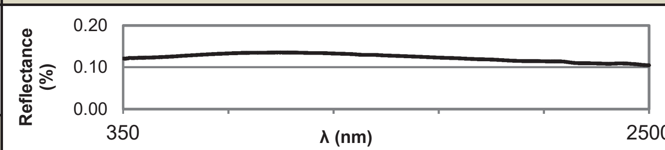

XRD

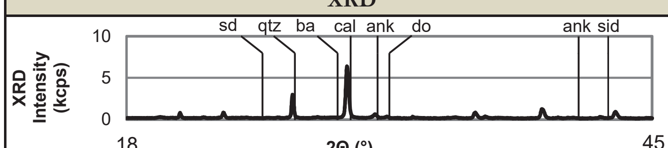

Stable Isotope (‰)

$\delta^{13}C_{VPDB}$	$\delta^{18}O_{VPDB}$
1A Sample	
-5.19	-10.84
1B Sample	
-4.75	-10.27
2A Sample	
-5.08	-11.31
2B Sample	
-5.39	-10.96

Well ID: Strong #1 (31107264660000)	Formation: Oatka Creek Formation	Sample ID:	3-TCC1
Location: Tioga, NY	Member: Cherry Valley Member	Depth (ft):	4187.25

Fossiliferous, baritic, calcareous mudstone

Matrix Composition and Microtexture

matrix is primarily calcite micrite

Diagenetic Minerals

mictric matrix comprises primarily calcite with select portions of the sample including barite; minor framboidal pyrite associated with degraded organic material

Diagenetic Texture and Fabric

neomorphism of calcite microspar destroys original depositional textures, creating a chunky or coarsely crystalline texture

Detrital Grains and Fossils

fossil fragments are recrystallized and typically include calcite overgrowths or replacement by barite

Additional comments:

images are SE (left) and BSE (right) pairs

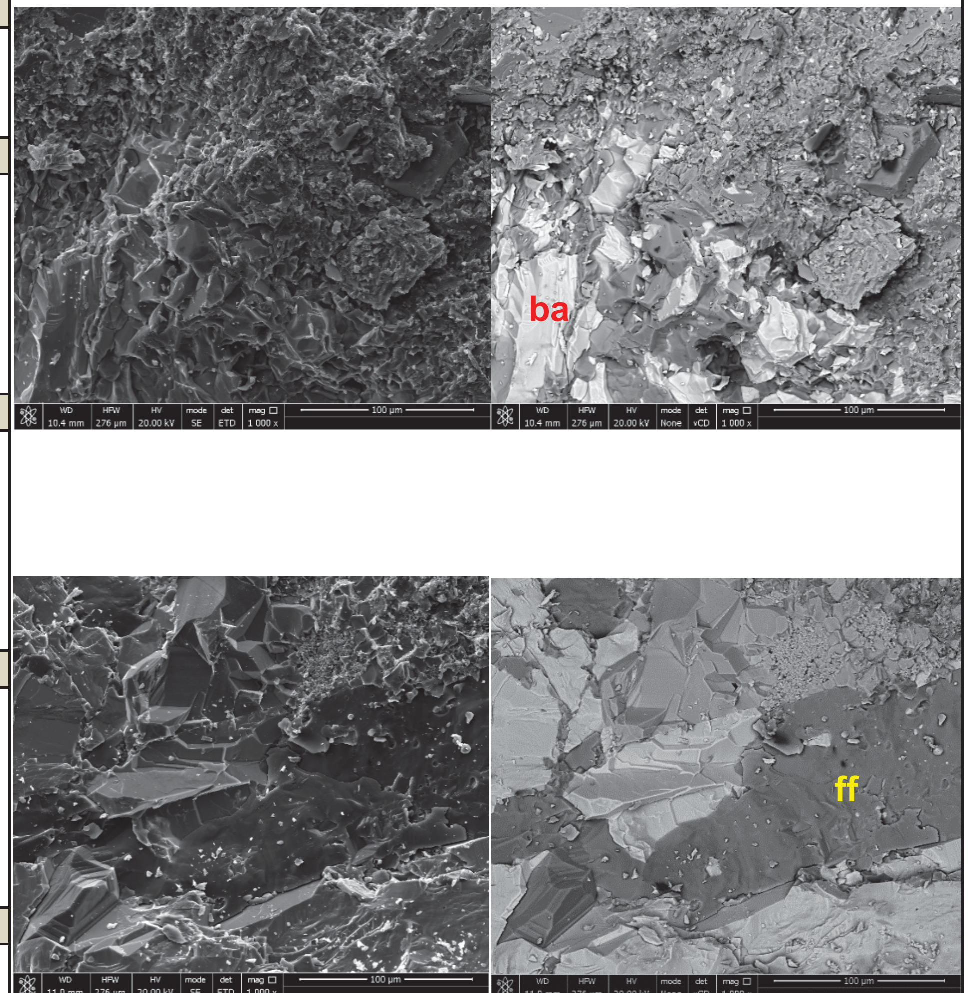

Well ID: Strong #1 (31107264660000)	Formation: Oatka Creek Formation	Sample ID:	13-TCC2
Location: Tioga, NY	Member: Cherry Valley Member	Depth (ft):	4187.33

Baritic wackestone

Matrix Composition

mostly calcite with lesser dolomite cement, some illitic clay

Texture

weakly laminated, mostly defined by aligned shell fragments

Diagenetic Minerals

final calcite overprint recrystallized other carbonate stages; calcite rhombs were likely originally dolomite; dolomite rhombs scattered throughout, with fewer ferroan dolomite; sparse zones of dolomite cement; euhedral barite with ferroan calcite rims fill vugs

Allochemical or Detrital Grains

fine quartz silt disseminated throughout

Fossils

mostly dacryoconarids (Styliolina) with several larger nondescript fragments; rare phosphatic bone fragments; brachiopods stretch width of thin section along bedding

Fractures

organic-filled, irregular, anastomosing stylolite and ferroan calcite-healed fracture oriented normal to bedding

Additional Comments

organic material-filled vertical seam as well as disseminated in the matrix

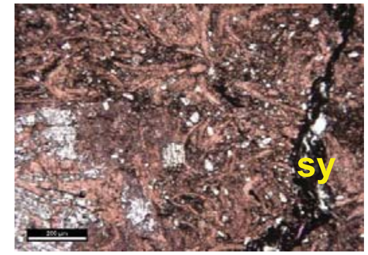

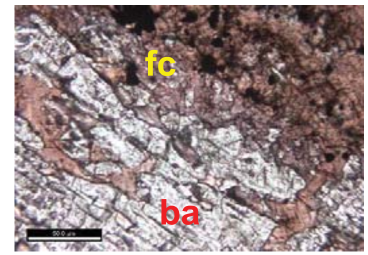

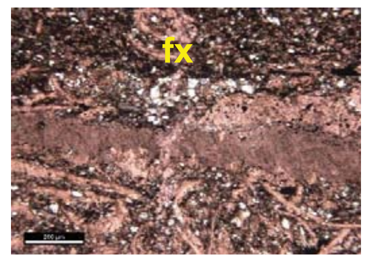

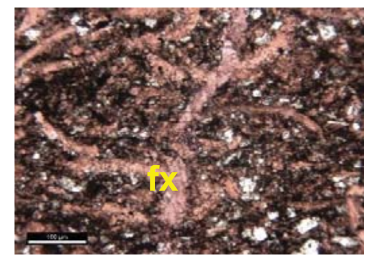

SWIR

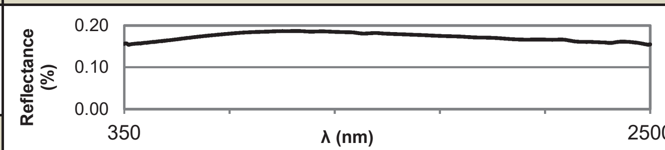

XRD

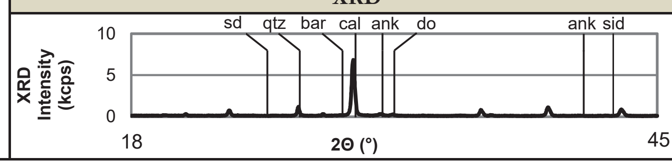

Stable Isotope

$\delta^{13}C_{VPDB}$ (‰)	$\delta^{18}O_{VPDB}$ (‰)
1A Sample	
N/A	N/A
1B Sample	
N/A	N/A

Well ID: Strong #1 (31107264660000)	Formation: Oatka Creek Formation	Sample ID:	13-TCC2
Location: Tioga, NY	Member: Cherry Valley Member	Depth (ft):	4187.33

Baritic wackestone

Matrix Composition and Microtexture

calcite cementation or recrystallization lends to a nonlaminated microtexture

Diagenetic Minerals

calcite is the most abundant diagenetic mineral; barite is crystallized in select portions of the calcareous matrix or as a replacement in fossils; minor dolomite rhombohedra are crystallized within the matrix; framboidal pyrite is associated with organic material

Diagenetic Texture and Fabric

neomorphism of micrite gives the matrix a homogenized or massive appearance; minor clays have been deformed and cemented; bladed barite crystals are replaced by calcite, as they were likely the result of an earlier diagenetic stage

Detrital Grains and Fossils

fossils are likely recrystallized based of their crystalline appearance, though are not compositionally distinct enough from calcite in the matrix; textural relationship between the matrix and detritus or fossils has largely been overprinted

Additional comments:

images are SE (top) and BSE (bottom) pair

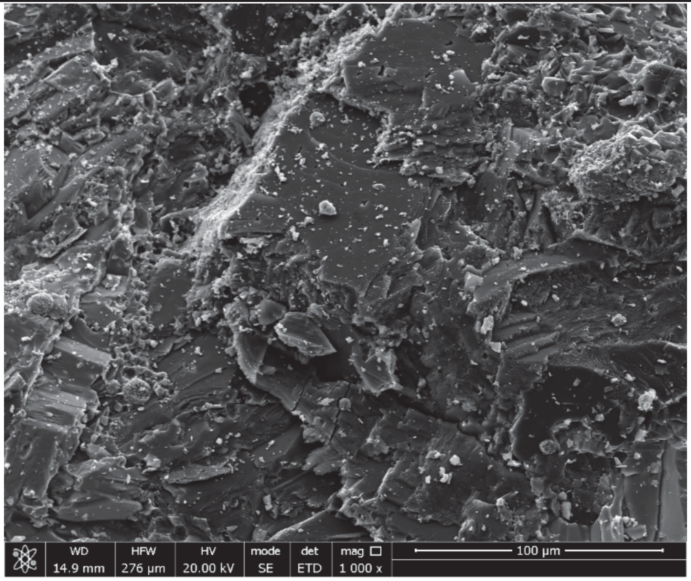

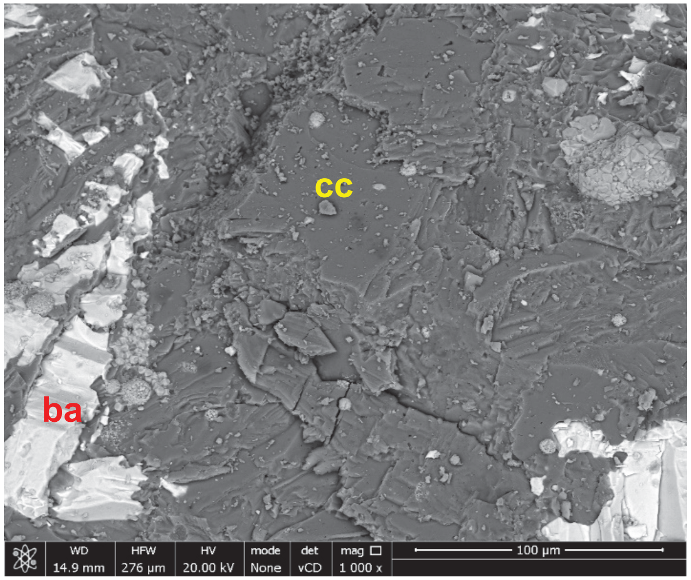

Well ID: Strong #1 (31107264660000)	Formation: Oatka Creek Formation	Sample ID:	14-TCC2
Location: Tioga, NY	Member: Cherry Valley Member	Depth (ft):	4187.50

Baritic wackestone

Matrix Composition

mostly calcite with minor dolomite cementation, minor illitic clay content

Texture

weakly laminated in the bottom portion, defined by fossil fragments aligning with bedding

Diagenetic Minerals

calcite cements or recrystallizes a majority of this sample; minor dolomitization in the bottom portion, mostly seen as rhombohedra; several calcite-healed fractures that terminate in the nodule (upper); euhedral barite in pores at bottom

Allochemical or Detrital Grains

minor quartz silt disseminated in the lower portion

Fossils

dacryoconarids (Styliolina) with several larger brachiopod fragments, phosphatic bone fragments, ostracods, and perhaps gastropods; many fragments are recrystallized and are not identifiable

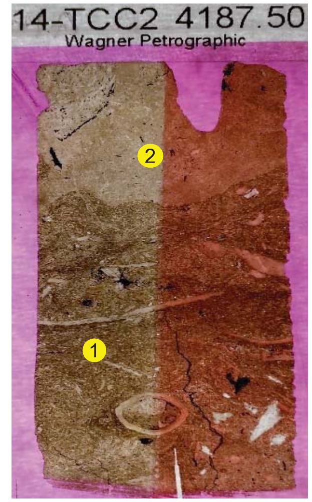

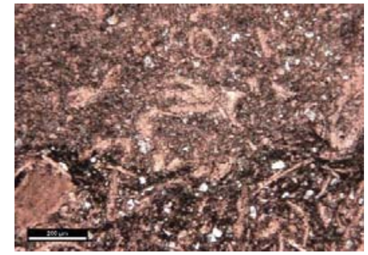

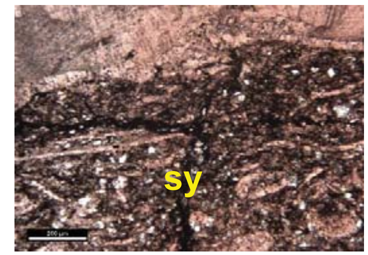

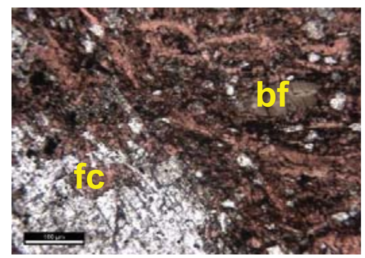

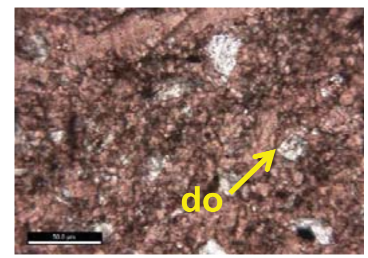

Fractures

irregular, anastomosing stylolites are filled with organic material and propagate normal to bedding, though they do not dissect larger fossils or heavily cemented portions such as the top of the thin section

Additional Comments

organic material-filled seams or fluid-escape structures and disseminated throughout matrix

SWIR

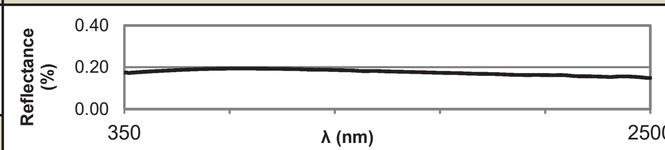

XRD

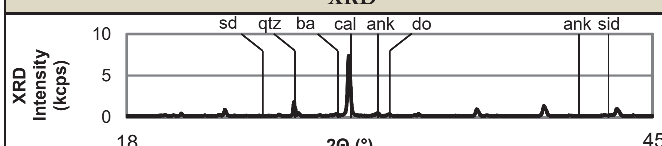

Stable Isotope (‰)

$\delta^{13}C_{VPDB}$	$\delta^{18}O_{VPDB}$
1A Sample	
-4.06	-9.40
1B Sample	
-3.54	-7.92
2A Sample	
-10.13	-8.86
2B Sample	
-10.35	-9.34

Well ID: Strong #1 (31107264660000)	Formation: Oatka Creek Formation	Sample ID:	14-TCC2
Location: Tioga, NY	Member: Cherry Valley Member	Depth (ft):	4187.50

Baritic wackestone

Matrix Composition and Microtexture

calcite cementation or recrystallization lends to a nonlaminated microtexture

Diagenetic Minerals

calcite is the most abundant diagenetic mineral; barite is crystallized in select portions of the calcareous matrix as a cement; minor dolomite rhombohedra are crystallized within the matrix; framboidal pyrite is associated with organic material

Diagenetic Texture and Fabric

neomorphism of micrite gives the matrix a homogenized or massive appearance; minor clays have been deformed and cemented; barite cement is partially replaced by calcite in many areas

Detrital Grains and Fossils

fossils are likely recrystallized based of their crystalline appearance, though are not compositionally distinct enough from calcite in the matrix; textural relationship between the matrix and detritus or fossils has largely been overprinted

Additional comments:

images are SE (top) and BSE (bottom) pair

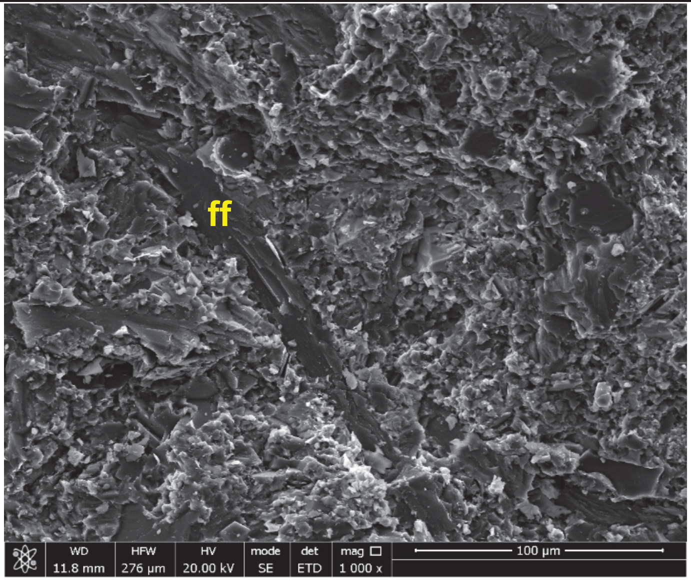

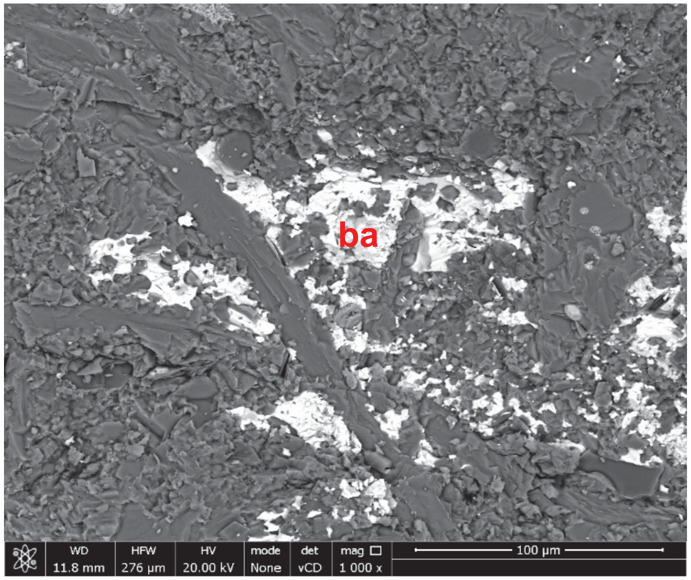

Well ID: Strong #1 (31107264660000)	**Formation: Oatka Creek Formation**	**Sample ID:**	**15-TCC2**
Location: Tioga, NY	**Member: Cherry Valley Member**	**Depth (ft):**	**4187.71**

Felted, baritic, calcareous/dolomitic mudstone

Matrix Composition

mostly calcite with minor dolomite and remaining illitic clay

Texture

weakly laminated; primary depositional fabric largely destroyed by diagenesis

Diagenetic Minerals

final stage of diagenesis likely calcite cementation; bladed barite crystals are mostly replaced by calcite; calcite nearest organic-filled seams are slightly ferroan; minor dolomite cements and rhombs

Allochemical or Detrital Grains

minor quartz silt scattered throughout clay-rich laminae

Fossils

dacryoconarids (Styliolina) with less common, more robust shell fragments; phosphatic bone fragments

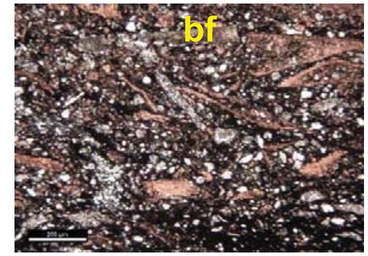

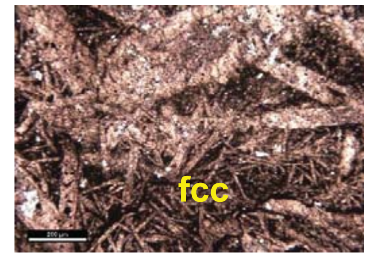

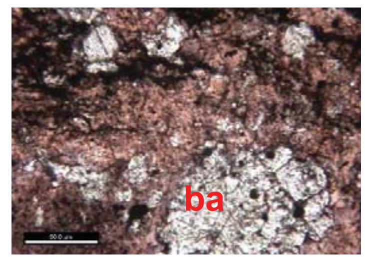

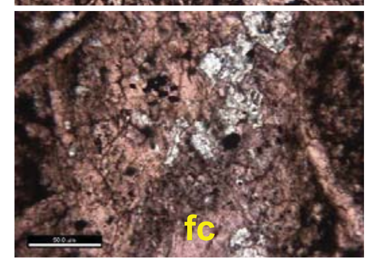

Fractures

abundant organic material-filled fractures or seams

Additional Comments

barite crystal size dependent on surrounding rock - clay-rich and OM-rich seams have the larger barite crystals, some of which have not been entirely replaced by calcite yet, while fossil-rich portions have smaller crystals

SWIR

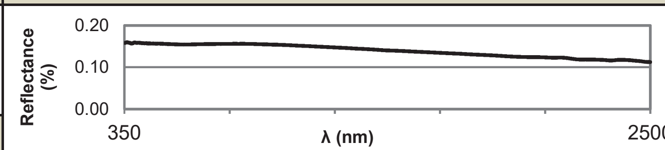

XRD

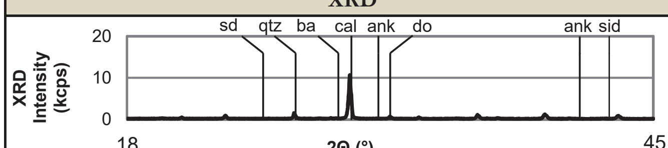

Stable Isotope (‰)

$\delta^{13}C_{VPDB}$	$\delta^{18}O_{VPDB}$
1A Sample	
-7.67	-8.45
1B Sample	
N/A	N/A
2A Sample	
-8.57	-7.71
2B Sample	
-7.79	-7.78

Well ID: Strong #1 (31107264660000)	Formation: Oatka Creek Formation	Sample ID:	15-TCC2
Location: Tioga, NY	Member: Cherry Valley Member	Depth (ft):	4187.71

Felted, baritic, calcareous/dolomitic mudstone

Matrix Composition and Microtexture

matrix is primarily calcite micrite with minor baritic and pyritic cements

Diagenetic Minerals

micritic matrix comprises primarily calcite with select portions of the sample including barite; minor framboidal pyrite is generally associated with degraded organic material; barite is crystallized in select portions of the calcareous matrix as a cement

Diagenetic Texture and Fabric

neomorphism of calcite microspar destroys original depositional textures, creating a chunky or coarsely crystalline texture

Detrital Grains and Fossils

fossil fragments are recrystallized and typically include calcite overgrowths or replacement by barite

Additional comments:

images are SE (left) and BSE (right) pair

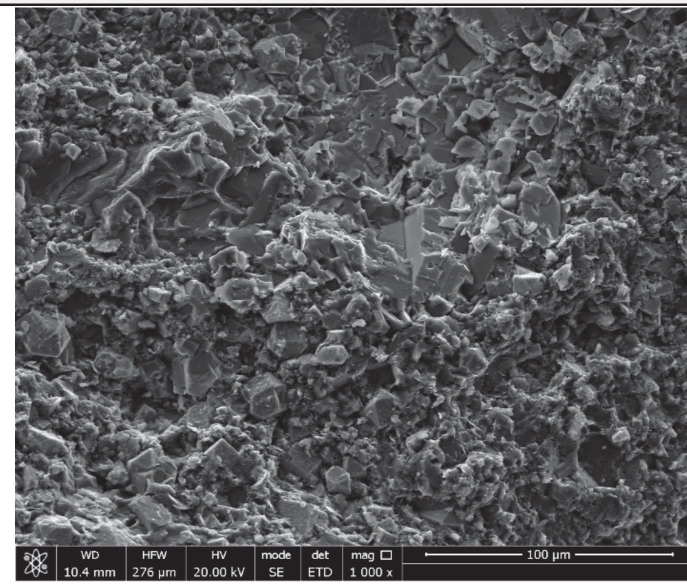

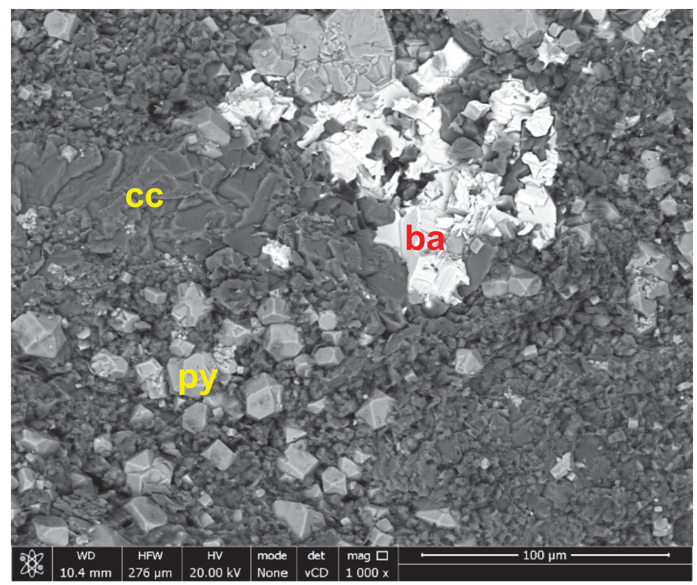

Well ID: Strong #1 (31107264660000)	Formation: Oatka Creek Formation	Sample ID:	16-TCC2
Location: Tioga, NY	Member: Cherry Valley Member	Depth (ft):	4187.83

Organic, pyritic, argillaceous mudstone

Matrix Composition

illitic clays almost exclusively comprise the matrix composition

Texture

well-laminated; minor disruptions are caused by pyrite crystallization; aligned organic particles/solids, mica flakes

Diagenetic Minerals

widespread pyrite crystallization, both blocky and framboidal forms; no apparent cements, mostly clay and organic material

Allochemical or Detrital Grains

silt-sized quartz at <5%

Fossils

nondescript shell fragments

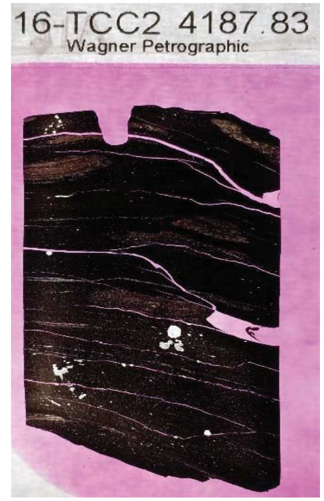

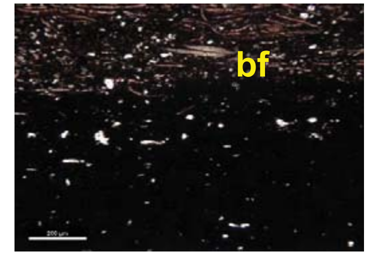

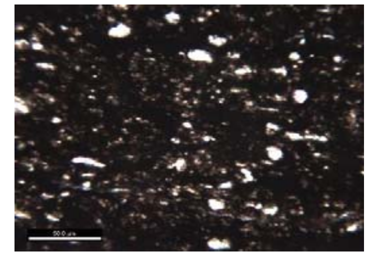

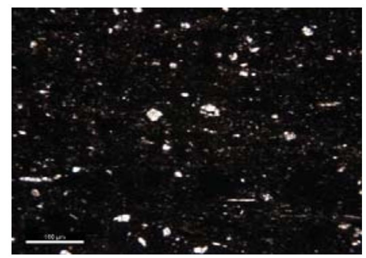

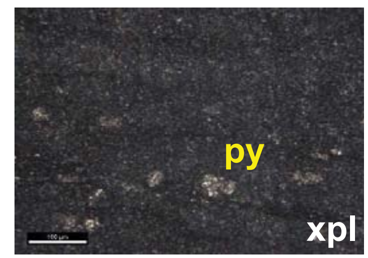

Fractures

none

Additional Comments

rare clumps of mica and silt grains, may be some sort of clast or flocculated bunch that has been cemented; elongate organic particles or solids are disseminated throughout, often in association with pyrite; matrix is nearly opaque, indicating a significant of kerigenous residue

SWIR

N/A

XRD

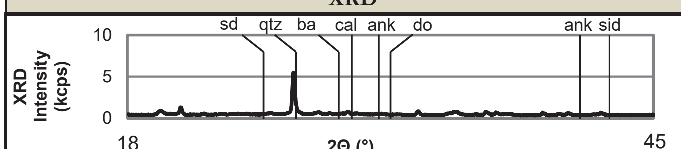

Stable Isotope

	$\delta^{13}C_{VPDB}$ (‰)	$\delta^{18}O_{VPDB}$ (‰)
1A Sample	N/A	N/A
1B Sample	N/A	N/A

Well ID: Strong #1 (31107264660000)	**Formation: Oatka Creek Formation**	**Sample ID:**	**17-TCC2**
Location: Tioga, NY	**Member: Cherry Valley Member**	**Depth (ft):**	**4188.00**

Felted, microsparitic crystalline carbonate

Matrix Composition

calcite

Texture

non-laminated; recrystallization, which appears to include several phases, has destroyed depositional fabric

Diagenetic Minerals

final phase is calcite cementation; pebbly texture of calcite matrix/cement suggests one time dolomitization; calcite replacement of felted or bladed barite in top fractured zones; minor ferroan calcite and dolomite near or within the organic- and clay-filled seam.

Allochemical or Detrital Grains

no detrital grains

Fossils

dacryoconarids (nondescript); collapsed organic-walled cysts

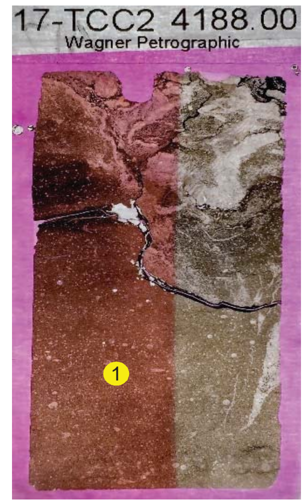

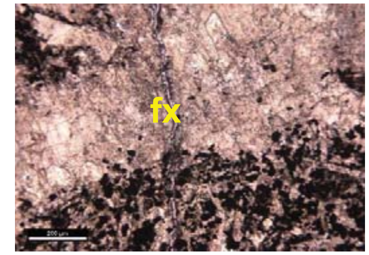

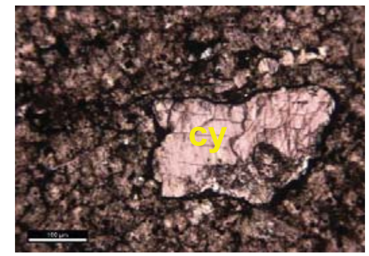

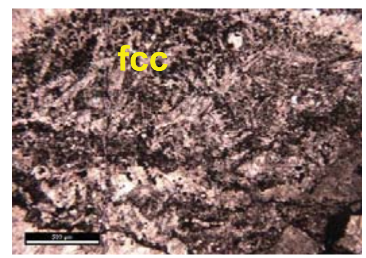

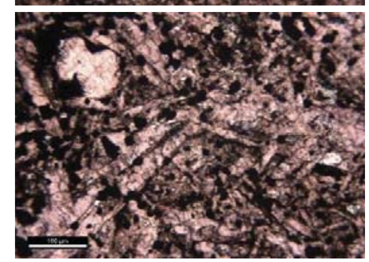

Fractures

organic material, clay, and pyrite fill undulating seam or fracture; organic-rich seam also includes calcite-filled fractures that run parallel to seam; fragments of either calcite fossils or allochems in fractured portion

Additional Comments

SWIR

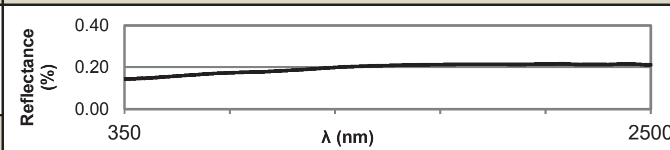

XRD

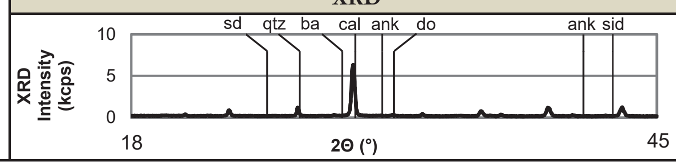

Stable Isotope

	$\delta^{13}C_{VPDB}$ (‰)	$\delta^{18}O_{VPDB}$ (‰)
1A Sample	-10.43	-7.82
1B Sample	-10.03	-9.34

Well ID: Strong #1 (31107264660000)	**Formation: Oatka Creek Formation**	**Sample ID:**	**17-TCC2**
Location: Tioga, NY	**Member: Cherry Valley Member**	**Depth (ft):**	**4188.00**

Felted, microsparitic crystalline carbonate

Matrix Composition and Microtexture

matrix is primarily calcite micrite with minor baritic and pyritic cements

Diagenetic Minerals

micritic matrix comprises primarily calcite with select portions of the sample including barite; minor framboidal pyrite is generally associated with degraded organic material; barite is crystallized in select portions of the calcareous matrix as a cement

Diagenetic Texture and Fabric

neomorphism of calcite microspar destroys original depositional textures, creating a coarsely crystalline texture

Detrital Grains and Fossils

fossil fragments are recrystallized

Additional comments:

images are SE (left) and BSE (right) pairs

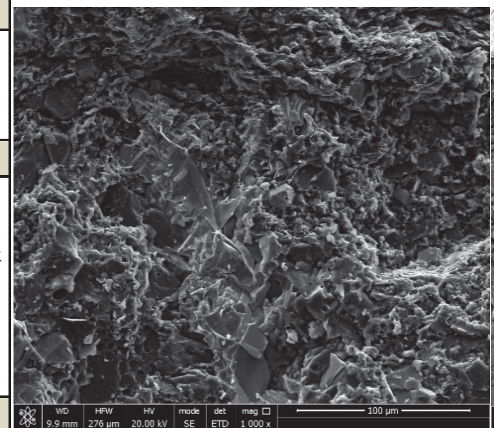

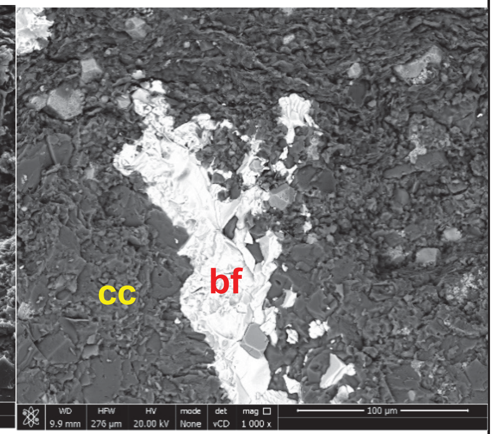

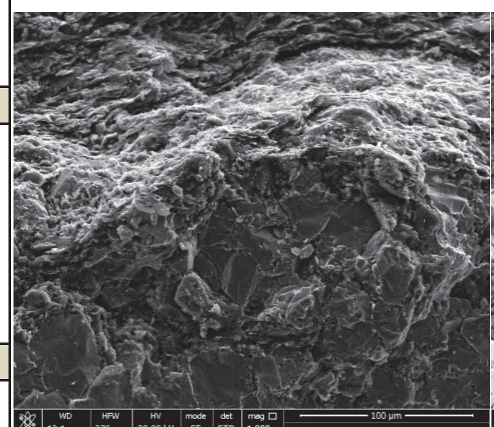

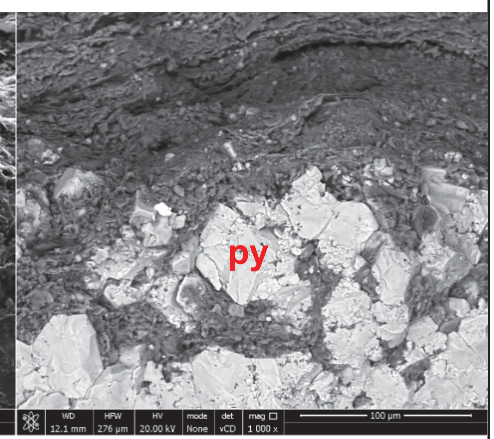

Well ID: Strong #1 (31107264660000) | **Formation: Oatka Creek Formation** | **Sample ID:** 4-TCC1

Location: Tioga, NY | **Member: Cherry Valley Member** | **Depth (ft):** 4188.25

Felted, baritic, microsparitic crystalline carbonate

Matrix Composition

calcite plus some other euhedral, bladed barite; minor clays

Texture

moderately laminated; microsparitic in calcareous laminations, then calcite fills in around some of the barite blades

Diagenetic Minerals

calcite, barite are the major cements; barite is mostly euhedral and felted or bladed; apparent that calcite and fossils have undergone several stages of recrystallization; lost stage of dolomitization may be covered by calcite, determined by the pebbly texture of the cement

Allochemical or Detrital Grains

none

Fossils

heavily recrystallized, nondescript fossils; collapsed organic-walled cysts

Fractures

none

Additional Comments

organic material restricted to select laminae that are horizontal, one of which is where the slide broke across the middle; spindly, wandering, and whispy organic particles; kerigenous residue abundant as the sparry portions are quite dark and often lined with organic material between crystals; organic material often associated with spherical fossils

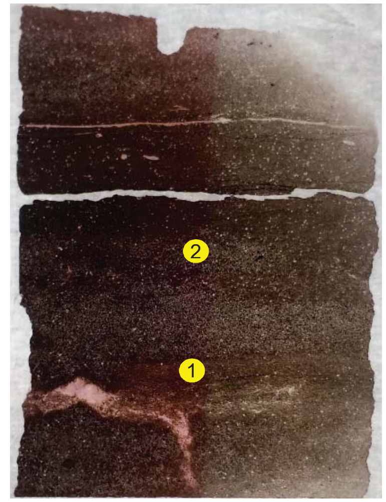

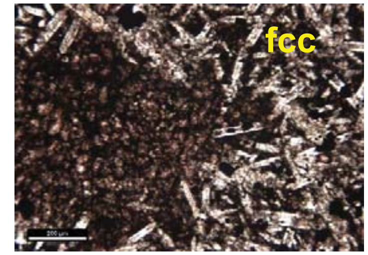

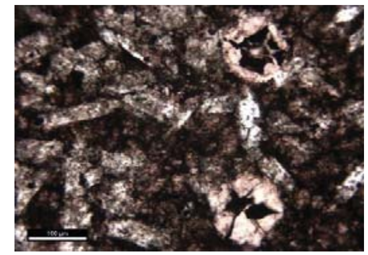

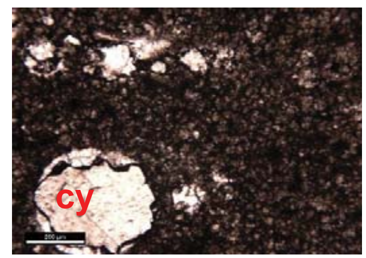

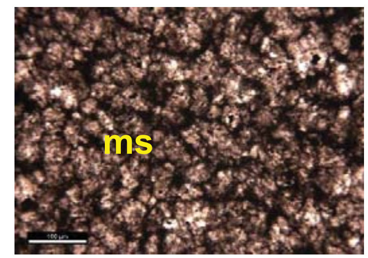

SWIR

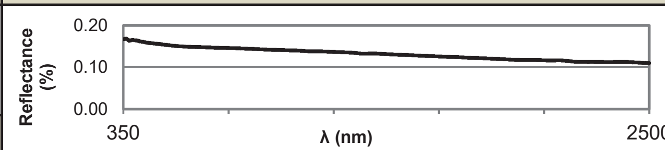

XRD

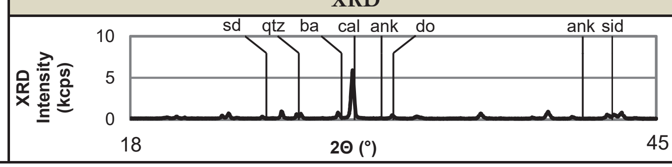

Stable Isotope (‰)

$\delta^{13}C_{VPDB}$	$\delta^{18}O_{VPDB}$
1A Sample	
-10.38	-8.78
1B Sample	
-10.51	-7.42
2A Sample	
N/A	N/A
2B Sample	
N/A	N/A

Well ID: Strong #1 (31107264660000)	Formation: Oatka Creek Formation	Sample ID:	4-TCC1
Location: Tioga, NY	Member: Cherry Valley Member	Depth (ft):	4188.25

Felted, baritic, microsparitic crystalline carbonate

Matrix Composition and Microtexture

calcite cementation or recrystallization lends to a nonlaminated microtexture

Diagenetic Minerals

calcite is the most abundant diagenetic mineral; bladed barite pervasive throughout the rock; pyrite crystallized within barite blades

Diagenetic Texture and Fabric

neomorphism of micrite gives the matrix a homogenized or massive appearance; minor clays have been deformed and cemented; bladed barite crystals are replaced by calcite

Detrital Grains and Fossils

fossils barely recognizable against the calcite matrix; textural relationship between the matrix and detritus or fossils has largely been overprinted

Additional comments:

images are SE (top) and BSE (bottom) pair

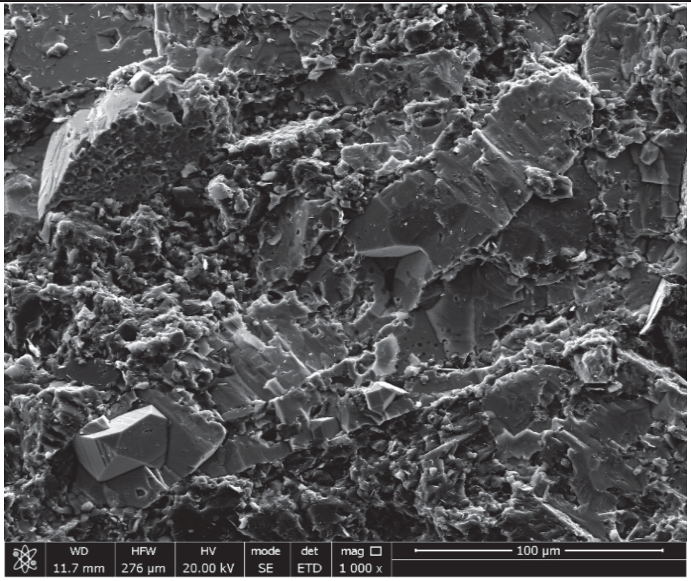

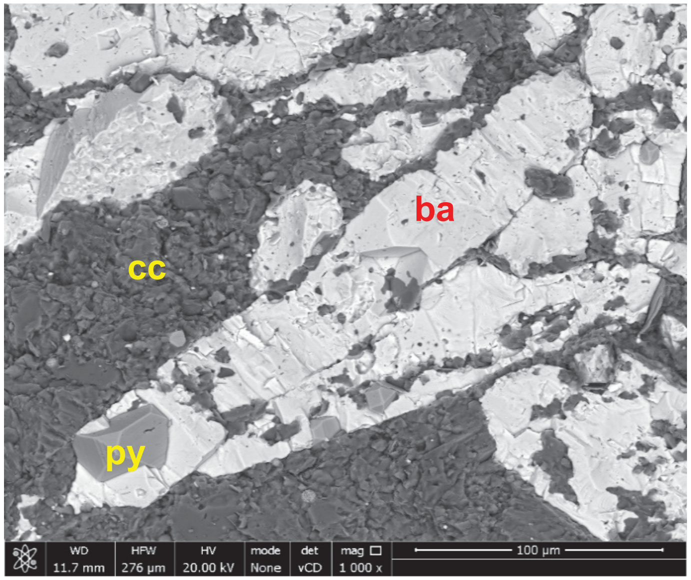

Well ID: Strong #1 (31107264660000)	**Formation: Oatka Creek Formation**	**Sample ID:**	**5-TCC1**
Location: Tioga, NY	**Member: Cherry Valley Member**	**Depth (ft):**	**4188.50**

Organic, pyritic, argillaceous mudstone

Matrix Composition

illitic clays almost exclusively comprise the matrix composition

Texture

well-laminated; aligned organic particles/solids, mica flakes; rare clumps of mica and silt grains

Diagenetic Minerals

widespread pyrite crystallization, both blocky and framboidal forms; no visible cements; may be some authigenic kaolinite

Allochemical or Detrital Grains

silt-sized quartz at <5%

Fossils

few nondescript shell fragments

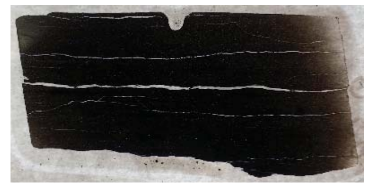

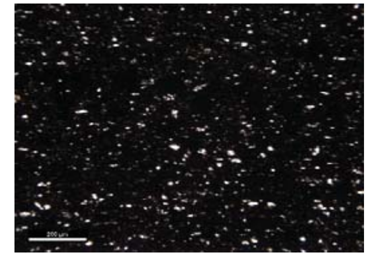

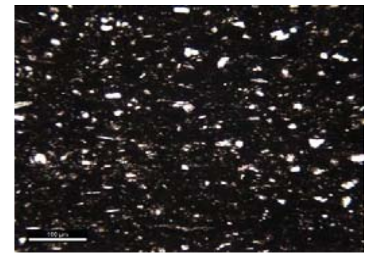

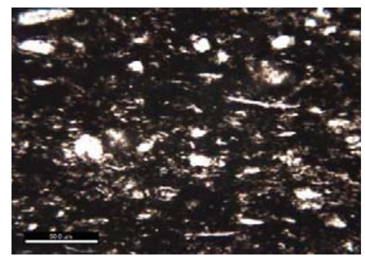

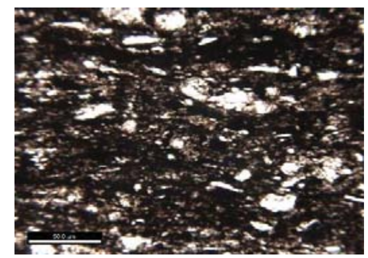

Fractures

none

SWIR

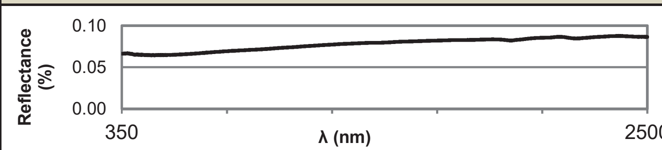

Additional Comments

elongate particles or solids are disseminated throughout, often in association with pyrite; matrix is nearly opaque, indicating a significant amount of kerigenous residue

XRD

N/A

Stable Isotope

	$\delta^{13}C_{VPDB}$ (‰)	$\delta^{18}O_{VPDB}$ (‰)
1A Sample	N/A	N/A
1B Sample	N/A	N/A

Well ID: Strong #1 (31107264660000)	**Formation: Oatka Creek Formation**	**Sample ID:**	**18-TCC2**
Location: Tioga, NY	**Member: Cherry Valley Member**	**Depth (ft):**	**4188.50**

Microsparitic crystalline carbonate

Matrix Composition

calcite

Texture

non-laminated with several larger recrystallized fossils defining a subtle bedding plane

Diagenetic Minerals

final phase is calcite cementation; pebbly texture of calcite matrix/cement suggests one time dolomitization; calcite replacement of bladed barite in top fractured zones; minor ferroan calcite and dolomite near or within the organic- and clay-filled seam; blocky barite fills pores

Allochemical or Detrital Grains

none

Fossils

all fossils are highly recrystallized and do not retain many identifying components; larger fragments are likely bivalves; collapsed organic-walled cysts

Fractures

organic-rich seam also includes calcite-filled fractures that run parallel to each other; fractures at top have larger calcite crystal size than rest of sample

Additional Comments

organic material fills seam or fracture runs normal to bedding, in some cases propagating parallel to bedding

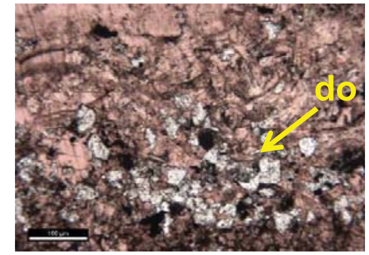

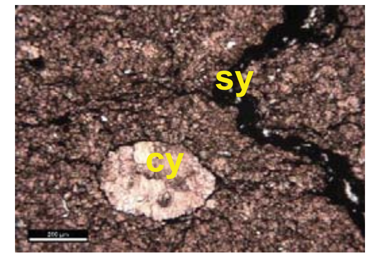

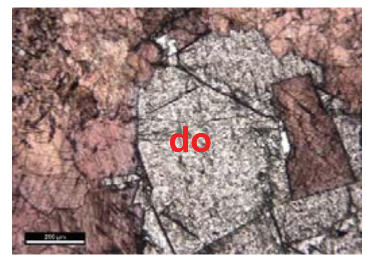

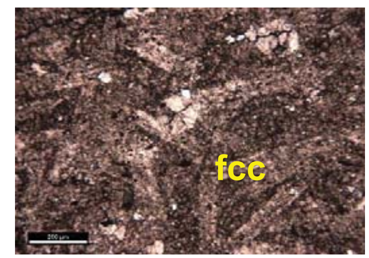

SWIR

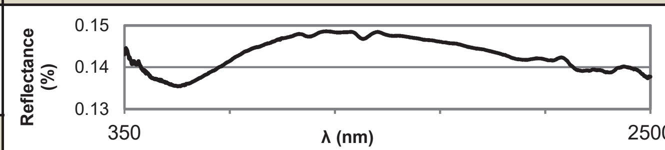

XRD

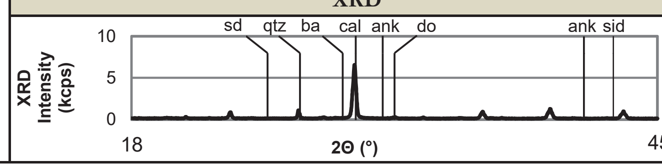

Stable Isotope (‰)

$\delta^{13}C_{VPDB}$	$\delta^{18}O_{VPDB}$
1A Sample	
-14.46	23.90
1B Sample	
-14.46	26.10
2A Sample	
N/A	N/A
2B Sample	
N/A	N/A

Well ID: Strong #1 (31107264660000)	Formation: Oatka Creek Formation	Sample ID:	18-TCC2
Location: Tioga, NY	Member: Cherry Valley Member	Depth (ft):	4188.50

Microsparitic crystalline carbonate

Matrix Composition and Microtexture

calcite cementation or recrystallization lends to a nonlaminated microtexture

Diagenetic Minerals

calcite is the most abundant diagenetic mineral; rare barite cement

Diagenetic Texture and Fabric

neomorphism of micrite gives the matrix a homogenized or massive appearance; minor clays have been deformed and cemented

Detrital Grains and Fossils

fossils barely recognizable against the calcite matrix; textural relationship between the matrix and detritus or fossils has largely been overprinted; in a rare instance, an organic-walled cyst is observed

Additional comments:

images are SE (top) and BSE (bottom) pair

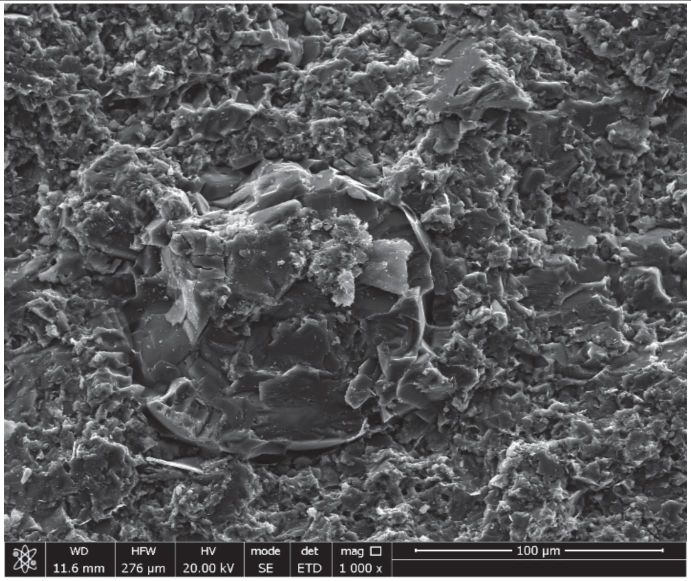

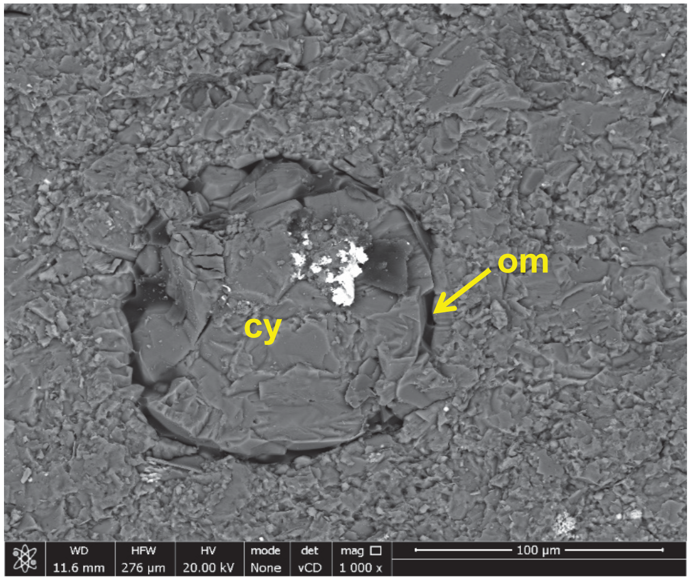

Well ID: Strong #1 (31107264660000)	Formation: Oatka Creek Formation	Sample ID:	19-TCC2
Location: Tioga, NY	Member: Cherry Valley Member	Depth (ft):	4188.75

Microsparitic crystalline carbonate

Matrix Composition

calcite

Texture

non-laminated with several larger recrystallized fossils defining a subtle bedding plane

Diagenetic Minerals

final phase is calcite cementation; pebbly texture of calcite matrix/cement suggests one time dolomitization; calcite replaces bladed barite in top fractured zone; minor retained dolomite; minor ferroan calcite and dolomite associated with organic- and clay-filled seams; blocky barite occludes pores

Allochemical or Detrital Grains

none

Fossils

nondescript fossils with dolomitic tests and calcite fill; bivalves or gastropods fragments; collapsed organic-walled cysts

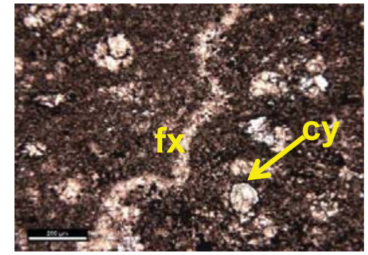

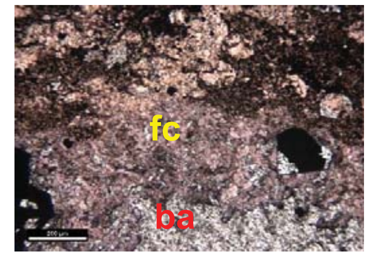

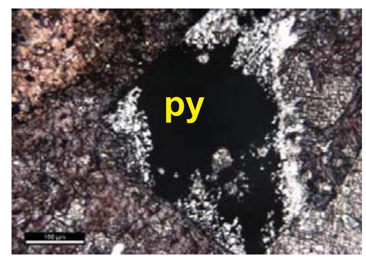

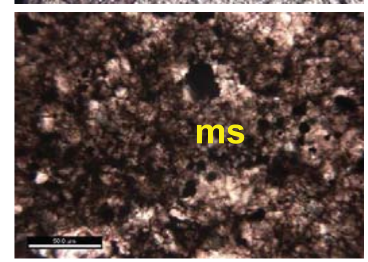

Fractures

organic material fills seam or fracture runs normal to bedding, propagating parallel to bedding; fractures at bottom have larger calcite crystal, with haloes of barite at center, ferroan calcite, and then calcite on the edge

Additional Comments

SWIR

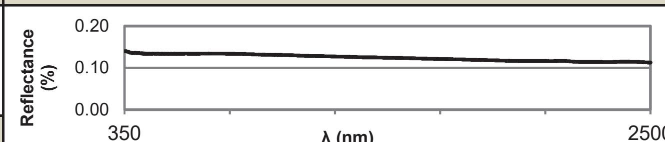

XRD

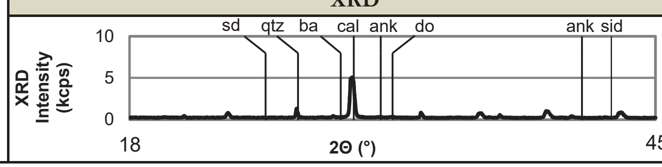

Stable Isotope

$\delta^{13}C_{VPDB}$ (‰)	$\delta^{18}O_{VPDB}$ (‰)
1A Sample	
-9.51	-10.80
1B Sample	
-9.18	-10.71

Well ID: Strong #1 (31107264660000)	**Formation: Oatka Creek Formation**	**Sample ID:**	**19-TCC2**
Location: Tioga, NY	**Member: Cherry Valley Member**	**Depth (ft):**	**4188.75**

Microsparitic crystalline carbonate

Matrix Composition and Microtexture

calcite cementation or recrystallization lends to a nonlaminated microtexture

Diagenetic Minerals

calcite is the most abundant diagenetic mineral; rare barite cement; pyritic and baritic seam runs normal to bedding

Diagenetic Texture and Fabric

neomorphism of micrite gives the matrix a homogenized or massive appearance; minor clays have been deformed and cemented

Detrital Grains and Fossils

fossils barely recognizable against the calcite matrix; textural relationship between the matrix and detritus or fossils has largely been overprinted

Additional comments:

images are SE (top) and BSE (bottom) pair

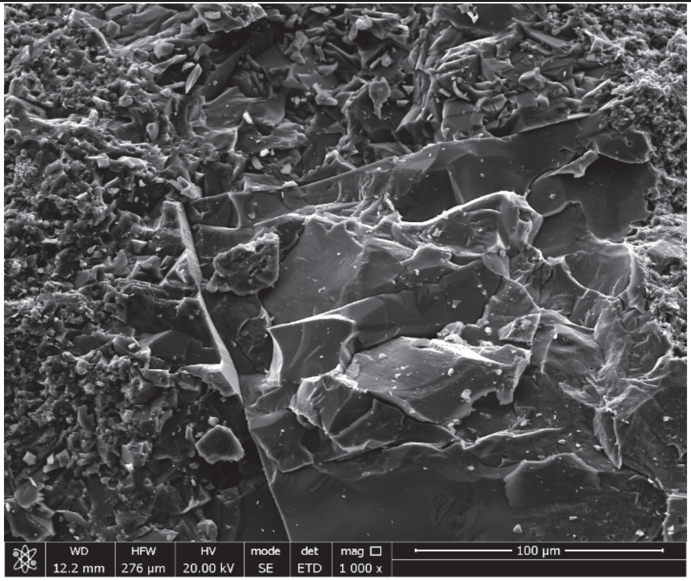

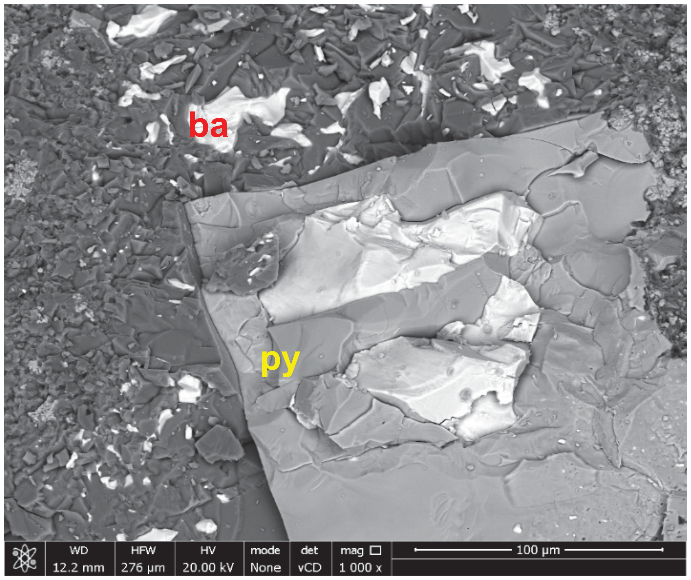

Well ID: Strong #1 (31107264660000)	**Formation: Oatka Creek Formation**	**Sample ID:**	**6-TCC1**
Location: Tioga, NY	**Member: Cherry Valley Member**	**Depth (ft):**	**4189.00**

Felted, microsparitic crystalline carbonate

Matrix Composition

calcite is the dominant cement with comparatively minor portions of the matrix comprising illitic clays and organic material

Texture

chaotic texture with original depositional horizons disturbed during compaction

Diagenetic Minerals

diagenetic calcite stages of fossil recrystallization and replacement of bladed barite; original crystallographic orientations in fossils have been overprinted; minor glauconite; calcite that forms void-fill or cements is slightly higher in iron

Allochemical or Detrital Grains

little siliciclastic detritus; allochemical grains are disseminated throughout, likely from the breakup of some of the more robust fossils fragments

Fossils

despite the abundance of fossils, recrystallization renders identification difficult; possible algal mats; thin-shelled fragments in the small mudstone section at the top; collapsed organic-walled cysts

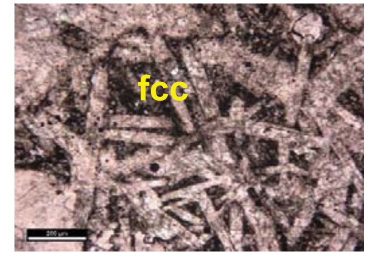

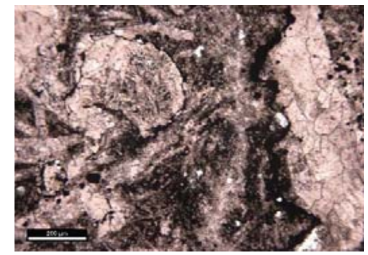

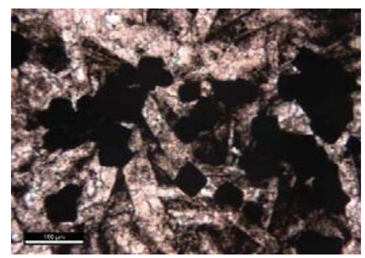

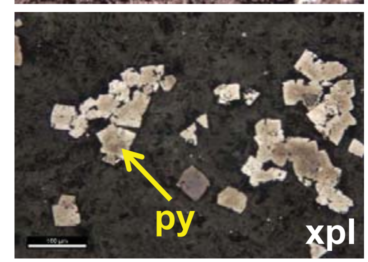

Fractures

organic- and clay-filled seams that likely formed during compaction; subvertical and bedding-parallel fractures are filled predominantly with calcite, though several of the horizontal fractures have dolomite

Additional Comments

organic material present throughout the sample in the matrix along with clays; stringers or kerigenous residue, not particles/solids

SWIR

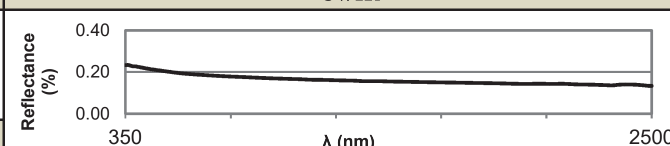

XRD

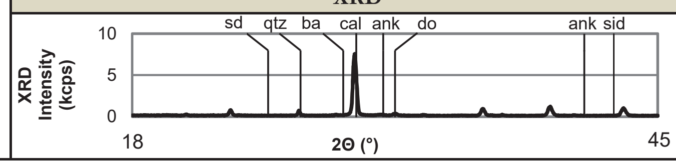

Stable Isotope (‰)

$\delta^{13}C_{VPDB}$	$\delta^{18}O_{VPDB}$
1A Sample	
-11.74	-7.32
1B Sample	
-9.68	-8.30
2A Sample	
-9.02	-5.62
2B Sample	
N/A	N/A

Well ID: Strong #1 (31107264660000)	Formation: Oatka Creek Formation	Sample ID:	6-TCC1
Location: Tioga, NY	Member: Cherry Valley Member	Depth (ft):	4189.00

Felted, microsparitic crystalline carbonate

Matrix Composition and Microtexture

calcite cementation or recrystallization lends to a nonlaminated microtexture

Diagenetic Minerals

calcite is the most abundant diagenetic mineral; pyrite is common and not generally associated with organic material

Diagenetic Texture and Fabric

neomorphism of micrite gives the matrix a homogenized or massive appearance; minor clays have been deformed and cemented; felted texture not apparent at this scale

Detrital Grains and Fossils

none observed

Additional comments:

images are SE (top) and BSE (bottom) pair

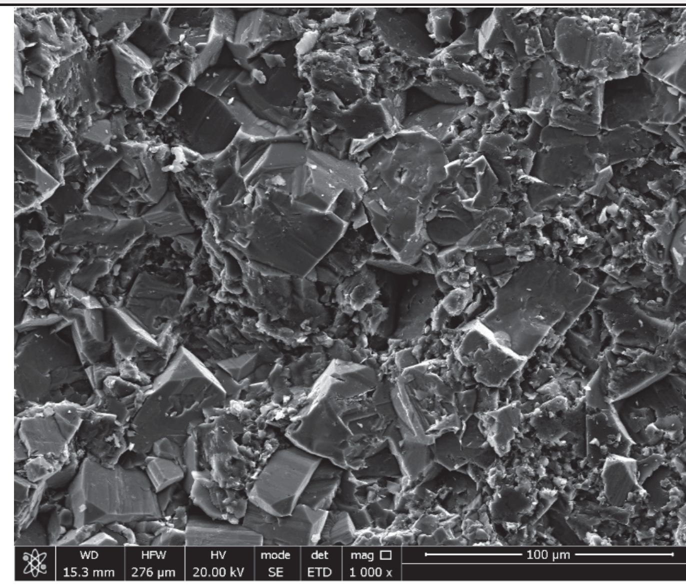

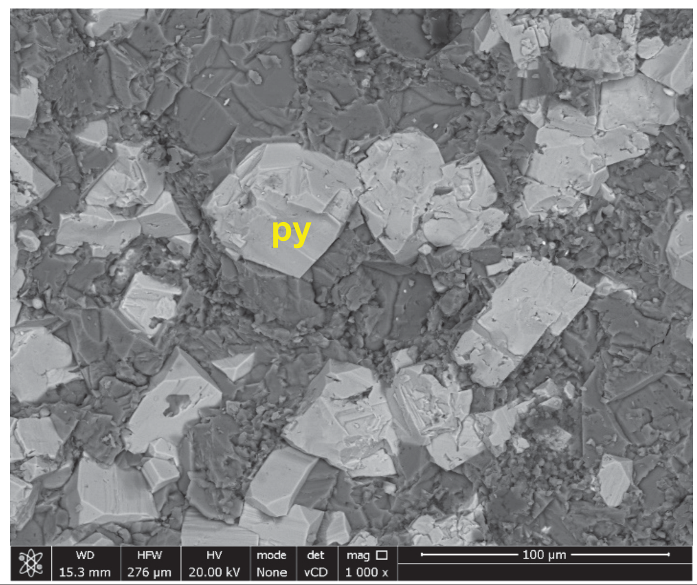

Well ID: Strong #1 (31107264660000)	Formation: Union Springs Formation	Sample ID:	20-TCC2
Location: Tioga, NY	Member: Bakoven Member	Depth (ft):	4189.21

Argillaceous mudstone

Microsparitic crystalline carbonate

Matrix Composition

calcite in nodule (bottom), illitic clays in mudstone (top)

Texture

weakly laminated - depositional structures remain but fabric is largely overprinted by calcite cement

Diagenetic Minerals

final stage calcite replacement of dolomite and barite in the wackestone; septarian cracks propagate normal to bedding and are filled with ferroan calcite; sphalerite also fill void-space in these cracks; minor dolomite remains in wackestone and is typically within the same laminations

Allochemical or Detrital Grains

quartz silt and micas in the upper portion

Fossils

algal mats separate the mudstone (top) from the wackestone (bottom), but they may be early fractures; few elongate shell fragments; collapsed organic-walled cysts

Fractures

top of nodule is cracked perpendicular to bedding

Additional Comments

organic material common in mudstone portion as a matrix component, and is likely disseminated throughout wackestone as rims to the calcite crystals (fine amorphous kerogen)

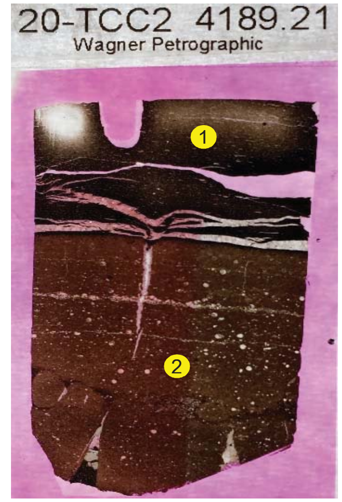

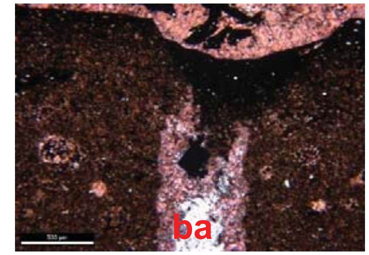

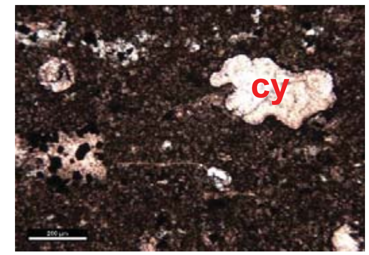

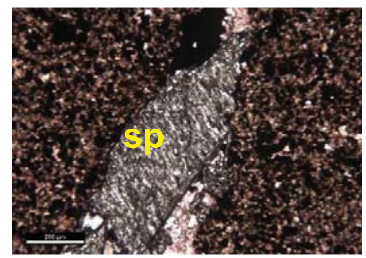

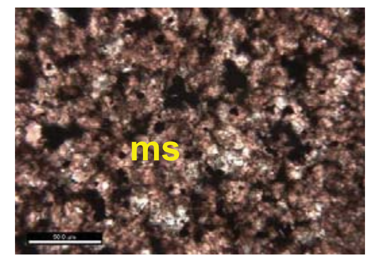

SWIR

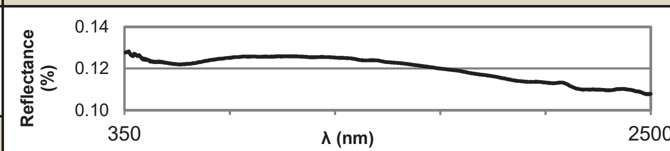

XRD

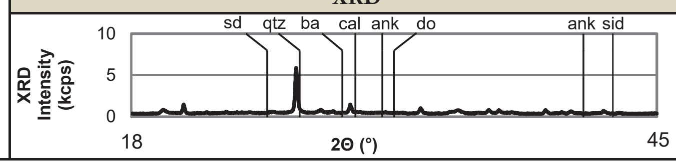

Stable Isotope (‰)	
$\delta^{13}C_{VPDB}$	$\delta^{18}O_{VPDB}$
1A Sample	
N/A	N/A
1B Sample	
N/A	N/A
2A Sample	
N/A	N/A
2B Sample	
-12.00	-9.28

Well ID: Strong #1 (31107264660000)	Formation: Union Springs Formation	Sample ID:	21-TCC2
Location: Tioga, NY	Member: Bakoven Member	Depth (ft):	4189.42

Argillaceous mudstone

Matrix Composition

illitic clay and calcite or dolomite cement

Texture

well-laminated by the alignment of fossils, organics, clays, micas; few zones of disruption

Diagenetic Minerals

calcite in fossils is largely original in composition, protected by organic linings of the fossil fragments with a halo of calcite in the matrix; subtle calcite or dolomite cement may be masked by organic material

Allochemical or Detrital Grains

fair amount of detrital grains, mostly quartz, compared with other mudstones in the suite; 5-7.5%

Fossils

nondescript, elongate shell fragments, likely dacryoconarids, disseminated throughout

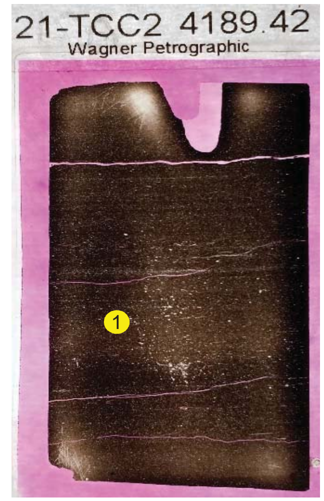

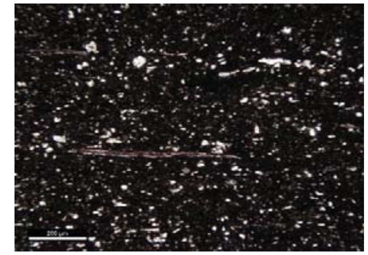

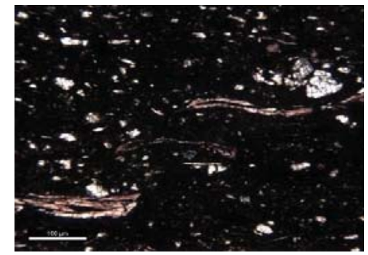

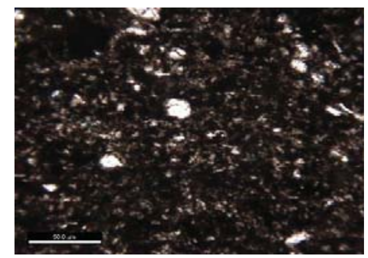

Fractures

none

Additional Comments

widely disseminated organic particles/solids and kerigenous residues

SWIR

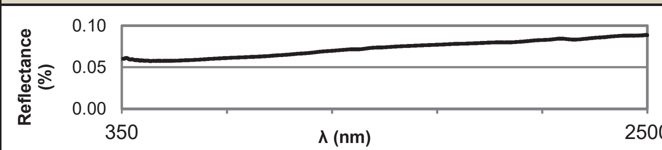

XRD

N/A

Stable Isotope

	$\delta^{13}C_{VPDB}$ (‰)	$\delta^{18}O_{VPDB}$ (‰)
1A Sample	N/A	N/A
1B Sample	N/A	N/A

Well ID: Strong #1 (31107264660000)	Formation: Union Springs Formation	Sample ID:	7-TCC1
Location: Tioga, NY	Member: Bakoven Member	Depth (ft): 41	4189.67

Fossiliferous, organic, pyritic, argillaceous mudstone

Matrix Composition
illitic clay and calcite cementation to an unknown extent, as seen in thinner/wedged parts of the slide

Texture
well-laminated by the alignment of fossils, organics, clays, micas; zones of disruption

Diagenetic Minerals
calcite in fossils is largely original in composition, protected by organic linings of the dacryoconarids with haloes of calcite; pyrite is common; pyrite growths have deformed surrounding matrix, causing cracks that have been filled by calcite

Allochemical or Detrital Grains
few detrital grains, mostly quartz which appear to be preferentially deposited, perhaps biotic influence, in silt-rich laminae

Fossils
nondescript dacryoconarids disseminated throughout

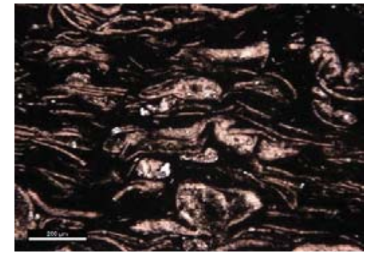

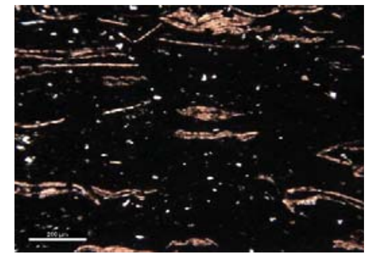

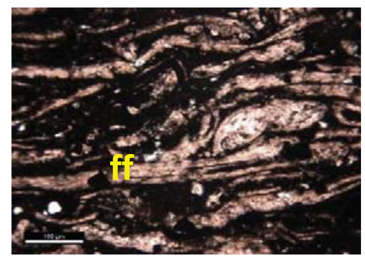

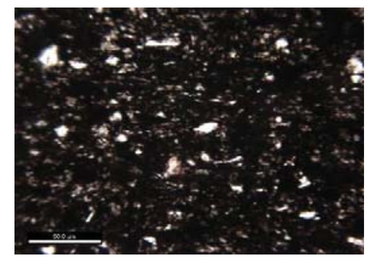

Fractures
none

Additional Comments
widely disseminated organic particles/solids and kerigenous residues, lending to an opaque matrix

SWIR
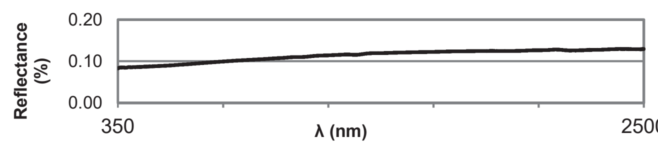

XRD
N/A

Stable Isotope

	$\delta^{13}C_{VPDB}$ (‰)	$\delta^{18}O_{VPDB}$ (‰)
1A Sample	N/A	N/A
1B Sample	N/A	N/A

Well ID: Strong #1 (31107264660000)	Formation: Union Springs Formation	Sample ID:	22-TCC2
Location: Tioga, NY	Member: Bakoven Member	Depth (ft): 41	4189.88

Argillaceous mudstone

Matrix Composition

illitic clay cemented by calcite

Texture

well-laminated by the alignment of fossils, organics, clays, micas; more disruption in microfabric

Diagenetic Minerals

calcite in fossils is largely original in composition, protected by organic linings of the dacryoconarids with a halo of calcite; subtle calcite or dolomite cement may be masked by organic material

Allochemical or Detrital Grains

fair amount of detrital grains, mostly quartz, compared with other mudstones in the suite; 5-7.5%

Fossils

nondescript dacryoconarids disseminated throughout, generally fractured into pieces and flattened

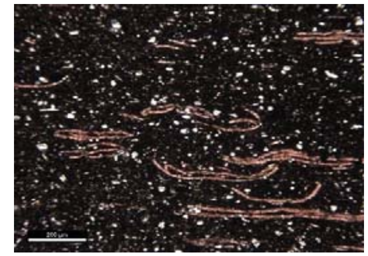

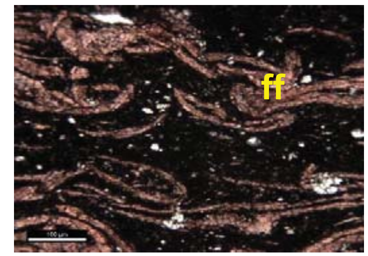

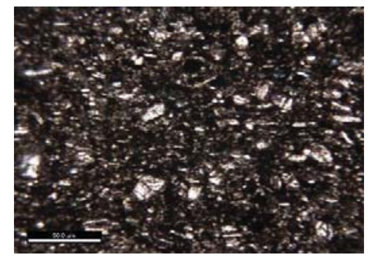

Fractures

none

Additional Comments

widely disseminated organic particles/solids and kerigenous residues

SWIR

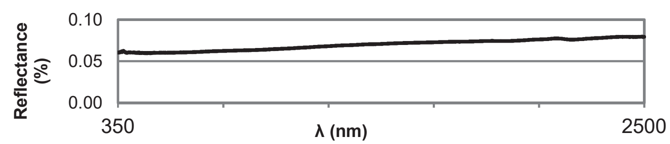

XRD

N/A

Stable Isotope

	$\delta^{13}C_{VPDB}$ (‰)	$\delta^{18}O_{VPDB}$ (‰)
1A Sample	N/A	N/A
1B Sample	-4.44	-8.68

Well ID: Strong #1 (31107264660000)	**Formation: Union Springs Formation**	**Sample ID:**	**8-TCC1**
Location: Tioga, NY	**Member: Bakoven Member**	**Depth (ft):**	**4190.33**

Argillaceous mudstone

Matrix Composition

Mostly illitic clay with minor silica cements in upper half; mix of calcite and clay in lower half

Texture

well-laminated texture; aligned fossils, organic particles, and micas; texture is disrupted by a bivalve that is filled with pyrite

Diagenetic Minerals

calcite cement generally more ferroan than that in fossils; close association of ferroan calcites and adjacent pyritization; pyritic lamination right below pyrite nodules includes fossils and calcite cement; minor dolomite rhombs disseminated throughout and some have ferroan dolomite rims

Allochemical or Detrital Grains

10-15% quartz silt throughout much of the sample, maybe less in the lower fossiliferous half; upper half includes nondescript allochems that are composed of an iron-rich calcite

Fossils

lower half contains abundant nondescript dacryoconarids; few fossils in upper half; phosphatic bone fragments; pyrite-filled, millimeter-scale bivalve structure; phosphatic spore-like features at top; collapsed organic-walled cysts

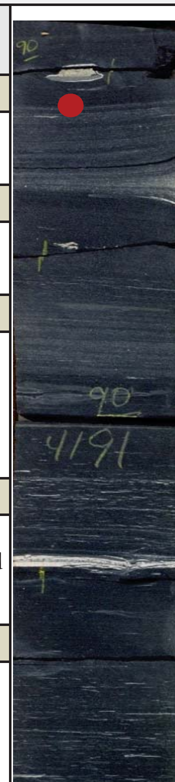

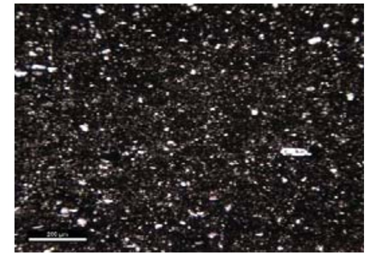

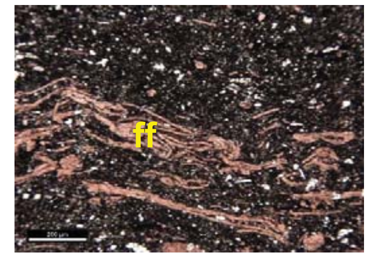

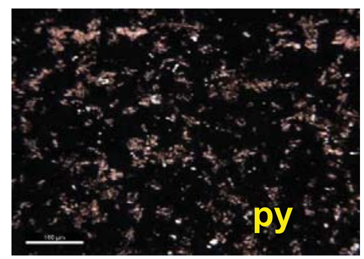

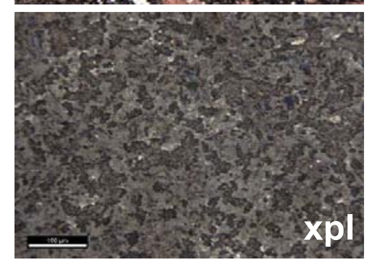

Fractures

none

Additional Comments

disseminated kerigenous residues apparent in darker areas; organic stringers/particles/solids common throughout clay-rich portions

SWIR

N/A

XRD

N/A

Stable Isotope

	$\delta^{13}C_{VPDB}$ (‰)	$\delta^{18}O_{VPDB}$ (‰)
1A Sample	N/A	N/A
1B Sample	N/A	N/A

Well ID: Strong #1 (31107264660000)
Location: Tioga, NY

Formation: Union Springs Formation
Member: Bakoven Member

Sample ID: 9-TCC1
Depth (ft): 4190.58

Pyritic, argillaceous mudstone

Matrix Composition

illitic clay-rich in bottom half, calcareous and dolomitic in top half

Texture

well-laminated, though bedding has been significantly disrupted by nodular pyrite

Diagenetic Minerals

microspar and framboidal pyrite is pervasive throughout the nodular bed; framboidal pyrite common throughout the clay-rich portions; dolomite with ferroan dolomite rims scattered throughout in small quantities

Allochemical or Detrital Grains

10-15% quartz silt throughout the bottom, clay-rich portion, with sparse detritus in the upper half; distinct rounded fossil fragments/allochems composed of ferroan calcite with ferroan dolomite rims in nodular bed

Fossils

abundant dacryoconarids in the upper portion (above the nodular bed); upper half fossils difficult to identify due to recrystallization; collapsed organic-walled cysts

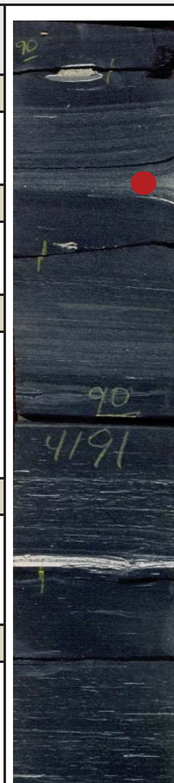

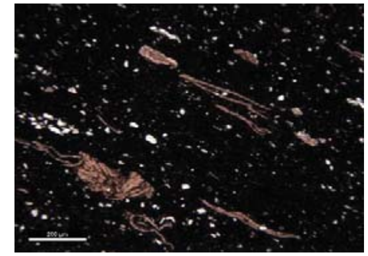

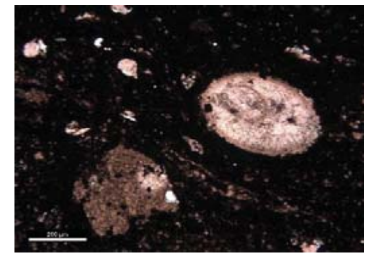

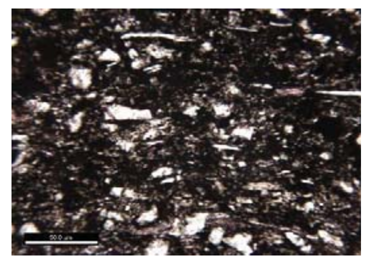

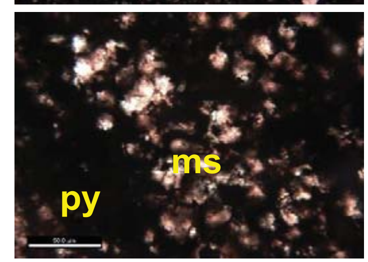

Fractures

pyritized fractures, presumably formed prior to lithification, cut across the calcareous bed that the nodule is normal to bedding; these fractures do not continue into bedding above or below this lamination

Additional Comments

organic stringers/particles/solids throughout the matrix; likely kerigenous residues disseminated

SWIR

N/A

XRD

N/A

Stable Isotope

	$\delta^{13}C_{VPDB}$ (‰)	$\delta^{18}O_{VPDB}$ (‰)
1A Sample	N/A	N/A
1B Sample	N/A	N/A

Well ID: Strong #1 (31107264660000)	Formation: Union Springs Formation	Sample ID:	23-TCC2
Location: Tioga, NY	Member: Bakoven Member	Depth (ft):	4191.17

Fossiliferous, argillaceous mudstone

Matrix Composition

illitic clay with minor calcite cement

Texture

well-laminated as defined by aligned algal mats that stretch the width of the thin section and fossil fragments

Diagenetic Minerals

dolomite replaces or comprises some of the algal mats; subtle calcite overprinting throughout, though clays remain the dominant matrix material

Allochemical or Detrital Grains

minor quartz silt

Fossils

few nondescript dacryoconarid shells that are fractured and compacted; stacked algal mats, with the largest at the bottom of the section

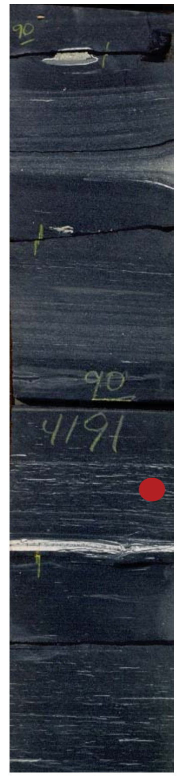

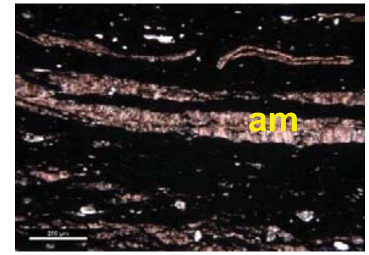

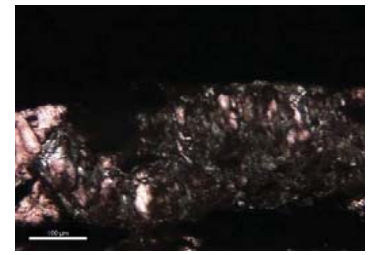

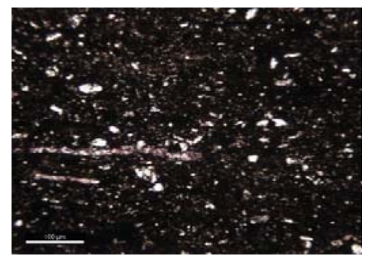

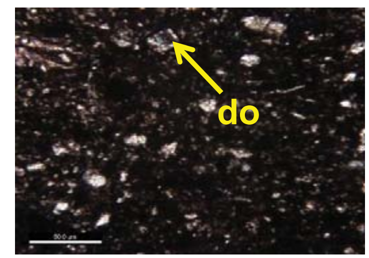

Fractures

none

Additional Comments

organic material distributed throughout the matrix as fine, amorphous, kerigenous residues, lending to a dark matrix

SWIR

N/A

XRD

N/A

Stable Isotope	
$\delta^{13}C_{VPDB}$ (‰)	$\delta^{18}O_{VPDB}$ (‰)
1A Sample	
N/A	N/A
1B Sample	
N/A	N/A

Well ID: EGSP NY-4 / Valley Vista View 1 (31101152680000)	Formation: Oatka Creek Formation	Sample ID:	NY4-20
Location: Steuben, NY	Member: Cherry Valley Member	Depth (ft):	3844.45

Microsparitic wackestone

Matrix Composition

calcite

Texture

poorly laminated; recrystallization has overprinted depositional textures; calcite matrix is microsparitic, equigranular, and xenotopic

Diagenetic Minerals

calcite is the predominant diagenetic mineral; other minerals are not present by visual estimation; calcite overgrowths on fossils are overprinted but distinguishable

Allochemical or Detrital Grains

none

Fossils

nondescript fossil fragments are not identifiable due to calcite recrystallization; collapsed organic-walled cysts

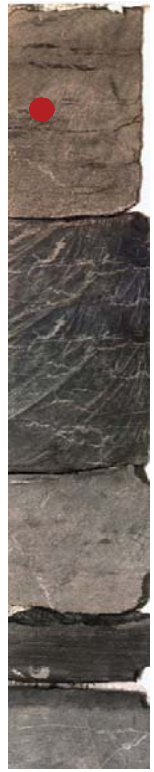

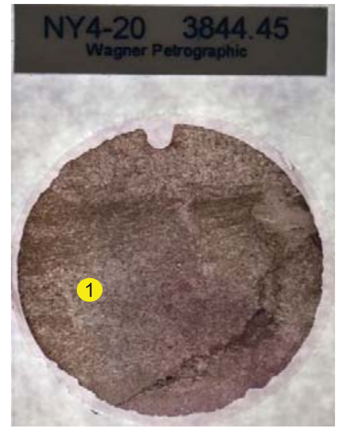

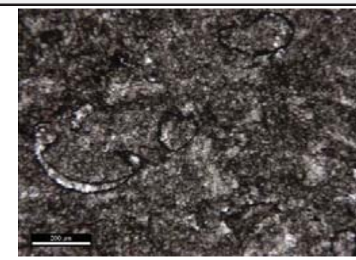

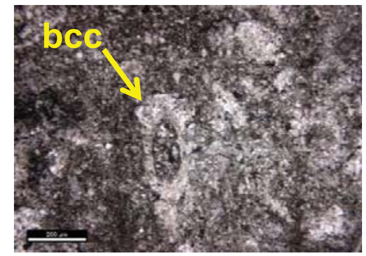

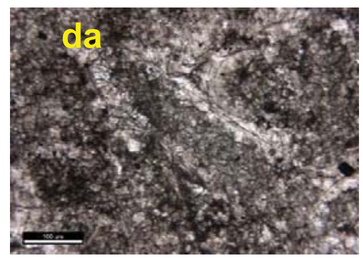

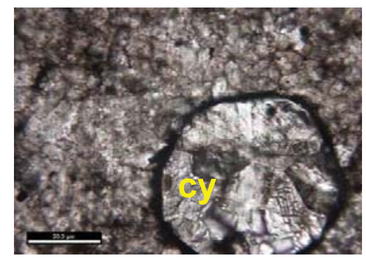

Fractures

none

Additional Comments

organic material outlines fossils and preserves the larger calcite crystals within

SWIR

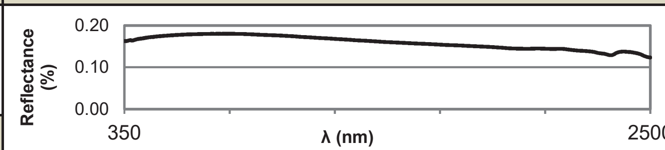

XRD

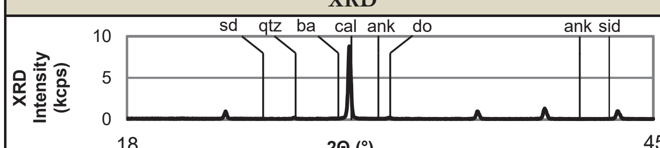

Stable Isotope

$\delta^{13}C_{VPDB}$ (‰)	$\delta^{18}O_{VPDB}$ (‰)
1A Sample	
-12.07	-0.76
1B Sample	
-11.71	-1.98

Well ID: EGSP NY-4 / Valley Vista View 1 (31101152680000)	Formation: Oatka Creek Formation	Sample ID:	NY4-20
Location: Steuben, NY	Member: Cherry Valley Member	Depth (ft):	3844.45

Microsparitic wackestone

Matrix Composition and Microtexture

massive matrix microtexture caused by calcite recrystallization; calcite is primary matrix constituent with minor clays and dolomite

Diagenetic Minerals

calcite, dolomite, pyrite

Diagenetic Texture

calcite crystallized as a micron-scale microspar or single-crystal replacement of fossils; interface between calcite cement and matrix components, such as fossils or detritus, is tight

Pore Structure

equant pores are hosted within calcite cement; minor organic-hosted porosity

Depositional Fabric

depositional fabrics are generally overprinted by diagenesis

Additional comments:

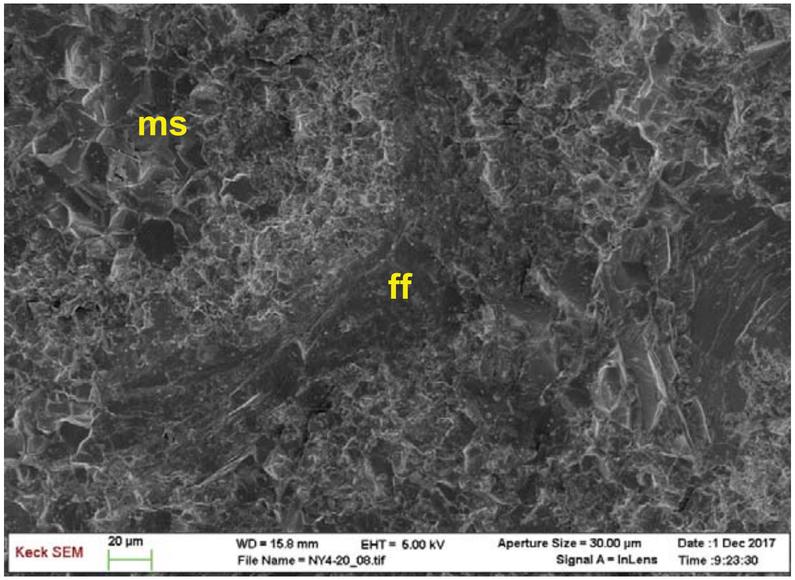

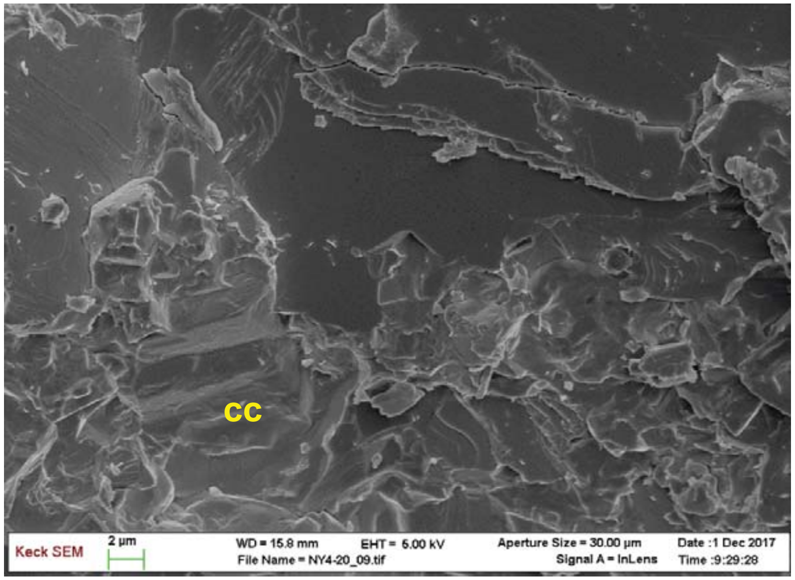

Well ID: EGSP NY-4 / Valley Vista View 1 (31101152680000)	Formation: Oatka Creek Formation	Sample ID:	NY4-22
Location: Steuben, NY	Member: Cherry Valley Member	Depth (ft):	3844.70

Felted, microsparitic crystalline carbonate

Matrix Composition

calcite

Texture

no depositional textures present; felted calcite is recrystallized, likely from original bladed, nodular barite; calcite is inequigranular and xenotopic

Diagenetic Minerals

calcite is the dominant diagenetic mineral; previous stages of carbonate diagenesis are overprinted by calcite; phase that originally produced the felted texture - likely barite - is entirely replaced by calcite; calcite in fractures display separate crystal texture, resembling the elongate prisms in some bivalves

Allochemical or Detrital Grains

none

Fossils

spherical and elongate tests, likely dacryoconarids

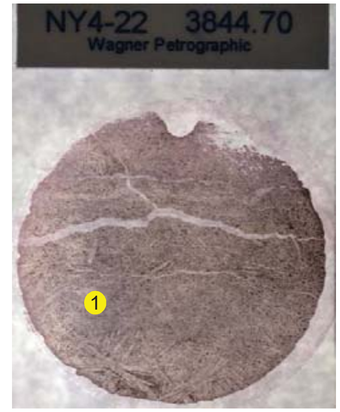

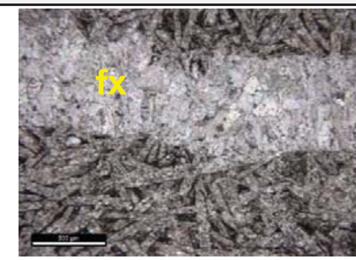

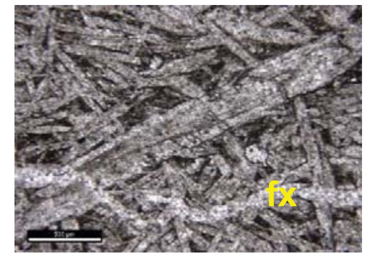

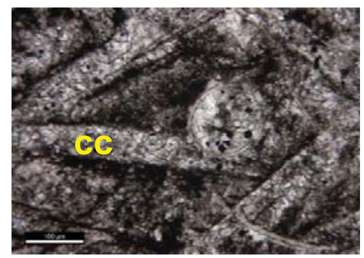

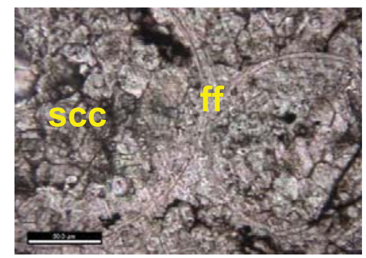

Fractures

fractures that measure several inches on the core are common in this dark grey-blue bed, and they only occur parallel to bedding

Additional Comments

organic seams are common and weave through bladed structures or fossils, but do not typically fracture these components

SWIR

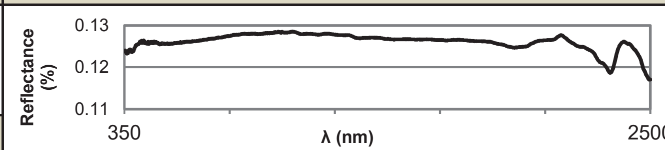

XRD

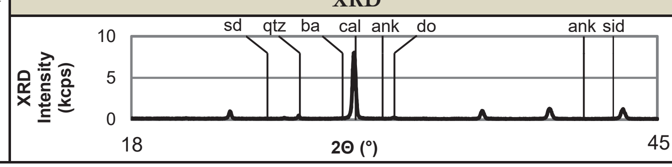

Stable Isotope

	$\delta^{13}C_{VPDB}$ (‰)	$\delta^{18}O_{VPDB}$ (‰)
1A Sample	-3.99	-3.80
1B Sample	-4.23	-3.69

Well ID: EGSP NY-4 / Valley Vista View 1 (31101152680000)	Formation: Oatka Creek Formation	Sample ID:	NY4-22
Location: Steuben, NY	Member: Cherry Valley Member	Depth (ft):	3844.70

Felted, microsparitic crystalline carbonate

Matrix Composition and Microtexture

massive matrix microtexture caused by calcite recrystallization; calcite is primary matrix constituent with minor clays and dolomite

Diagenetic Minerals

calcite, dolomite, pyrite

Diagenetic Texture

calcite crystallized as a micron-scale microspar or bladed crystals, potentially a replacement texture from recrystallized barite; calcite fills fractures with crystals that elongate perpendicular to the plane of propagation; dolomite rhombohedra are disseminated

Pore Structure

equant pores are hosted within calcite cement; minor organic-hosted porosity

Depositional Fabric

advanced neomorphism has overprinted all depositional fabrics, including the replacement of likely bladed barite by calcite

Additional comments:

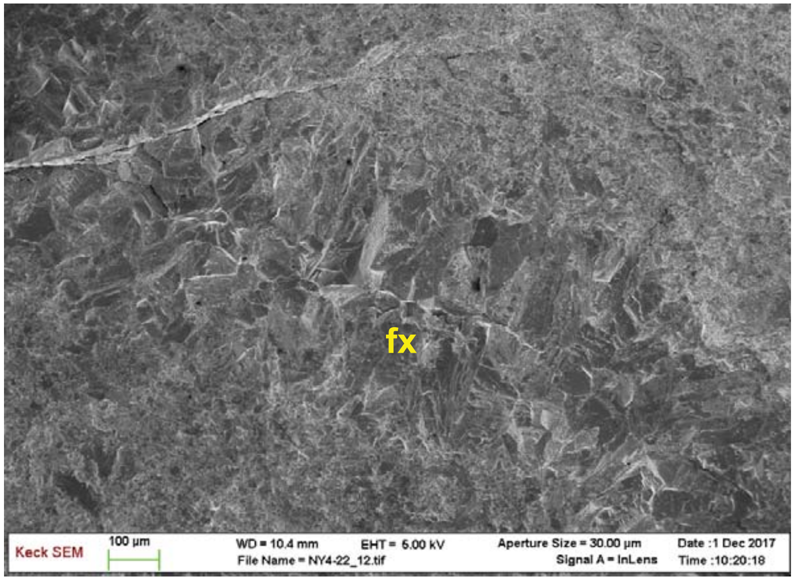

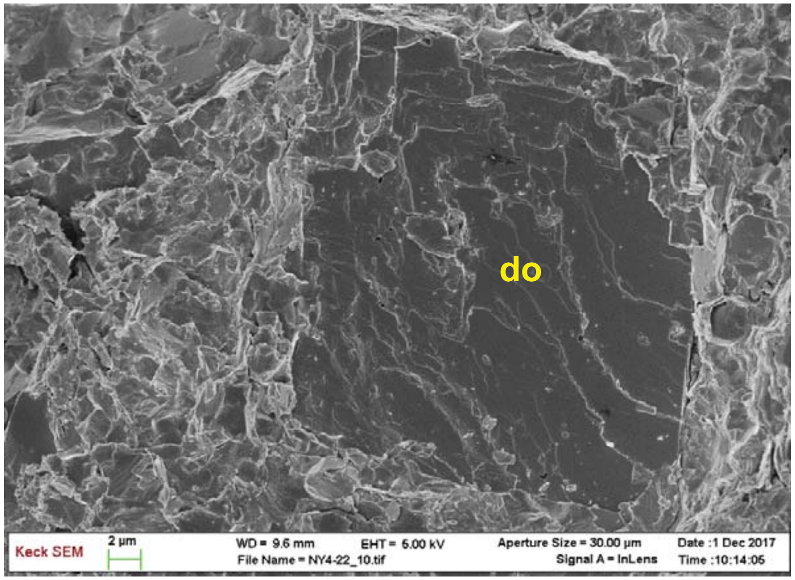

Well ID: EGSP NY-4 / Valley Vista View 1 (31101152680000)	Formation: Oatka Creek Formation	Sample ID:	NY4-24
Location: Steuben, NY	Member: Cherry Valley Member	Depth (ft):	3844.95

Felted, microsparitic crystalline carbonate

Matrix Composition

calcite

Texture

no depositional textures present; felted calcite is recrystallized, likely from original bladed, nodular barite; calcite is inequigranular and xenotopic

Diagenetic Minerals

calcite is the dominant diagenetic mineral; previous stages of carbonate diagenesis are overprinted by calcite; phase that originally produced the felted texture - likely barite - is entirely replaced by calcite; calcite in fractures display separate crystal texture, resembling the elongate prisms in some bivalves

Allochemical or Detrital Grains

none

Fossils

spherical and elongate tests, likely dacryoconarids; collapsed organic-walled cysts

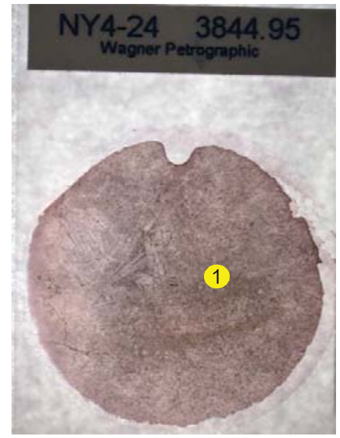

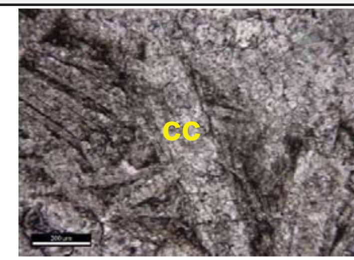

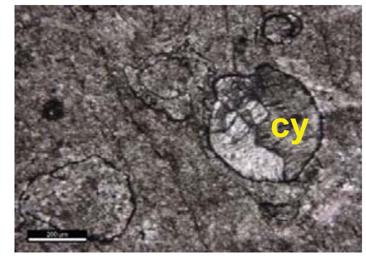

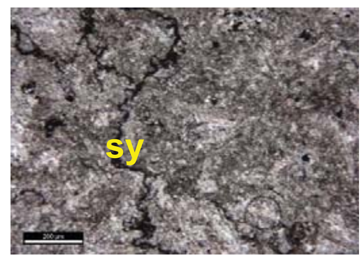

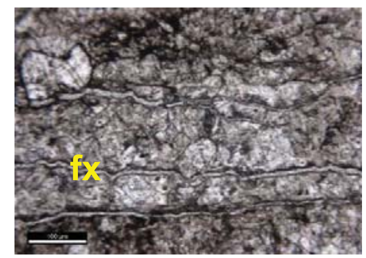

Fractures

fractures that measure several inches on the core are common in this dark grey-blue bed, and they only occur parallel to bedding; 10 μm-wide, bedding-parallel fractures are filled with silica

Additional Comments

organic-filed stylolites are common and do not show preferred orientation; organic material lines some fossils and preserves larger crystal growth within

SWIR

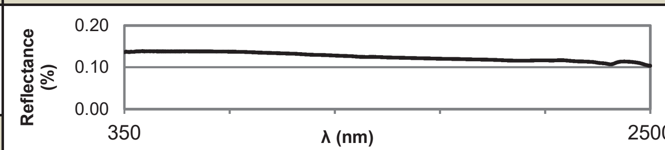

XRD

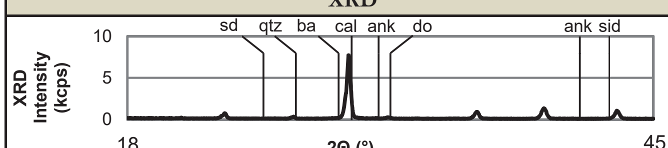

Stable Isotope

	$\delta^{13}C_{VPDB}$ (‰)	$\delta^{18}O_{VPDB}$ (‰)
1A Sample	-4.65	-3.74
1B Sample	-4.86	-3.70

Well ID: EGSP NY-4 / Valley Vista View 1 (31101152680000) | **Formation: Oatka Creek Formation** | **Sample ID:** NY4-29
Location: Steuben, NY | **Member: Cherry Valley Member** | **Depth (ft):** 3845.50

Microsparitic wackestone

Matrix Composition
calcite

Texture
poorly laminated; depositional horizon is visible, though much of the rock is recrystallized with equigranular and hypidiotopic calcite

Diagenetic Minerals
calcite is the primary diagenetic mineral; equant calcite growth on interior of fossils

Allochemical or Detrital Grains
none

Fossils
nondescript dacryoconarids; nondescript shell fragments

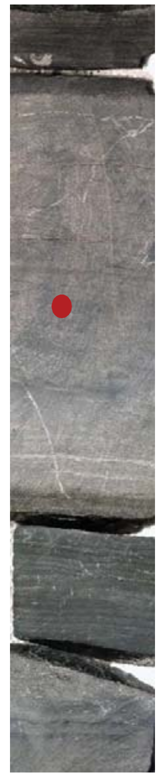

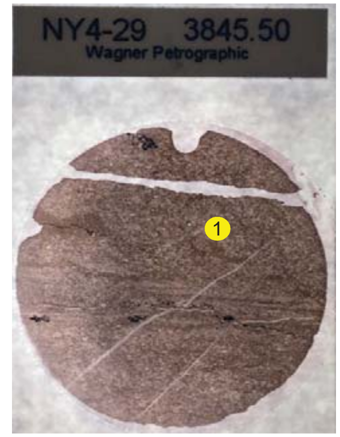

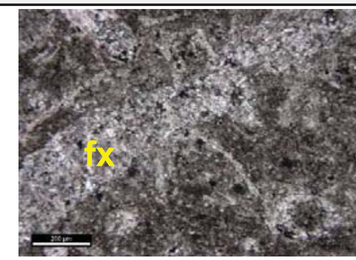

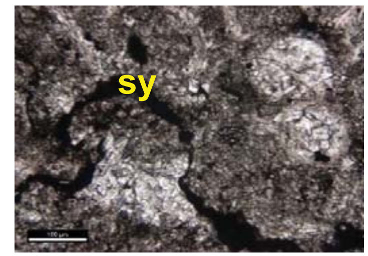

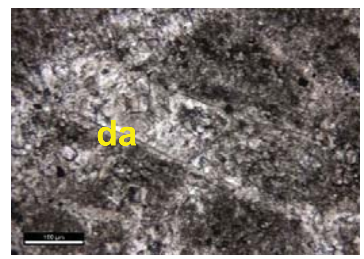

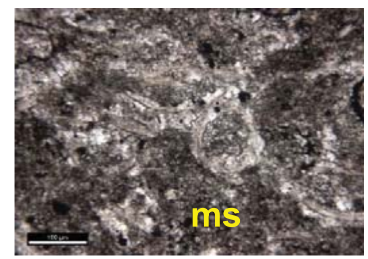

Fractures
0.5mm-wide, calcite-filled fracture set oblique to bedding; bedding-parallel, organic-filled, irregular anastomosing stylolites

Additional Comments
organic material lines some fossils and preserves larger crystal growth within

SWIR

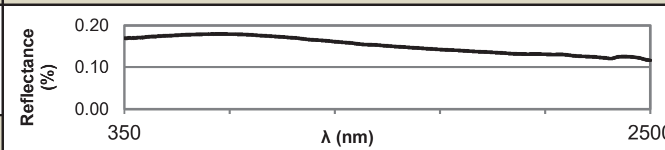

XRD

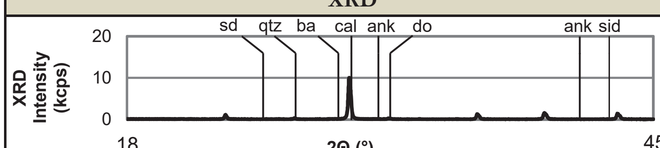

Stable Isotope

	$\delta^{13}C_{VPDB}$ (‰)	$\delta^{18}O_{VPDB}$ (‰)
1A Sample	-3.17	-2.48
1B Sample	-3.31	-3.04

Well ID: EGSP NY-4 / Valley Vista View 1 (31101152680000)	Formation: Oatka Creek Formation	Sample ID:	NY4-35
Location: Steuben, NY	Member: Cherry Valley Member	Depth (ft):	3846.36

Microsparitic wackestone

Matrix Composition

calcite; minor clay content in muddier portions of the rock

Texture

poorly laminated; micritic matrix recrystallized by xenotopic and equigranular calcite

Diagenetic Minerals

calcite is dominant diagenetic mineral; equant, circumgranular calcite crystal growth around fossils; rare dolomite rhombohedra

Allochemical or Detrital Grains

none

Fossils

nondescript dacryoconarids; nondescript shell fragments; collapsed organic-walled cysts

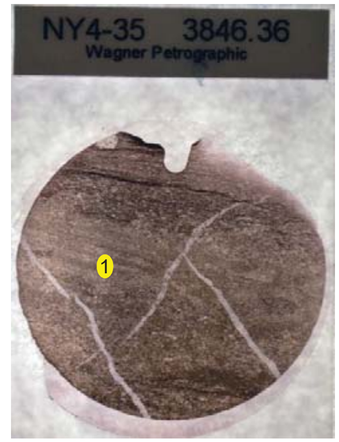

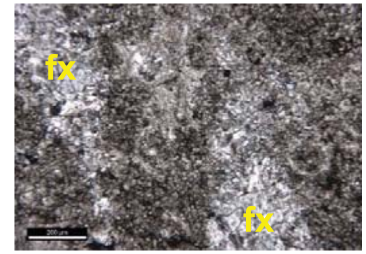

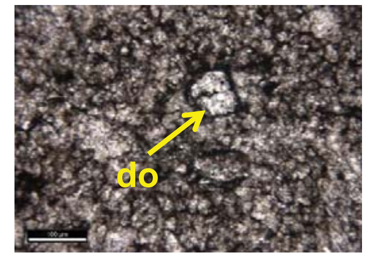

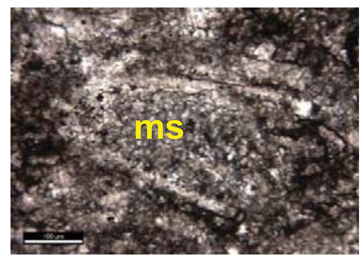

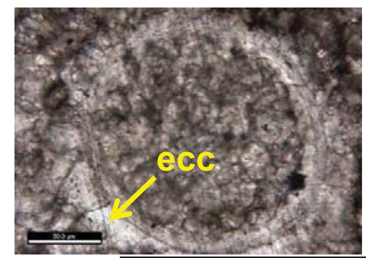

Fractures

0.5mm-wide, calcite-filled fracture set oblique to bedding; bedding-parallel, organic-filled, irregular anastomosing stylolites crosscut calcite-filled fractures

Additional Comments

muddy portions of the rock, such as the beds at the top of this thin section, contain elevated organic content

SWIR

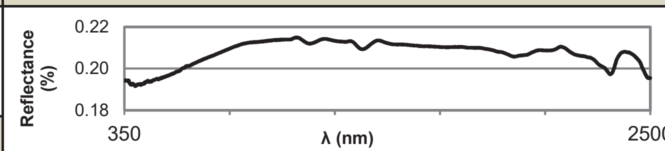

XRD

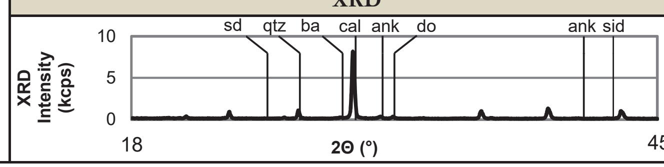

Stable Isotope

$\delta^{13}C_{VPDB}$ (‰)	$\delta^{18}O_{VPDB}$ (‰)
1A Sample	
-3.84	-2.86
1B Sample	
-3.08	-3.11

Well ID: EGSP NY-4 / Valley Vista View 1 (31101152680000)	Formation: Oatka Creek Formation	Sample ID:	NY4-35
Location: Steuben, NY	Member: Cherry Valley Member	Depth (ft):	3846.36

Microsparitic wackestone

Matrix Composition and Microtexture

massive matrix microtexture caused by calcite recrystallization; calcite is primary matrix constituent with minor clays and dolomite

Diagenetic Minerals

calcite, dolomite; framboidal pyrite associated with highly degraded organic material

Diagenetic Texture

calcite crystallized as a micron-scale microspar or single-crystal replacement of fossils; fossil tests lined with equant or sparry calcite overgrowths

Pore Structure

equant pores are hosted within calcite cement; minor organic-hosted porosity

Depositional Fabric

depositional fabrics are generally overprinted by diagenesis, though select, clay-rich laminae preserve a depositional surface

Additional comments:

prominent fractures that are apparent at thin-section scale were not observed on SEM, likely due to sampling

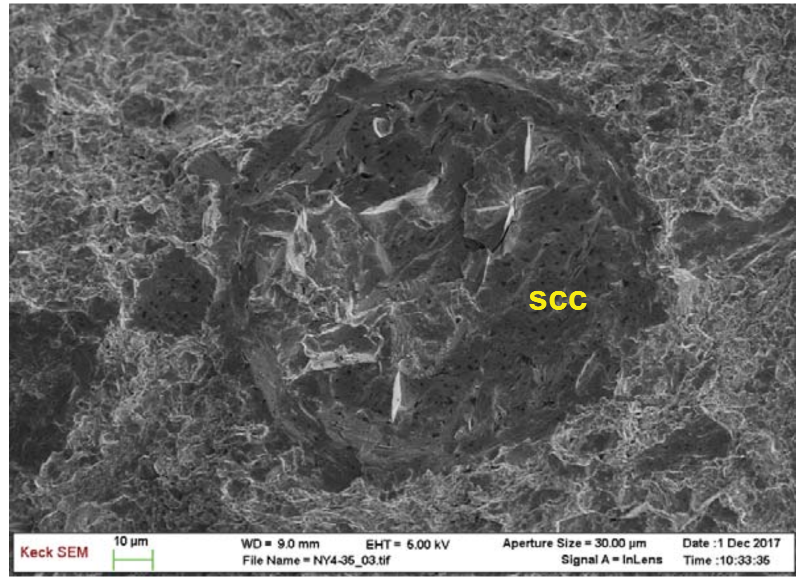

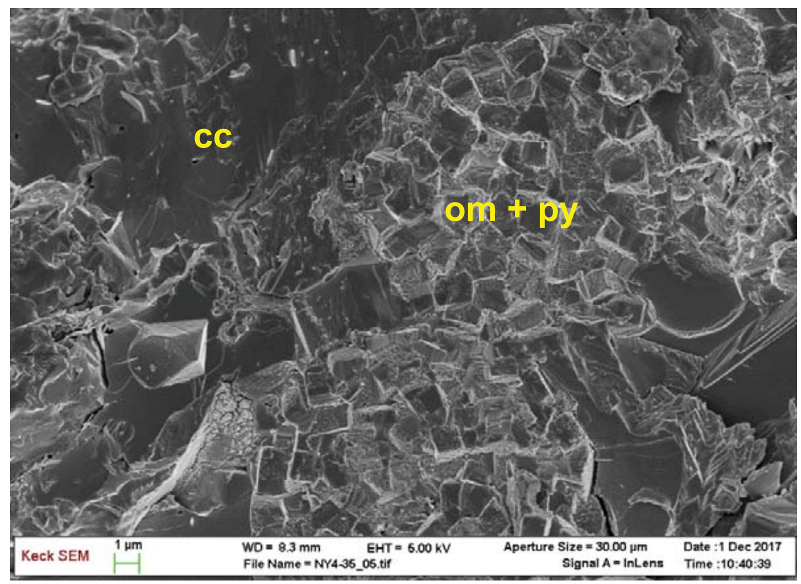

Well ID: EGSP NY-4 / Valley Vista View 1 (31101152680000)	Formation: Oatka Creek Formation	Sample ID: NY4-39
Location: Steuben, NY	Member: Cherry Valley Member	Depth (ft): 3846.78

Microsparitic wackestone

Matrix Composition
calcite

Texture
primarily nonlaminated, with bedding interfaces recognizable by change in fossil content

Diagenetic Minerals
calcite is the dominant diagenetic mineral; matrix calcite recrystallized to xenotopic and equigranular microspar; fossils have circumgranular calcite growth of equant or bladed crystals; poikilotopic fabric in sparry cements

Allochemical or Detrital Grains
none

Fossils
nondescript dacryoconarids; nondescript fossil fragments; collapsed organic-walled cysts

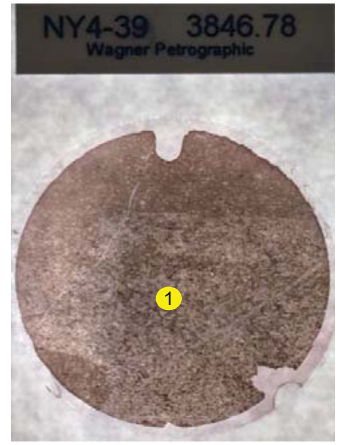

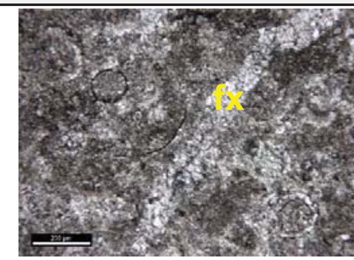

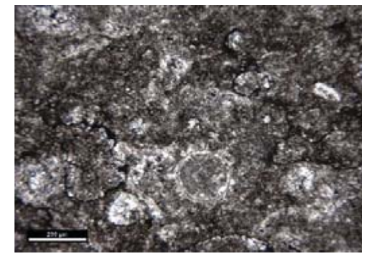

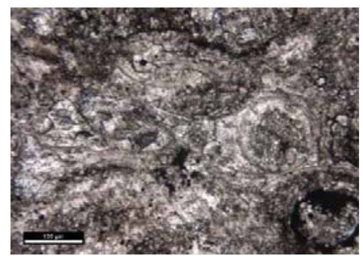

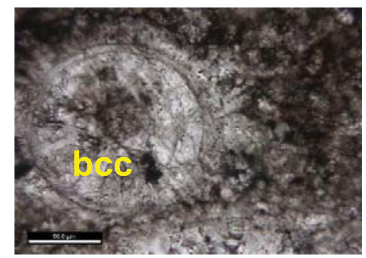

Fractures
0.5mm-wide, calcite-filled fracture set oblique to bedding; bedding-parallel, organic-filled, irregular anastomosing stylolites crosscut calcite-filled fractures

Additional Comments
organic material lines some fossils and preserves larger crystal growth within

SWIR
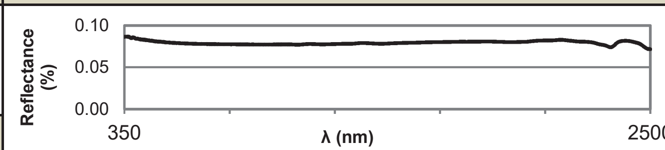

XRD
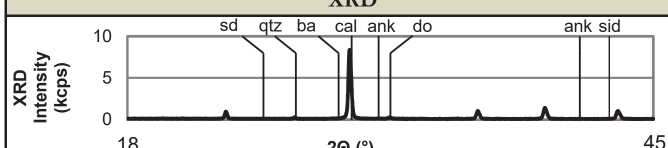

Stable Isotope

	$\delta^{13}C_{VPDB}$ (‰)	$\delta^{18}O_{VPDB}$ (‰)
1A Sample	-2.95	-2.32
1B Sample	-7.16	-3.37

Well ID: EGSP NY-4 / Valley Vista View 1 (31101152680000)	Formation: Oatka Creek Formation	Sample ID:	NY4-43
Location: Steuben, NY	Member: Cherry Valley Member	Depth (ft):	3847.33

Microsparitic wackestone

Matrix Composition

calcite

Texture

nonlaminated, though bedding horizons can be distinguished by change in calcite recrystallization fabrics

Diagenetic Minerals

calcite is the dominant diagenetic mineral; darker portions of this rock are characterized by microsparitic, xenotopic, equigranular calcite; sparry cement, likely recrystallized fossils, form poikilotopic crystals; several distinguishable fossils show earlier circumgranular, equant calcite growth

Allochemical or Detrital Grains

none

Fossils

nondescript fossil fragments; collapsed organic-walled cysts

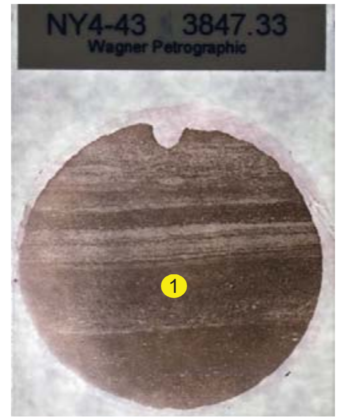

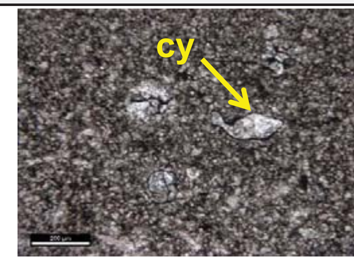

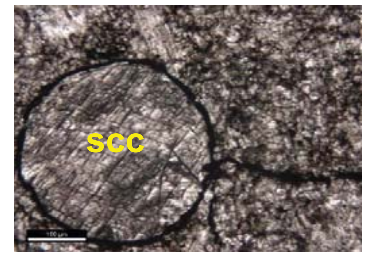

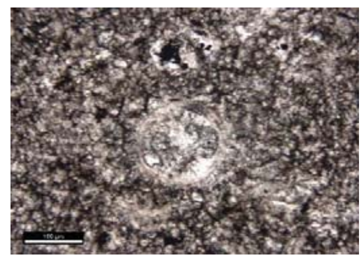

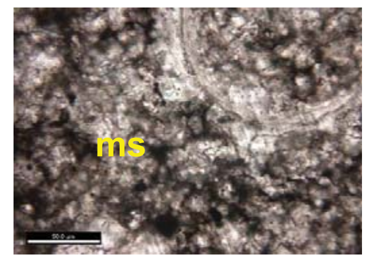

Fractures

none

Additional Comments

organic material lines some fossils and preserves larger crystal growth within

SWIR

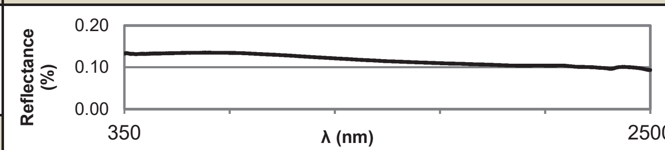

XRD

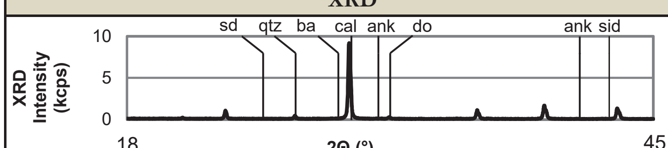

Stable Isotope

	$\delta^{13}C_{VPDB}$ (‰)	$\delta^{18}O_{VPDB}$ (‰)
1A Sample	-1.66	-2.56
1B Sample	-2.81	-2.99

Well ID: EGSP NY-4 / Valley Vista View 1 (31101152680000)	Formation: Oatka Creek Formation	Sample ID:	NY4-43
Location: Steuben, NY	Member: Cherry Valley Member	Depth (ft):	3847.33

Microsparitic wackestone

Matrix Composition and Microtexture

massive matrix microtexture caused by calcite recrystallization; calcite is primary matrix constituent with minor clays and dolomite; minor clay minerals

Diagenetic Minerals

calcite, dolomite; framboidal pyrite associated with highly degraded organic material

Diagenetic Texture

calcite crystallized as a micron-scale microspar or single-crystal replacement of fossils; fossil tests lined with equant or sparry calcite overgrowths

Pore Structure

equant pores are hosted within calcite cement; minor organic-hosted porosity

Depositional Fabric

depositional fabrics are generally overprinted by diagenesis, though select, clay-rich laminae preserve a depositional surface

Additional comments:

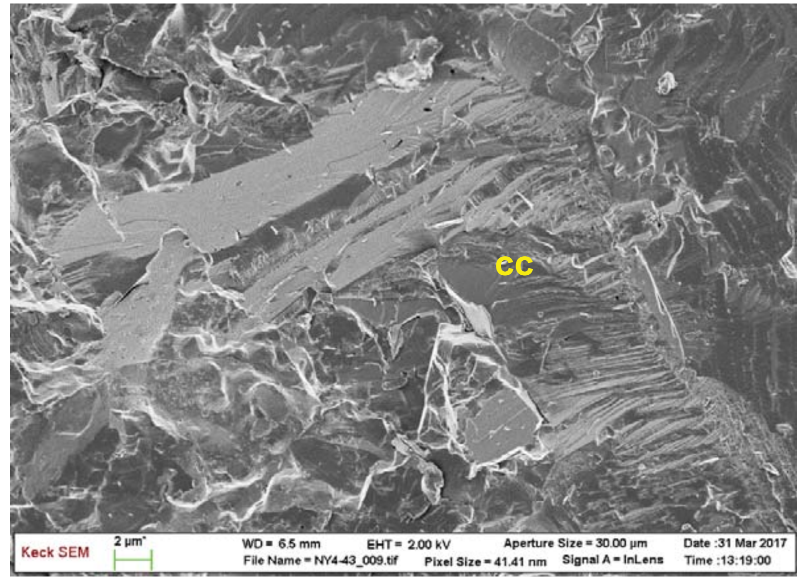

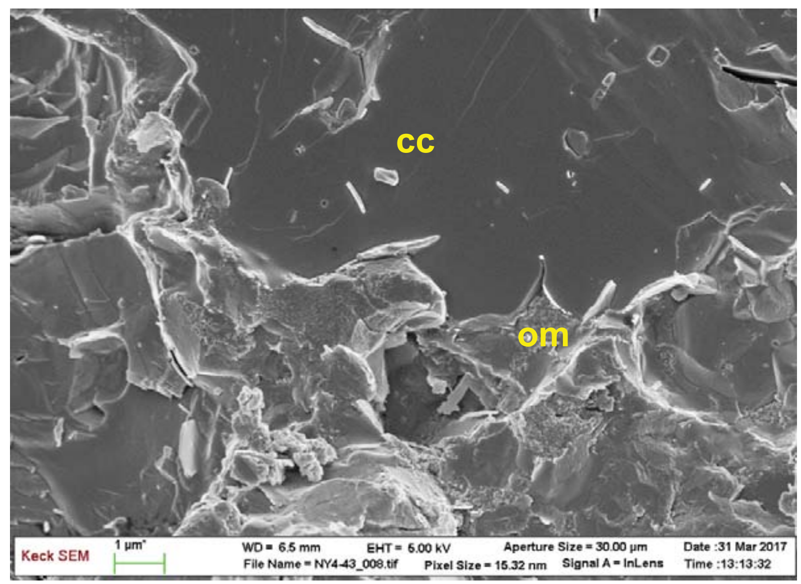

Well ID: EGSP NY-4 / Valley Vista View 1 (31101152680000)	**Formation: Oatka Creek Formation**	**Sample ID:**	**NY4-47**
Location: Steuben, NY	**Member: Cherry Valley Member**	**Depth (ft):**	**3847.92**

Microsparitic wackestone

Matrix Composition

calcite

Texture

poorly laminated; calcite recrystallization pervasive throughout rock, typically as equigranular and xenotopic microspar

Diagenetic Minerals

calcite is the primary diagenetic mineral; fossils may have circumgranular, equant calcite crystals; select fossil-rich portions display a poikilotopic fabric in sparite

Allochemical or Detrital Grains

none

Fossils

nondescript dacryoconarids; nondescript shell fragments; collapsed organic-walled cysts

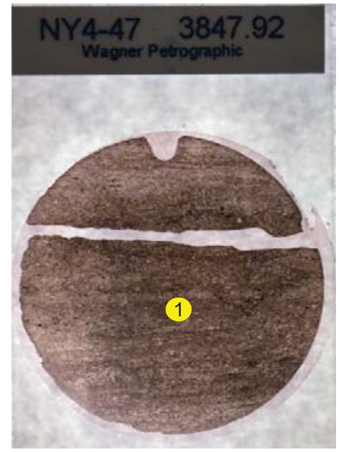

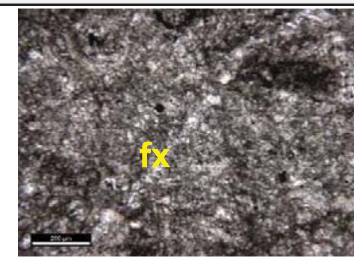

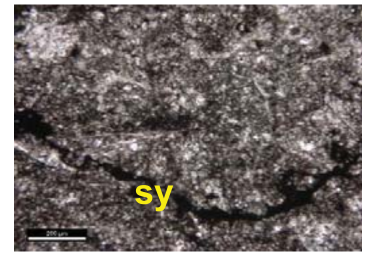

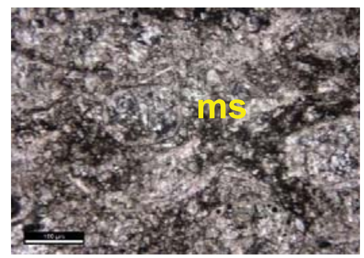

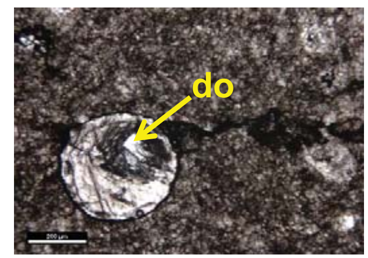

Fractures

faint calcite-healed fractures propagate oblique to bedding and are seemingly recrystallized; irregular anastomosing stylolites filled with organic material

Additional Comments

organic material lines some fossils and preserves larger crystal growth within; phosphate particles

SWIR

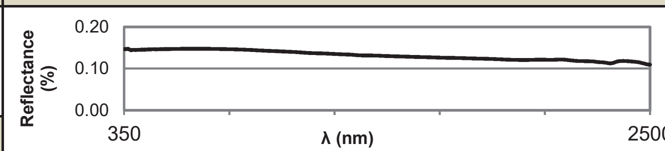

XRD

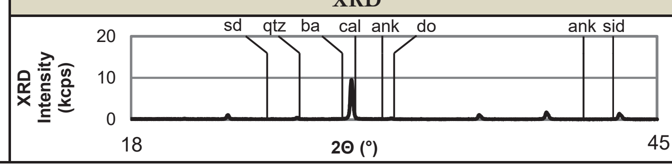

Stable Isotope

$\delta^{13}C_{VPDB}$ (‰)	$\delta^{18}O_{VPDB}$ (‰)
1A Sample	
-1.25	-3.44
1B Sample	
-2.56	-2.35

Well ID: EGSP NY-4 / Valley Vista View 1 (31101152680000)	Formation: Oatka Creek Formation	Sample ID:	NY4-50
Location: Steuben, NY	Member: Cherry Valley Member	Depth (ft):	3848.25

Microsparitic packstone

Fossiliferous, calcareous mudstone

Matrix Composition

calcite in both lithologies

Texture

packstone is largely nonlaminated and recrystallized to equigranular and xenotopic microspar; micrite in mudstone is hypidiotopic

Diagenetic Minerals

calcite is the dominant diagenetic mineral; equant calcite rims the inside of fossil tests; pyrite cements between poikilotopic calcite crystals in septarian-style fracture in packstone

Allochemical or Detrital Grains

none

Fossils

dacryoconarids (Styliolina); nondescript shell fragments

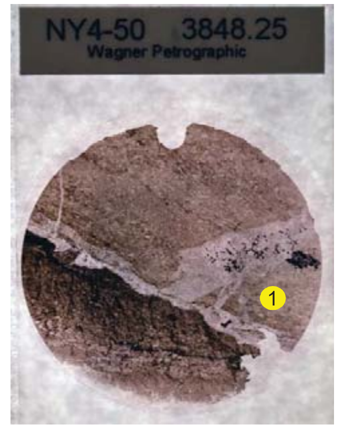

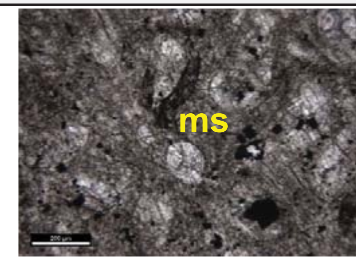

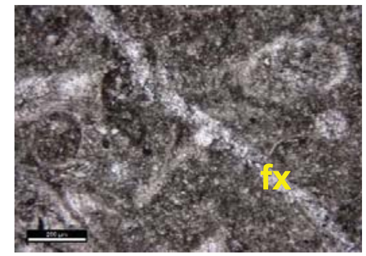

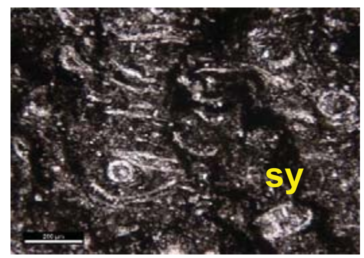

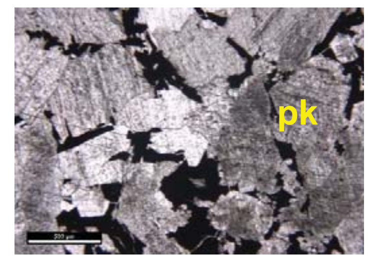

Fractures

fracture (or reaction front) along interface between packstone and mudstone, crystallized with millimeter-scale bladed crystals; irregular anastomosing stylolites propagate through packstone; septarian-style fracture in packstone

Additional Comments

stylolite-like structures, filled with organic material, streak through the mudstone at oblique angle to interface with packstone; isotope sample only taken from packstone portion due to insufficient material

SWIR

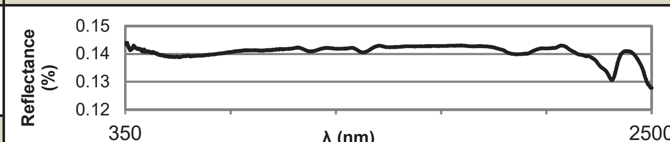

XRD

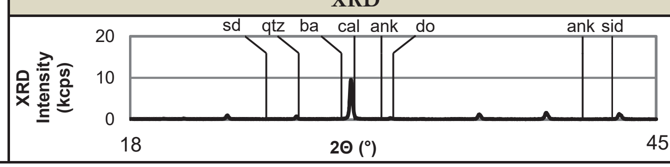

Stable Isotope

	$\delta^{13}C_{VPDB}$ (‰)	$\delta^{18}O_{VPDB}$ (‰)
1A Sample	-1.31	-4.85
1B Sample	-1.23	-4.50

Well ID: EGSP NY-4 / Valley Vista View 1 (31101152680000)	Formation: Oatka Creek Formation	Sample ID:	NY4-52
Location: Steuben, NY	Member: Cherry Valley Member	Depth (ft):	3848.58

Microsparitic wackestone

Matrix Composition

calcite

Texture

neomorphosed calcite microspar overprints lamina-scale textures, though beds are preserved by varying fossil content

Diagenetic Minerals

calcite is the dominant diagenetic mineral; matrix, presumably micritic in origin, is xenotopic and inequigranular; fossils are rimmed with equant calcite crystals that may entirely occlude the interior of the test

Allochemical or Detrital Grains

none

Fossils

dacryoconarids (Styliolina); nondescript shell fragments

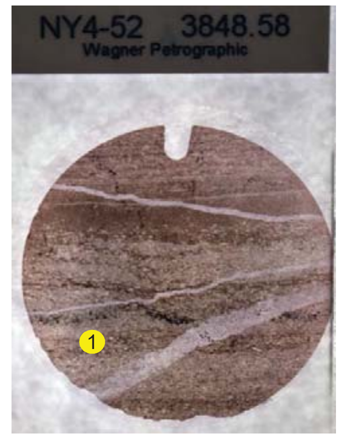

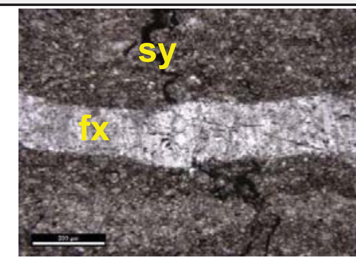

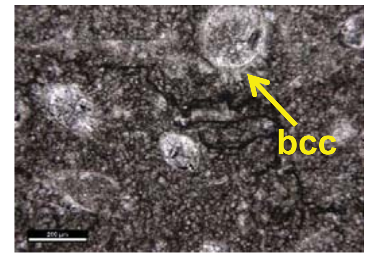

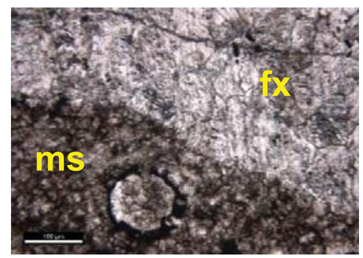

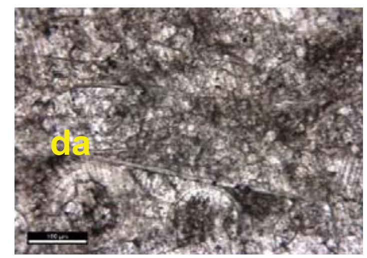

Fractures

septarian-style, millimeter-scale fractures are randomly oriented; irregularly anastomosing stylolites do not show preferential orientation; fractures bisect stylolites

Additional Comments

organic material lines some fossils and preserves larger crystal growth within; phosphate particles

SWIR

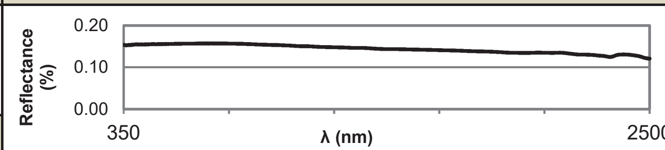

XRD

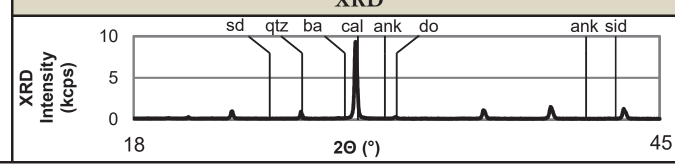

Stable Isotope

	$\delta^{13}C_{VPDB}$ (‰)	$\delta^{18}O_{VPDB}$ (‰)
1A Sample	-0.96	-5.67
1B Sample	-2.94	-5.00

Well ID: Beaver Meadow 1 (31017230060000)	Formation: Oatka Creek Formation	Sample ID:	BMC-NYSM-2
Location: Chenango, NY	Member: East Berne Member	Depth (ft):	1900.00

Organic, argillaceous mudstone

Matrix Composition

illitic clays with minor calcite cementation near fossils

Texture

moderately well-laminated; bedding and laminae defined by aligned fossils, organic particles, and mica flakes

Diagenetic Minerals

minor leaching of fossil calcite into surrounding clay matrix; dolomite is crystallized as fossil fill and disseminated rhombohedra

Allochemical or Detrital Grains

quartz silt (<5%) and detrital micas

Fossils

nondescript dacryoconarids; nondescript fossil fragments

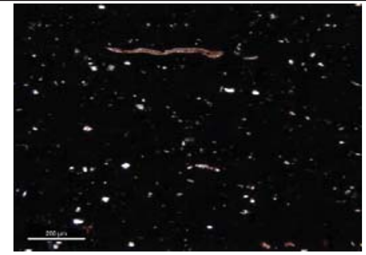

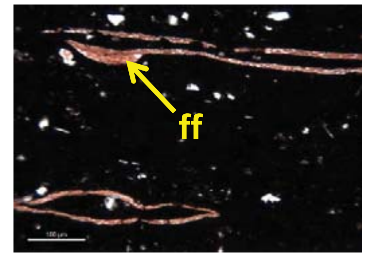

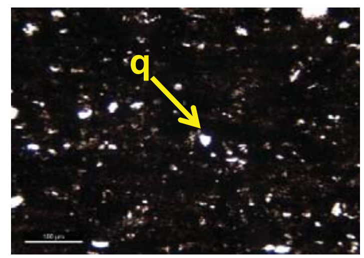

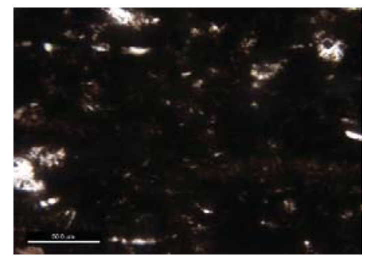

Fractures

none

Additional Comments

organic particles abundant throughout; thin section loaned from NYSM (no extra material available for SEM, XRD, or geochemical testing)

SWIR

N/A

XRD

N/A

Stable Isotope

	$\delta^{13}C_{VPDB}$ (‰)	$\delta^{18}O_{VPDB}$ (‰)
1A Sample	N/A	N/A
1B Sample	N/A	N/A

Well ID: Beaver Meadow 1 (31017230060000)	**Formation: Oatka Creek Formation**	**Sample ID:**	**BMC-NYSM-3**
Location: Chenango, NY	**Member: East Berne Member**	**Depth (ft):**	**1901.00**

Fossiliferous, calcareous mudstone

Matrix Composition

calcite and illitic clays

Texture

moderately laminated; aligned shell fragments

Diagenetic Minerals

calcite is the dominant diagenetic mineral; micritic matrix is marginally neomorphosed, nearing microspar in select portions of the rock; fossil cavities are typically fully occluded by sparry calcite; uncommon dolomite rhombohedra

Allochemical or Detrital Grains

quartz silt (<5%)

Fossils

dacryoconarids (Viriatellina); robust, nondescript shell fragments; phosphatic bone fragments; algal mat structures that define bedding planes and span the width of the thin section

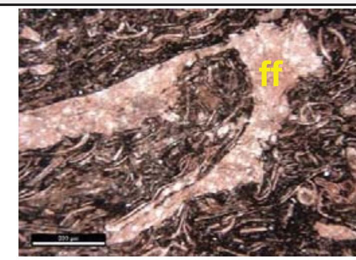

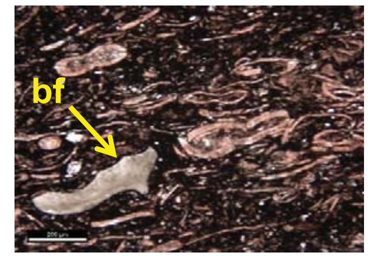

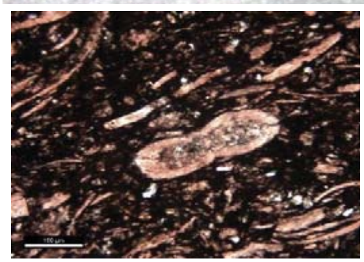

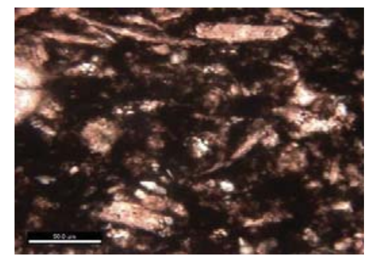

Fractures

none

SWIR

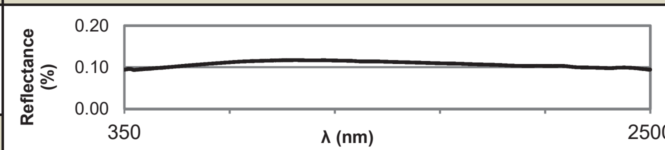

Stable Isotope

$\delta^{13}C_{VPDB}$ (‰)	$\delta^{18}O_{VPDB}$ (‰)
1A Sample	
N/A	N/A
1B Sample	
N/A	N/A

Additional Comments

organic material disseminated within matrix, likely as fine, amorphous kerogen; thin section loaned from NYSM (no extra material available for SEM, XRD, or geochemical testing)

XRD

N/A

Well ID: Beaver Meadow 1 (31017230060000)	Formation: Oatka Creek Formation	Sample ID:	BMC-13
Location: Chenango, NY	Member: Cherry Valley Member	Depth (ft):	1902.58

Microsparitic wackestone

Matrix Composition

calcite

Texture

nonlaminated and chaotic; alignment of fossils is undulatory; micrite is recrystallized to xenotopic microspar

Diagenetic Minerals

calcite is the dominant diagenetic mineral; micrite has largely been neomorphosed to microspar, though select portions of the rock display larger, nearly poikilotopic crystalline textures; pyrite is associated with stylolites; equant or dog tooth calcite crystallized inside fossil tests

Allochemical or Detrital Grains

trace quartz silt

Fossils

nondescript dacryoconarids; nondescript shell fragments; possible algal mat fragments

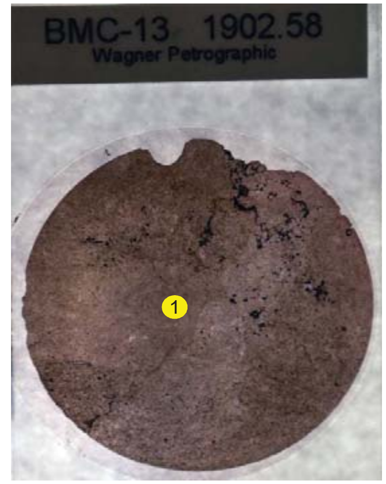

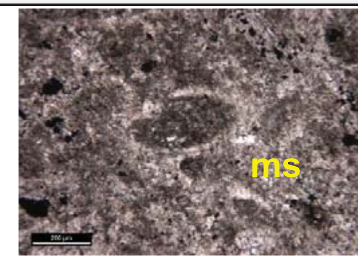

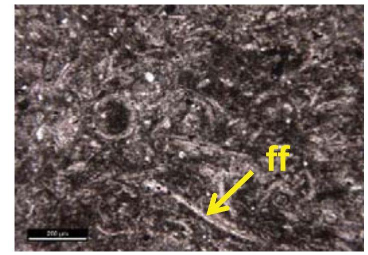

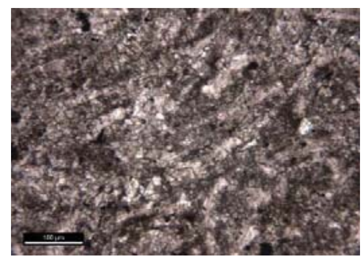

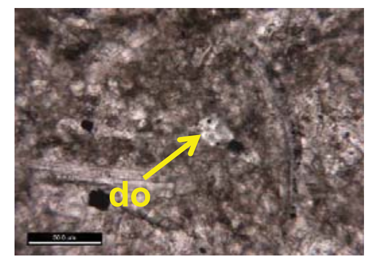

Fractures

micron-scale vertical fracture normal to bedding; irregular anastomosing stylolites do not propagate in a preferred orientation, but do follow more fossil-poor portions of the

Additional Comments

organic material stains microspar and fills stylolites

SWIR

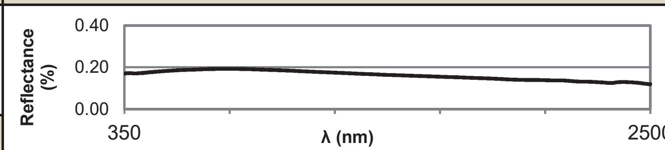

XRD

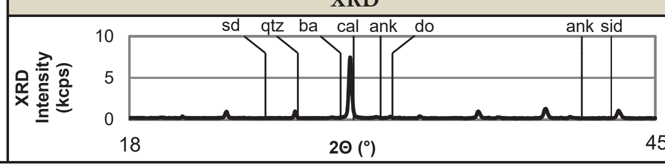

Stable Isotope

	$\delta^{13}C_{VPDB}$ (‰)	$\delta^{18}O_{VPDB}$ (‰)
1A Sample	N/A	N/A
1B Sample	N/A	N/A

Well ID: Beaver Meadow 1 (31017230060000)	Formation: Oatka Creek Formation	Sample ID:	BMC-13
Location: Chenango, NY	Member: Cherry Valley Member	Depth (ft):	1902.58

Microsparitic wackestone

Matrix Composition and Microtexture

massive matrix microtexture caused by calcite recrystallization; calcite is primary matrix constituent with minor clays and dolomite

Diagenetic Minerals

calcite, dolomite, pyrite

Diagenetic Texture

calcite crystallized as a micron-scale microspar or single-crystal replacement of fossils; dolomite is sparse and disseminated as rhombohedra; interface between calcite cement and matrix components, such as fossils or detritus, is tight

Pore Structure

equant pores are hosted within calcite cement; minor organic-hosted porosity

Depositional Fabric

depositional fabrics are generally overprinted by diagenesis; patches of depositional clay minerals observed

Additional comments:

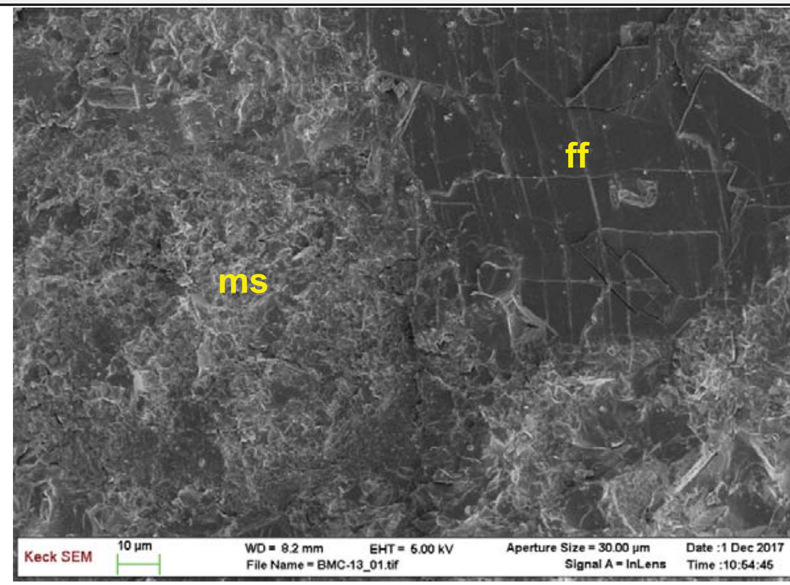

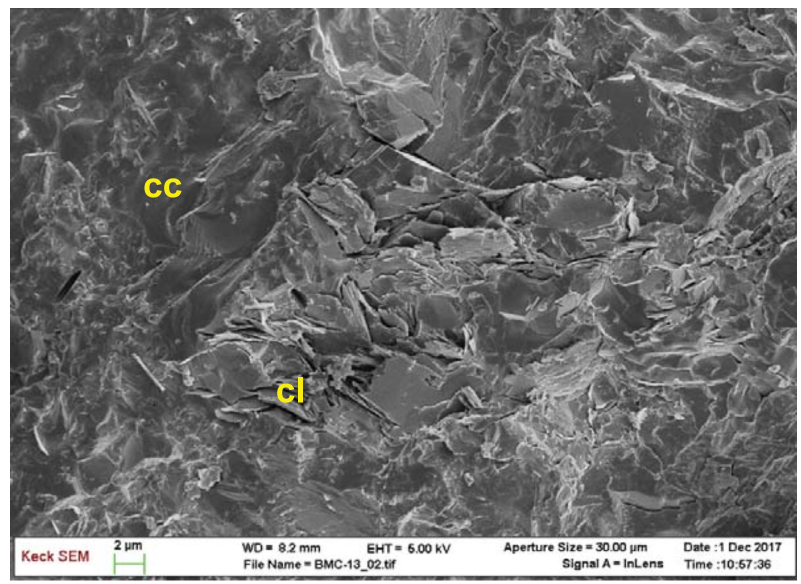

Well ID: Beaver Meadow 1 (31017230060000)	Formation: Oatka Creek Formation	Sample ID:	BMC-NYSM-4
Location: Chenango, NY	Member: Cherry Valley Member	Depth (ft):	1903.00

Silty wackestone

Matrix Composition
calcite with lesser clays

Texture
poorly laminated; microtexture is chaotic, with fossils and detrital mica showing little preference to bedding planes and possible bioturbation

Diagenetic Minerals
calcite is the dominant diagenetic mineral, most commonly as a cement; minor dolomite cementation; select fossils are filled with dolomite; disseminated dolomite rhombohedra

Allochemical or Detrital Grains
quartz silt and detrital micas (< 25% by visual estimate); single millimeter-scale allochem, likely a pre-existing carbonate fragment rather than a fossil

Fossils
nondescript dacryoconarids; nondescript shell fragments

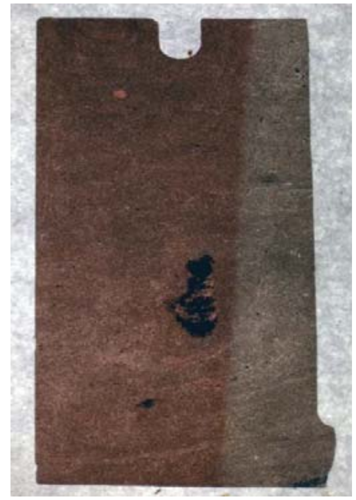

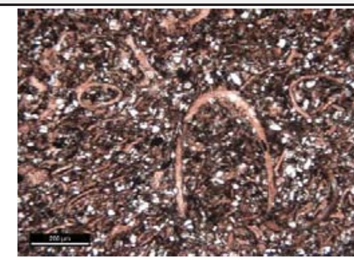

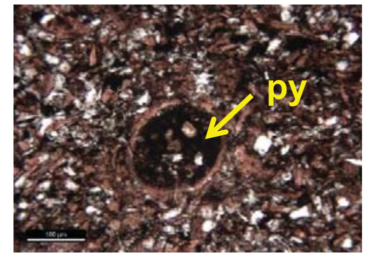

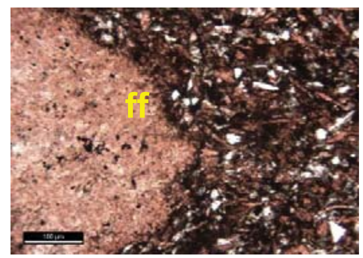

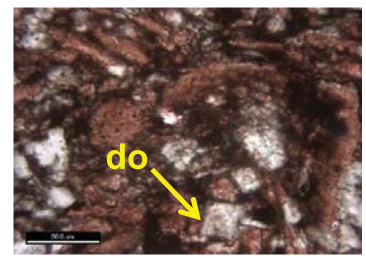

Fractures
none

Additional Comments
organic material disseminated throughout matrix, likely as a fine, amorphous kerogen, and also fills select fossil tests; thin section loaned from NYSM (no extra material available for SEM, XRD, or geochemical testing)

SWIR

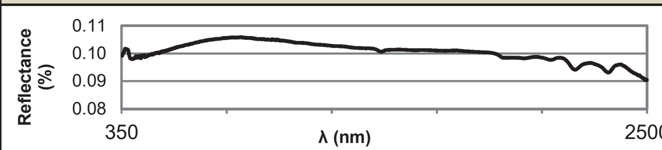

XRD
N/A

Stable Isotope

	$\delta^{13}C_{VPDB}$ (‰)	$\delta^{18}O_{VPDB}$ (‰)
1A Sample	N/A	N/A
1B Sample	N/A	N/A

Well ID: Beaver Meadow 1 (31017230060000)	Formation: Oatka Creek Formation	Sample ID:	BMC-21
Location: Chenango, NY	Member: Cherry Valley Member	Depth (ft):	1903.50

Microsparitic packstone

Matrix Composition

calcite

Texture

nonlaminated; calcite is typically xenotopic and has overprinted most depositional fabrics

Diagenetic Minerals

calcite is the dominant diagenetic mineral, having cemented or recrystallized the entire rock; sparry calcite cement displays poikilotopic textures in select areas; circumgranular, equant calcite growth on fossils; minor dolomite crystallization in select fossils

Allochemical or Detrital Grains

minor (< 10%) quartz silt and detrital micas

Fossils

nondescript dacryoconarids; nondescript shell fragments;

Fractures

vertical, calcite-filled fractures propagate normal to bedding

Additional Comments

organic material largely absent; not enough sample to complete second stable isotope measurement

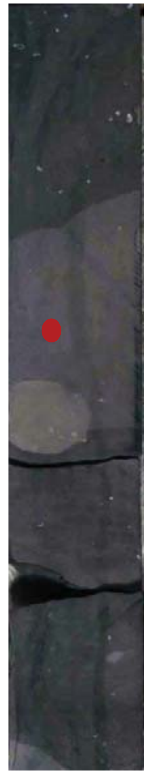

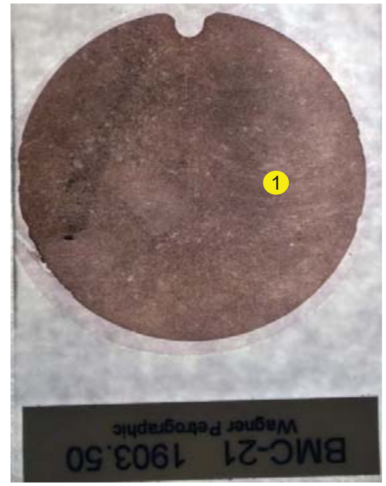

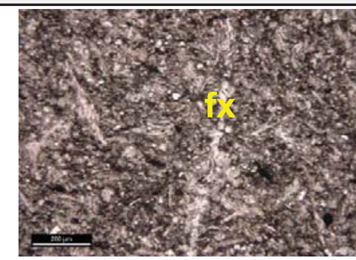

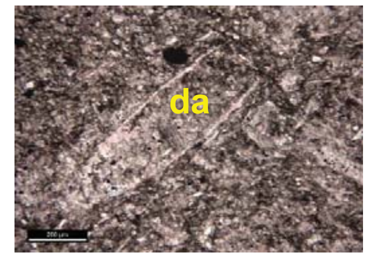

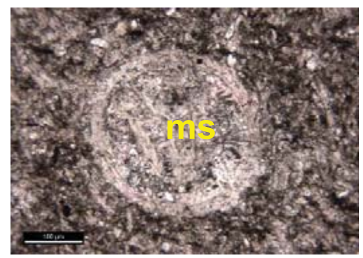

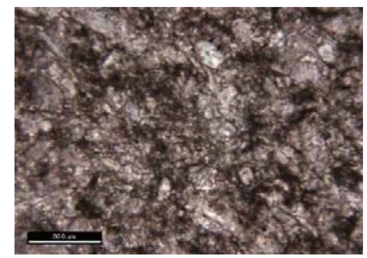

SWIR

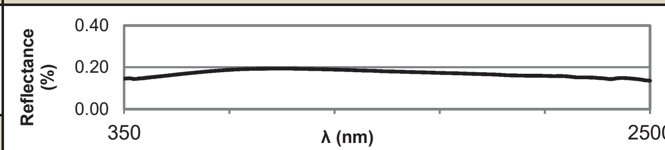

XRD

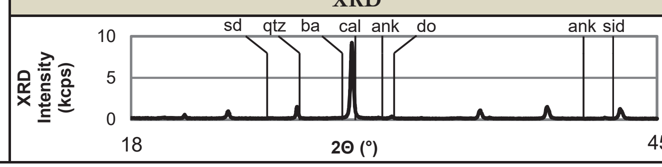

Stable Isotope

	$\delta^{13}C_{VPDB}$ (‰)	$\delta^{18}O_{VPDB}$ (‰)
1A Sample	-0.41	-7.21
1B Sample	N/A	N/A

Well ID: Beaver Meadow 1 (31017230060000)	Formation: Oatka Creek Formation	Sample ID:	BMC-21
Location: Chenango, NY	Member: Cherry Valley Member	Depth (ft):	1903.50

Microsparitic packstone

Matrix Composition and Microtexture

massive matrix microtexture caused by calcite recrystallization; calcite is primary matrix constitutent with minor clays and dolomite

Diagenetic Minerals

calcite, dolomite, pyrite

Diagenetic Texture

calcite crystallized as a micron-scale microspar or single-crystal replacement of fossils; calcite overgrowths are observed on fossil exteriors; dolomite is sparse and disseminated as rhombohedra; interface between calcite cement and matrix components, such as fossils or detritus, is tight

Pore Structure

equant pores are hosted within calcite cement; minor organic-hosted porosity

Depositional Fabric

depositional fabrics are overprinted by diagenesis; some detrital material, including chlorite laths and other clay minerals, are preserved

Additional comments:

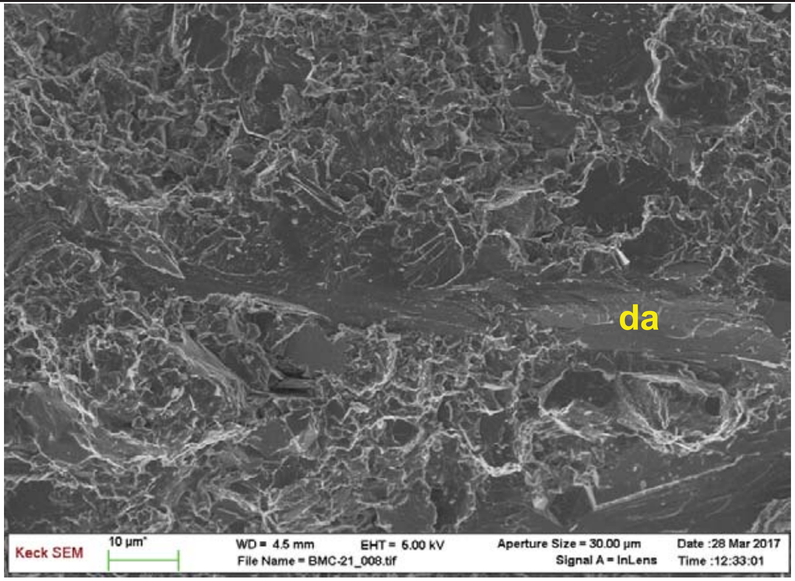

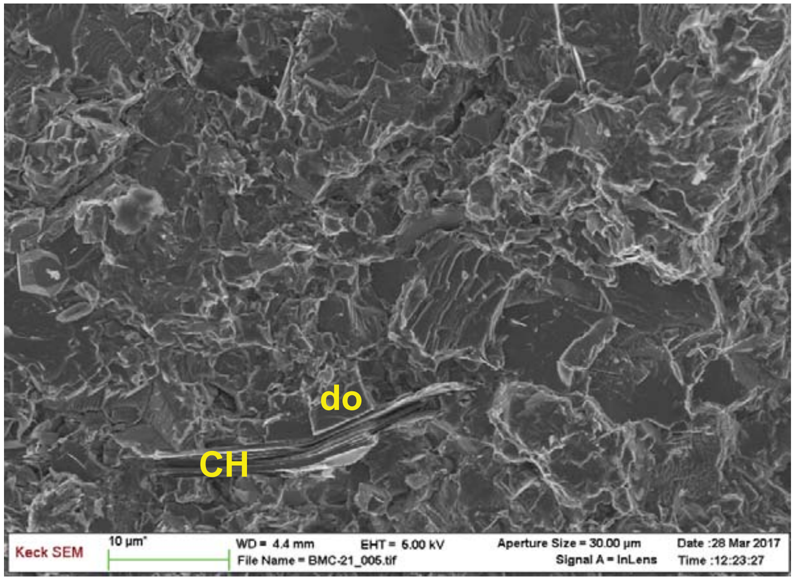

Well ID: Beaver Meadow 1 (31017230060000)	Formation: Oatka Creek Formation	Sample ID:	BMC-26
Location: Chenango, NY	Member: Cherry Valley Member	Depth (ft):	1904.25

Microsparitic wackestone

Matrix Composition

calcite

Texture

poorly laminated; matrix is recrystallized to xenotopic and inequigranular microspar in most of the rock

Diagenetic Minerals

calcite is the dominant diagenetic mineral; micrite remains in some portions of the rock, but is largely neomorphosed to microspar; equant calcite or dolomite is crystallized on fossil interiors

Allochemical or Detrital Grains

minor (< 5%) quartz silt

Fossils

dacryoconarids (Styliolina); nondescript shell fragments; few robust fossil fragments, likely bivalves

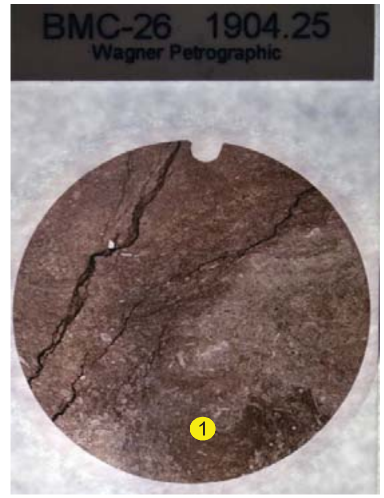

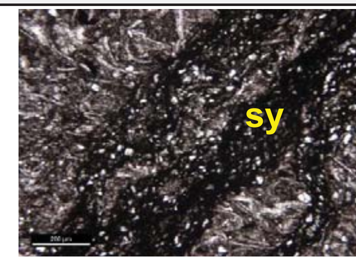

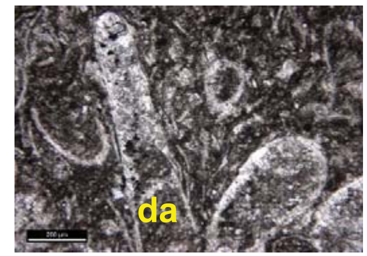

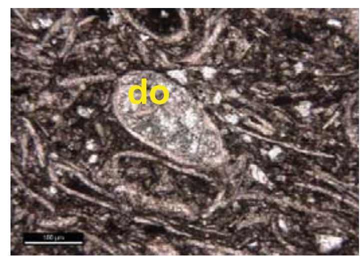

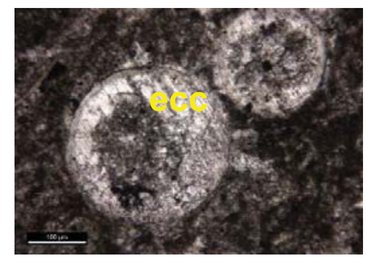

Fractures

irregular anastomosing stylolites cross bedding planes and do propagate through more micritic sections

Additional Comments

organic material is mostly relegated to stylolites

SWIR

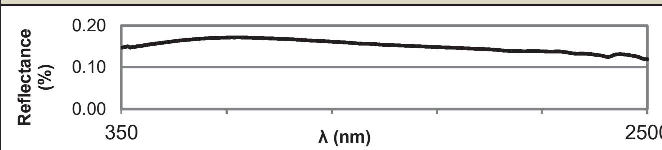

XRD

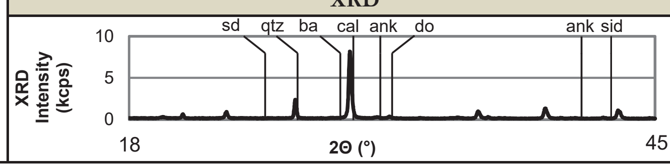

Stable Isotope

	$\delta^{13}C_{VPDB}$ (‰)	$\delta^{18}O_{VPDB}$ (‰)
1A Sample	N/A	N/A
1B Sample	N/A	N/A

Well ID: Beaver Meadow 1 (31017230060000)	**Formation: Oatka Creek Formation**	**Sample ID:**	**BMC-30**
Location: Chenango, NY	**Member: Cherry Valley Member**	**Depth (ft):**	**1904.75**

Microsparitic packstone

Matrix Composition

calcite

Texture

nonlaminated; matrix is recrystallized to xenotopic and inequigranular microspar

Diagenetic Minerals

calcite is the dominant diagenetic mineral; matrix is neomorphosed to microspar; fossils are rimmed with equant or dog-tooth calcite;

Allochemical or Detrital Grains

none

Fossils

dacryoconarids (Styliolina); nondescript fossil fragments

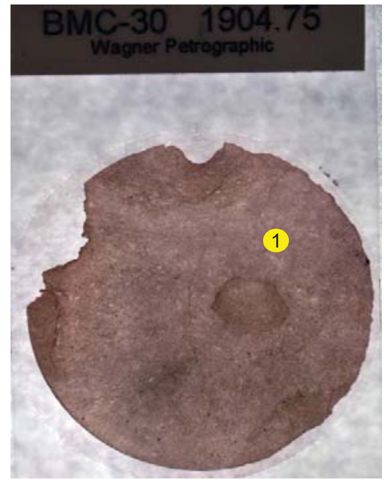

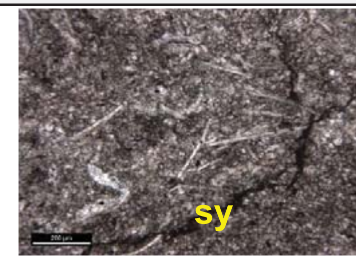

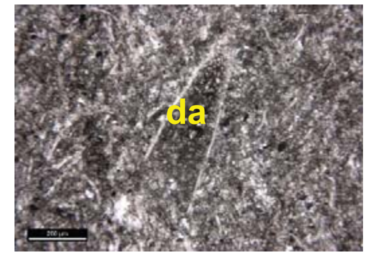

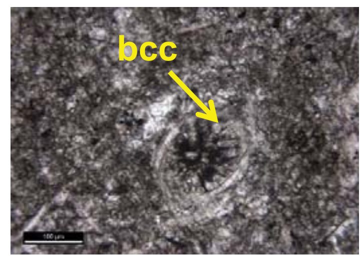

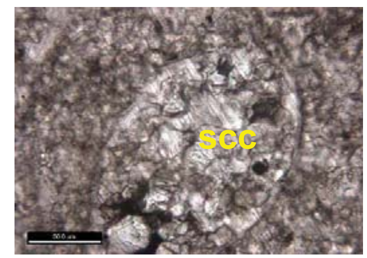

Fractures

recrystallized, subvertical fracture that presumably propagated prior to the last stage of calcite recrystallization; stylolites are discontinuous and do not show a preferred orientation

Additional Comments

organic material is largely restricted to stylolites

SWIR

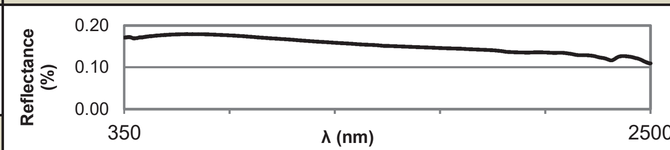

XRD

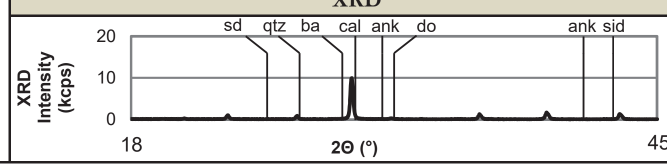

Stable Isotope

$\delta^{13}C_{VPDB}$ (‰)	$\delta^{18}O_{VPDB}$ (‰)
1A Sample	
N/A	N/A
1B Sample	
N/A	N/A

Well ID: Beaver Meadow 1 (31017230060000)	Formation: Oatka Creek Formation	Sample ID:	BMC-35
Location: Chenango, NY	Member: Cherry Valley Member	Depth (ft):	1905.33

Microsparitic wackestone

Matrix Composition
calcite

Texture
poorly laminated; matrix is largely neomorphosed to microspar, though aligned fossil material define bedding planes

Diagenetic Minerals
calcite is the dominant diagenetic mineral; minor dolomite cements and worn rhombohedra; dog tooth calcite crystallized on surface of fossils

Allochemical or Detrital Grains
trace quartz silt

Fossils
nondescript dacryoconarids; nondescript shell fragments; phosphatic bone fragments; stromatoporoids, with well-preserved radial, chambered "fingers"; crinoid, by U-shaped arm plate

Fractures
irregular anastomosing stylolites propagate normal to bedding

Additional Comments
organic material fills stylolites and select fossils

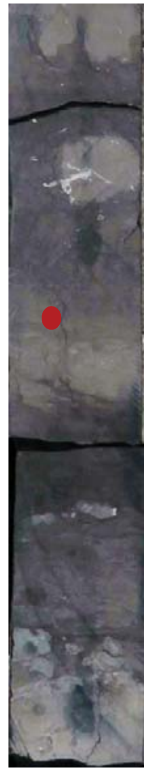

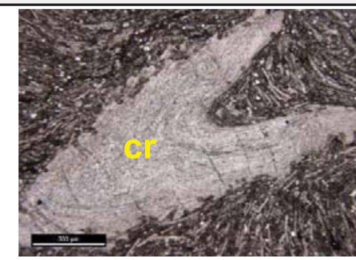

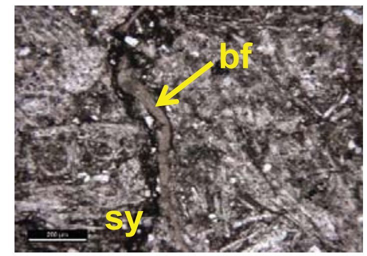

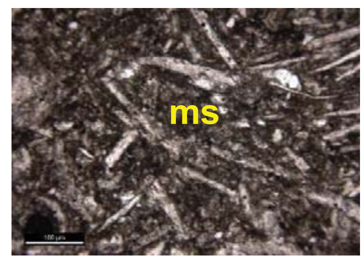

SWIR

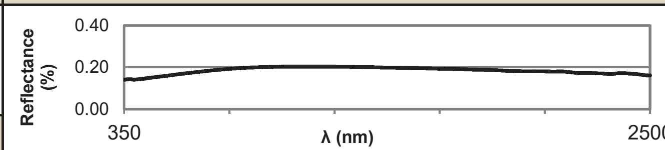

XRD

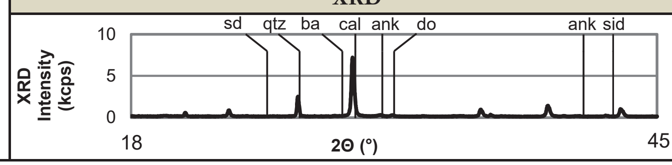

Stable Isotope

	$\delta^{13}C_{VPDB}$ (‰)	$\delta^{18}O_{VPDB}$ (‰)
1A Sample	N/A	N/A
1B Sample	N/A	N/A

Well ID: Beaver Meadow 1 (31017230060000)	Formation: Oatka Creek Formation	Sample ID:	BMC-40
Location: Chenango, NY	Member: Cherry Valley Member	Depth (ft):	1905.83

Microsparitic wackestone

Matrix Composition

calcite

Texture

nonlaminated; xenotopic, inequigranular microspar replaces micritic matrix; silty lenses may indicate burrowing

Diagenetic Minerals

calcite is the dominant diagenetic mineral; matrix is neomorphosed to microspar; fossils are typically rimmed with equant calcite; minor dolomite fossil fill; pyrite framboids partially fill select fossils; siderite fills fracture or crack

Allochemical or Detrital Grains

quartz silt (< 10%) and detrital micas

Fossils

dacryoconarids (Styliolina); trilobites; nondescript shell fragments

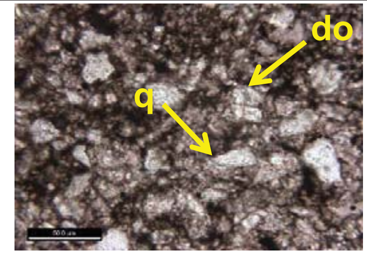

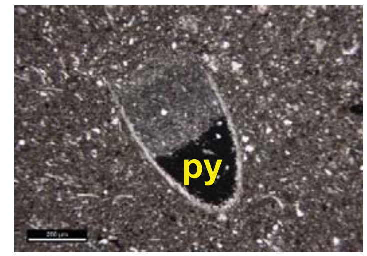

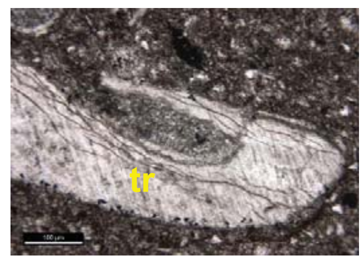

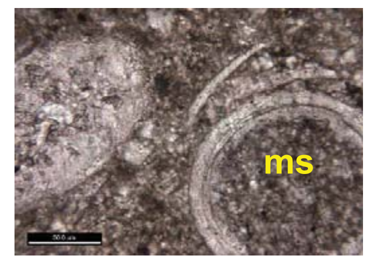

Fractures

single fracture, or crack, filled with siderite

Additional Comments

hydrocarbon staining apparent by solitary blotches in the rock; not enough sample to complete second stable isotope measurement

SWIR

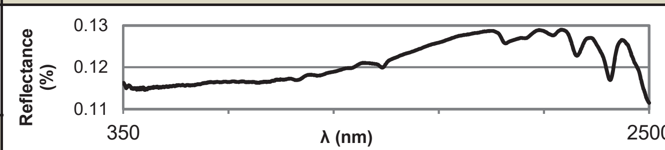

XRD

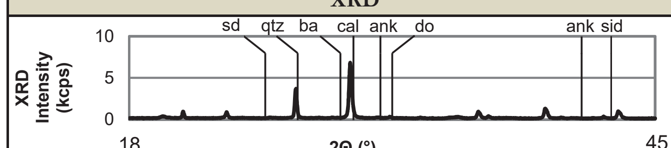

Stable Isotope

	$\delta^{13}C_{VPDB}$ (‰)	$\delta^{18}O_{VPDB}$ (‰)
1A Sample	-1.20	-8.41
1B Sample	N/A	N/A

Well ID: Beaver Meadow 1 (31017230060000)	Formation: Oatka Creek Formation	Sample ID:	BMC-43
Location: Chenango, NY	Member: Cherry Valley Member	Depth (ft):	1906.17

Microsparitic wackestone

Matrix Composition

calcite

Texture

nonlaminated, with abundant fossils not deposited with preferred orientations; neomorphosed microspar overprints depositional microtextures

Diagenetic Minerals

calcite is the dominant diagenetic mineral; matrix likely micritic in origin and neomorphosed to hypidiotopic, equigranular microspar; equant or dog tooth calcite rims fossils; framboidal pyrite associated with organic material

Allochemical or Detrital Grains

trace quartz silt

Fossils

dacryoconarids (Styliolina); trilobites; crinoids; nondescript shell fragments; phosphatic bone fragments

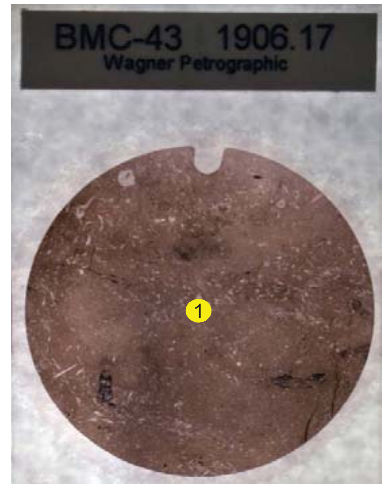

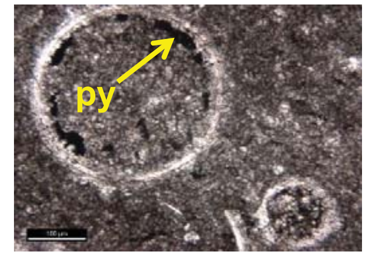

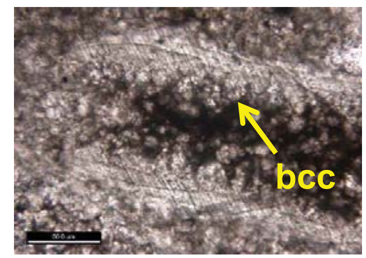

Fractures

none

Additional Comments

organic material fills select fossils; not enough sample to complete second stable isotope measurement

SWIR

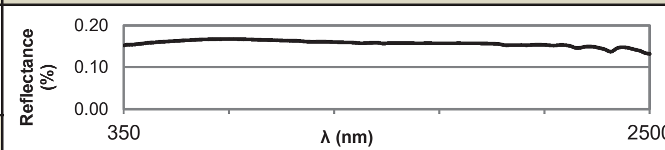

XRD

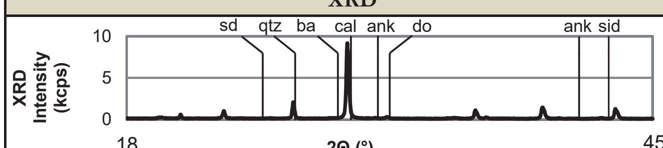

Stable Isotope

$\delta^{13}C_{VPDB}$ (‰)	$\delta^{18}O_{VPDB}$ (‰)
1A Sample	
-3.21	-7.60
1B Sample	
N/A	N/A

Well ID: Beaver Meadow 1 (31017230060000)	Formation: Oatka Creek Formation	Sample ID:	BMC-43
Location: Chenango, NY	Member: Cherry Valley Member	Depth (ft):	1906.17

Microsparitic wackestone

Matrix Composition and Microtexture

massive matrix microtexture caused by calcite recrystallization; calcite is primary matrix constitutent with minor clays and dolomite

Diagenetic Minerals

calcite, dolomite, pyrite

Diagenetic Texture

calcite crystallized as a micron-scale microspar or single-crystal replacement of fossils; calcite overgrowths are observed on fossil exteriors; dolomite is sparse and disseminated as rhombohedra; interface between calcite cement and matrix components, such as fossils or detritus, is tight

Pore Structure

equant pores are hosted within calcite cement; minor organic-hosted porosity

Depositional Fabric

depositional fabrics are overprinted by diagenesis

Additional comments:

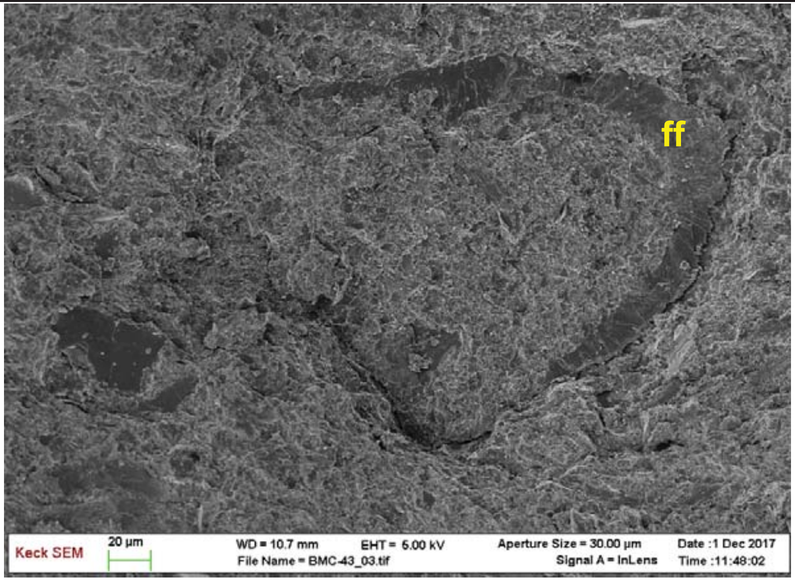

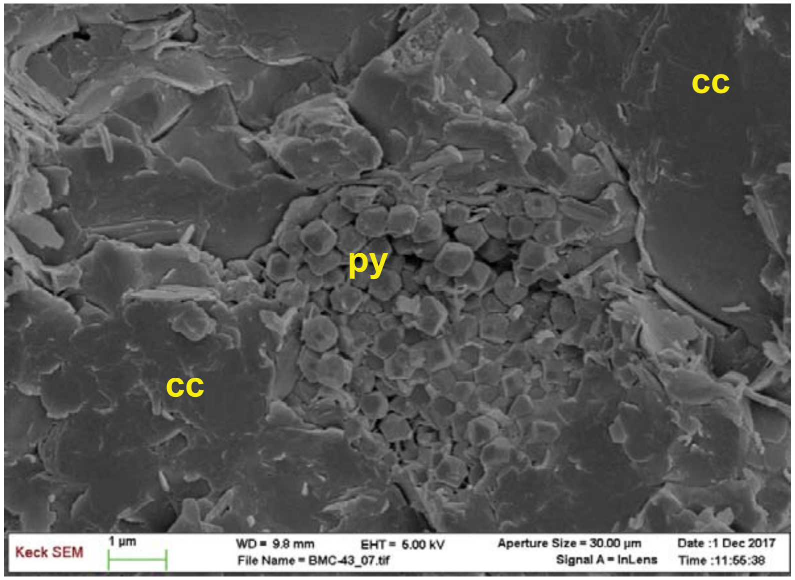

Well ID: Beaver Meadow 1 (31017230060000)	**Formation: Oatka Creek Formation**	**Sample ID:**	**BMC-NYSM-5**
Location: Chenango, NY	**Member: Cherry Valley Member**	**Depth (ft):**	**1906.50**

Microsparitic crystalline carbonate

Matrix Composition
calcite

Texture
nonlaminated, with abundant fossils not deposited with preferred orientations; neomorphosed microspar overprints depositional microtextures

Diagenetic Minerals
calcite is the dominant diagenetic mineral; matrix likely micritic in origin and neomorphosed to hypidiotopic, equigranular microspar; equant or dog tooth calcite rims fossils; framboidal pyrite associated with organic material; minor dolomite cement

Allochemical or Detrital Grains
trace quartz silt

Fossils
dacryoconarids (Styliolina); ostracods; crinoids; trilobites; nondescript shell fragments

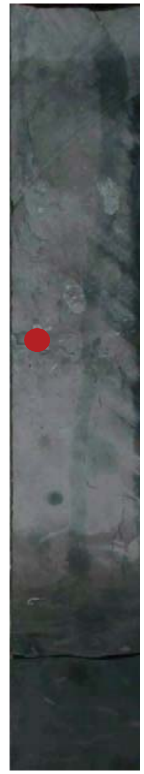

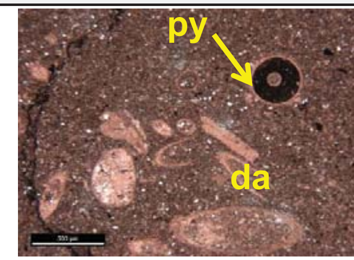

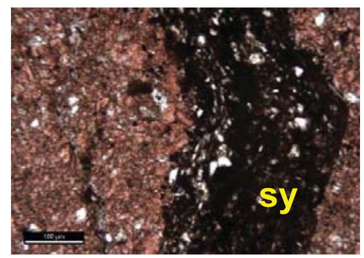

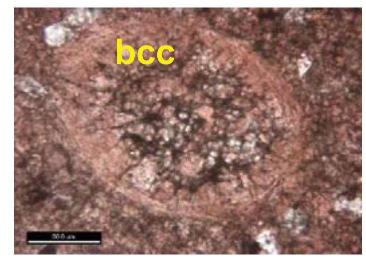

Fractures
millimeter-scale, organic- and clay-filled stylolite or fracture propagates normal to bedding through thin section

Additional Comments
organic material fills select fossils; thin section loaned from NYSM (no extra material available for SEM, XRD, or geochemical testing)

SWIR

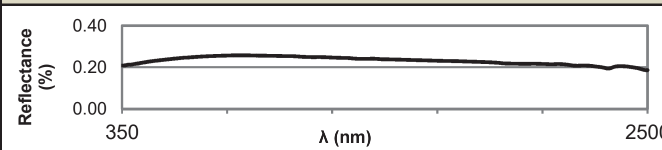

XRD
N/A

Stable Isotope

	$\delta^{13}C_{VPDB}$ (‰)	$\delta^{18}O_{VPDB}$ (‰)
1A Sample	N/A	N/A
1B Sample	N/A	N/A

Well ID: Beaver Meadow 1 (31017230060000)	Formation: Oatka Creek Formation	Sample ID:	BMC-48
Location: Chenango, NY	Member: Cherry Valley Member	Depth (ft):	1906.75

Microsparitic crystalline carbonate

Matrix Composition

calcite

Texture

nonlaminated; matrix is neomorphosed to xenotopic, equigranular microspar

Diagenetic Minerals

calcite is the dominant diagenetic mineral; recrystallization overprints depositional textures; equant calcite crystallizes on the surfaces of fossils

Allochemical or Detrital Grains

trace quartz silt

Fossils

dacryoconarids (Styliolina); crinoids; stromatoporoids; nondescript shell fragments

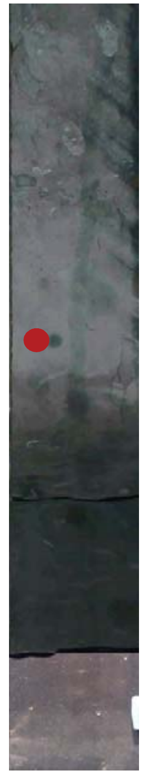

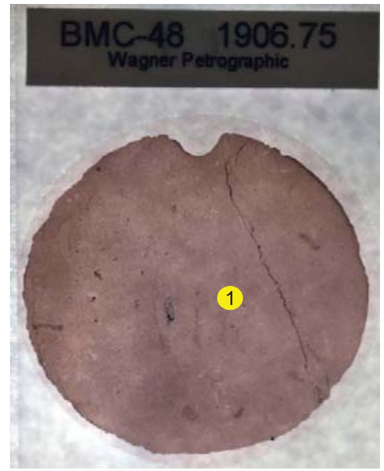

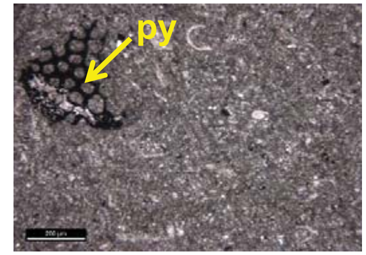

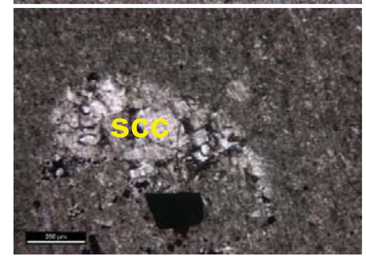

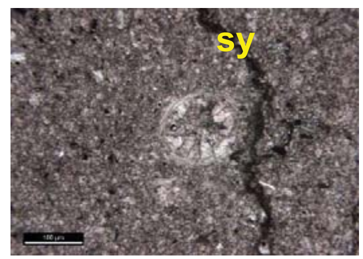

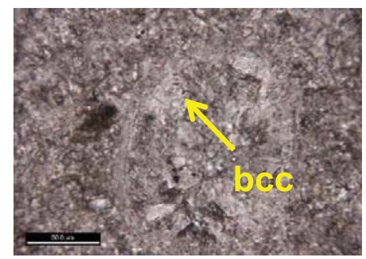

Fractures

irregular anastomosing stylolites propagate normal to bedding and are filled with clay and organic material

Additional Comments

select fossils have been dissolved and filled with organic material and framboidal pyrite

SWIR

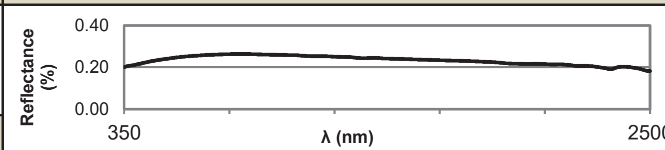

XRD

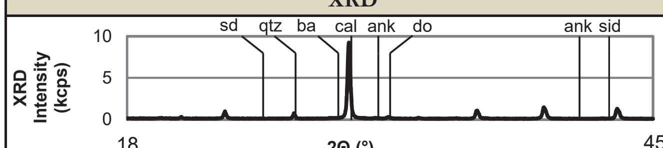

Stable Isotope

$\delta^{13}C_{VPDB}$ (‰)	$\delta^{18}O_{VPDB}$ (‰)
1A Sample	
-0.08	-7.31
1B Sample	
-0.51	-8.55

Well ID: Beaver Meadow 1 (31017230060000)	**Formation: Oatka Creek Formation**	**Sample ID:**	**BMC-48**
Location: Chenango, NY	**Member: Cherry Valley Member**	**Depth (ft):**	**1906.75**

Microsparitic crystalline carbonate

Matrix Composition and Microtexture

massive matrix microtexture caused by calcite recrystallization; calcite is primary matrix constitutent with minor clays and dolomite

Diagenetic Minerals

calcite, dolomite, pyrite

Diagenetic Texture

calcite crystallized as a micron-scale microspar or single-crystal replacement of fossils; calcite overgrowths are observed on fossil exteriors; dolomite is sparse and disseminated as rhombohedra; interface between calcite cement and matrix components, such as fossils or detritus, is tight

Pore Structure

equant pores are hosted within calcite cement; minor organic-hosted porosity

Depositional Fabric

depositional fabrics are overprinted by diagenesis

Additional comments:

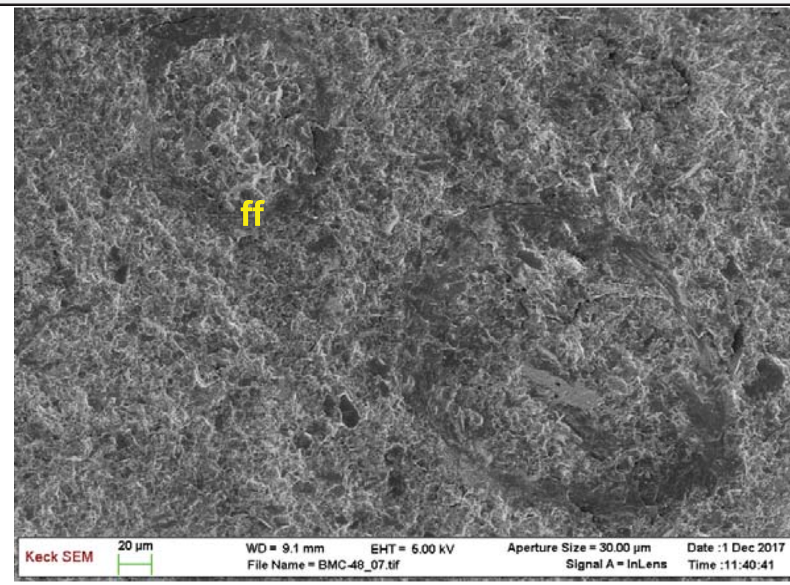

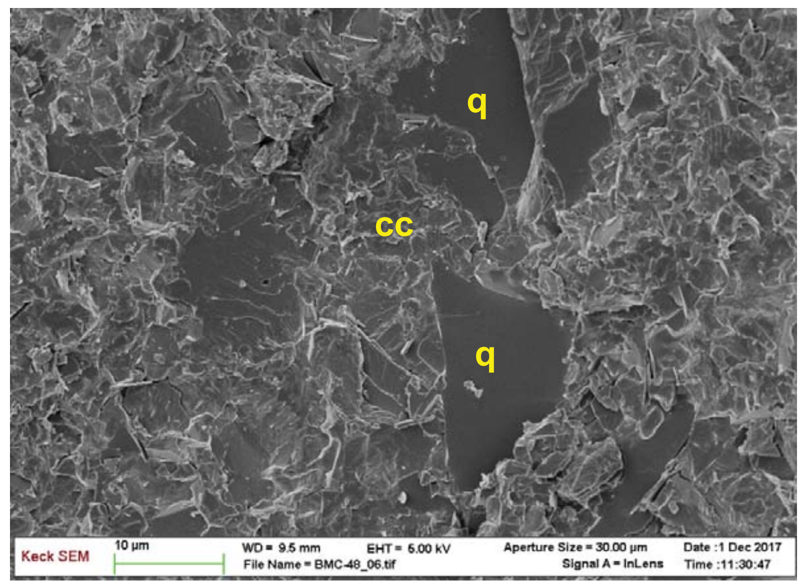

Well ID: Beaver Meadow 1 (31017230060000)	**Formation: Union Springs Formation**	**Sample ID:**	**BMC-NYSM-6**
Location: Chenango, NY	**Member: Bakoven Member**	**Depth (ft):**	**1909.00**

Silty, fossiliferous, calcareous mudstone

Matrix Composition

calcite and illitic clays

Texture

moderately well-laminated

Diagenetic Minerals

argillaceous matrix clays are cemented by calcite; fossils exhibit a calcite-rich halo; minor dolomite cement and disseminated rhombohedra; framboidal pyrite is associated with organic material

Allochemical or Detrital Grains

quartz silt (< 10%)

Fossils

nondescript shell fragments; phosphatic bone fragments

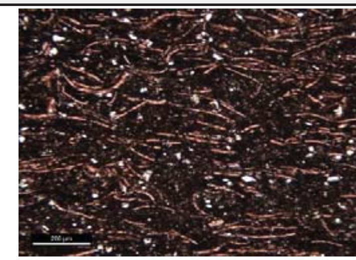

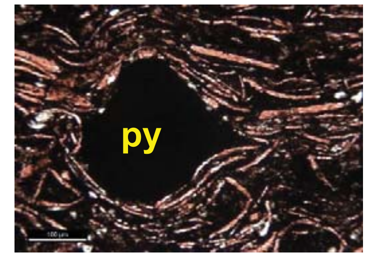

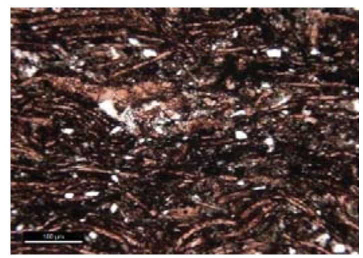

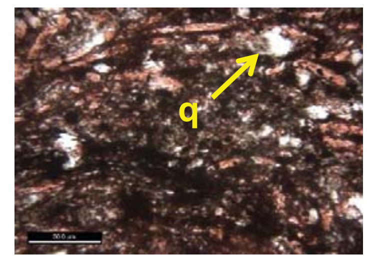

Fractures

none

Additional Comments

elevated organic content lends to opaque areas of the sample; thin section loaned from NYSM (no extra material available for SEM, XRD, or geochemical testing)

SWIR

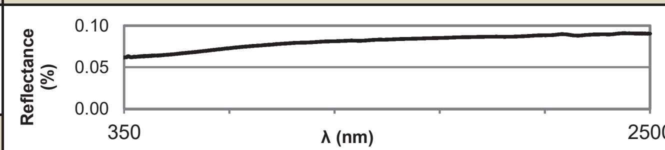

XRD

N/A

Stable Isotope

	$\delta^{13}C_{VPDB}$ (‰)	$\delta^{18}O_{VPDB}$ (‰)
1A Sample	N/A	N/A
1B Sample	N/A	N/A

REFERENCES

Aharon, P., & Fu, B. (2000). Microbial sulfate reduction rates and sulfur and oxygen isotope fractionations at oil and gas seeps in deepwater Gulf of Mexico. *Geochimica et Cosmochimica Acta*, *64*(2), 233-246.

Algeo, T. J., & Rowe, H. (2012). Paleoceanographic applications of trace-metal concentration data. *Chemical Geology*, *324*, 6-18.

Allison, P. A., & Pye, K. (1994). Early diagenetic mineralization and fossil preservation in modern carbonate concretions. *Palaios*, 561-575.

Anderson, E. J., Brett, C. E., Fisher, D. W., Goodwin, P. W., Kloc, G. J., Landing, E., & Lindemann, R. H. (1988). Upper Silurian to Middle Devonian stratigraphy and depositional controls, east-central New York. In *The Canadian paleontology and biostratigraphy seminar, New York State Museum Bulletin* (Vol. 462, pp. 111-134).

ASD Inc., a PANalytical Company. (2015). *TerraSpec 4: User Manual.* Boulder, CO: Author.

Banner, J. L., & Hanson, G. N. (1990). Calculation of simultaneous isotopic and trace element variations during water-rock interaction with applications to carbonate diagenesis. *Geochimica et Cosmochimica Acta*, *54*(11), 3123-3137.

Barker, S. L., Dipple, G. M., Dong, F., & Baer, D. S. (2011). Use of laser spectroscopy to measure the 13C/12C and 18O/16O compositions of carbonate minerals. *Analytical chemistry*, *83*(6), 2220-2226.

Bartholomew, A. J., & Brett, C. E. (2007). Correlation of Middle Devonian Hamilton Group-equivalent strata in east-central North America: implications for eustasy, tectonics and faunal provinciality. *Geological Society, London, Special Publications*, *278*(1), 105-131.

Beaumont, C., Quinlan, G. M., & Hamilton, J. (1987). The Alleghanian orogeny and its relationship to the evolution of the eastern interior, North America.

Bedell, R., Crósta, A. P., & Grunsky, E. R. I. C. (2009). Remote sensing and spectral geology. *Reviews in Economic Geology*, *16*, 266.

Blackmer, G. C., Omar, G. I., & Gold, D. P. (1994). Post-Alleghanian unroofing history of the Appalachian Basin, Pennsylvania, from apatite fission track analysis and thermal models. *Tectonics*, *13*(5), 1259-1276.

Blood, D. R., & Lash, G. G. (2015). Dynamic redox conditions in the Marcellus Shale as recorded by pyrite framboid size distributions. *Geological Society of America Special Papers*, *515*, 153-168.

Bojanowski, M. J., & Clarkson, E. N. (2012). Origin of Siderite Concretions in Microenvironments of Methanogenesis Developed in a Sulfate Reduction Zone: an exception or a rule?. *Journal of Sedimentary Research*, *82*(8), 585-598.

Bojanowski, M. J., Barczuk, A., & Wetzel, A. (2014). Deep-burial alteration of early-diagenetic carbonate concretions formed in Palaeozoic deep-marine greywackes and mudstones (Bardo Unit, Sudetes Mountains, Poland). *Sedimentology*, *61*(5), 1211-1239.

Bowen, G. J., Daniels, A. L., & Bowen, B. B. (2008). Paleoenvironmental isotope geochemistry and paragenesis of lacustrine and palustrine carbonates, Flagstaff Formation, Central Utah, USA. *Journal of Sedimentary Research*, *78*(3), 162-174.

Brand, U. (2004). Carbon, oxygen and strontium isotopes in Paleozoic carbonate components: an evaluation of original seawater-chemistry proxies. *Chemical Geology*, *204*(1-2), 23-44.

Brand, U., & Veizer, J. (1981). Chemical diagenesis of a multicomponent carbonate system-2: stable isotopes. *Journal of Sedimentary Research*, *51*(3).

Brand, U., Tazawa, J. I., Sano, H., Azmy, K., & Lee, X. (2009). Is mid-late Paleozoic ocean-water chemistry coupled with epeiric seawater isotope records?. *Geology*, *37*(9), 823-826.

Bréhéret, J. G., & Brumsack, H. J. (2000). Barite concretions as evidence of pauses in sedimentation in the Marnes Bleues Formation of the Vocontian Basin (SE France). *Sedimentary Geology*, *130*(3), 205-228.

Brett, C. E., & Baird, G. C. (1996). Middle Devonian sedimentary cycles and sequences in the northern Appalachian Basin. *SPECIAL PAPERS-GEOLOGICAL SOCIETY OF AMERICA*, 213-242.

Brett, C. E., Baird, G. C., Bartholomew, A. J., DeSantis, M. K., & Ver Straeten, C. A. (2011). Sequence stratigraphy and a revised sea-level curve for the Middle Devonian of eastern North America. *Palaeogeography, Palaeoclimatology, Palaeoecology*, *304*(1), 21-53.

Brett, C. E., Goodman, W. M., & LoDuca, S. T. (1990). Sequences, cycles, and basin dynamics in the Silurian of the Appalachian Foreland Basin. *Sedimentary Geology*, *69*(3-4), 191-244.

Brett, C. E., Ivany, L. C., Bartholomew, A. J., DeSantis, M. K., & Baird, G. C. (2009). Devonian ecological-evolutionary subunits in the Appalachian Basin: a revision and a test of persistence and discreteness. *Geological Society, London, Special Publications*, *314*(1), 7-36.

Brocke, R., Fatka, O., Lindemann, R. H., Schindler, E., & Ver Straeten, C. A. (2016). Palynology, dacryoconarids and the lower Eifelian (Middle Devonian) Basal Choteč Event: case studies from the Prague and Appalachian basins. *Geological Society, London, Special Publications*, *423*(1), 123-169.

Brocke, R., Fatka, O., Lindemann, R. H., Schindler, E., & Ver Straeten, C. A. (2016). Palynology, dacryoconarids and the lower Eifelian (Middle Devonian) Basal Choteč Event: case studies from the Prague and Appalachian basins. *Geological Society, London, Special Publications*, *423*(1), 123-169.

Bruner, K. R., Walker-Milani, M., & Smosna, R. (2015). Lithofacies of the Devonian Marcellus Shale in the Eastern Appalachian Basin, USA. *Journal of Sedimentary Research*, *85*(8), 937-954.

Buchardt, B., & Nielsen, A. T. (1985). Carbon and oxygen isotope composition of Cambro-Silurian limestone and anthraconite from Bornholm: Evidence for deep burial diagenesis. *Bulletin of the Geological Society of Denmark*, *33*, 415-435.

Call, T. (2012). *Geomechanical properties of Marcellus Shale core samples within a sequence stratigraphic framework* (Master's thesis). The Pennsylvania State University, State College, Pennsylvania.

Carpenter, S. J., & Lohmann, K. C. (1997). Carbon isotope ratios of Phanerozoic marine cements: Re-evaluating the global carbon and sulfur systems. *Geochimica et Cosmochimica Acta*, *61*(22), 4831-4846.

Carpenter, S. J., Erickson, J. M., Lohmann, K. C., & Owen, M. R. (1988). Diagenesis of fossiliferous concretions from the Upper Cretaceous Fox Hills Formation, North Dakota. *Journal of Sedimentary Research*, *58*(4).

Cate, A. S. (1963). Lithostratigraphy of some Middle and Upper Devonian rocks in the subsurface of southwestern Pennsylvania. *Pennsylvanian Topographic and Geological Survey*, *39*, 229-440.

Chen, R. (2016). *Dominant controls on organic-rich shale deposition: Geochemical evidences from the Marcellus Shale in the Appalachian basin* (Doctoral dissertation). West Virginia University, Morgantown, West Virginia.

Chen, R., & Sharma, S. (2016). Role of alternating redox conditions in the formation of organic-rich interval in the Middle Devonian Marcellus Shale, Appalachian Basin, USA. *Palaeogeography, Palaeoclimatology, Palaeoecology*, *446*, 85-97.

Chen, R., Sharma, S., Bank, T., Soeder, D., & Eastman, H. (2015). Comparison of isotopic and geochemical characteristics of sediments from a gas-and liquids-prone wells in Marcellus shale from Appalachian Basin, West Virginia. *Applied Geochemistry*, *60*, 59-71.

Choquette, P. W., & James, N. P. (1987). Diagenesis# 12. Diagenesis in Limestones-3. The deep burial environment. *Geoscience Canada*, *14*(1).

Coleman, M. E. (2005). *The Geologic History of Connecticut's Bedrock*. Connecticut Department of Environmental Protection.

Deines, P., Langmuir, D., & Harmon, R. S. (1974). Stable carbon isotope ratios and the existence of a gas phase in the evolution of carbonate ground waters. *Geochimica et Cosmochimica Acta*, *38*(7), 1147-1164.

DeSantis, M. K., & Brett, C. E. (2011). Late Eifelian (Middle Devonian) biocrises: timing and signature of the pre-Kačák Bakoven and Stony Hollow events in eastern North America. *Palaeogeography, Palaeoclimatology, Palaeoecology*, *304*(1), 113-135.

DeSantis, M. K., & Brett, C. E. (2011). Late Eifelian (Middle Devonian) biocrises: timing and signature of the pre-Kačák Bakoven and Stony Hollow events in eastern North America. *Palaeogeography, Palaeoclimatology, Palaeoecology*, *304*(1), 113-135.

DeSantis, M. K., Brett, C. E., & Ver Straeten, C. A. (2007). Persistent depositional sequences and bioevents in the Eifelian (early Middle Devonian) of eastern Laurentia: North American evidence of the Kačák Events?. *Geological Society, London, Special Publications*, *278*(1), 83-104.

Dorobek, S. L. (1987). Petrography, geochemistry, and origin of burial diagenetic facies, Siluro-Devonian Helderberg Group (carbonate rocks), central Appalachians. *AAPG bulletin*, *71*(5), 492-514.

Engelder, T., & Gold, D. (2008). Structural geology of the Marcellus and other Devonian gas shales: Geological conundrums involving joints, layer-parallel shortening strain, and the contemporary tectonic stress field: Field Trip Guidebook. In *AAPG–Society of Exploration Geophysicists Eastern Section Meeting, Pittsburgh, Pennsylvania.*

Engelder, T., Lash, G. G., & Uzcátegui, R. S. (2009). Joint sets that enhance production from Middle and Upper Devonian gas shales of the Appalachian Basin. *AAPG bulletin*, *93*(7), 857-889.

Engelder, T., Slingerland, R., Arthur, M., Lash, G., Kohl, D., Gold, D. P., & Ciampaglio, C. N. (2011). An introduction to the structure and stratigraphy in the proximal portion of the Middle Devonian Marcellus and Burket/Geneseo black shales in the central Appalachian Valley and Ridge. In *From the Shield to the Sea: Geological Field Trips form the 2011 Joint Meeting of the GSA Northeastern and North-Central Sections: Geological Society of America Field Guide*(Vol. 20, pp. 17-44).

Engle, M. A., & Rowan, E. L. (2014). Geochemical evolution of produced waters from hydraulic fracturing of the Marcellus Shale, northern Appalachian Basin: A multivariate compositional data analysis approach. *International Journal of Coal Geology*, *126*, 45-56.

Enomoto, C. B., Coleman Jr, J. L., Haynes, J. T., Whitmeyer, S. J., McDowell, R. R., Lewis, J. E., Spear, T.P., & Swezey, C. S. (2012). *Geology of the Devonian Marcellus Shale--Valley and Ridge province, Virginia and West Virginia--a field trip guidebook for the American Association of Petroleum Geologists Eastern Section Meeting, September 28-29, 2011* (No. 2012-1194, pp. i-48). US Geological Survey.

Ettensohn, F. R. (1985). The Catskill delta complex and the Acadian orogeny: A model. *Geological Society of America Special Papers*, *201*, 39-50.

Fairchild, I. J., & Spiro, B. (1987). Petrological and isotopic implications of some contrasting Late Precambrian carbonates, NE Spitsbergen. *Sedimentology*, *34*(6), 973-989.

Flügel, E. (2010). *Microfacies of Carbonate Rocks*. Springer Berlin Heidelberg.

Frank, T. D., & Bernet, K. (2000). Isotopic signature of burial diagenesis and primary lithological contrasts in periplatform carbonates (Miocene, Great Bahama Bank). *Sedimentology*, *47*(6), 1119-1134.

Frank, T. D., & Lohmann, K. C. (1996). Diagenesis of fibrous magnesian calcite marine cement: Implications for the interpretation of δ18O and δ13C values of ancient equivalents. *Geochimica et Cosmochimica Acta*, *60*(13), 2427-2436.

Frappier, A. B., Lindemann, R. H., & Frappier, B. R. (2015). Stable isotope analysis of Dacryoconarid carbonate microfossils: a new tool for Devonian oxygen and carbon isotope stratigraphy. *Rapid Communications in Mass Spectrometry*, *29*(8), 764-774.

Given, R. K., & Lohmann, K. C. (1986). Isotopic evidence for the early meteoric diagenesis of the reef facies, Permian Reef Complex of West Texas and New Mexico. *Journal of Sedimentary Research*, *56*(2).

Graber, K. K., & Chafetz, H. S. (1990). Petrography and origin of bedded barite and phosphate in the Devonian Slaven Chert of central Nevada. *Journal of Sedimentary Research*, *60*(6).

Griffing, D. H., & Ver Straeten, C. A. (1991). Stratigraphy and depositional environments of the lower part of the Marcellus Formation (Middle Devonian) in eastern New York State. In *New York State Geological Association, 63rd Annual Meeting Field Trip Guidebook* (pp. 205-234).

Halley, S. (2016, May). *Mineralogy Maps from SWIR data; what works, what doesn't work and why*. Presentation presented at the TeamWA Workshops: Hyperspectral Analysis for Exploration, Kensington, Australia.

Heizler, M. T., & Harrison, T. M. (1998). The thermal history of the New York basement determined from 40Ar/39Ar K-feldspar studies. *Journal of Geophysical Research: Solid Earth*, *103*(B12), 29795-29814.

Herwanger*, J. V., Bottrill, A. D., & Mildren, S. D. (2015, July). Uses and abuses of the brittleness index with applications to hydraulic stimulation. In *Unconventional Resources Technology Conference, San Antonio, Texas, 20-22 July 2015*(pp. 1215-1223). Society of Exploration Geophysicists, American Association of Petroleum Geologists, Society of Petroleum Engineers.

Hilliard, V. L. (2015). *Sequence Stratigraphy and Reservoir Characterization of the Middle Devonian Marcellus Formation for a Cored Well in Harrison County, West Virginia* (Master's thesis). West Virginia University, Morgantown, West Virginia.

Hoefs, J. (2015). Isotope fractionation processes of selected elements. In *Stable Isotope Geochemistry* (pp. 47-190). Springer, Cham.

Hosseininejad, S., Pedersen, P. K., Spencer, R. J., & Uwuilekhue, F. M. Use of NIR spectroscopy in mineral identification in shale.

Hosterman, J. W., & Whitlow, S. I. (1983). *Clay mineralogy of Devonian shales in the Appalachian Basin* (No. 1298). US Geological Survey.

Howe, H., Chipera, S., & Alcantar-Lopez, L. (2016). Iron Content of Organogenic Dolomite as a Reflection of Chemical Reactions within the Zone of Sulfate Reduction: A Potential Tool for Depositional Studies of Organic-Rich Mudstones. Unconventional Resources Technology Conference (URTEC).

Hudson, J. D. (1977). Stable isotopes and limestone lithification. *Journal of the Geological Society*, *133*(6), 637-660.

Huntington, K. W., Budd, D. A., Wernicke, B. P., & Eiler, J. M. (2011). Use of clumped-isotope thermometry to constrain the crystallization temperature of diagenetic calcite. *Journal of Sedimentary Research*, *81*(9), 656-669.

Hurley, N. F., & Lohmann, K. C. (1989). Diagenesis of Devonian reefal carbonates in the Oscar Range, Canning Basin, Western Australia. *Journal of Sedimentary Research*, *59*(1).

Husson, J. M., Schoene, B., Bluher, S., & Maloof, A. C. (2016). Chemostratigraphic and U–Pb geochronologic constraints on carbon cycling across the Silurian–Devonian boundary. *Earth and Planetary Science Letters*, *436*, 108-120.

Irwin, H., Curtis, C., & Coleman, M. (1977). Isotopic evidence for source of diagenetic carbonates formed during burial of organic-rich sediments. *Nature*, *269*(5625), 209-213.

Jackson, M., McCabe, C., Ballard, M. M., & Van der Voo, R. (1988). Magnetite authigenesis and diagenetic paleotemperatures across the northern Appalachian basin. *Geology*, *16*(7), 592-595.

Jarvie, D. M., Hill, R. J., Ruble, T. E., & Pollastro, R. M. (2007). Unconventional shale-gas systems: The Mississippian Barnett Shale of north-central Texas as one model for thermogenic shale-gas assessment. *AAPG bulletin*, *91*(4), 475-499.

Joachimski, M. M., Breisig, S., Buggisch, W., Talent, J. A., Mawson, R., Gereke, M., ... & Weddige, K. (2009). Devonian climate and reef evolution: insights from oxygen isotopes in apatite. *Earth and Planetary Science Letters*, *284*(3-4), 599-609.

Johnsson, M. J. (1986). Distribution of maximum burial temperatures across northern Appalachian Basin and implications for Carboniferous sedimentation patterns. *Geology*, *14*(5), 384-387.

Jones, B., & Manning, D. A. (1994). Comparison of geochemical indices used for the interpretation of palaeoredox conditions in ancient mudstones. *Chemical Geology*, *111*(1-4), 111-129.

Jones, B., Pleydell, S. M., Ng, K. C., & Longstaffe, F. J. (1989). Formation of poikilotopic calcite-dolomite fabrics in the Oligocene-Miocene Bluff formation of Grand Cayman, British West Indies. *Bulletin of Canadian Petroleum Geology*, *37*(3), 255-265.

Karaca, C. (2012). *Characterization Of The Union Springs Formation, Finger Lakes Region, NY: An Integrated High Resolution Facies, Geochemical And Sequence Stratigraphical Approach* (Doctoral dissertation). Cornell University, Ithaca, New York.

Klofak, S. M., & Landman, N. H. (2012). Internal features of Ammonitellas of Tornoceratids from the Middle Devonian Cherry Valley Limestone, New York State, USA. *Geobios*, *45*(1), 49-56.

Kohl, D., Slingerland, R., Arthur, M., Bracht, R., & Engelder, T. (2014). Sequence stratigraphy and depositional environments of the Shamokin (Union Springs) Member, Marcellus Formation, and associated strata in the middle Appalachian Basin. *AAPG bulletin*, *98*(3), 483-513.

Lash, G. G. (2015). Authigenic barite nodules and carbonate concretions in the Upper Devonian shale succession of western New York–a record of variable methane flux during burial. *Marine and Petroleum Geology*, *59*, 305-319.

Lash, G. G., & Blood, D. R. (2014). Organic matter accumulation, redox, and diagenetic history of the Marcellus Formation, southwestern Pennsylvania, Appalachian basin. *Marine and Petroleum Geology*, *57*, 244-263.

Lash, G. G., & Engelder, T. (2009). Tracking the burial and tectonic history of Devonian shale of the Appalachian Basin by analysis of joint intersection style. *Geological Society of America Bulletin*, *121*(1-2), 265-277.

Lash, G. G., & Engelder, T. (2011). Thickness trends and sequence stratigraphy of the Middle Devonian Marcellus Formation, Appalachian Basin: Implications for Acadian foreland basin evolution. *AAPG bulletin*, *95*(1), 61-103.

Lash, G., Loewy, S., & Engelder, T. (2004). Preferential jointing of Upper Devonian black shale, Appalachian Plateau, USA: evidence supporting hydrocarbon generation as a joint-driving mechanism. *Geological Society, London, Special Publications*, *231*(1), 129-151.

Laughrey, C. D., & Baldassare, F. J. (1998). Geochemistry and origin of some natural gases in the Plateau Province, central Appalachian Basin, Pennsylvania and Ohio. *AAPG bulletin*, *82*(2), 317-335.

Laughrey, C. D., Ruble, T. E., Lemmens, H., Kostelnik, J., Butcher, A. R., Walker, G., & Knowles, W. (2011). AV black shale diagenesis: insights from integrated high-definition analyses of post-mature Marcellus Formation Rocks, Northeastern Pennsylvania. In *Annual Convention and Exhibition, AAPG*.

Lazar, O. R., Bohacs, K. M., Macquaker, J. H., Schieber, J., & Demko, T. M. (2015). Capturing key attributes of fine-grained sedimentary rocks in outcrops, cores, and thin sections: nomenclature and description guidelines. *Journal of Sedimentary Research*, *85*(3), 230-246.

Lindemann, R. H., & Karabinos, P. (2002). Dacryoconarid bioevents of the Onondaga Formation and the Marcellus Subgroup, Cherry Valley, New York. *Guidebooks for fieldtrips in New York and Vermont B*, *7*.

Lohmann, K. C. (1988). Geochemical patterns of meteoric diagenetic systems and their application to studies of paleokarst. In *Paleokarst* (pp. 58-80). Springer New York.

Lokier, S. W., & Al Junaibi, M. (2016). The petrographic description of carbonate facies: are we all speaking the same language?. *Sedimentology*, *63*(7), 1843-1885.

Lovering, T. G., & Van Heyl, A. (1989). *Mineral belts in western Sierra County, New Mexico, suggested by mining districts, geology, and geochemical anomalies* (No. 1876). USGPO; For sale by the Books and Open-File Reports Section, US Geological Survey,.

Loyd, S. J., Dickson, J. A. D., Boles, J. R., & Tripati, A. K. (2014). Clumped-isotope constraints on cement paragenesis in septarian concretions. *Journal of Sedimentary Research*, *84*(12), 1170-1184.

Lynch-Stieglitz, J., Curry, W. B., & Slowey, N. (1999). A geostrophic transport estimate for the Florida Current from the oxygen isotope composition of benthic foraminifera. *Paleoceanography*, *14*(3), 360-373.

Majewski, W. (2003). Middle Jurassic concretions from Częstochowa (Poland) as indicators of sedimentation rates. *Acta Geologica Polonica*, *50*(4), 431-439.

Manning, E. B., & Elmore, R. D. (2015). An integrated paleomagnetic, rock magnetic, and geochemical study of the Marcellus shale in the Valley and Ridge province in Pennsylvania and West Virginia. *Journal of Geophysical Research: Solid Earth*, *120*(2), 705-724.

Mason, J. L. (2017). *High-resolution facies variability and connections to compositional and mechanical heterogeneity in the union springs formation of central New York* (Doctoral dissertation). Cornell University, Ithaca, New York.

Maynard, J. B. (1981). Carbon isotopes as indicators of dispersal patterns in Devonian-Mississippian shales of the Appalachian Basin. *Geology*, *9*(6), 262-265.

Mazzullo, S. J. (2000). Organogenic dolomitization in peritidal to deep-sea sediments. *Journal of Sedimentary Research*, *70*(1), 10-23.

McKeon, R. E., Zeitler, P. K., Pazzaglia, F. J., Idleman, B. D., & Enkelmann, E. (2014). Decay of an old orogen: Inferences about Appalachian landscape evolution from low-temperature thermochronology. *Geological Society of America Bulletin*, *126*(1-2), 31-46.

Miller, D. S., & Duddy, I. R. (1989). Early Cretaceous uplift and erosion of the northern Appalachian Basin, New York, based on apatite fission track analysis. *Earth and Planetary Science Letters*, *93*(1), 35-49.

Milliken, K. L., Rudnicki, M., Awwiller, D. N., & Zhang, T. (2013). Organic matter–hosted pore system, Marcellus formation (Devonian), Pennsylvania. *AAPG bulletin*, *97*(2), 177-200.

Moldovanyi, E. P., & Lohmann, K. C. (1984). Isotopic and petrographic record of phreatic diagenesis: Lower Cretaceous Sligo and Cupido Formations. *Journal of Sedimentary Research*, *54*(3).

Mozley, P. S., & Burns, S. J. (1993). Oxygen and carbon isotopic composition of marine carbonate concretions: an overview. *Journal of Sedimentary Research*, *63*(1).

Munnecke, A., Westphal, H., Reijmer, J. J., & Samtleben, C. (1997). Microspar development during early marine burial diagenesis: a comparison of Pliocene carbonates from the Bahamas with Silurian limestones from Gotland (Sweden). *Sedimentology*, *44*(6), 977-990.

Murata, K. J., Friedman, I., & Madsen, B. M. (1969). *Isotopic composition of diagenetic carbonates in marine Miocene formations of California and Oregon*. US Government Printing Office.

Murphy, A. E., Sageman, B. B., Hollander, D. J., Lyons, T. W., & Brett, C. E. (2000). Black shale deposition and faunal overturn in the Devonian Appalachian Basin: clastic starvation, seasonal water-column mixing, and efficient biolimiting nutrient recycling. *Paleoceanography*, *15*(3), 280-291.

Obermajer, M., Fowler, M. G., Goodarzi, F., & Snowdon, L. R. (1997). Organic petrology and organic geochemistry of Devonian black shales in southwestern Ontario, Canada. *Organic Geochemistry*, *26*(3-4), 229-246.

Osborn, S. G., & McIntosh, J. C. (2010). Chemical and isotopic tracers of the contribution of microbial gas in Devonian organic-rich shales and reservoir sandstones, northern Appalachian Basin. *Applied Geochemistry*, *25*(3), 456-471.

Parnell, J. (2002). Diagenesis and fluid flow in response to uplift and exhumation. *Geological Society, London, Special Publications*, *196*(1), 433-446.

Pitman III, W. C., & Talwani, M. (1972). Sea-floor spreading in the North Atlantic. *Geological Society of America Bulletin*, *83*(3), 619-646.

Pommer, L., Gale, J. F., Eichhubl, P., Fall, A., & Laubach, S. E. (2013, August). Using structural diagenesis to infer the timing of natural fractures in the Marcellus Shale. In *Unconventional Resources Technology Conference* (pp. 1639-1644). Society of Exploration Geophysicists, American Association of Petroleum Geologists, Society of Petroleum Engineers.

Quinlan, G. M., & Beaumont, C. (1984). Appalachian thrusting, lithospheric flexure, and the Paleozoic stratigraphy of the eastern interior of North America. *Canadian Journal of Earth Sciences*, *21*(9), 973-996.

Raiswell, R., & Fisher, Q. J. (2000). Mudrock-hosted carbonate concretions: a review of growth mechanisms and their influence on chemical and isotopic composition. *Journal of the Geological Society*, *157*(1), 239-251.

Reddy, J. E., & Kappel, W. M. (2010). *Hydrogeologic and geospatial data for the assesment of focused recharge to the Carbonate-Rock Aquifer in Genesee County, New York* (No. 3132). US Geological Survey.

Reed, J. S., Spotila, J. A., Eriksson, K. A., & Bodnar, R. J. (2005). Burial and exhumation history of Pennsylvanian strata, central Appalachian Basin: An integrated study. *Basin Research*, *17*(2), 259-268.

Repetski, J. E., Ryder, R. T., Weary, D. J., Harris, A. G., & Trippi, M. H. (2008). Thermal Maturity Patterns (CAI and% Ro) in Upper Ordovician and Devonian Rocks of the Appalachian Basin. A Major Revision of USGS Map I–917–E Using New Subsurface Collections. *US Geological Survey Scientific Investigations Map*, *3006*, 26.

Rickard, L. V. (1984). Correlation of the subsurface Lower and Middle Devonian of the Lake Erie region. *Geological Society of America Bulletin*, *95*(7), 814-828.

Roden, M. K., & Miller, D. S. (1989). Apatite fission-track thermochronology of the Pennsylvania Appalachian Basin. *Geomorphology*, *2*(1-3), 39-51.

Roden, M. K. (1991). Apatite fission-track thermochronology of the southern Appalachian basin: Maryland, West Virginia, and Virginia. *The Journal of Geology*, *99*(1), 41-53.

Roden-Tice, M. K., Tice, S. J., & Schofield, I. S. (2000). Evidence for differential unroofing in the Adirondack Mountains, New York State, determined by apatite fission-track thermochronology. *The Journal of geology*, *108*(2), 155-169.

Rosales, I., & Pérez-Garcia, A. (2010). Porosity development, diagenesis and basin modelling of a Lower Cretaceous (Albian) carbonate platform from northern Spain. *Geological Society, London, Special Publications*, *329*(1), 317-342.

Ryder, R. T., Trippi, M. H., Swezey, C. S., Crangle, R. D., Hope, R. S., Rowan, E. L., & Lentz, E. E. (2012). Geologic Cross Section CC' Through the Appalachian Basin from Erie County, North-central Ohio, to the Valley and Ridge Province, Bedford County, South-central Pennsylvania.

Sageman, B. B., Murphy, A. E., Werne, J. P., Ver Straeten, C. A., Hollander, D. J., & Lyons, T. W. (2003). A tale of shales: the relative roles of production, decomposition, and dilution in the accumulation of organic-rich strata, Middle–Upper Devonian, Appalachian basin. *Chemical Geology*, *195*(1), 229-273.

Sak, P.B., McQuarrie, N., Oliver, B.P., Lavdovsky, N. and Jackson, M.S., 2012. Unraveling the central Appalachian fold-thrust belt, Pennsylvania: The power of sequentially restored balanced cross sections for a blind fold-thrust belt. *Geosphere*, *8*(3), pp.685-702.

Savin, S. M. (1982). Stable isotopes in climatic reconstructions. *Climate and Earth History. Natl. Acad. Press, Washington, DC*, 164.

Schindler, E. (2012). Tentaculitoids–an enigmatic group of Palaeozoic fossils. In *Earth and Life* (pp. 479-490). Springer Netherlands.

Scholle, P. A., & Ulmer-Scholle, D. S. (2003). *A Color Guide to the Petrography of Carbonate Rocks: Grains, Textures, Porosity, Diagenesis, AAPG Memoir* (Vol. 77). AAPG.

Selleck, B., & Koff, D. (2008). Stable isotope signature of Middle Devonian seawater from Hamilton Group brachiopods, central New York State. *Northeastern Geology & Environmental Sciences*, *30*(4), 330-343.

Slingerland, R., & Furlong, K. P. (1989). Geodynamic and geomorphic evolution of the Permo-Triassic Appalachian Mountains. *Geomorphology*, *2*(1-3), 23-37.

Suess, E., & Whiticar, M. (1989). Methane-derived CO2 in pore fluids expelled from the Oregon subduction zone. *Palaeogeography, Palaeoclimatology, Palaeoecology*, *71*(1-2), 119-136.

Swart, P. K. (2015). The geochemistry of carbonate diagenesis: The past, present and future. *Sedimentology*, *62*(5), 1233-1304.

Tada, R., & Siever, R. (1989). Pressure solution during diagenesis. *Annual Review of Earth and Planetary Sciences*, *17*(1), 89-118.

Thompson, A. J. (1999). Alteration mapping in exploration: Application of short wave infrared (SWIR) spectroscopy. *Econ. Geol. Newsl.*, *30*, 13.

Torres, M. E., Brumsack, H. J., Bohrmann, G., & Emeis, K. C. (1996). Barite fronts in continental margin sediments: a new look at barium remobilization in the zone of sulfate reduction and formation of heavy barites in diagenetic fronts. *Chemical Geology*, *127*(1-3), 125-139.

Tribovillard, N., Algeo, T. J., Lyons, T., & Riboulleau, A. (2006). Trace metals as paleoredox and paleoproductivity proxies: an update. *Chemical geology*, *232*(1), 12-32.

Tucker, R. D., Bradley, D. C., Ver Straeten, C. A., Harris, A. G., Ebert, J. R., & McCutcheon, S. R. (1998). New U–Pb zircon ages and the duration and division of Devonian time. *Earth and Planetary Science Letters*, *158*(3), 175-186.

Vandeginste, V., & John, C. M. (2012). Influence of climate and dolomite composition on dedolomitization: insights from a multi-proxy study in the central Oman Mountains. *Journal of Sedimentary Research*, *82*(3), 177-195.

Van Geldern, R., Joachimski, M. M., Day, J., Jansen, U., Alvarez, F., Yolkin, E. A., & Ma, X. P. (2006). Carbon, oxygen and strontium isotope records of Devonian brachiopod shell calcite. *Palaeogeography, Palaeoclimatology, Palaeoecology*, *240*(1-2), 47-67.

Ver Straeten, C. A. (2004). K-bentonites, volcanic ash preservation, and implications for Early to Middle Devonian volcanism in the Acadian orogen, eastern North America. *Geological Society of America Bulletin*, *116*(3-4), 474-489.

Ver Straeten, C. A. (2007). Basinwide stratigraphic synthesis and sequence stratigraphy, upper Pragian, Emsian and Eifelian stages (Lower to Middle Devonian), Appalachian Basin. *Geological Society, London, Special Publications*, *278*(1), 39-81.

Ver Straeten, C. A., & Brett, C. E. (2006). Pragian to Eifelian strata (middle Lower to lower Middle Devonian), northern Appalachian Basin-stratigraphic nomenclatural changes. *Northeastern Geology and Environmental Sciences*, *28*(1), 80.

Ver Straeten, C. A., Baird, G., Brett, C., Lash, G., Over, J., Karaca, C., & Blood, R. (2011). The Marcellus subgroup in its type area, Finger Lakes area of New York, and beyond. In *New York State Geological Association, 83rd Annual Meeting Field Trip Guidebook (pp. 23-86).*

Ver Straeten, C. A., Brett, C. E., & Sageman, B. B. (2011). Mudrock sequence stratigraphy: a multi-proxy (sedimentological, paleobiological and geochemical) approach, Devonian Appalachian Basin. *Palaeogeography, Palaeoclimatology, Palaeoecology*, *304*(1), 54-73.

Ver Straeten, C. A., Griffing, D. H., & Brett, C. E. (1994). The lower part of the Middle Devonian Marcellus "Shale," central to western New York State; stratigraphy and depositional history. In *New York State Geological Association, 66th Annual Meeting Field Trip Guidebook* (pp. 271-321).

Vinn, O., & Zatoń, M. (2012). Phenetic phylogenetics of tentaculitoids–extinct, problematic calcareous tube-forming organisms. *GFF*, *134*(2), 145-156.

Walker-Milani, M. E. (2011). *Outcrop lithostratigraphy and petrophysics of the Middle Devonian Marcellus Shale in West Virginia and adjacent states* (Master's thesis). West Virginia University, Morgantown, West Virginia.

Wang, G., & Carr, T. R. (2013). Organic-rich Marcellus Shale lithofacies modeling and distribution pattern analysis in the Appalachian Basin. *AAPG bulletin*, *97*(12), 2173-2205.

Wang, J. (2014). *The origin of a basin-scale thin limestone: the Middle Devonian Cherry Valley Member, Marcellus Formation* (Master's thesis). The Pennsylvania State University, State College, Pennsylvania.

Wei, F., Gong, Y., & Yang, H. (2012). Biogeography, ecology and extinction of Silurian and Devonian tentaculitoids. *Palaeogeography, Palaeoclimatology, Palaeoecology*, *358*, 40-50.

Wendt, A. K., Arthur, M. A., Slingerland, R., Kohl, D., Bracht, R., & Engelder, T. (2015). Geochemistry and depositional history of the Union Springs Member, Marcellus Formation in central Pennsylvania. *Interpretation*, *3*(3), SV17-SV33.

Werne, J. P., Sageman, B. B., Lyons, T. W., & Hollander, D. J. (2002). An integrated assessment of a "type euxinic" deposit: evidence for multiple controls on black shale deposition in the Middle Devonian Oatka Creek Formation. *American Journal of Science*, *302*(2), 110-143.

Wierzbowski, H., & Joachimski, M. (2007). Reconstruction of late Bajocian–Bathonian marine palaeoenvironments using carbon and oxygen isotope ratios of calcareous fossils from the Polish Jura Chain (central Poland). *Palaeogeography, Palaeoclimatology, Palaeoecology*, *254*(3), 523-540.

Wilson, M. E., Wah, E. C. E., Dorobek, S., & Lunt, P. (2013). Onshore to offshore trends in carbonate sequence development, diagenesis and reservoir quality across a land-attached shelf in SE Asia. *Marine and Petroleum Geology*, *45*, 349-376.

Wilson, T. H. (2000). Seismic evaluation of differential tectonic subsidence, compaction, and loading in an interior basin. *AAPG bulletin*, *84*(3), 376-398.

Wintsch, R. P., & Kvale, C. M. (1994). Differential mobility of elements in burial diagenesis of siliciclastic rocks. *Journal of Sedimentary Research*, *64*(2).

Wittmer, J. M., & Miller, A. I. (2011). Dissecting the global diversity trajectory of an enigmatic group: The paleogeographic history of tentaculitoids. *Palaeogeography, Palaeoclimatology, Palaeoecology*, *312*(1), 54-65.

Zaini, N., van der Meer, F., & van der Werff, H. (2012). Effect of grain size and mineral mixing on carbonate absorption features in the SWIR and TIR wavelength regions. *Remote sensing*, *4*(4), 987-1003.

Zaini, N., van der Meer, F., & van der Werff, H. (2014). Determination of carbonate rock chemistry using laboratory-based hyperspectral imagery. *Remote Sensing*, *6*(5), 4149-4172.

Zapata, A. (2014). *Geological characterization of the Union Springs Formation, Lower Marceullus Shale in the Appalachian Basin, central New York* (Master's thesis). Brooklyn College, Brooklyn, New York.

Zatoń, M., Machocka, S., Wilson, M. A., Marynowski, L., & Taylor, P. D. (2011). Origin and paleoecology of Middle Jurassic hiatus concretions from Poland. *Facies*, *57*(2), 275-300.

Zempolich, W. G., Wilkinson, B. H., & Lohmann, K. C. (1988). Diagenesis of late Proterozoic carbonates: the Beck Spring Dolomite of eastern California. *Journal of Sedimentary Research*, *58*(4).

Zhou, J., Rush, P., & Miller, R. (2017). Barite in the Middle Devonian Marcellus Shale, Appalachian Basin: Occurrence, petrography, geochemistry and its implications. In *AAPG Annual Convention and Exhibition*.